THE UNIVERSITY
of EDINBURGH

Modification of Poly(lactic acid) *via* Olefin Cross-Metathesis

Fern Sinclair

A thesis submitted at the University of Edinburgh
for the Degree of Doctor of Philosophy
2017

Abstract

Poly(lactic acid), PLA, is a viable replacement to petroleum derived polymers due to its renewable feedstock, biodegradability and bioassimilability, yet improvements in its physical, thermal and mechanical properties are required before it can fully enter all commodity markets. This thesis investigates olefin cross-metathesis (CM) as a synthetic strategy to modify the properties of PLA. The use of novel lanthanide and actinide catalysts on the microstructure control of PLA are also explored.

The Tebbe reagent was used in a new synthetic strategy to produce a novel olefin derivative of lactide (MML). Olefin CM of MML with hex-1-ene was successful but polymerisation pre- and post-CM was unsuccessful due to monomer instability. CM of another olefin derivative of lactide, 3-methylenated lactide (3-ML) was successful with aliphatic alkenes; hex-1-ene to dodec-1-ene. To overcome competing alcoholysis of the functionalised monomers, which prevented polymerisation, hydrogenation was used to remove the olefin entity followed by successful ring-opening polymerisation (ROP) to produce polymers of low glass-transition temperatures (T_g).

Post-polymerisation CM on an olefin containing polymer P(β-heptenolactone) P(β-HL), with methyl acrylate and an epoxide, generated functionalised homopolymers with increased T_g's. Co-polymerisation of lactide with β-HL generated novel gradient-copolymers. Olefin CM with 15 different cross-partners produced functionalised co-polymers with different thermal properties. Based on this route a new methodology was created to introduce two unique functionalities into the polymer backbone by manipulation of the olefin reactivities.

Finally, in a collaborative project, uranium and cerium catalysts, $Me_3SiOU(OArP)_3$ and $Me_3SiOCe(OArP)_3$ - designed out-with the group- were tested and compared as ROP catalysts for lactide. Both catalysts were active in living polymerisations of L-lactide and under immortal conditions the activity and rates of the catalysts were switched, accounted for by a change in the coordination sphere due to ligand displacement. ROP of rac-lactide using the uranium analogue produced heterotactic-biased PLA with a $P_r = 0.79$.

Lay Summary

Poly(lactic acid), PLA, is a viable replacement to petroleum derived polymers due to its renewable feedstock and biodegradability, yet improvements in its physical, thermal and mechanical properties are required before it can fully enter all commodity markets. This thesis investigates the viability of olefin cross-metathesis (CM) as a route to alter the thermal properties of PLA.

Olefin CM reactions require an olefin moiety to work. Thus in order to modify the properties of PLA this work explores the incorporation of an olefin moiety into lactide, the monomer of PLA. Successful CM reactions generated functionalised lactide monomers that after further manipulations produced polymers with altered thermal properties. Copolymers of lactide with a different olefin containing monomer generated copolymers that were capable of modification *via* olefin CM. 15 different functional groups were incorporated to demonstrate changes in thermal properties. A novel methodology was also developed to introduce two unique functionalities into the copolymer.

Finally, in a collaborative project uranium and cerium catalysts were tested and compared in the polymerisation of lactide. The uranium analogue was capable of producing PLA with a controlled monomer sequence.

Declaration

The work described in this thesis is of my own, unless I have acknowledged help from a named person or referenced a published source. This thesis has not been submitted, in whole or in part, for any other degree.

Signature:

Date:

Acknowledgements

The work in this thesis would not have been possible without the continued support and encouragement from work colleagues, friends and family. Firstly, I would like to thank my supervisor Dr Michael Shaver. He has given scientific support throughout my research but more importantly encouraged development out-with the laboratory, supporting my entrepreneurial training and has constantly kept me on my toes. I would like to thank the Principal's Career Development Scholarship for the funding that has made this PhD possible.

I would like to thank both past and present lab colleagues, and now friends of the Green Materials Laboratory for all the laughs and support throughout the years; Dave, Kevin, Stefan, Jake, Meng, Jaclyn, Gerry, Mohammad, James.M, Vishal, Yasmeen, Joanne, Eszter, and all undergraduates. A special thanks to previous postdoctorates of the group; Laura for initial laboratory training and Vincent for his input with aiding with the purification of my more challenging monomers. A huge thanks to Ben, Dan.C and Catherine for reading through my thesis. A special thanks to Joe, Amy, James.P, Emily, Jarret and Genny who were there from the start. In particular, Emily whose support in my first couple of years was greatly appreciated. Thanks to fellow groups, the Tasker's and the Pulham's of whom I shared office space with during my final year, and who helped me over the last hurdle. I would also like to thank Nalas Engineering for taking me on a four month placement and who helped shape my career path.

Thanks are also given to the many people who helped with analytical support; Dr Lorna Murray and Mr Juraj Bella with NMR spectroscopy, Long Chen and Dr Barnaby Greenland for DSC measurements and the McKeown group for allowing use of their TGA machine. Thanks to Jordann Wells, Dr Johann Hilna and Professor Polly Arnold for catalyst synthesis. The work in this thesis could not be done without all their help.

Lastly, I would like to thank my family and friends who have always believed in me and provided kind and supportive words during stressful times. In particular, I would like to thank Dan for making my PhD experience unforgettable. His patience and understanding is unparalleled and he made the hard days easier. We shared many adventures and he kept me smiling the whole way, I could not have done this without him.

Table of Contents

List of Abbreviations

°C	degree Celsius
3-BL	3-bromomethylenated lactide
3-HL	3-hexenyl lactide
3-HHL	3-hydrogenated hexenyl lactide
3-ML	3-methylenated lactide
β -BL	β-butyrolactone
β-HL	β-heptenolactone
β-VL	β-valerolactone
β-HAL	β-heptanolactone
μL	microliters
ADMET	acylic diene metathesis
ATBC	acetyl tri-n-butyl citrate
BnOH	benzyl alcohol
CM	cross-metathesis
ᵗBu	tertiary butyl
CL	caprolactone
CO	carbon monoxide
COSY	homonuclear correlation spectroscopy
Đ	dispersity
Da	daltons
dn/dc	differential index of refraction
DBU	diazabicyclo[5. 4.0]unde-7-ene
DCM	dichloromethane
DLC	diamond-like carbon
DML	dimethylenated lactide
DMAP	4-dimethylaminopyridine

DME	dimethoxyethane
DSC	differential scanning calorimetry
d	doublet resonance
EO	ethylene oxide
EtOAc	ethyl acetate
ESI	electrospray ionisation mass spectrometry
g	grams
GPC	gel permeation chromatography
HMBC	heteronuclear multiple bond correlation
HML	hexenyl-methylenated lactide
HSQC	heteronuclear single quantum correlation
h	hour
Hz	hertz
J	NMR coupling constant
LA	lactide
M_n	number average molecular weight
M_w	weight average molecular weight
MALDI	matrix assisted laser desorption ionisation
Mes	mesitylene
min	minutes
mL	millilitre
MML	mono-methylenated lactide
MMT	montmorillonite
mol	mole
mol%	mole percent
NaOH	sodium hydroxide
NHCs	N-heterocyclic carbenes
NMR	nuclear magenetic resonsance
P_r	probability of racemic linkages
P(3HB)	poly(3-hydroxybutyrate)

P(β-HL)	poly(β-heptenolactone)
PDLA	poly(D-lactic acid)
PEG	polyethyleneglycol
PFT	perflurotoluene
Ph	phenyl
PHB	polyhydroxybutyrate
PLA	poly(lactic acid)
PLLA	poly(L-lactic acid)
P(LA_{87}-co-β-HL_4)	poly(lactide$_{87}$-co-β-heptenolactone$_4$)
P(LA_{85}-co-β-HL_{19})	poly(lactide$_{85}$-co-β-heptenolactone$_{19}$)
PPh_2	triphenylphosphine
^{i}Pr	isopropyl
psi	pounds per square inch
q	quartet resonance
rac	racemic
RCM	ring-closing metathesis
ROMP	ring-opening metathesis polymerisation
ROP	ring-opening polymerisation
R.T	room temperature
$Sn(Oct)_2$	tin(II) 2-ethylhexanoate
t	triplet resonance
T_g	glass transition temperature
T_m	melting temperature
T_{max}	temperature at maximum weight loss
$T_{5\%}$	onset thermal degradation temperature
TBD	1, 5, 7-triazabicyclo[4. 4.0]dec-5-ene
TEG	triethylene glycol
TGA	thermal gravimetric analysis
THF	tetrahydrofuran
TMS	trimethylsilyl

Compound Abbreviations

In this thesis the following compounds have been given abbreviations due to their high appearance throughout a chapter. Other compounds appear as numbers.

Chapter 2 compounds and abbreviations:

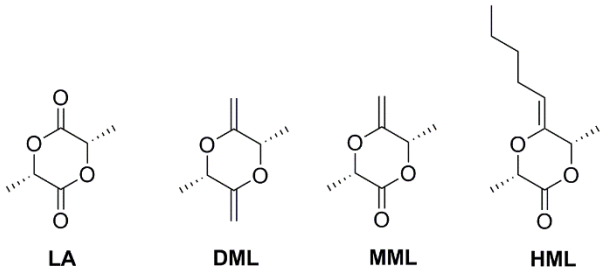

Chapter 3 compounds and abbreviations:

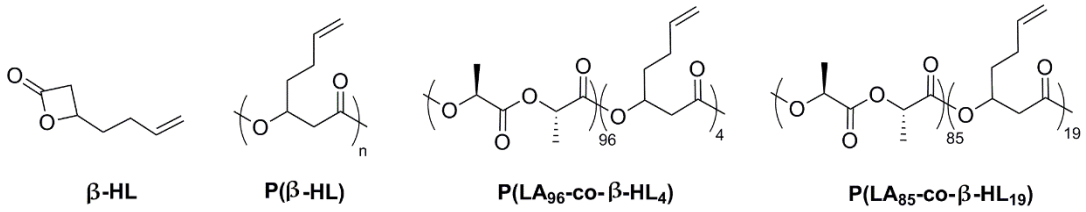

Chapter 4 compounds and abbreviations:

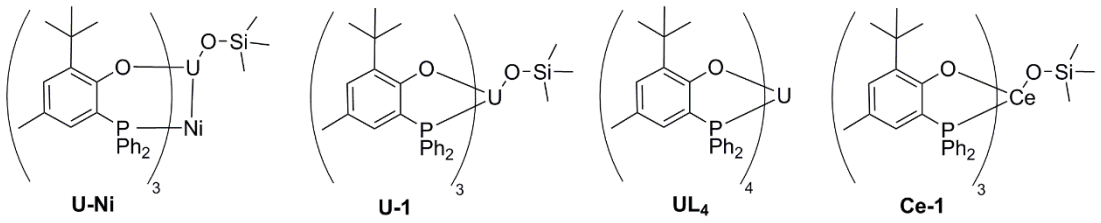

Publications

F. Sinclair, J. A. Hilna, J. A. L. Wells, M. P. Shaver and P. L Arnold, Ring opening polymerisation of lactide with uranium(IV) and cerium(IV) phosphinoaryloxide complexes. *Dalton transactions,* **2017**, 46, 10786-10790

F. Sinclair, M. Alkattan, J. Prunet and M. P. Shaver, Olefin cross metathesis and ring-closing metathesis in polymer chemistry, *Polymer Chemistry*, **2017**, 8, 3385-3398

F. Sinclair, L. Chen, B. W. Greenland and M. P. Shaver, Installing Multiple Functional Groups on biodegradable Polyesters via Post-Polymerisation Olefin Cross-Metathesis, *Macromolecules*, **2016**, 49, 6826-6834

"I have yet to see any problem, however complicated, which, when you looked at it in the right way, did not become still more complicated"

Poul Anderson

Chapter 1. Introduction

1.1 Polymers and sustainability

Polymers are essential to our lives, underpinning advances in material development for everyday commodity and speciality applications including plastics, textiles and medical devices. Petroleum-derived polymers dominate the world's polymer production, including a range of commercial polymers; poly(vinyl chloride), polystyrene, polyethylene and polypropylene. These polymers exhibit good thermal, physical and mechanical properties and their cost of production is low,[1,2] yet various factors are causing a shift in industry attention towards alternative feedstocks that reduce our dependence on petroleum resources. Declining oil and gas resources coupled with fluctuating feedstock prices enforce a need for alternative resources.[1,3] More pressing is the environmental implication of these persistent polymers that reside in landfills for many years. Renewably sourced biodegradable polymers offer a solution and attractive replacement to petroleum derived polymers. Biodegradable materials are ones which can degrade by the presence of naturally occurring microorganisms.[4] Bio-based polymers are prevalent in nature and can be produced from genetically modified bacteria, such as poly(hydroxyalkonates), or extracted directly from natural raw materials for example polysaccharides and proteins.[1] Despite their prevalence, matching the properties of petroleum-based polymer remains a challenge. An alternative option is to chemically synthesise biodegradable polymers derived from renewable feedstock, to allow flexibility and control over the material properties.

1.2 Poly(lactic acid)

1.2.1 Lactic acid and poly(lactic acid) production

Poly(lactic acid) (PLA) is emerging as a viable replacement for petroleum derived materials. It is a high modulus thermoplastic that is both biodegradable and

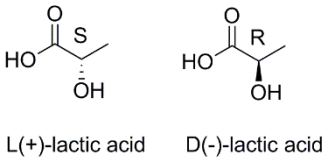

L(+)-lactic acid D(-)-lactic acid

Figure 1.1 *Two enantiomers of lactic acid L(+)- and D(-)- lactic acid.*

bioassimilable.[5,6] It is derived from lactic acid, a renewable resource derived from plants such as corn. Lactic acid exists as two enantiomers, L(+)- and D(-)- lactic acid, where the former is the most prevalent in nature (**Figure 1.1**).[5–7] 90% of the worldwide production of lactic acid is performed *via* the bacterial fermentation of carbohydrates, which favours a selected isomer dependent on the organism used.[6,7]

Two major routes exist for the synthesis of PLA starting from lactic acid: polycondensation and ring-opening polymerisation (ROP). Polycondensation involves reaction of the hydroxyl and carboxylic acid entities of lactic acid and is normally carried out in the melt. Removal of water formed during the condensation is critical to drive the reaction towards polymer formation. To aid this, polymerisation is carried out under vacuum at high temperatures, however, unwanted transesterification can lead to the formation of ring structures, the smallest of which is lactide. Transesterification is most prominent at temperatures >200 °C, thus reaction temperatures are kept below this but at the expense of a reduced reaction rate.[8] Consequently, achieving high molecular weight PLA is difficult *via* polycondensation and normally chain extension is used to increase the overall molecular weight.[6,8] Similarly, polycondensation in solution using azeotropic dehydration is another route to yield PLA with the added advantage of achieving higher molecular weight polymers with easier water removal.[1,8] However, extra labour intensive steps are required and the boiling point of the solvent restricts the reaction temperature.[8] The various routes to PLA production are shown in **Scheme 1.1**.

The industrially significant route to PLA synthesis is *via* ROP of lactide. This route can be separated into three stages; polycondensation to form low molecular weight oligomers, lactide formation *via* depolymerisation, and finally ring-opening polymerisation to yield high molecular weight PLA (**Scheme 1.1**).[8] From an environmental stand point the main advantages of PLA manufacturing compared to petroleum derived polymers are firstly, the overall net CO_2 production is negative, giving rise to positive implications on global warming and secondly the associated reduction in landfill waste.[1,9] PLA can either degrade

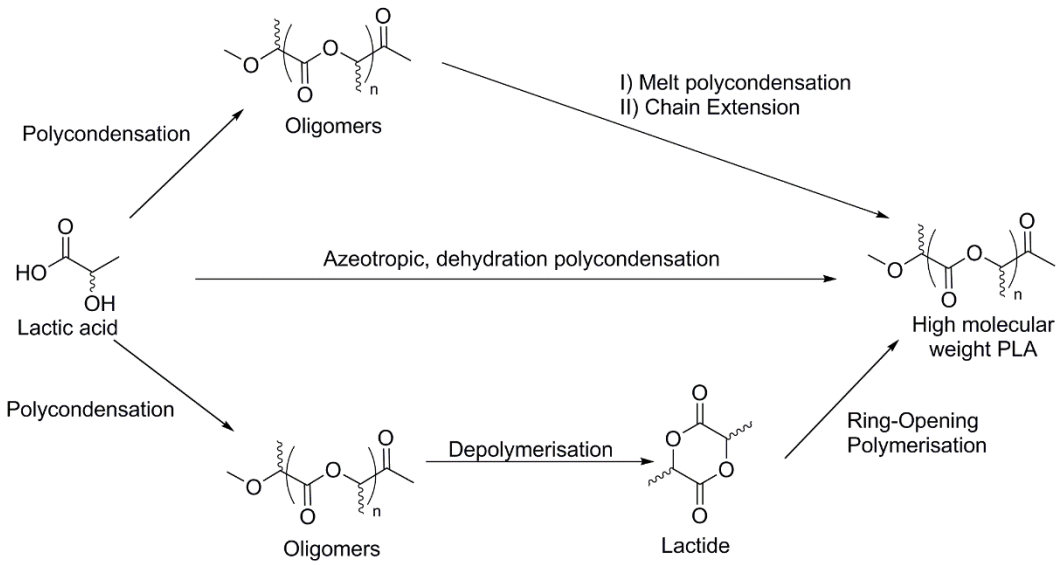

Scheme 1.1 *Synthetic routes to PLA: polycondensation, azetropic polycondensation, and ring-opening polymerisation.*

to CO_2 and H_2O in the presence of microorganisms at elevated temperatures (~60 °C), or it can be recycled *via* the depolymerisation to lactide or hydrolysis to lactic acid.[1,7,10] ROP is favoured compared to polycondensation as it can provide high molecular weight polymers with tuneable and controllable microstructures based on the lactide feedstock.

1.2.2 Ring-opening polymerisation and tacticity

The two enantiomers of lactic acid give rise to three stereoisomers of lactide; L-(S,S), D-(R,R) or meso- (S,R) lactide (**Figure 1.2**), formed from either depolymerisation of two identical enantiomeric lactic acid units or in the case of meso-lactide, depolymerisation of two opposite enantiomeric lactic acid units. Consequently, homopolymerisation, copolymerisation and blends of the diastereomers can give rise to stereoregular polymers of differing tacticities and properties based on the chirality of the repeating units

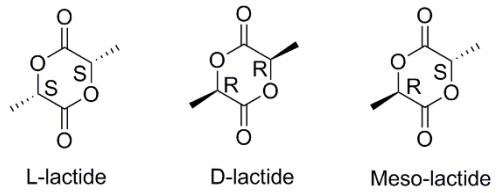

Figure 1.2 *Three stereoisomers of lactide.*

Figure 1.3). Polymerisation of enantiopure L- or D- lactide gives rise to isotactic poly(L-lactic acid) (PLLA) and poly(D-lactic acid) (PDLA) respectively, where all the chiral centres in the repeat units are identical (either (S) for PLLA or (R) for PDLA). These structures are semi-crystalline with a glass transition temperature (T_g) between 60-70 °C, and a melting temperature (T_m) in the range of 170-180 °C.[5,11] Syndiotactic PLA contains alternating chiral centres (-SRSR-) and is formed from polymerisation of meso-lactide if ring-opening occurs at the same chiral centre. Syndiotactic polymers tend to have lower T_m's ~150 °C.[12] However, if no chiral preference exists, random amorphous, atactic PLA is formed. Rac-lactide, a 1:1 mixture of L- and D- lactide, offers routes to various stereoregular structures. If the catalyst has no chiral preference then an amorphous atactic polymer is formed.[6] Otherwise, an alternating preference of L- and D- lactide can result in heterotactic (-SSRRSS-) PLA, which is typically amorphous.[12] Alternatively, rac-lactide can produce isotactic-stereoblock PLA which contains repeating blocks of chiral centres (-RRRRRSSSS-) with a typically higher T_m than isotactic PLA.[13] However, the highest T_m is observed with sterecomplex isotactic PLA with a T_m of between 220-230 °C.[3,14] This polymer is formed from a 1:1 mixture of isotactic PLLA and PDLA. Thus, changing the tacticity of PLA can substantially alter the properties of the resulting polymer, which is dictated largely by the choice of catalyst.

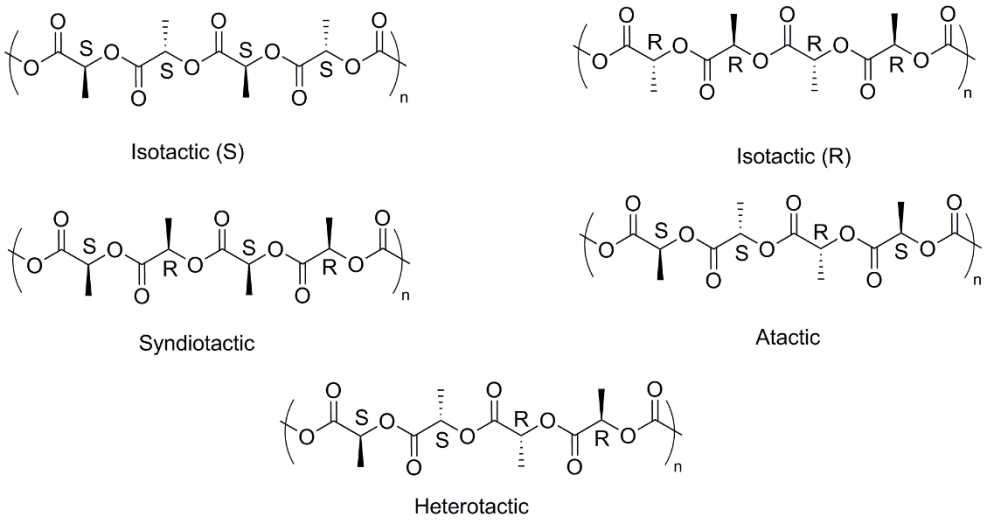

Figure 1.3 *Different tacticities of PLA: isotactic, syndiotactic, atactic and heterotactic.*

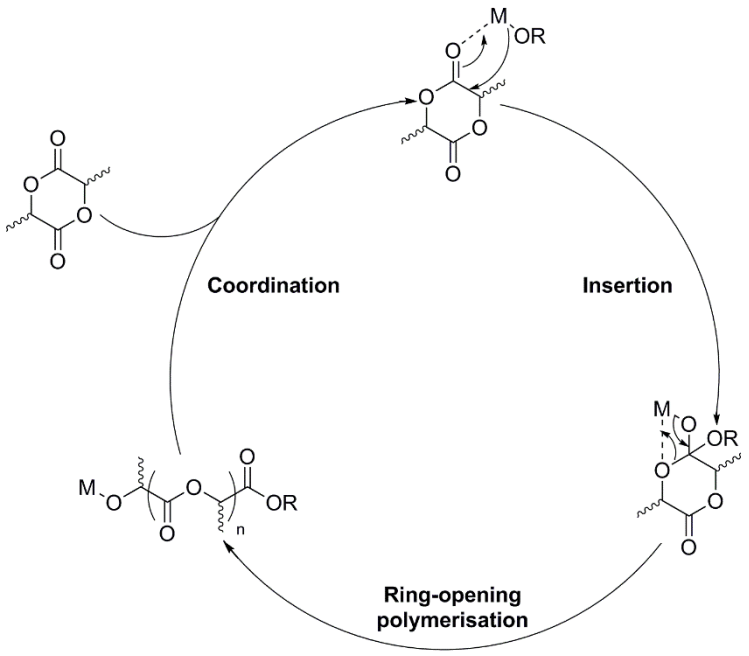

Scheme 1.2 *Coordination insertion mechanism for the ROP of lactide.*

The mechanism for coordination-insertion is shown in **Scheme 1.2**. The reaction proceeds *via* coordination of lactide to a typical Lewis acidic metal alkoxide. The monomer then inserts into the metal-alkoxide bond and then undergoes acyl-bond cleavage to generate a linear growing chain, which acts as a new metal alkoxide to propagate further coordination insertion. The polymerisation is terminated by a large excess of a protic source, to form hydroxyl terminated PLA.

A range of metal alkoxides have been reported for ROP of lactide with retention of configuration to yield isotactic or atactic PLA.[15–17] Of the most explored complexes for stereocontrolled polymerisation of lactide are the aluminium salen species. Spassky designed an enatiomerically pure chiral aluminium salen complex for the kinetic resolution of rac-lactide (**1**, **Figure 1.4**). This catalyst displayed a 20:1 preference for D- lactide over L- lactide to generate a stereocomplex of PLA.[18] Coates *et al.* extended the work of this chiral catalyst using a bulkier alkoxide to afford highly syndiotactic PLA during the ROP of meso-lactide (**2**, **Figure 1.4**).[19] A rac-analogue, of this chiral complex **2**, produced heterotactic PLA in the presence of meso-lactide, which was proposed to occur *via* a polymer exchange mechanism between the catalytic chiral centres. Interestingly, applying **2** to rac-lactide enabled the formation of an isotactic stereoblock PLA (P_i = 0.98).[13] Similarly, Feijen *et al.* designed rac-chiral aluminium salen, **3**, **Figure 1.4**, for the synthesis

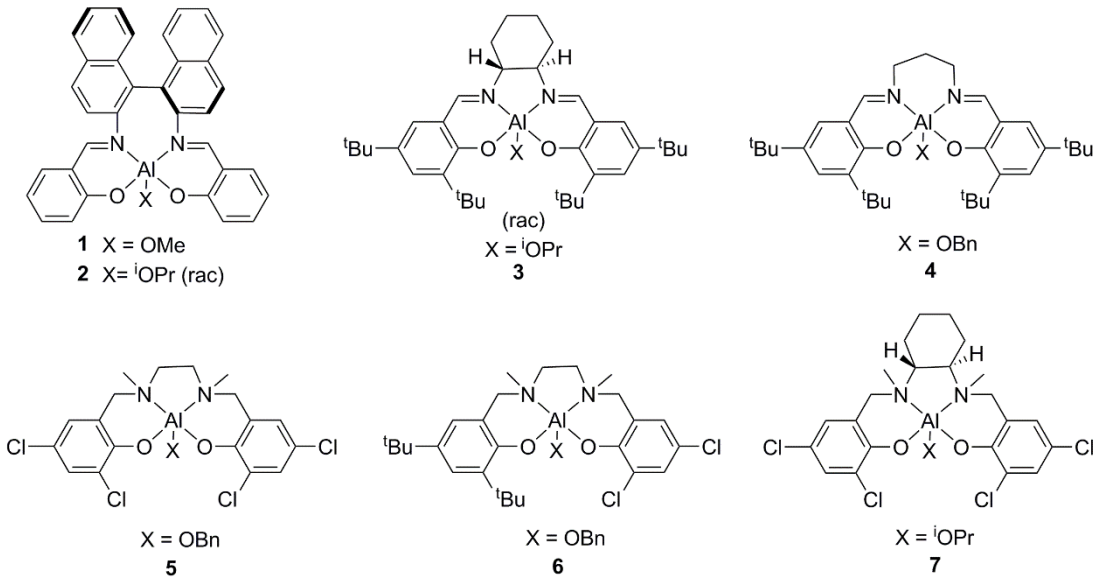

Figure 1.4 *Aluminium (salen) and (salan) complexes used in stereocontrolled ROP of rac-and meso-lactide.*[18-24]

of isotactic stereoblock PLA from rac-lactide, which demonstrated a 14:1 preference for L -lactide over D-Lactide (P_i = 0.93).[20]

These examples discussed exemplify enantiomorphic site control where stereoselectivity is dictated by ligand chirality. Alternatively, chain-end-control can be used to direct stereoselectivity, whereby the stereogenic centre of the last repeating unit in the propagating chain can determine the insertion of an incoming monomer. This route is more financially attractive due to elimination of expensive chiral ligands. Gibson *et al.* compared the stereocontrol imparted by a library of Al(salen) catalysts for the ROP of rac-lactide.[21] It was discovered that a long, flexible amine bridge along with bulky phenoxy substituents favoured an increase in isotacticity as seen with complex **4**, (**Figure 1.4**) P_i = 0.88.

Structurally similar but less explored than the aluminium salen complexes are the aluminium salan complexes. Gibson *et al.* were the first to report this new family of aluminium ROP catalysts.[22] Through altering phenoxy substituents it was found unsubstituted phenoxides promoted high isoselectivity, while inclusion of substituents switched the tacticity to a heterotactic bias. Chloro-functionalised phenoxides led to the highest heterotacticity (P_r = 0.96) (**5**, **Figure 1.4**). Following, Hormnirun synthesised the first asymmetric aluminium salan complexes which contained one phenolic ring with tert-butyl substituents and a second ring with varied substituents.[23] Again, chloro-

functionalised analogues gave the highest heterotacticity (**6**, **Figure 1.4**). The first polymerisation of meso lactide using an aluminium salan catalyst was carried out by Feijen *et al.*[24] They used chiral aluminium salan complex **7 (Figure 1.4)**, which yielded syndiotactically biased PLA (P_r = 0.70).

Alternatively, organocatalysts can be used in the ROP of lactide. However, due to high reactivity's, susceptibility to racemization and transesterification tends to be high,[7] thus more control over polymer microstructure is generally attained with the use of specially designed metal catalysts. Tin 2-ethylhexanoate ($Sn(Oct)_2$) is used for commercial production of PLA but issues with transesterification and lack of stereocontrol warrant continued research into new initiators for the ROP of lactide.[25,26]

1.2.3 Applications of poly(lactic acid)

The market leader in PLA is NatureWorks®, who have a large scale plant capable of manufacturing 140,000 metric tons per annum. While they are based in the USA, other PLA manufacturers are present in both Asia and Europe.[1] PLA has many commercial applications, promoted under the trademark Inego™ (NatureWorks®); it can be processed as fibres for use as clothes and pillows, either alone or as blends with cotton and wool,[27] it has a dominant presence in the plastic market, for use as bottles,[1] or as foam packaging for fresh food such as fruit, veg or deli meats.[28] Aside from commodity applications PLA is also used as a speciality polymer in the biomedical field due to its biodegradability and bioassimability, including its use in sutures, bone fixation, drug delivery and tissue engineering.[6,26] L-Lactic acid is a natural metabolite in the body thus PLLA is more commonly used in these applications. In the biomedical field PLA is often copolymerised with other biocompatible monomers such as glycolide and ethylene oxide to generate Poly(lactic-co-glycolic acid) and poly(lactic acid)-poly(ethylene glycol) copolymers respectively.[3,6,29] Although PLA has an established commercial prevalence, it has limitations. Current short comings include low thermal resistance, poor toughness, brittleness and poor gas barrier properties. These drawbacks make PLA processing difficult and narrows the end application scope.

1.2.4 Modification of poly(lactic acid)

Current strategies exist to overcome these drawbacks and continued research is still ongoing in both science and engineering to enable PLA to be a viable competitor to rival petroleum based polymers. To improve thermal stability and strength, PLA nanocomposites are synthesised. Work has been carried out using clay nanocomposites such as montmorillonite (MMT). Both Ogata *et al.* and Lee *et al.* demonstrated that PLA-organoclay nanocomposites from MMT demonstrate improved mechanical and thermal properties with an associated increase in Young's modulus and heat resistance.[30–33] More recently, Gui *et al.* demonstrated that the use of co-modified MMT not only improved the Young's modulus and thermal resistance of PLA nanocomposites but also its fire resistance was enhanced.[34]

PLA blends can increase the flexibility of the polymer. Examples include non-biodegradable blends such as poly(lactic acid)/polystyrene and biodegradable blends such as poly(lactic acid)/poly(caprolactone). However, miscibility with the blended polymer is not always easy.[33]

The limiting factor restraining PLA to cold temperature food packaging is its low gas barrier properties, which allow oxygen penetration through the plastic, which can affect the lifetime of food. A method to counteract this is to use diamond-like carbon (DLC) films as a surface coating. DLC films exhibit high gas barrier properties, high recyclability and high biocompatibility.[36]

To improve the inherent brittleness of PLA, plasticisers have been used to lower the T_g and increase the elasticity.[37] Small molecules such as lactic acid can be used as a plasticiser but these molecules risk evaporation during melt processing making them unattractive for end use applications.[37] Jacobsen and Fritz *et al.* demonstrated polyethylene glycol (PEG) can successfully act as a plasticiser and successfully increase the elongation at break thus generating a more elastic PLA.[38] Baiardo *et al.*, investigated the use of acetyl tri-n-butyl citrate (ATBC) and PEG as plasticisers for PLA and concluded that an increase in plasticiser content leads to a reduction in T_g with an increase in elongation at break but at the expense of a decrease in stiffness.[39]

A powerful alternative to physical modification, is chemical modification of PLA *via* copolymerisation.[37] Besides the most common copolymers of PLA and PEG, discussed previously for biomedical applications, lactone-type monomers have been a popular choice. Linear random copolymers of lactide (LA) with caprolactone (CL) generate poly(CL-co-LA) and dependent on both monomer ratio and enantiomer of lactide, polymers with various properties can be made.[40,41] Abadie *et al.* designed a new approach to generate diblock structures of LA and CL with each block being randomised itself to generate an elastomer.[42] Synthesis of star and linear block copolymers have been reported to toughen PLA including the work of Grijpma *et al.* They prepared block copolymers using a multifunctional initiator to generate star shaped AB or ABA block copolymers of LA with CL and β-methyl-δ-valerolactone.[37] Polyhydroxybutyrate (PHB) is another key player as a popular alternative to petroleum derived plastics and its copolymers with lactide are discussed later in Chapter 3. Telechelic polymers, that contain reactive end-groups capable of further polymerisation/modification, represent another route to modify the properties of PLA.[43,44] Moreover, graft copolymers and cross-linked copolymers of PLA have been shown to increase elongation and strength with respect to neat PLA.[37,45,46]

PLA does not possess reactive side-chain functional groups, consequently modification of the backbone through chemical transformations is a challenge. Only a handful of reports exist on pre-polymerisation modification of lactide, which will be discussed in Chapter 2.

1.3 Olefin metathesis

1.3.1 Mechanism of olefin metathesis

Synthetic chemistry drives development and advancement in new medicines, biology and materials. At the core of synthetic chemistry is catalyst discovery and catalytic olefin metathesis is a powerful and popular tool in organic synthesis. Carbon- carbon bond formation is one of the most useful transformations in organic synthesis. The word metathesis derives from Greek, meaning to "change position," thus olefin metathesis can be described as the rearrangement of carbon-carbon double bonds. The discovery of

olefin metathesis, its mechanistic understanding and the development of the robust catalysts used today stretches over six decades.

The first report of olefin metathesis dates back to 1931 when the pyrolysis of propene at 852 °C led to ethene and 2-butene.[47] In 1960, catalytic olefin metathesis was successfully utilised and Eleuterio observed the polymerisation of norbornene using $WCl_6/AlEt_2Cl$.[48] Catalytic olefin metathesis made a big step forward in 1964 due to three important discoveries. Firstly, scientists Bank and Bailey published the disproportionation of propene to ethene and 2-butene using a heterogeneous system- Molybdenum (metal, oxide, or $Mo(CO)_6$) supported on alumina.[48] Secondly, Natta disclosed homogeneous polymerisation of cyclopentene using tungsten or molybdenum halides[49] and thirdly, Fischer introduced the existence of a new metal- carbon bond- carbenes.[50] Although these discoveries appeared unrelated, they were the foundation that led to the now accepted mechanism of olefin metathesis. Yves Chauvin recognised that both disproportionation and ring-opening polymerisation were a result of the same mechanism and set out to investigate its pathway.[51] Calderon also identified the link between these two reactions and in 1967 coined the term "olefin metathesis."[48] Attention turned to understanding the mechanism of this mysterious transformation and in this same year Bradshaw proposed the formation of a cyclobutane-metal intermediate, which was supported by Calderon.[52,53] In 1971, Pettit suggested an alternative tetramethylene complex intermediate[54] and in 1972 Grubbs hypothesised a re-arranging metallacyclopentane intermediate.[55] These pairwise mechanisms shown in **Scheme 1.3** were incorrect as they could not account for the product distributions observed during olefin metathesis.[51,56] However, in the same year as Pettit, 1971, Yves Chauvin presented his hypothesis that was often overlooked in the literature. His mechanism proposed a metal carbene-complex initiated catalysis, through a metallacyclobutane intermediate.[51] Experimental evidence to support his theory was found in the metathesis of cyclopentene with 2-pentene using $WOCl_4/AlEt_2Cl$ to give C_9, C_{10} and C_{11} products (**Scheme 1.4**). This result disproved a pairwise mechanism, which would only produce the C_{10} product.

Following, Chauvin and other scientists Casey, Burkhardt, Katz, Grubbs and Schrock all provided further experimental evidence in support of his carbene mechanism.[51,57–59] However, it was Richard Schrock that made a monumental breakthrough in catalyst development. In 1980 Schrock synthesised the first active metal-alkylidene for olefin

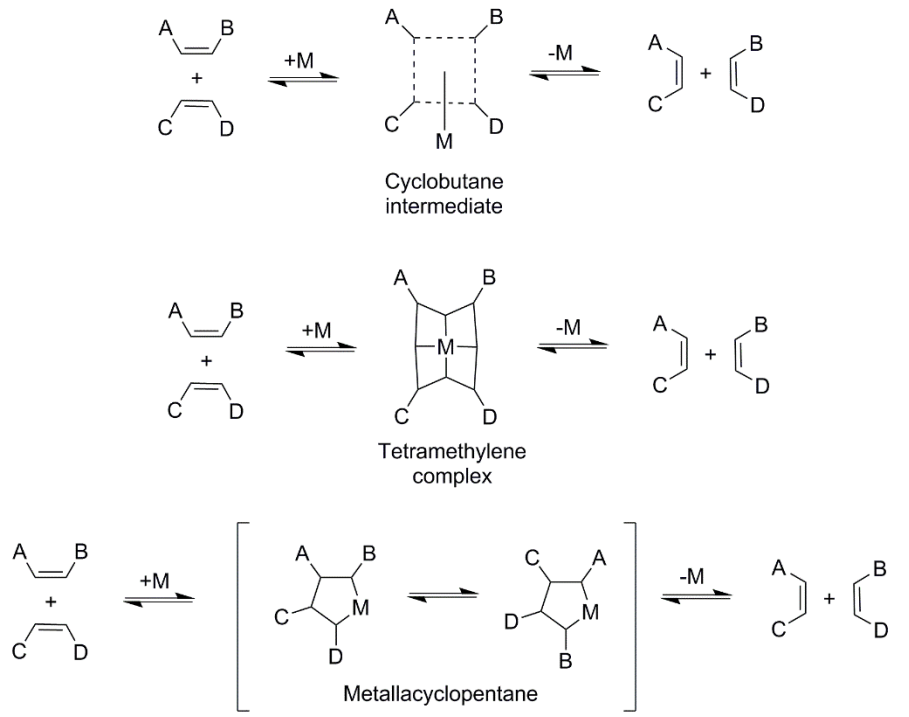

Scheme 1.3 *Incorrect mechanisms proposed for olefin cross-metathesis: cyclobutane, tetramethylene and metallacylopentane formation.*[52-55]

metathesis, [Ta(=CH-*t*-Bu)(Cl)(PMe_3)(O-*t*-Bu)$_2$], which provided the first real evidence for Chauvin's mechanism.[60] In that same year Grubbs isolated a metallocylobutane using the Tebbe reagent and 3-methyl-1-butene, to provide the first proof of the existence of this intermediate.[61]

The now accepted mechanism of olefin metathesis is illustrated in **Scheme 1.5**. The reaction involves a [2+2] cycloaddition between a transition metal carbene and an olefin

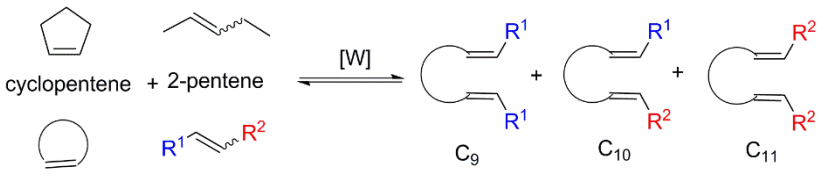

Scheme 1.4 *Olefin cross-metathesis of cyclopentene with 2-pentene to produce a product mixture which disproves a pairwise mechanism.*

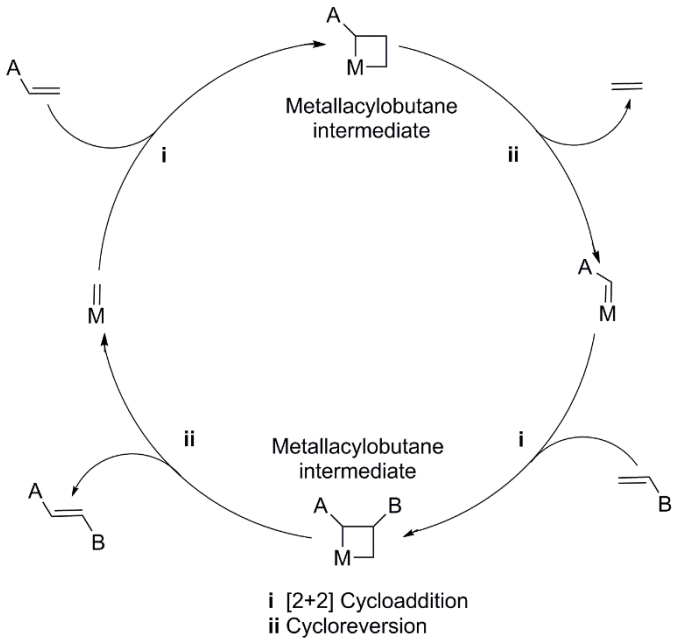

Scheme 1.5 *The mechanism for olefin CM, proposed by Chauvin involving a metal carbene and a metallacylcobutane intermediate.*

to yield a metallacyclobutane intermediate which undergoes cycloreversion to release a new olefin and a new metal carbene that re-enters the catalytic cycle.

1.3.2 Development of olefin metathesis catalysts

With the mechanism of olefin metathesis established, rationale catalyst design was fundamental to the success and scope of the reaction. While many scientists contributed to catalyst development, Schrock and Grubbs undisputedly led the efforts to design the catalysts that have allowed the capacity of olefin metathesis to be recognised.

Schrock, the pioneer in olefin metathesis catalysts, centred his research on the optimisation of tungsten and molybdenum alkylidenes. Early tungsten catalysts contained oxo ligands, and were active as cationic 16 e- species in the presence of Lewis acids (**8**, **Figure 1.5**).[48,62,63,64] It was soon identified that oxo ligands were not bulky enough to suppress bimolecular decomposition that led to the limited activity of these catalysts.[65] Imido ligands thus replaced oxo ligands alongside chloride replacement with alkoxides to produce a library of stable, 4-coordinate, 14 e- W and Mo alkylidene catalysts.[65] Optimisation led to the development of **9**, **Figure 1.5**, known today as Schrock's

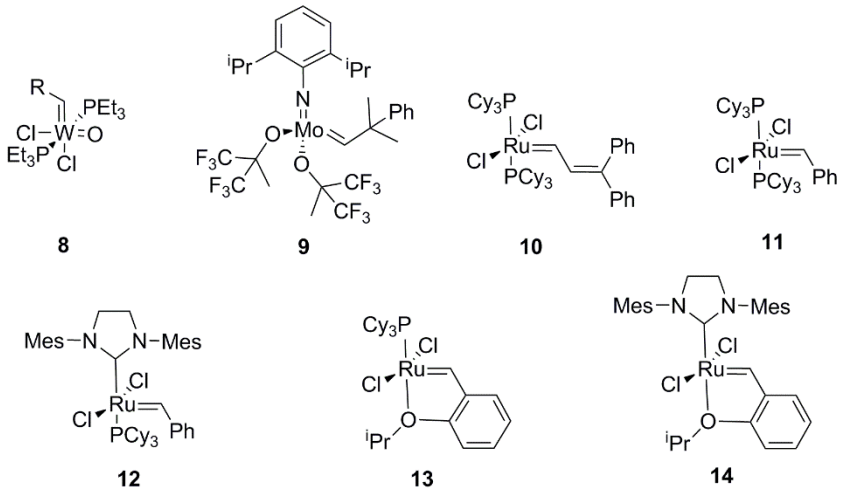

Figure 1.5 *Development of olefin metathesis catalysts of tungsten, molybdenum and ruthenium.*[64,65,71,72,77-79]

catalyst.[65,66] The activity of this catalyst can be attributed to careful iterations in the ligand framework. Electron withdrawing alkoxide groups increase the electrophilicity of the metal centre and strengthen the Mo-N bond, while steric bulk of both the imido ligand and the alkoxide groups effectively stabilise an electron deficient metal centre.[65] The high oxidation state Mo(VI) generates a nucleophilic carbene and a highly active metathesis catalyst. However, the high oxophilicity of molybdenum makes Schrock's catalyst highly sensitive to oxygen and moisture, consequently it must be handled under Ar/N_2 using dry solvents and substrates.[65] Moreover, its sensitivity limits its substrate scope. Metals on the left hand side of the periodic table react preferentially with acids and alcohols while metals on the right hand side react preferentially with olefins.[67] One such metal that has a preference for olefins is ruthenium.

Although now the preferred choice of metal for olefin metathesis, ruthenium was not always an obvious choice. The potential of ruthenium was unlocked by Grubbs, whose interest in polymeric materials led to the development of Ru(II) salt catalysts for ring-opening metathesis polymerisation. These catalysts showed unexpectedly high activity in water, showcasing the robust nature of Ru to aqueous medium.[68,69] However, only a small percentage of the ruthenium was active and the structure of the active species was unknown making optimisation difficult. Following on from Schrock's breakthrough, Grubbs aimed to synthesis the first well-defined active Ru-carbene and in 1992 he successfully achieved this.[70] This catalyst was limited to ROMP of low-strained monomers but it provided the scaffold for further design, and based on ligand rationale established

by Schrock, Grubbs attempted to mimic the same trends with ruthenium. Unexpectedly, the use of less basic phosphine ligands resulted in a decrease in activity.[67] While Schrock observed an increase in activity with more e- withdrawing groups, Grubbs observed the opposite trend and instead larger and more basic phosphines increased activity. Thus, replacement of PPh_3 with PCy_3 produced the first Ru-catalyst that was active for the metathesis of acyclic olefins (**10**, **Figure 1.5**).[71] Ruthenium was able, to perform the same olefin metathesis transformations as molybdenum except on a bench. Difficulties in large scale synthesis of catalyst **10** led to the formation of Grubbs 1st generation catalyst **11**, **Figure 1.5**. [72] Low oxidation state Ru(II) has a preference for soft Lewis-bases and Lewis acids (eg. olefins), over harder bases such as oxygen, accounting for its tolerance to air and water and preference to olefin functional groups. It is also able to initiate metathesis in the presence of alcohols and carboxylic acids and represents a milestone in the development of metathesis catalysts.[67,73] Compared to Schrock's active 14 e- species Grubbs' catalyst exists as a stable 16 e- complex which requires loss of one of the neutral ligands to generate the active 14 e- species. This initiation step is dependent on the ligand environments. Sterically bulky, electron rich, neutral ligands promote phosphine dissociation and stabilise the 14 e- intermediate.[67] On the other hand, smaller electron withdrawing halogens increase olefin coordination due to the trans-influence.[67] In 1998, Hermann introduced a new ligand set into the framework and replaced both phosphine ligands with N-heterocyclic carbenes (NHCs) but this resulted in slightly lower catalyst activity than **11**.[74,75] Based on Herrmann's work, in 1999 Grubbs produced mono-substituted derivatives and replaced only one of the phosphines with a NHC to generate Grubbs 2nd generation catalyst (**12**, **Figure 1.5**).[76,77] NHC's are bulkier, stronger σ- donors and less labile than phosphines, producing a more active metathesis catalyst.[67,74]

Later in 1999, Hoveyda synthesised the first recyclable metal-based homogenous olefin metathesis catalyst, Hoveyda-Grubbs 1st Generation catalyst (**13**, **Figure 1.5**), which contained an internal oxygen chelate and was based on Grubbs 1st Generation catalyst.[78] A year later this catalyst was soon optimised by replacement of the phosphine with an NHC to generate Hoveyda-Grubbs 2nd generation catalyst (**14**, **Figure 1.5**).[79]

Schrock, Grubbs and Hoveyda provided the groundwork for olefin metathesis active catalysts and variations in ligand environment has seen a multitude of versions of Mo and Ru metathesis catalysts emerge, including chiral catalysts for tacticity control in ROMP,

asymmetric ring-closing metathesis and asymmetric ring-opening metathesis (ROM).[65,80–82]

1.4 Olefin cross-metathesis

Olefin metathesis represents an umbrella for a series of transformations; cross metathesis (CM), ring-opening metathesis (ROM), ring-closing metathesis (RCM), ring-opening metathesis polymerisation (ROMP) and acyclic diene metathesis (ADMET). The latter three are well recognised in the realm of polymer chemistry offering routes to polymerisation and control over polymer architectures[83–86] while the former two, CM and ROM, have found dominance in small molecule synthesis.[87,88] Metathesis reactions are reversible requiring a thermodynamic driving force to prevent statistical mixtures of starting materials and products being produced. In the case of CM, RCM and ADMET, evolution of the volatile ethylene gas by-product, formed during the metathesis, shifts the equilibrium in favour of the products as in accordance to le Chatelier's principle. Alternatively ROM and ROMP capitalise on ring strain and the associated energy release as a favourable driving force. Of the aforementioned olefin metathesis reactions olefin CM is the least explored mainly due to challenges with selectivity. Grubbs devised an empirical model to help overcome this problem and aid in the design of selective CM.[89]

The model categorises olefins based on their ability to homodimerise (react with themselves) and the ability of the formed homodimers to participate in a second CM reaction. Four categories exist, ranging from very active to inactive olefins (**Scheme 1.6**). Type I olefins are the most active in CM and undergo fast homodimerisation; the homodimers formed are readily able to participate in a second CM reaction. Type II olefins undergo slow homodimerisation, with the homodimers formed only sparingly consumed in secondary metathesis. Type III olefins are the least active and are unable to homodimerise but can react with olefins of a different type (I or II). The final category, Type IV olefins, are inert to CM but with no de-activation of the catalyst.

Electronic and steric factors influence olefin categorisation. To generalise, electron rich, sterically unhindered olefins are the most active and are categorised as Type I olefins such as 5-hexenyl acetate and hex-1-ene. At the other extreme, electron-deficient, sterically hindered olefins are inert to CM and can be categorised as inactive Type IV olefin such

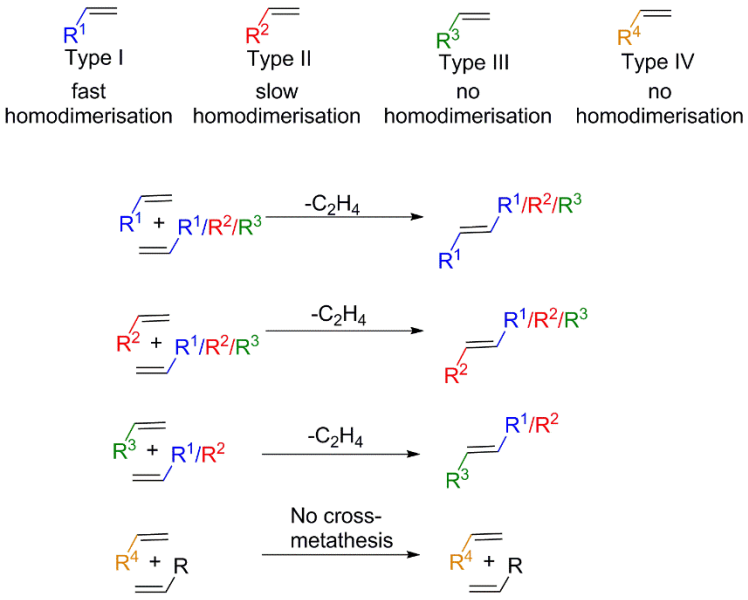

Scheme 1.6 *Olefin Type categorisation (Type I, II, III or IV) and reactivity.*

as vinyl nitro olefins and tri-substituted allyl alcohols. A gradient of reactivity exists within each category and the key to achieving selective CM is to react olefins from different categories, where there is no competition between the rates of homodimerisation. To elaborate, CM between a Type I olefin and a Type II olefin should lead to selective CM (**Scenario 1**, **Scheme 1.7**). The rate of homodimerisation of the Type II olefin is slow and will preferentially react with the Type I olefin instead (**Scenario 2**, **Scheme 1.7**). Conversely, the rate of homodimerisation of the Type I olefin is fast and will afford a new olefin that is able to participate in secondary metathesis with the Type II olefin to provide

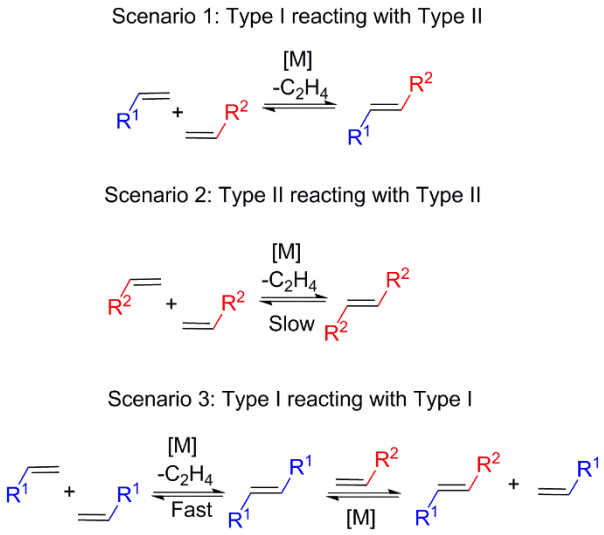

Scheme 1.7 *Selectivity in olefin cross-metathesis: reaction of a Type I olefin with a Type II olefin.*

an alternative pathway to the desired cross-product (**Scenario 3**, **Scheme 1.7**). Consequently, selective CM in the presence of two different Type I olefins is challenging due to similar reactivity profiles. Normally this reaction results in a statistical product mixture that requires a large excess (~10 times) of one of the cross partners. In CM reactions an excess of the less reactive reagent is routinely used to promote selective CM.

Catalyst development is largely responsible for the increase in scope of cross-partners available for CM. In particular, the introduction of NHCs into Ru olefin-metathesis catalysts saw an expansion of available cross partners including acrylates, vinyl ketones, and those that were previously inactive such as 1,1-disubstituted olefins.[89]

1.4.1 Pre-polymerisation olefin cross-metathesis

CM is an established tool in small molecule transformations, yet few reports have exploited this methodology for monomer synthesis. Pre-polymerisation modification is an advantageous route as it produces fully functionalised polymers that are not always achieved *via* post polymerisation modification. Research into using CM for the generation of renewable fatty acids as potential precursors for step-growth polymerisation is abundant in the literature, including the work of Dixneuf, Brunea and Meier.[90–94] Nevertheless, only a handful of reports demonstrate pre-polymerisation CM followed by successful polymerisation to the functionalised polymer. Examples include the work of Cadiz *et al.* who in 2010 used olefin CM to functionalise vegetable oils with a phosphonate containing styrene derivative (**Scheme 1.8**).[95] This newly functionalised monomer was copolymerised with soybean oil and other styrene derivatives to produce vegetable oil

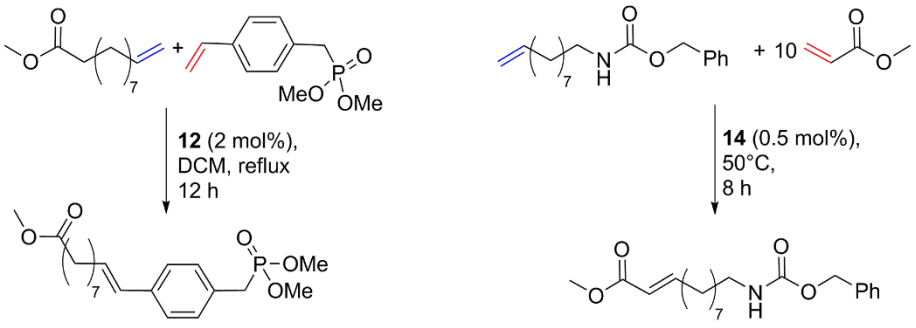

Scheme 1.8 *Pre-polymerisation olefin cross-metathesis. Left: work of Cadiz. Right: work of Meier and Winkler.*[95,96]

based thermosets with reduced flammability, a consequence of the inherent flame retardant properties of phosphonates. More recently, in 2014, Meier and Winkler *et al.* generated renewable polyamides by CM of a protected amine substrate containing a terminal olefin with methyl acrylate (**Scheme 1.8**).[96] This monomer was subsequently de-protected and polymerised to produce a polyamide matching the thermal performance of commercial polyamides.

1.4.2 Post-polymerisation olefin cross-metathesis

Alternatively, a more robust methodology is post-polymerisation CM. This route has been applied to a wide array of polymer backbones including end-group functionalisation[97,98] and cross-linking for self-healing polymers.[99,100] However, less work is observed in the functionalisation of polymer backbones which is of growing importance.[101–105]

The first example of this was in 2004, where Coates *et al.* functionalised alkene containing poly(olefins) of a Type I nature, with seven different olefins in order to modify the polymer properties (**15**, **Figure 1.6**).[101] The olefins included 4-penten-1-ol (Type I) to introduce polarity, ethyl acrylate (Type II) to add non-protic polarity and fluorinated acrylates (Type II) to increase phase separation. Incorporation of the acrylates resulted in the highest incorporation (>90 %).

In 2012, Hoogenboom and Meier *et al.*, used a "grafting onto approach," similar to earlier work by Kolbe and Meier,[106] to functionalise a renewably derived polymer, poly(2-oxazoline) (**16**, **Figure 1.6**).[102] This polymer, likely categorised as a Type I olefin, was reacted in a CM with various Type II acrylate cross partners. Optimisation of the reaction conditions led to >99 % functional group incorporation and identified that increasing either temperature or catalyst loading increased conversion, while a decrease in acrylate equivalents increased conversion. Moreover, dilute conditions favoured less self-metathesis and therefore minimised undesired polymer cross-linking. Additionally, they discovered that larger acrylates also minimise self-metathesis; bulky groups installed on the polymer chain hinder interaction between two separate chains, effectively preventing self-metathesis. Optimisation of reaction conditions including solvent, quantity of cross

partner, catalyst concentration and temperature is critical to achieve the highest conversion to cross-product and limit self-metathesis of polymer chains.

Grubbs' model of olefin categorisation is a general model to help aid with selectivity difficulties in CM, however, within each category there exists a gradient of reactivity. The work of Zedník *et al.*, in 2014, showcases this.[103] He investigated the CM between poly(5-vinyl-2-norborene) with an array of Type I olefin cross partners; cis-1,4-diacetoxybutene, 5-hexenyl acetate, allyl acetoacetate and allytrimethylsilane (**17**, **Figure 1.6**). Work of the previous authors discussed above led to high functional group incorporation, in particular CM in the presence of Type II acrylate cross partners. Selectivity is high in these cases because there is no competition between the rates of homodimerisation; the Type II acrylates, will preferentially react with the Type I polymers, as opposed to reacting with themselves. Conversely in the work of Zedník *et al.,* low incorporation (10-60%) is observed dependent on the cross partner used. In this work competition exists between the rates of homodimerisation and secondary metathesis of the Type I cross-partners and the Type I polymer. The highest degree of polymer functionalisation was observed with a 2-fold excess of cis-1,4-diacetoxybutene, while the lowest was seen with allyltrimethylsilane. In the former case the rate of homodimerisation of cis-1,4,-diacetoxybutene is slower than the rate of selective cross metathesis with the polymer, whereas in the latter case the preference of allyltrimethylsilane to homodimerise effectively inhibits CM functionalisation. The steric bulk of allyltrimethylsilane will also hinder polymer functionalisation. Thus, this work highlights the variation in individual reagent reactivity within an olefin category.

Polysaccharides that are derived exclusively from nature prevail in medical applications including drug delivery and antimicrobials.[107] Properties and thus applications of polysaccharides can be tuned by functional group incorporation. In 2014, Edgar *et al.* demonstrated the first successful olefin CM of an unsaturated cellulose ester with acrylic acid and later extended the scope to include acrylate cross partners (**18**, **Figure 1.6**).[104] The long linker between the cellulose backbone and the terminal olefin likely categorises this olefin as a Type I olefin, which in the presence of the Type II cross-partners led to complete functional group incorporation.

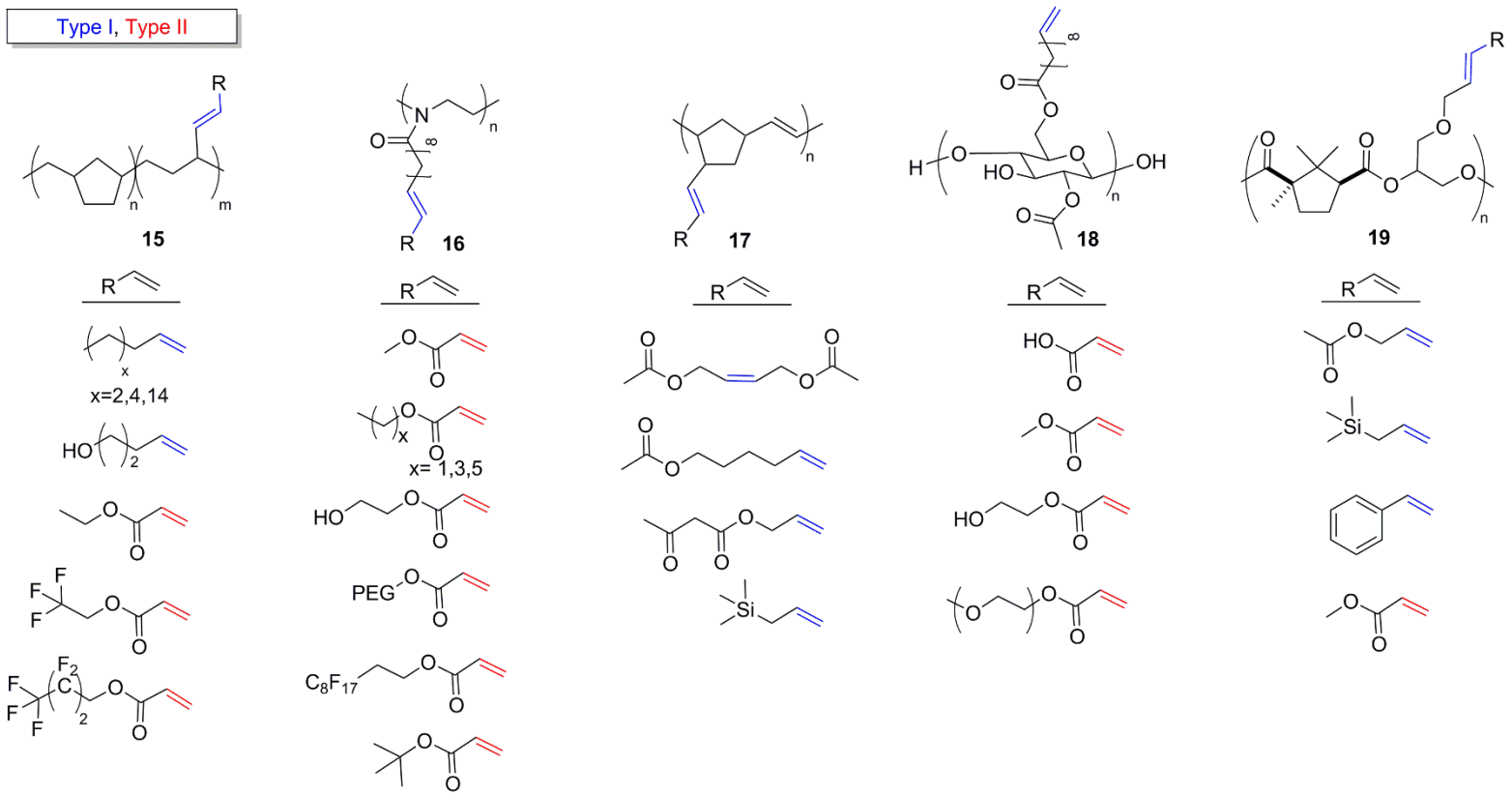

Figure 1.6 *Post-polymerisation olefin cross-metathesis. From left to right the work of Coates, Hoogenboom and Meier, Zedník, Edgar and Thomas and Prunet.*[101,102,103 105 107]

Most recently, in 2016, Thomas and Prunet *et al.*, reported the first modification of a polyester *via* olefin CM.[105] The authors synthesised four different copolymers of camphoric anhydride with various olefin containing epoxides that represented Type I, Type II and Type III olefins. They discovered that reacting the Type II and Type III olefin polymers with a Type I cross partner (allyltrimethylsilane) resulted in no selective CM. These polymers contained short pendent olefin arms which would generate a more sterically encumbered environment for the cross-partner to access. Alternatively, CM of the Type I olefin polymer with Type II, methyl acrylate, yielded high conversion (> 90%) with no traces of self-metathesis (**19**, **Figure 1.6**). The high reactivity of this polymer allowed the scope of the reaction to be expanded to include, Type I cross partners styrene, allyltrimethylsilane and allyl acetate. All functional group incorporations resulted in a substantial increase in the T_g of the resultant polymers.

CM can also be applied to the functionalisation of dendrimers. Although more commonly used in RCM strategies to generate new cyclic architectures,[108–110] dendrimers can act as an effective scaffold for CM reactions to introduce new functionalities into the polymer architecture. Dendrimers are spherical macromolecules containing a central core that are synthesised *via* two routes; divergent synthesis (the structure is assembled from a multifunctional core out) or convergent synthesis (the dendrimer is constructed from the periphery inwards with attachment to a central core). Literature exists that use CM as part of an iterative sequence to build dendrimers,[111] yet few examples exist that use CM to directly functionalise the polymer architecture.[112–114] The pioneer in dendrimer functionalisation *via* CM is Astruc, who constructed dendrimer **20**, (**Scheme 1.9**) and in a CM reaction with acrylic acid and methyl acrylate generated functionalised dendrimers **21a** and **21b** (**Scheme 1.9**).[112] As observed with CM reactions on aliphatic polymers, selective CM is achieved by limiting self-metathesis (cross-linking). In the case of dendrimer CM, competing self-metathesis results in RCM. To limit RCM, Astruc *et al.* lengthened the dendrimer tether *via* hydrosilyation to disfavour ring-closing due to the resultant ring size (**22**, **Scheme 1.9**). Water soluble poly(carboxylic acid) dendrimers and responsive dendrimers, *via* incorporation of ferrocenyl acrylates, were then able to be synthesised.[113]

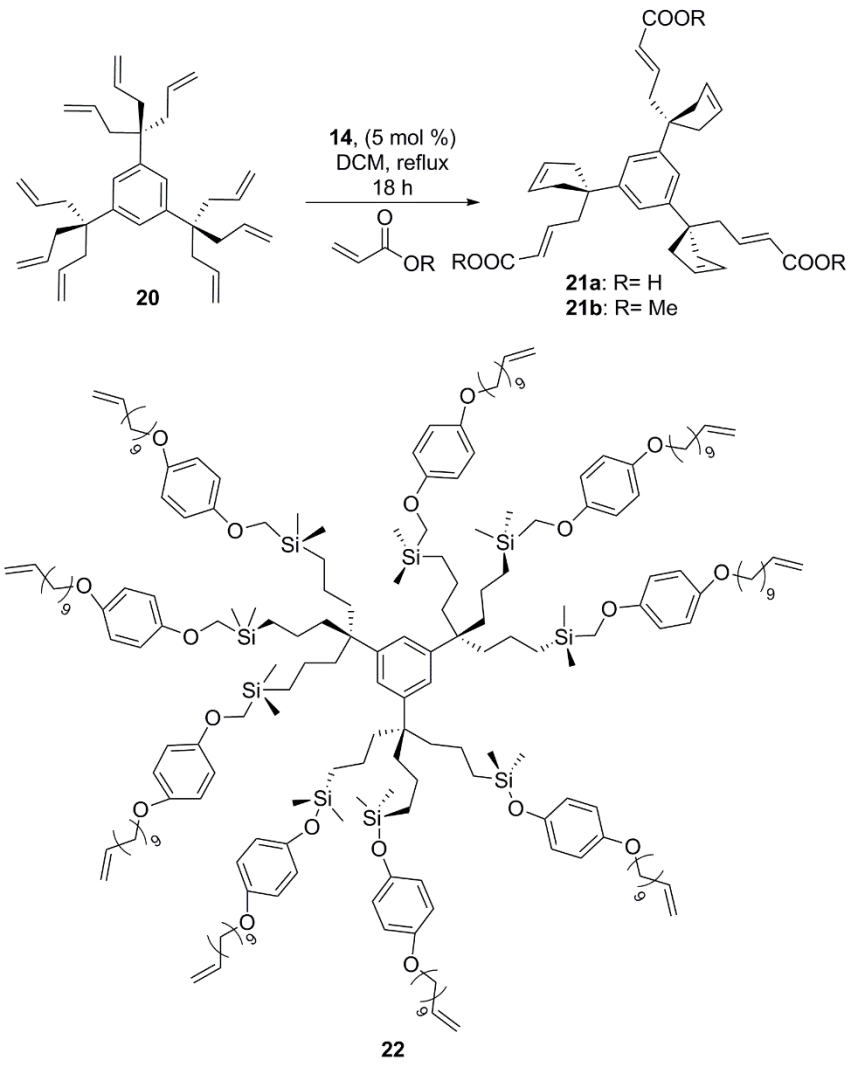

Scheme 1.9 *Olefin cross-metathesis of a dendrimer and a lengthened dendrimer tether via hydrosilyation.*[112,113]

1.5 Project aims

The overall aim of this research is to modify the thermal properties of poly(lactic acid) *via* chemical modification using olefin CM. A low T_g limits the expansion of PLA into applications involving high temperatures. Contrary, lowering the T_g further will improve the flexibility and reduce the inherent brittleness of PLA. Thus functional group incorporation was investigated to target tuning of the T_g while monitoring the corresponding effects on T_m and T_c. Chapter 2 is focussed on pre-polymerisation olefin CM. Methodologies to introduce olefin functionality into lactide were investigated. Olefin categorisation and substrate scope of these olefin monomers of lactide in CM reactions were explored. Degradation pathways for these monomers were monitored to gain further

understanding of their stability profiles. Finally, hydrogenation was studied and compared as a stabilisation tool prior to ROP with a selection of catalysts.

In Chapter 3, the suitability of biodegradable ester β-heptenolactone as a reactive olefin in CM reactions is explored. Olefin categorisation and substrate scope in CM reactions were investigated. Pre-polymerisation olefin CM was compared to post-polymerisation olefin CM as strategies to generate fully functionalised homopolymers. It was hypothesised that co-polymers of β-heptenolactone with lactide would allow for the modification of the properties of PLA *via* CM. An array of 15 different olefin cross-partners, ranging from Type I to Type III were used on two copolymers with different ratios of β-heptenolactone. Thermal properties of the functionalised copolymers were analysed *via* thermal gravimetric analysis and differential scanning calorimetry.

Lastly, Chapter 4 explores a collaborative project comparing uranium and cerium complexes in the ROP of lactide. It was hypothesised that the nature of these catalysts would produce different reaction profiles. Living and immortal polymerisations were compared for the two metal centres and kinetic studies were taken to gain further understanding into their mechanism of polymerisation. The influence these catalysts induced on the stereochemistry of PLA was also explored.

1.6 References

(1) Jamshidian, M.; Tehrany, E. A.; Imran, M.; Jacquot, M.; Desobry, S. *Compr. Rev. Food Sci. Food Saf.* **2010**, *9* (5), 552–571.

(2) Hopewell, J.; Dvorak, R.; Kosior, E. *Philos. Trans. R. Soc. B Biol. Sci.* **2009**, *364* (1526), 2115–2126.

(3) Madhavan Nampoothiri, K.; Nair, N. R.; John, R. P. *Bioresour. Technol.* **2010**, *101* (22), 8493–8501.

(4) Amass, W.; Amass, A; Tighe, B. *Polym. Int.* **1998**, *47* (2), 89–144.

(5) Saeidlou, S.; Huneault, M. A.; Li, H.; Park, C. B. *Prog. Polym. Sci.* **2012**, *37* (12), 1657–1677.

(6) Lasprilla, A. J. R.; Martinez, G. A. R.; Lunelli, B. H.; Jardini, A. L.; Filho, R. M. *Biotechnol. Adv.* **2012**, *30* (1), 321–328.

(7) Garlotta, D. *J. Polym. Environ.* **2001**, *9* (2), 63–84.

(8) Sodergard, A.; Stolt, M. *Poly(lactic acid) Synth. Struct. Prop. Process. Appl.* **2010**, No. iii, 27–41.

(9) Gironi, F.; Piemonte, V. *Energy Sources, Part A Recover. Util. Environ. Eff.* **2011**, *33* (21), 1949–1959.

(10) Drumright, R. E.; Gruber, P. R.; Henton, D. E. *Adv. Mater.* **2000**, *12* (23), 1841–1846.

(11) Perego, G.; Cella, G. D. *Poly(Lactic Acid) Synth. Struct. Prop. Process. Appl.* **2010**, 141–153.

(12) Buffet, J.-C.; Okuda, J. *Polym. Chem.* **2011**, *2*, 2758.

(13) Ovitt, T. M.; Coates, G. W. *J Polym Sci A Polym Chem* **2000**, *38*, 4686–4692.

(14) Tsuji, H. *Macromol. Biosci.* **2005**, *5* (7), 569–597.

(15) Kricheldorf, H. R.; Lee, S.-R.; Bush, S. *Macromolecules* **1996**, *29* (5), 1375–1381.

(16) Dubois, P.; Jacobs, C.; Jérôme, R.; Teyssié, P. *Macromolecules* **1991**, *24*, 2266–2270.

(17) Kowalski, A.; Duda, A.; Penczek, S. *Macromolecules* **2000**, *33* (3), 689–695.

(18) Spassky, N.; Wisniewski, M.; Pluta, C.; Le Borgne, A. *Macromol. Chem. Phys.* **1996**, *197*, 2627–2637.

(19) Ovitt, T. M.; Coates, G. W. *J. Am. Chem. Soc.* **2002**, *124* (7), 1316–1326.

(20) Zhong, Z.; Dijkstra, P. J.; Feijen, J. *J. Am. Chem. Soc.* **2003**, *125* (37), 11291–11298.

(21) Hormnirun, P.; Marshall, E. L.; Gibson, V. C.; Pugh, R. I.; White, A. J. P. *Proc. Natl. Acad. Sci. U. S. A.* **2006**, *103* (42), 15343–15348.

(22) Hormnirun, P.; Marshall, E. L.; Gibson, V. C.; White, A. J. P.; Williams, D. J. *J. Am. Chem. Soc.* **2004**, *126* (9), 2688–2689.

(23) Sumrit, P.; Hormnirun, P. *Macromol. Chem. Phys* **2013**, *214*, 1845–1851.

(24) Du, H.; Velders, A. H.; Dijkstra, P. J.; Sun, J.; Zhong, Z.; Chen, X.; Feijen, J. *Chem. - A Eur. J.* **2009**, *15* (38), 9836–9845.

(25) Dechy-Cabaret, O.; Martin-Vaca, B.; Bourissou, D. *Chem. Rev.* **2004**, *104*, 6147–6176.

(26) Mehta, R.; Kumar, V.; Bhunia, H.; Upadhyay, S. N. *J. Macromol. Sci. Part C Polym. Rev.* **2005**, *45* (4), 325–349.

(27) Avinc, O.; Khoddami, A. *Fibre Chem.* **2009**, *41* (6), 391–401.

(28) Parker, K.; Garancher, J.; Shah, S.; Weal, S.; Fernyhough, A. *Handb. Bioplastics Biocomposites Eng. Appl.* **2011**, 161–175.

(29) Erbetta, C. D. C.; Alves, R. J.; Reseende, J. M.; Freitas, R. F. S.; Sousa, R. G. *J. Biomater. Nanobiotechnol.* **2012**, *3*, 208–225.

(30) Ogata, N.; Jimenez, G.; Kawai, H.; Ogihara, T. *J. Polym. Sci. Part B Polym. Phys.* **1997**, *35*, 389–396.

(31) Lee, J. H.; Park, T. G.; Park, H. S.; Lee, D. S.; Lee, Y. K.; Yoon, S. C.; Nam, J. Do. *Biomaterials* **2003**, *24* (16), 2773–2778.

(32) Ray, S. S. *Poly(Lactic Acid) Synth. Struct. Prop. Process. Appl.* **2010**, No. i, 311–322.

(33) Balakrishnan, H.; Hassan, A.; Imran, M.; Wahit, M. U. *Polym. Plast. Technol. Eng.* **2012**, *51* (2), 175–192.

(34) Liu, J.; Zhou, K.; Wen, P.; Wang, B.; Hu, Y.; Gui, Z. *Polym. Adv. Technol.* **2015**, *26* (6), 626–634.

(35) Detyothin, S.; Kathuria, A.; Jaruwattanayon, W.; Selke, S. E. M.; Auras, R. *Poly(Lactic Acid) Synth. Struct. Prop. Process. Appl.* **2010**, 227–271.

(36) Tashiro, H.; Nakaya, M.; Hotta, A. *Diam. Relat. Mater.* **2013**, *35*, 7–13.

(37) Liu, H.; Zhang, J. *J. Polym. Sci. Part B Polym. Phys.* **2011**, *49* (15), 1051–1083.

(38) Jacobsen, S.; Fritz, H. G. *Polym. Eng. Sci.* **1999**, *39* (7), 1303–1310.

(39) Baiardo, M.; Frisoni, G.; Scandola, M.; Rimelen, M.; Lips, D.; Ruffieux, K.; Wintermantel, E. *J. Appl. Polym. Sci.* **2003**, *90*, 1731.

(40) Della Monica, F.; Luciano, E.; Buonerba, A.; Grassi, A.; Milione, S.; Capacchione, C. *RSC Adv.* **2014**, *4* (93), 51262–51267.

(41) Seppälä, J.; Karjalainen, T.; Hiljanen-Vainio, M. *J. Appl. Polym. Sci* **1996**, *59*, 1281–1288.

(42) Lipik, V. T.; Kong, J. F.; Chattopadhyay, S.; Widjaja, L. K.; Liow, S. S.; Venkatraman, S. S.; Abadie, M. J. M. *Acta Biomater.* **2010**, *6* (11), 4261–4270.

(43) Kember, M. R.; Copley, J.; Buchard, A.; Williams, C. K. *Polym. Chem.* **2012**, *3* (5), 1196–1201.

(44) Coullerez, G.; Lowe, C.; Pechy, P.; Kausch, H. H.; Hilborn, J. *J. Mater. Sci. Mater. Med.* **2000**, *11* (8), 505–510.

(45) Theryo, G.; Jing, F.; Pitet, L. M.; Hillmyer, M. A. *Macromolecules* **2010**, *43* (18), 7394–7397.

(46) Helminen, A. O.; Korhonen, H.; Seppälä, J. V. *Macromol. Chem. Phys* **2002**, No.

203, 2630–2639.

(47) Singh, O. M. *J. Sci. Ind. Res.* **2006**, *65*, 957–965.

(48) Astruc, A. *New J. Chem.* **2005**, *29*, 42–56.

(49) Natta, G.; Dall'Asta, G.; Mazzanti, G. *Angew. Chem. Int. Ed.* **1964**, *3* (11), 723–729.

(50) Fischer, E. .; Maasböl, A. *Angew. Chem. Int. Ed.* **1964**, *3* (8), 3–4.

(51) Chauvin, Y. *Angew. Chem. Int. Ed.* **2006**, *45* (23), 3741–3747.

(52) Bradshaw, C. P. C.; Howman, E. J.; L, T. *J. Catal.* **1967**, *7*, 269–276.

(53) Calderon, N.; Ofstead, E. A.; Ward, J. P.; Judy, W. A.; Scott, K. W. *J. Am. Chem. Soc.* **1968**, *90* (15), 4133–4140.

(54) Pettit, R.; Lewandos, G. S. *J. Am. Chem. Soc.* **1971**, *93*, 7087–7088.

(55) Grubbs, R. H.; Brunck, T. K. *J. Am. Chem. Soc.* **1972**, *3794* (9), 2538–2540.

(56) Katz, T. J.; McGinnis, J. *J. Am. Chem. Soc.* **1975**, *97* (6), 1592–1594.

(57) Casey, C. P.; Burkhardt, T. J. *J. Am. Chem. Soc.* **1974**, *96* (25), 7808–7809.

(58) Grubbs, R. H.; Burk, P. L.; Carr, D. D. *J. Am. Chem. Soc.* **1975**, *97*, 3265–3267.

(59) McGinnis, J.; Katz, Thomas J.; Hurwitz, S. *J. Am. Chem. Soc.* **1976**, *98* (2), 605–606.

(60) Schrock, R.; Rocklage, S.; Wengrovius, J.; Rupprecht, G.; Fellmann, J. *J. Mol. Catal.* **1980**, *8*, 73–83.

(61) Howard, T. R.; Lee, J. B.; Grubbs, R. H. *J. Am. Chem. Soc.* **1980**, *102*, 6876–6880.

(62) Wengrovius, J. H.; Schrock, R. R. *J. Am. Chem. Soc.* **1980**, *102* (13), 4515–4516.

(63) Kress, J.; Wesolek, M.; Le Ny, J.-P.; Osborn, J. a. *J. Chem. Soc. Chem. Commun.* **1981**, 1039–1040.

(64) Kress, J. R. M.; Russell, M. J. M.; Wesolek, M. G.; Osborn, J. a. *J. Chem. Soc. Chem. Commun.* **1980**, 431–432.

(65) Schrock, R. R.; Hoveyda, A. H. *Angew. Chem. Int. Ed.* **2003**, *42* (38), 4592–4633.

(66) Murdzek, J. S.; Schrock, R. R. *Organometallics.* **1987**, *6*, 1373–1374.

(67) Trnka, T. M.; Grubbs, R. H. *Acc. Chem. Res.* **2001**, *34* (1), 18–29.

(68) Novak, B. M.; Grubbs, R. H. *J. Am. Chem. Soc.* **1988**, *110* (18), 7542–7543.

(69) McGrath, D. V; Grubbs, R. H. *J. Am. Chem. Soc.* **1991**, *113*, 3611–3613.

(70) Nguyen, S. T.; Johnson, L. K.; Grubbs, R. H. *J. Am. Chem. Soc.* **1992**, *114*, 3974–3975.

(71) Nguyen, S. T.; Grubbs, R. H. *J. Am. Chem. Soc.* **1993**, *115*, 9858–9859.

(72) Schwab, P.; Grubbs, R. H.; Ziller, J. W. *J. Am. Chem. Soc.* **1996**, *118* (1), 100–110.

(73) Monsaert, S.; Lozano Vila, A.; Drozdzak, R.; Van Der Voort, P.; Verpoort, F. *Chem. Soc. Rev.* **2009**, *38* (12), 3360–3372.

(74) Samojłowicz, C.; Bieniek, M.; Grela, K. *Chem. Rev.* **2009**, *109* (8), 3708–3742.

(75) Weskamp, T.; Schattenmann, W. C.; Spiegler, M.; Herrmann, W. A. *Angew. Chem. Int. Ed.* **1998**, *37* (18), 2490–2493.

(76) Scholl, M.; Trnka, T. M.; Morgan, J. P.; Grubbs, R. H. *Tetrahedron Lett.* **1999**, *40*, 2247–2250.

(77) Scholl, M.; Ding, S.; Lee, C. W.; Grubbs, R. H. *Org. Lett.* **1999**, *1* (6), 953–956.

(78) Kingsbury, J. S.; Harrity, J. P. A.; Bonitatebus, P. J.; Hoveyda, A. H. *J. Am. Chem. Soc.* **1999**, *121*, 791–799.

(79) Garber, S. B.; Kingsbury, J. S.; Gray, B. L.; Hoveyda, A. H. *J. Am. Chem. Soc.* **2000**, *122* (34), 8168–8179.

(80) Mcconville, D. H.; Wolf, J. R.; Schrock, R. R. *J. Am. Chem. Soc.* **1993**, *115*, 4413–4414.

(81) Seiders, T. J.; Ward, D. W.; Grubbs, R. H. *Org. Lett.* **2001**, *3* (20), 3225–3228.

(82) Van Veldhuizen, J. J.; Garber, S. B.; Kingsbury, J. S.; Hoveyda, A. H. *J. Am. Chem. Soc.* **2002**, *124* (18), 4954–4955.

(83) Bielawski, C. W.; Grubbs, R. H. *Angew. Chem. Int. Ed.* **2000**, *39* (16), 2903–2906.

(84) Mutlu, H.; Montero de Espinosa, L.; Meier, M. a R. *Chem. Soc. Rev.* **2011**, *40* (3), 1404–1445.

(85) Coates, G. W.; Grubbs, R. H. *J. Am. Chem. Soc.* **1996**, *118* (1), 229–230.

(86) Sugai, N.; Yamamoto, T.; Tezuka, Y. *Macro Lett.* **2012**, *1* (7), 902–906.

(87) Prunet, J. *European J. Org. Chem.* **2011**, *2011* (20–21), 3634–3647.

(88) Herndon, J. W. *Coord. Chem. Rev.* **2016**, *329*, 53–162.

(89) Chatterjee, A. K.; Choi, T. L.; Sanders, D. P.; Grubbs, R. H. *J. Am. Chem. Soc.* **2003**, *125* (37), 11360–11370.

(90) Miao, X.; Dixneuf, P. H.; Fischmeister, C.; Bruneau, C. *Green Chem.* **2011**, *13* (9), 2258.

(91) Rybak, A.; Fokou, P. A.; Meier, M. A. R. *Eur. J. Lipid Sci. Technol.* **2008**, *110* (9), 797–804.

(92) Miao, X.; Fischmeister, C.; Dixneuf, P. H.; Bruneau, C.; Dubois, J.-L.; Couturier, J.-L. *Green Chem.* **2012**, *14* (8), 2179.

(93) Von Czapiewski, M.; Kreye, O.; Mutlu, H.; Meier, M. A. R. *Eur. J. Lipid Sci. Technol.* **2013**, *115* (1), 76–85.

(94) Miao, X.; Fischmeister, C.; Bruneau, C.; Dixneuf, P. H. *ChemSusChem* **2009**, *2* (6), 542–545.

(95) Sacristán, M.; Ronda, J. C.; Galià, M.; Cádiz, V. *J. Appl. Polym. Sci.* **2011**, *122* (3), 1649–1658.

(96) Winkler, M.; Meier, M. A. R. *Green Chem.* **2014**, *16*, 3335–3340.

(97) Nagarkar, A. A.; Crochet, A.; Fromm, K. M.; Kilbinger, A. F. M. *Macromolecules* **2012**, *45* (11), 4447–4453.

(98) Lee, H.-K.; Bang, K.-T.; Hess, A.; Grubbs, R. H.; Choi, T.-L. *J. Am. Chem. Soc.* **2015**, *137* (29), 9262–9265.

(99) Lu, Y.-X.; Guan, Z. *J. Am. Chem. Soc.* **2012**, *134* (34), 14226–14231.

(100) Neal, J. A.; Mozhdehi, D.; Guan, Z. *J. Am. Chem. Soc.* **2015**, *137* (14), 4846–4850.

(101) Mathers, R. T.; Coates, G. W. *Chem. Commun.* **2004**, No. 4, 422–423.

(102) Espinosa, L. M. De; Kempe, K.; Schubert, U. S.; Hoogenboom, R.; Meier, M. A R. *Macromol. Rapid Commun.* **2012**, *33*, 2023–2028.

(103) Balcar, H.; Shinde, T.; Lamač, M.; Sedláček, J.; Zedník, J. *J. Polym. Res.* **2014**, *21* (9), 557.

(104) Meng, X.; Edgar, K. J. *Carbohydr. Polym.* **2015**, *132*, 565–573.

(105) Fournier, L.; Robert, C.; Pourchet, S.; Gonzalez, A.; Williams, L.; Prunet, J.; Thomas, C. M. *Polym. Chem.* **2016**, *7* (22), 3700–3704.

(106) Kolb, N.; Meier, M. A. R. *Eur. Polym. J.* **2013**, *49* (4), 843–852.

(107) Dong, Y.; Matson, J. B.; Edgar, K. J. *Biomacromolecules* **2017**, *18*, 1661–1676.

(108) Arakawa, K.; Eguchi, T.; Kakinuma, K. *J. Org. Chem.* **1998**, *63* (14), 4741–4745.

(109) Bai, Y.; Xing, H.; Vincil, G. a.; Lee, J.; Henderson, E. J.; Lu, Y.; Lemcoff, N. G.; Zimmerman, S. C. *Chem. Sci.* **2014**, *5* (7), 2862.

(110) Cherian, A. E.; Sun, F. C.; Sheiko, S. S.; Coates, G. W. *J. Am. Chem. Soc.* **2007**, *129* (37), 11350–11351.

(111) Kreye, O.; Kugele, D.; Faust, L.; Meier, M. A. R. *Macromol. Rapid Commun.* **2014**, *35* (3), 317–322.

(112) Ornelas, C.; Méry, D.; Blais, J. C.; Cloutet, E.; Aranzaes, J. R.; Astruc, D. *Angew. Chem. Int. Ed.* **2005**, *44* (45), 7399–7404.

(113) Ornelas, C.; Méry, D.; Cloutet, E.; Aranzaes, J. R.; Astruc, D. *J. Am. Chem. Soc.* **2008**, *130* (4), 1495–1506.

(114) Liang, C. O.; Fréchet, J. M. J. *Macromolecules* **2005**, *38* (15), 6276–6284.

Chapter 2. Olefin Derivatives of Lactide

2.1 Chemical modification of lactide

Lactide does not offer versatile handles for modification that avoid ring-opening of the monomer. A common route to target functional derivatives of lactide is to start from substituted α-hydroxy acids.[1] In 1999, Baker *et al.* reported the synthesis of a family of derivatives of lactide centred on substitution at the α-carbon of lactic acid to produce biodegradable polymers with tuneable properties. The authors described three synthetic pathways to form substituted lactides (**Scheme 2.1**).[2] Route **a)** is analogous to the formation of lactide; oligomer formation *via* condensation of two substituted α-hydroxy acids followed by cracking under reduced pressure in the presence of a transesterification catalyst. Route **b)** offers more flexibility for creating unsymmetrical dimers, where an ester is formed from the condensation of an α-hydroxy acid with an α-bromoacyl bromide followed by ring closure to yield the cyclic dimer. Route **c)** is the direct acid catalysed dimerization of two α-hydroxy acids.

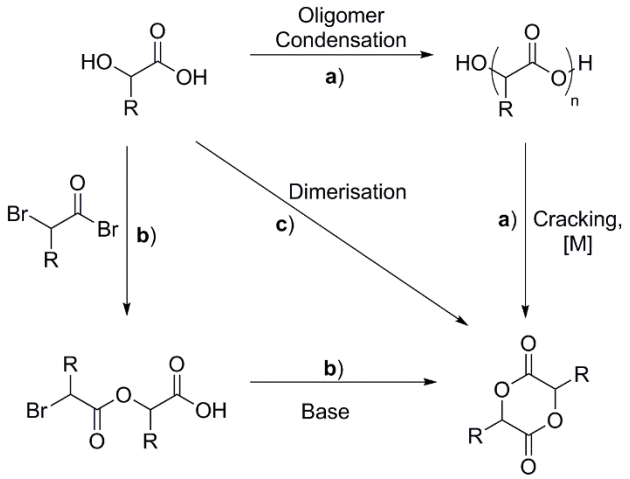

Scheme 2.1 *Synthetic routes to functionalised derivatives of lactide starting from α-hydroxy acids. Route a) oligomer condensation. Route b) condensation of α-hydroxy acids and α-bromoacyl bromides. Route c) dimerization.*

From these routes a variety of symmetrical functionalised lactide monomers were created (**23**-**25**, **Figure 2.1**). ROP of these dimers produced polymers with differing properties to PLA. The authors noted an increase in chain length gave rise to an associated decrease in T_g, with a corresponding increase in onset thermal degradation temperature. Monomer **26** was targeted to match the properties of commercial PS, however, the poly(phenyllactide) formed in the ROP of **26**, was amorphous with an associated T_g of 50 °C. The lack of crystallinity was explained by epimerization during melt ROP and the low T_g was accounted for by the flexibility of the methylene group linking the aromatic ring to the polymer chain. Thermal degradation of this polymer was confirmed to proceed primarily *via* depolymerisation to monomer which occurred more slowly than PLA due to the lower volatility of phenyllactide compared to lactide. Moreover an increase in hydrophobic nature of the polymer resulted in a decrease in hydrolytic degradation compared to PLA.[3]

To better match the properties of PS, Baker *et al.* successfully synthesised polymandelide *via* the ROP of mandelide, **27**. Although the T_g was increased substantially to 100 °C, this polymer exhibited poor thermal and photochemical stability rendering it impractical.[4] Additionally, Baker generated monomers **28-30** with associated T_g's of 98 °C, 73 °C and 41 °C respectively. Monomer **29** polymerised 10 times faster than **28** indicating preferential ROP at the carbonyl adjacent to the methyl group in **29**.[5]

Möller *et al.* targeted mono-substituted lactides and derived monomers **31-35.** The authors demonstrated that ROP conversions and rates could be improved in the presence of 4-dimethylaminopyridine (DMAP) compared to $Sn(Oct)_2$.[6]

Other examples of functionalised derivatives of lactide include the work of Vert *et al.* and Hennink *et al.* who synthesised monomers **36** and **37** respectively.[7–9] Hennink *et al.* showcased the versatility of the olefin fragment and carried out post-polymerisation epoxidation to generate amorphous co-polymers with lactide.[8] Following on from Hennink's work, Weck *et al.* synthesised monomer **38** *via* thiolene radical chemistry between allyl substituted lactide and tri(ethylene glycol) (TEG).[10] ROP produced a polymer capable of further functionalisaton at the azide. Similarly, Collard recently reported the synthesis of monomer **39**. Successive ROP and dehydrochlorination led to the formation of a PLA-containing olefin that has potential for thiolene addition.[11]

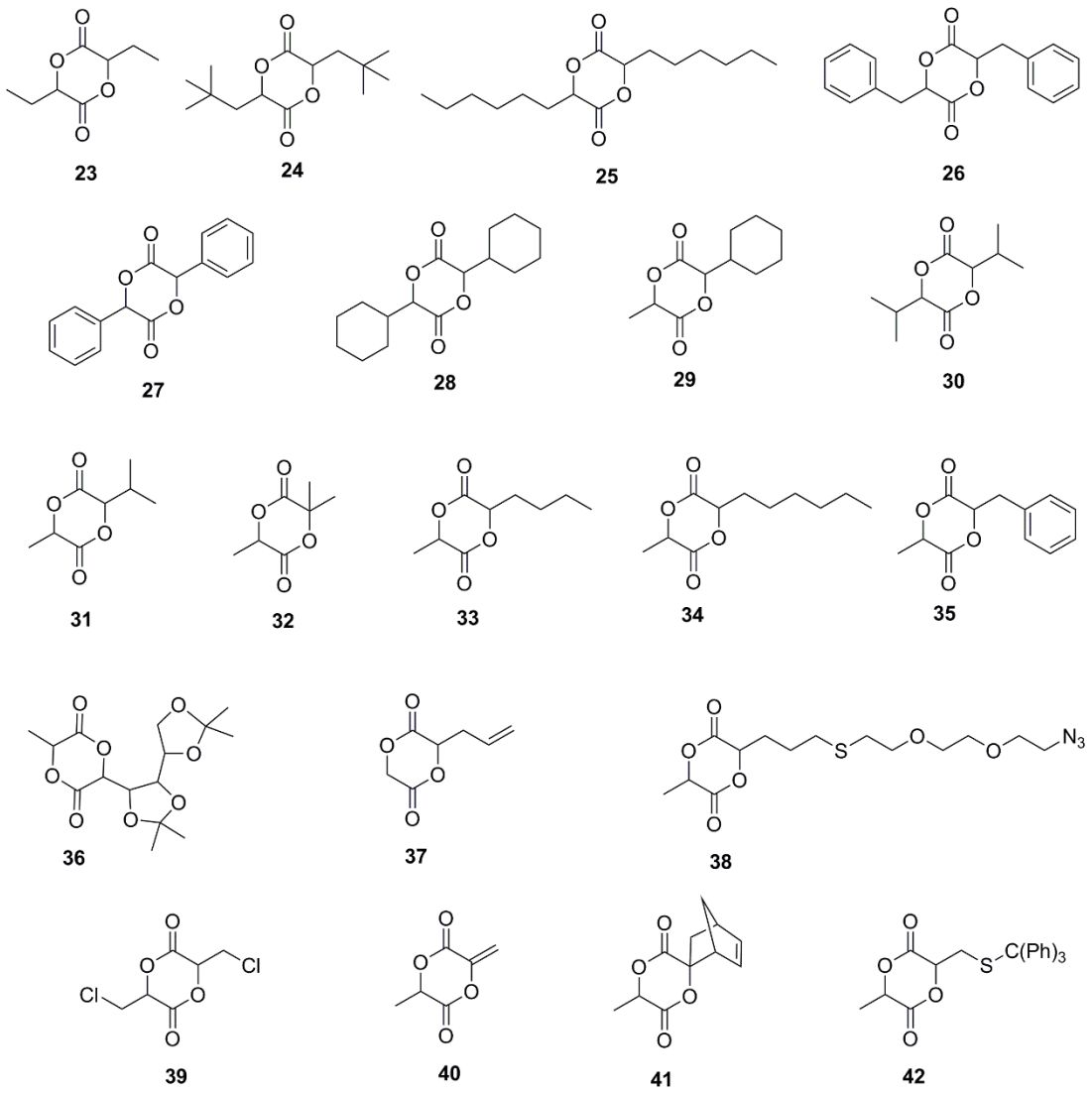

Figure 2.1 *Olefin derivatives of lactide.*[3-13, 15]

The aforementioned routes are useful for the generation of substituted lactides. More challenging is modification of the cyclic dimer lactide, with only a few reports currently demonstrating this. In 1969, Scheibelhoffer synthesised monomer **40** *via* a two-step bromination-elimination process[12] and in 2008 Hillmyer and Jing demonstrated its ability to act as a dienophile in a Diels Alder with cyclopentadiene to produce **41**.[13] The significance of **41** is its two polymerisable rings. ROP at the ester linkage versus ROMP at the olefin generated separate polymers with T_g's of 113 °C and 192 °C respectively. The bifunctional nature of **41** enabled dual polymerisation to generate a polybutadiene-graft-PLA copolymer with 1,5-cyclooctadiene. 20 Wt % incorporation of this copolymer during the ROP of rac-lactide led to PLA composites with toughened properties. Further

modification of **41** involved hydrogenation of the olefin pre-polymerisation to produce polymers with a decrease in T_g.[14] Alternatively, altering the size of the diene allowed further tailoring of T_g's such that using a larger diene, 1,3-cyclohexadiene, led to an increase in T_g while using a smaller diene, isoprene, led to a decrease in T_g.[14] Pappalardo recently reported thiol incorporation of **40** to produce **42**, which contained a protected thiol moiety. Copolymerisation was achieved with LA, CL and a mixture of the two. De-protection resulted in "free" pendant thiols that display potential for further modification.[15]

The lack of functional handles on lactide coupled with its reactive esters limit modification without losing the ring structure. An option that has yet to be reported for the modification of lactide is methylenation of a single carbonyl group, which is of interest as a precursor for CM.

2.2 Reagents for methylenation reactions

Methylenation of carbonyl functionalities to olefins can be achieved with a range of catalysts, most commonly the Wittig Reagent. Although an excellent choice for the reaction of aldehydes and ketones, its reactivity is limited in the presence of sterically hindered ketones and carboxylic acid derivatives, making it an unsuitable choice for the methylenation of lactide. An alternative choice is the Tebbe reagent, **43**, **Scheme 2.2**, originally reported in 1978 by Tebbe and co-workers.[16] It is an air sensitive reagent that is synthesised and handled under an inert atmosphere. In the presence of a Lewis base a

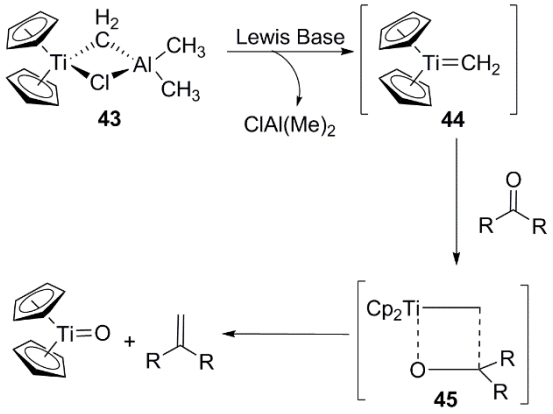

Scheme 2.2 *Formation of active methylidene from the Tebbe reagent and its reaction with carbonyl compounds.*

highly active titanocene methylidene complex **44**, is generated in addition to dimethylaluminium chloride. This highly active Schrock-type carbene complex can react with carbonyls to form an oxatitanacyclobutane intermediate, **45**, which yields a new methylenated product and a titanium oxide species.[17]

The Tebbe reagent has a wide substrate scope, including sterically hindered, or readily enolizable ketones and ketones containing leaving groups β- to a carbonyl functionality, which are typically difficult to achieve with phosphorous ylides. Moreover, it can react with esters, lactones, amides and imides and chemo-selective methylenation is possible in the presence of two carbonyl functionalities or in the presence of alkenes. The limitation of the Tebbe reagent lies with highly electrophilic acid anhydrides and acid halides which instead form titanium enolates.[18]

The Petasis reagent, dimethyltitanocene **46**, **Scheme 2.3**, is an attractive alternative to the Tebbe reagent due to its air and moisture tolerance with no associated acidic aluminium by-product. The reaction involves the formation of **44** through α-elimination at elevated temperatures (> 60 °C).[19] Its substrate scope matches that of the Tebbe reagent but extends to the methylenation of acid sensitive substrates.[18] Another advantage is the ability to generate dialkyltitanocenes, such as dibenzyltitanocene **47**, which can be used for the alkylidenation of carbonyls through active species **48**, but synthesis of dialkyltitanocenes is restricted by β-hydride elimination.[18] Both the Tebbe reagent and the Petasis reagent were explored as candidates for the methylenation of lactide.

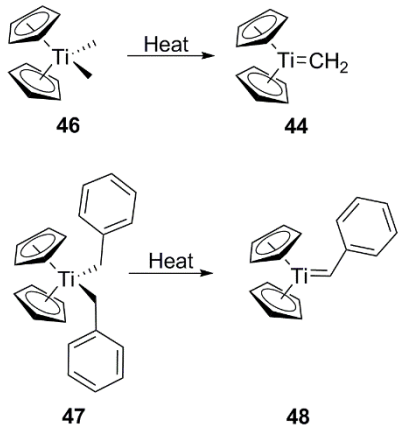

Scheme 2.3 *The Petasis reagent and dibenzyltitanocene with their corresponding active carbene complexes.*

2.3 Mono-methylenated lactide

2.3.1 The Tebbe and Petasis reagent

Initial studies focussed on using the Tebbe reagent for the methylenation of lactide. In order to produce a monomer suitable for ROP *via* acyl-oxygen bond cleavage it was critical to ensure mono-methylenation of the carbonyl groups. We aimed to optimise reaction conditions to achieve the greatest conversion to the desired mono-methylenated product. The Tebbe reagent was synthesised according to literature procedures and handled and stored under an inert atmosphere.[20] Initial experiments were carried out with 1 equivalent of the Tebbe reagent at 0 °C and left to react for 1 hour (**Table 2.1**). The reaction was quenched with a few drops of aqueous NaOH (10 mol%) and diluted with diethyl ether prior to work up. Analysis by ^{1}H NMR spectroscopy indicated almost a 50:50 mixture of residual lactide:mono-methylenated lactide (LA:MML), with a small amount of di-methylenated lactide (DML), (Entry 1). To investigate the effect of NaOH during quenching the reaction was repeated (for 2.5 hours) and a crude NMR spectrum was taken prior to quenching with a stronger solution of NaOH (15 mol%). As can be seen from Entry 2, the percentage of residual lactide decreased from 75 % to 0 % after quenching and resonances corresponding to PLA appeared. This result suggested NaOH removed

Table 2.1 *Methylenation of lactide using the Tebbe reagent.*

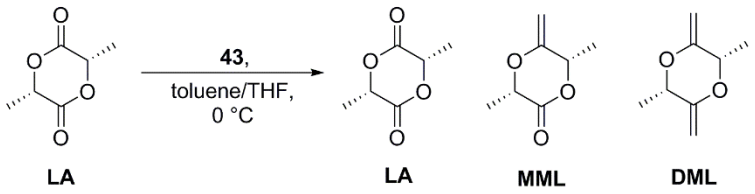

Entry	Time (h)	NaOH (%)	Residual **LA** (%)[a]	Conversion to **MML** (%)[a]	Conversion to **DML** (%)[a]	Conversion to **PLA** (%)[a]
1	1	10	44	43	13	0
2	2.5	15	75[b], 0[c]	20[b], 63[c]	5[b], 20[c]	0[b], 17[c]

[a]Determined by ^{1}H NMR spectroscopy monitored by appearance of olefin protons. [b]NMR spectrum taken prior to quenching with NaOH, [c]NMR spectrum taken after quenching with NaOH.

residual lactide from the mixture and at concentrations of 15 mol%, promoted the ROP of lactide to form PLA.

Following from these results, quenching the reaction with NaOH was removed. To target the formation of MML, reaction conditions (equivalents of Tebbe reagent, temperature of reaction and rate of Tebbe addition) were optimised as shown in **Table 2.2**. Comparing Entries 1 and 2 at 0 °C, doubling the equivalents of Tebbe reagent resulted in an increase in conversion to MML, while decreasing the temperature to -41 °C (Entries 3 and 4) gave no significant increase in conversion to MML (compare Entries 2 and 4).

With the aim to improve the conversion of lactide to MML the duration of the reaction was increased from 1 to 2 hours, yet no significant improvement was observed (Entries 4

Table 2.2 *Optimisation of reaction conditions for the methylenation of lactide using the Tebbe reagent.*

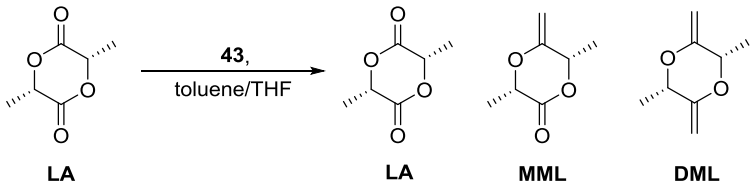

Entry	Equiv. of **43**	Rate of Addition (ml/min)	Temp. (°C)	Time (h)	Residual **LA** (%)[a]	Conversion to **MML** (%)[a]	Conversion to **DML** (%)[a]
1	1	Instantaneous	0	1	65	35	0
2	2	Instantaneous	0	1	35	50	15
3	1	Instantaneous	-41	1	64	34	2
4	2	Instantaneous	-41	1	31	55	14
5	2	Instantaneous	-41	2	34	58	8
6	2	0.1	-41	1	39	56	5
7	2	0.1	-72	1	54	41	5
8	2	0.1	0	1	26	60	14
9	3	0.1	0	1	32	30	38
10[b]	2	0.1	0	1	30	49	21
11	2	0.1	R.T	1	25	17	58

[a]Determined by ^{1}H NMR spectroscopy monitored by appearance of olefin protons. [b]Reaction diluted by 2-fold.

and 5). Next, the rate of addition of the Tebbe reagent was investigated. To limit formation of DML, it was hypothesised that a slower addition rate of the Tebbe reagent may favour mono-methylenation over dimethylenation of lactide. Entries 6-8 compare the effect of temperature (-41 °C, -72 °C and 0 °C) with an addition rate of 0.1 ml/min. The reaction performed at 0 °C (Entry 8), produced the highest conversion to MML (60 %). Comparing this result to the reaction carried out under identical conditions with instant Tebbe addition (Entry 2), the conversion to MML increased from 50 % to 60 %, in agreement with the hypothesis. To promote higher conversions to MML, the equivalents of Tebbe reagent was increased from 2 to 3 equivalents (Entry 9). Unfortunately, this resulted in higher conversion to DML. Dilution of the reaction also increased the conversion to DML (Entry 10). This would be expected due to the decreased probability of the Tebbe reagent interacting with another lactide monomer. Finally, performing the reaction at room temperature reduced selectivity and DML was the favoured product. This result highlights the importance of performing the reaction at 0 °C or below in order to maintain selectivity.

The Petasis reagent was considered for the methylenation of lactide, however formation of the active titanocene methylidene requires temperatures above 60 °C, which would potentially pose problems with selectivity. Initial screening gave no improvement compared to the Tebbe reagent. Thus, optimal reaction conditions were identified as 2 equivalents of the Tebbe reagent at an addition rate of 0.1 ml/min at 0 °C.

2.3.2 Degradation of mono-methylenated lactide

Purification and isolation of MML was carried out using column chromatography on silica gel. Separation of the three monomers LA, MML and DML was difficult, particularly due to the similar polarity of LA and MML. Separation was successful, however, upon concentration of the collected fractions (corresponding to MML), under reduced pressure, no mass of MML was obtained. This indicated the monomer must possess inherent stability issues degrading into volatile products capable of being removed under reduced pressure. In order to isolate MML, slow evaporation of the eluent system using

a stream of nitrogen in an ice bath was applied, generating a white solid in low yield (< 20%). A negligible yield of DML was isolated.

To probe further the instability of MML, a sample dissolved in $CDCl_3$ was heated (60-100 °C) for 5 days in a sealed Young NMR tube and its transformation was monitored *via* ^{1}H NMR spectroscopy (**Figure 2.2**). Interestingly, by day 2 of heating a new quartet and two new singlets emerged and by day 5 disappearance of the methylene protons was evident. 2D NMR spectroscopy (COSY, HSQC and HMBC) confirmed MML underwent thermal rearrangement to form **49**, **Scheme 2.4**. Interestingly, exposure of MML to air for 2 days resulted in disappearance of all sample. This indicated **49** undergoes degradation in its solid state, most likely producing volatile by-products. This proposition is consistent with the observed disappearance of MML under reduced pressure and accounts for the unexpected low yields. To limit degradation MML was stored in the freezer of a glove box.

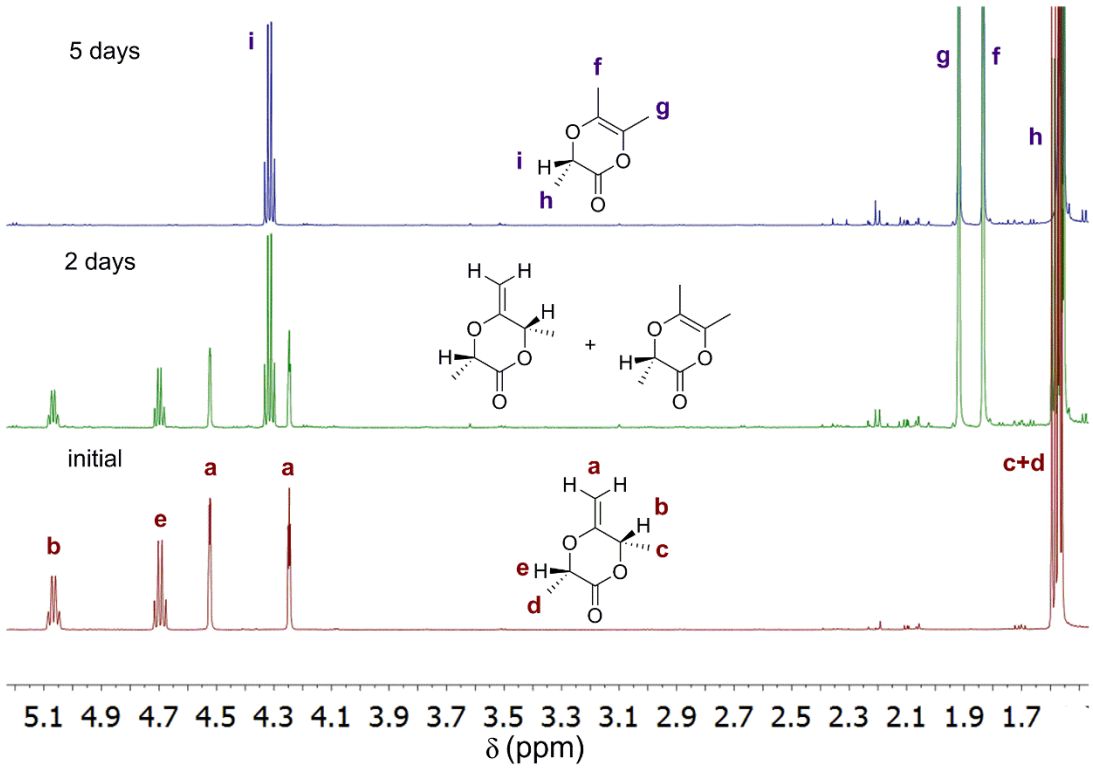

Figure 2.2 *Degradation of MML via ^{1}H NMR spectroscopy over the course of 5 days (60-100 °C).*

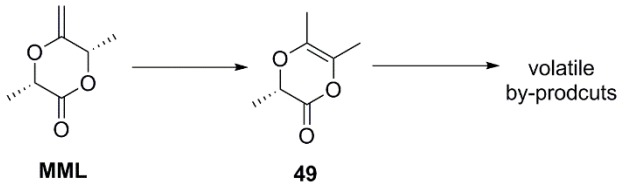

Scheme 2.4 *Hypothetical thermal degradation of MML.*

2.3.3 Olefin cross-metathesis of mono-methylenated lactide

Irrespective of the stability issues of MML, it was hypothesised that CM of the monomer may inhibit or reduce degradation. First, olefin Type determination was necessary to categorise MML and identify suitable cross partners. Hoveyda Grubbs second generation catalyst, **14**, was chosen for all CM reactions due to its high reactivity and wide substrate scope. Homodimerisation of MML led to no reaction (**Scheme 2.5**). According to the model devised by Grubbs,[21] Type I olefins undergo rapid homodimerisation, Type II olefins undergo slow homodimerisation, Type III olefins are unable to homodimerise and Type IV olefins are completely inert to metathesis. Based on this model, MML can be either categorised as a Type III or a Type IV olefin. Next, reaction with a Type II olefin,

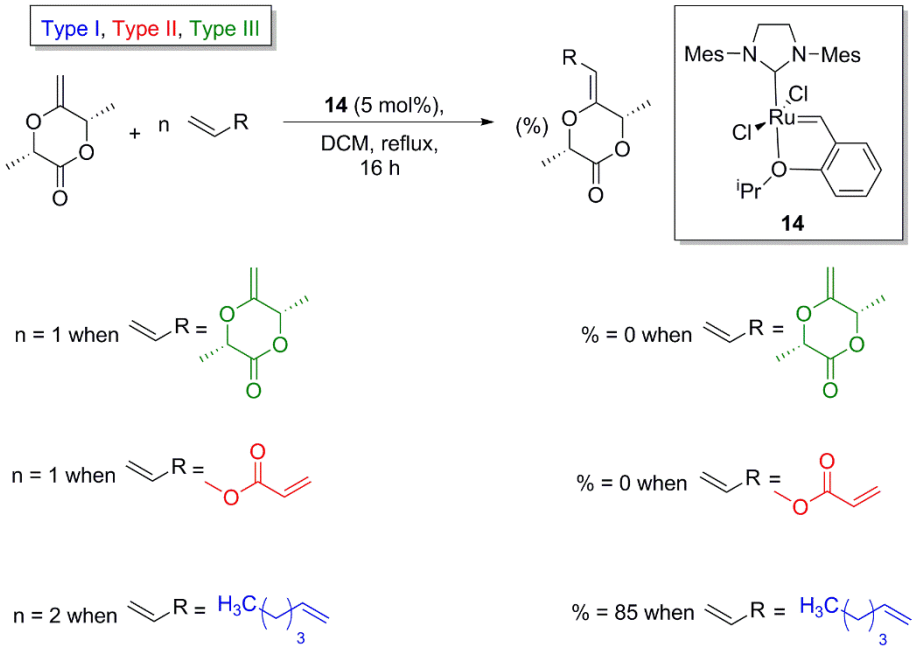

Scheme 2.5 *Olefin cross-metathesis of MML with itself, a Type I (hex-1-ene) and Type II (methyl acrylate) olefin.*

methyl acrylate, only generated the dimer of methyl acrylate and unreacted MML. Conversely, reaction in the presence of a Type I olefin, hex-1-ene, gave a conversion to 85 % of the targeted cross-product. Consequently, MML can be categorised as a Type III olefin, however, its inability to react with a type II olefin signifies its low reactivity within this category.

Purification and isolation of hexenyl-methylenated lactide (HML), **Scheme 2.6**, mirrored that of MML. Slow evaporation of the eluent system using a stream of nitrogen in an ice bath was used to limit any potential degradation, to form a pale yellow solid with a low yield (30 %). To investigate whether HML undergoes the same degradation pathway as MML, a sample dissolved in $CDCl_3$ was heated (60-100 °C) for 6 days in a sealed Young NMR tube and its transformation was monitored *via* ^{1}H NMR spectroscopy. 2D NMR spectroscopy (COSY, HSQC and HMBC) indicated the formation of **50**, **Scheme 2.6**, which confirmed HML also undergoes thermal rearrangement. When exposed to air for 2 days HML exhibited no degradation highlighting that the introduction of hex-1-ene into the monomer framework enhances stability, and reduces the rate of degradation.

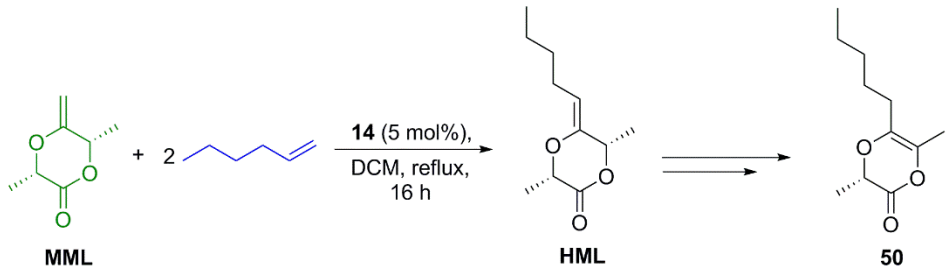

Scheme 2.6 *Olefin cross-metathesis of MML with Type I olefin hex-1-ene to form HML followed by its thermal rearrangement.*

2.3.4 Ring-opening polymerisation of modified and functionalised derivatives of lactide

ROP of both MML and HML was investigated using catalysts **51**, **52** and **53** (catalysts successful in the ROP of lactide) (**Table 2.3**). It was hypothesised that both MML and HML, would transform into **49** and **50**, respectively, under the ROP temperatures but should not inhibit polymerisation. ROP of MML was attempted using aluminium salen, **53** (**Table 2.3**, Entry 1), while ROP of HML was investigated using organo-catalyst **51**,

triazabicyclodecene (TBD) (Entry 2) and $Sn(Oct)_2$, **52** (Entry 3). Unfortunately polymerisation was unsuccessful for all attempts and surprisingly, no traces of rearranged derivatives **49** or **50** were observed during the reaction. Due to the instability of MML, and HML and the low yields obtained, research and optimisation of this route was abandoned. Attention turned to an alternative olefin-functionalised derivative of lactide.

Table 2.3 *Ring-opening polymerisation of novel derivatives of lactide under various reaction conditions.*

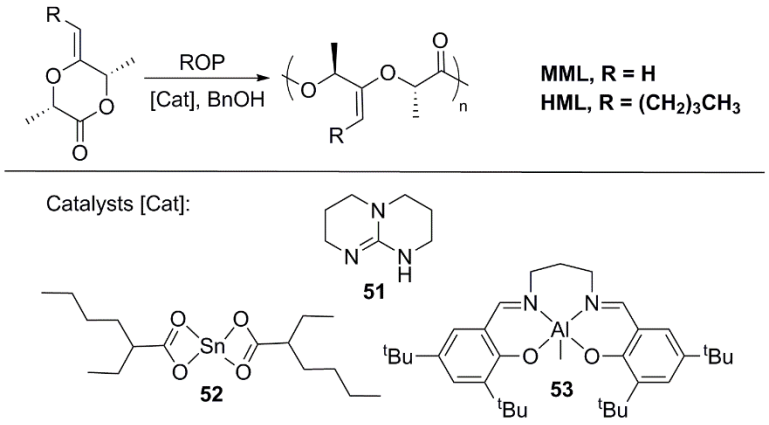

Entry	Monomer	Catalyst	Solvent	Temperature (°C)	Time (h)	Conversion (%)
1[a]	MML	**53**	Benzene-d_6	85	15	0
2[b]	HML	**51**	DCM-d_2	R.T	24	0
3[b]	HML	**52**	Toluene-d_8	120	24	0

[a]Monomer:catalyst:BnOH, 50:1:1. [b]Monomer:catalyst:BnOH, 30:1:1. [C]Conversion determined by ^1H NMR spectroscopy.

2.4 3-Methylenated lactide

2.4.1 Ring-opening polymerisation of 3-methylenated lactide

3-Methylenated lactide (3-ML) (**Scheme 2.7**), is currently the only example in the literature that is derived from the direct modification of lactide. As discussed previously, both Hillmyer *et al.* and Pappalardo *et al.* utilise the olefin moiety of 3-ML for further functionalisation,[13,15] yet olefin CM is yet to be investigated as a potential tool for the functionalisation of this monomer. Initial studies focussed on ROP to target a polymer

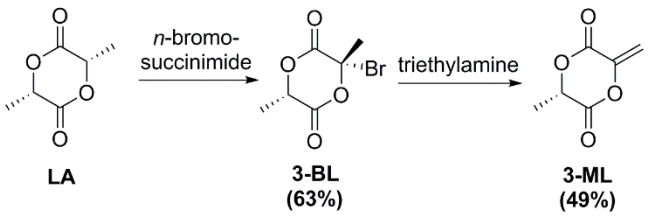

Scheme 2.7 *Synthesis of 3-ML via the bromination of lactide to produce 3-BL and subsequent elimination.*

with olefin functionality built within the polymer backbone. 3-ML was synthesised using a modified literature procedure[13] involving bromination to produce 3-brominated lactide (3-BL) followed by elimination to yield 3-ML with expected yields shown (**Scheme 2.7**).

ROP was attempted using aluminium salan and salen catalysts **53-55** that were synthesised according to literature procedures,[22,23] $Sn(Oct)_2$ **52**, and organocatalysts TBD **51** and 1,8-diazabicycloundec-7-ene (DBU) **56**, **Table 2.4**. Reaction conditions were altered including duration and temperature, yet as can be seen from **Table 2.4**, Entries **1-11**, none of the polymerisations were successful. Analysis by ^{1}H NMR spectroscopy of the crude sample of Entry 2 in the presence of an excess of MeOH showed an unexpected result, **Figure 2.3**. Disappearance of the methylene protons was evident indicating 3-ML had undergone a transformation during the polymerisation. 2D NMR spectroscopy (COSY, HSQC and HMBC) identified the formation of compound **57**, **Scheme 2.8**. It was apparent that 3-ML underwent alcoholysis in the presence of MeOH to produce ring-opened version **57**. A proposed mechanism is illustrated in **Scheme 2.8**. This finding suggested that the alcohol initiator present, BnOH, is likely consumed via alcoholysis generating a non-polymerisable derivative. To eliminate the possibility of alcoholysis, pre-initiation of the catalyst was attempted in the hope of promoting ROP *via* coordination insertion as opposed to nucleophilic ring-opening, which would consume all initiator required for the ROP (Entry 12, **Table 2.4**). Unfortunately this was also unproductive and no polymerisation occurred. Although "free" BnOH was eliminated through coordination to the catalyst, it is possible insertion of BnOH into 3-ML is favoured at the carbonyl adjacent to the methyl group as opposed to the carbonyl adjacent to the methylene group, which promotes degradation by ring-opening. To confirm that 3-ML was susceptible to alcoholysis in the presence of BnOH initiator, 3-ML was dissolved in toluene and reacted with 1.1 equivalents of BnOH at 70 °C for 24 hours. The reaction was effective and showed complete conversion to **58**, **Figure 2.4**. Based on this finding

a family of compounds were generated **57**-**62** *via* the alcoholysis of 3-ML with a variety of alcohols; including methanol **57**, benzyl alcohol **58**, allyl alcohol **59**, ethanol **60**, and isopropanol **61**. Moreover when exposed to air at room temperature, 3-ML formed **62**, illustrating the instability of this monomer. It was also evident that all alcoholysis reactions

Table 2.4 Ring-opening polymerisation of 3-ML under various reaction conditions.

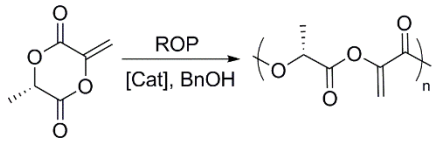

Catalysts [Cat]:

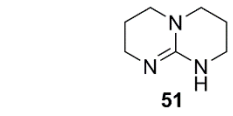

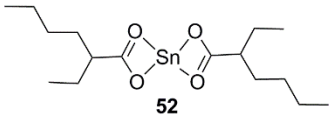

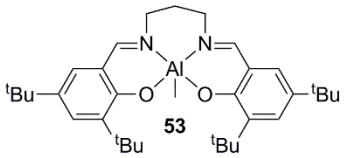

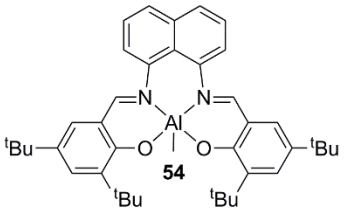

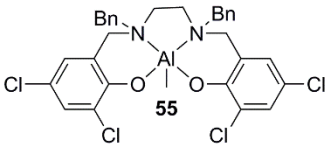

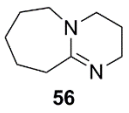

Entry	Catalyst	Solvent	Temperature (°C)	Time (h)	Conversion (%)[b]
1[a]	**54**	Toluene	85	8	0
2[a]	**52**	Toluene	85	2	0
3[a]	**55**	Toluene	80	5	0
4[a]	**51**	DCM	70	24	0
5[a]	**51**	DCM	R.T	24	0
6[a]	**51**	DCM	0	6	0
7[a]	**56**	DCM	70	24	0
8[a]	**56**	DCM	R.T	24	0
9[a]	**56**	DCM	120	24	0
10[a]	**53**	Toluene	85	2	0
11[a]	**53**	Toluene	85	24	0
12[a,c]	**53**	Toluene	85	24	0

[a]Monomer:catalyst:BnOH, 50:1:1. [b]Determined by ^{1}H NMR spectroscopy. [c]Pre-catalyst initiation.

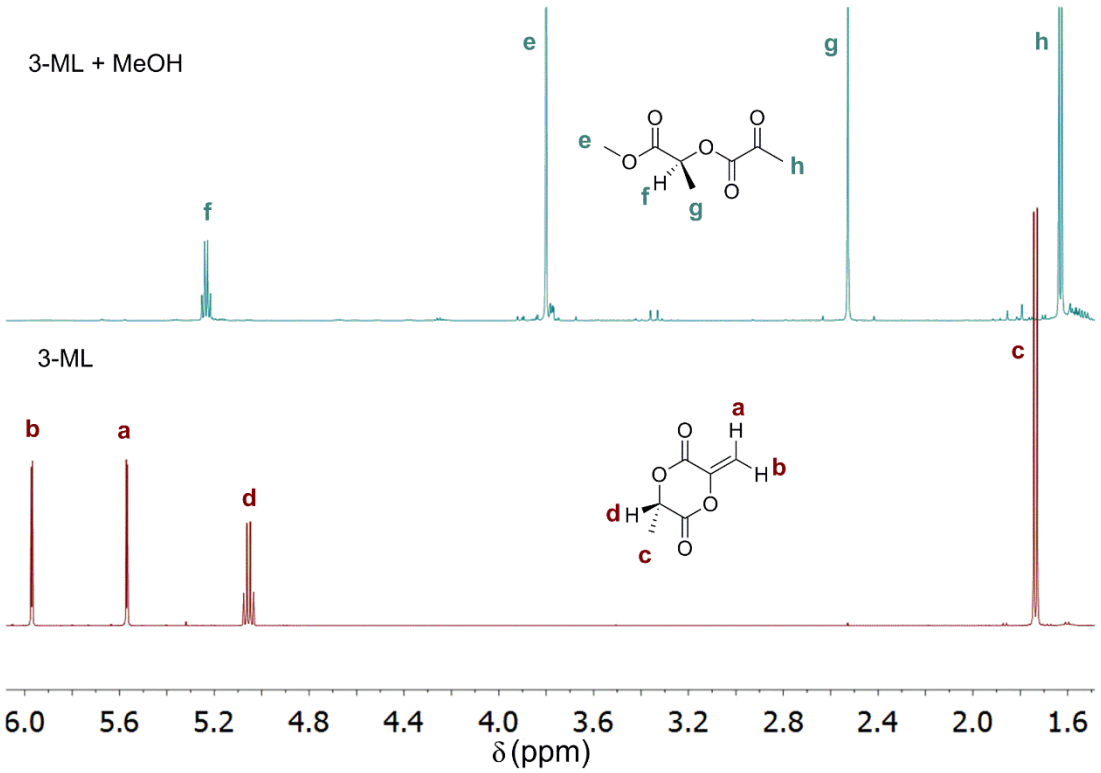

Figure 2.3 *Comparison ^{1}H NMR spectra of 3-ML to 3-ML in the presence of an excess of MeOH.*

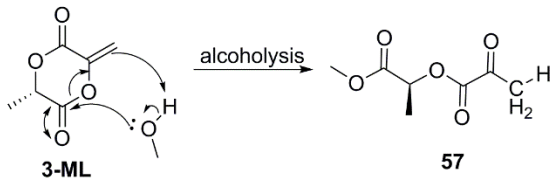

Scheme 2.8 *Proposed alcoholysis of 3-ML in the presence of methanol.*

were regioselective, with exclusive nucleophilic attack at the carbonyl adjacent to the methyl group as opposed to the one adjacent to the methylene group. This can be attributed to the conjugation of the methylene double bond with the latter carbonyl, de-activating this carbonyl towards nucleophilic attack. While this research was ongoing, a publication by Miyake *et al.* illustrated this very finding.[24] The authors examined the polymerisability of 3-ML *via* ROP with an array of anionic initiators, organocatalysts, frustrated Lewis pairs and coordination catalysts but none were successful. They observed the decomposition of 3-ML in air and alcoholysis of 3-ML in the presence of methanol and $(CF_3)_2CHOH$. Thus, Miyake *et al.* concluded that 3-ML is non-polymerisable in the presence of current ROP reagents that trigger breakdown as opposed to polymerisation.

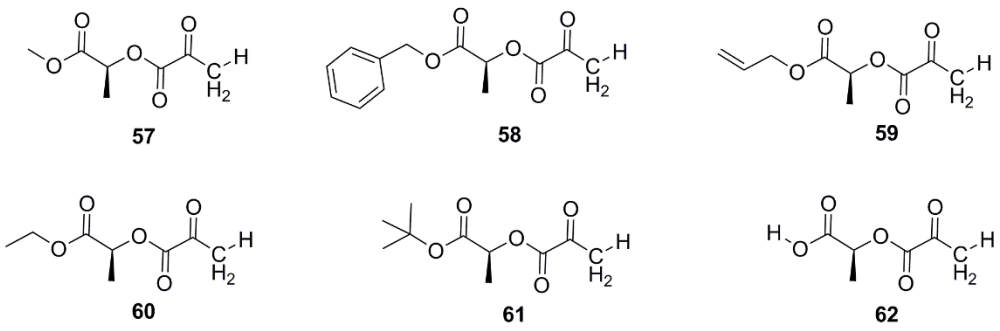

Figure 2.4 *Novel family of compounds generated via the alcoholysis of 3-ML in the presence of various alcohols.*

2.4.2 Olefin cross-metathesis of 3-methylenated lactide

The ability of 3-ML to act as an active olefin in CM reactions was examined. First, the olefin Type of 3-ML was determined to help identify suitable cross partners. Self-metathesis led to no homodimerisation deeming 3-ML as either a Type III or a Type IV olefin (Entry 1, **Table 2.5**). CM of 3-ML in the presence of a Type I olefin, dec-1-ene, gave full conversion to the desired cross-product (Entry 2), categorising 3-ML as a Type III olefin (unable to homodimersise but can react with olefins of a different Type). Next, optimisation of reactions conditions were explored using dec-1-ene as the cross-partner. First, the effect of catalyst concentration was investigated and it was observed that decreasing the catalyst concentration from 5 mol % to 2 mol % resulted in a decrease in the conversion to cross-product (compare Entries 2 and 3). However, decreasing the reaction volume to make the solution 5 times more concentrated in the presence of 2 mol % catalyst led to complete conversion to cross-product (compare Entries 3 and 4). Conversely diluting the reaction by a factor of 2 led to a decrease in conversion (compare Entries 2 and 5). These results show how both reaction concentration and catalyst loading can manipulate conversion.

The effect of cross-partner equivalents was then investigated. Using dec-1-ene:3-ML in a ratio of 0.1:1 resulted in a dramatic decrease in conversion to 16% (Entry 6). Similarly, reversing the ratio to 10:1 dec-1-ene:3-ML also revealed a low yield of 29 % (Entry 7) but repeating this reaction using a higher catalyst loading of 5 mol % saw an associated increase in yield to 92 % (Entry 8). To favour consumption of 3-ML an excess of

Table 2.5 *Olefin cross-metathesis of 3-ML with Type I and Type II olefin cross-partners.*

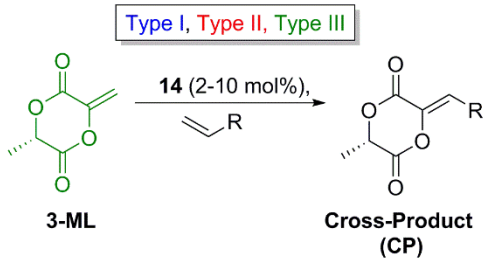

Entry	R	Equiv. of R	Catalyst (mol%)	Solvent	Temp. (°C)	Time	Conv. to CP (%)[a]
1	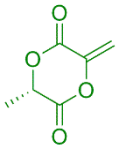	1	2	DCM	45-50	16 h	0
2		2	5	DCM	45-50	16 h	100
3		2	2	DCM	45-50	16 h	64
4[b]		2	2	DCM	45-50	16 h	100
5[c]		2	5	DCM	45-50	16 h	40
6		0.1	2	DCM	45-50	16 h	16
7		10	2	DCM	45-50	16 h	29
8		10	5	DCM	45-50	16 h	92
9		1.5	5	DCM	45-50	16 h	97
10		2	5	DCM	R.T	16 h	50
11		2	5	DCM	45-50	4 h	85
12		2	5	DCM	45-50	16 h	100
13		2	5	DCM	45-50	16 h	100
14		2	5	DCM	45-50	16 h	100

15	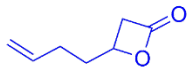	2	5	DCM	45-50	16 h	0
16	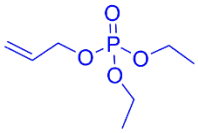	2	5	DCM	45-50	2.5 days	0
17	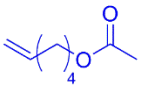	2	5	DCM	45-50	16 h	18
18	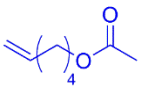	2	10	DCM	45-50	7 days	71
19	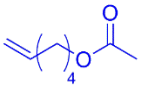	2	10	PFT	100	7 days	87
20	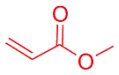	2	5	DCM	45-50	2.5 days	0
21	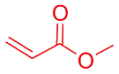	2	5	PFT	100	7 days	0
22	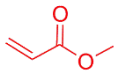	2	10	Toluene	100	7 days	0

[a]Determined by ^{1}H NMR spectroscopy monitored by consumption of 3-ML olefin protons and appearance of cross product protons. [b]Reaction concentrated by a factor of 5. [c]Reaction diluted by a factor of 2.

dec-1-ene is preferred, yet a large excess can also disfavour selective CM due to competing self-metathesis of dec-1-ene and catalyst exhaustion. Nevertheless, a higher catalyst loading can overcome the high excess of cross-partner to favour selective CM. Decreasing the equivalents of dec-1-ene to 1.5 instead of 2 also demonstrated a slight loss in conversion, indicating 2 equivalents is optimum (Entry 9).

Finally, both a reduction in duration to 4 hours from 16 hours and a decrease in temperature from reflux to R.T saw a decrease in conversion to cross-product (Entries 10 and 11 respectively). From the screening experiments conducted, the optimum reaction conditions chosen for further CM of 3-ML were 2 equivalents of cross-partner, with a catalyst loading of 5 mol% performed under reflux for 16 hours.

Using the optimum reaction conditions, CM with similar long chain aliphatic alkenes; dodec-1-ene, oct-1-ene and hex-1-ene, resulted in complete conversion to cross-product (Entries 12-14). To expand the substrate scope of cross-partners, Type I olefins β-6-

heptenolactone and allyl phosphonate (Entries 15 and 16 respectively) were used as functional cross-partners. Unfortunately, no selective CM occurred, potentially due to the steric bulk associated with both these cross-partners. To position the steric bulk further from the reactive olefin, 5-hexenyl acetate was investigated and results indicated a low conversion of 18 % (Entry 17). To promote conversion to the cross-product, the catalyst loading and reaction time was increased to 10 mol% and 7 days respectively. These conditions demonstrated a significant increase in conversion to 71 % (Entry 18). Perfluorotoluene (PFT) has been reported as an effective solvent for enhancing the activity of olefin metathesis catalysts.[25] Thus, the reaction was repeated using PFT at 100 °C which increased the conversion to 87 % (Entry 19).

Finally, the ability of 3-ML to react with a Type II olefin was examined using methyl acrylate. Under the optimised reaction conditions, no cross-product was observed, even after reaction times of one week (Entry 20). Following from the success of PFT as a solvent in the CM of 3-ML with 5-hexenyl acetate, it was used in the CM with methyl acrylate but it gave no improvement in yield (Entry 21). The solvent was switched to toluene but again no product formation was observed (Entry 22). These experiments confirmed that although 3-ML is categorised as a Type III olefin its reactivity profile is very low. Olefin CM of 3-ML is successful only with sterically unhindered long chain aliphatic alkenes (hex-1-ene to dodec-1-ene), though harsher reaction conditions can lead to CM with a functional olefin (5-hexenyl acetate).

2.4.3 Tandem olefin cross-metathesis and hydrogenation of 3-methylenated lactide

Olefin CM of 3-ML with hex-1-ene was repeated on a gram scale to produce 3-hexenyl lactide (3-HL) (**Scheme 2.9**). Purification of 3-HL was attempted using column chromatography on silica gel but surprisingly negligible material was collected. Analysis by ^{1}H NMR of the material collected identified the formation of **63** (**Scheme 2.9**). The susceptibility of 3-HL to alcoholysis was not seemingly eliminated by incorporation of hex-1-ene. The eluent system used during purification was DCM, which contained ethanol stabiliser, consequently alcoholysis of 3-HL with ethanol generated ring-opened version **63**.

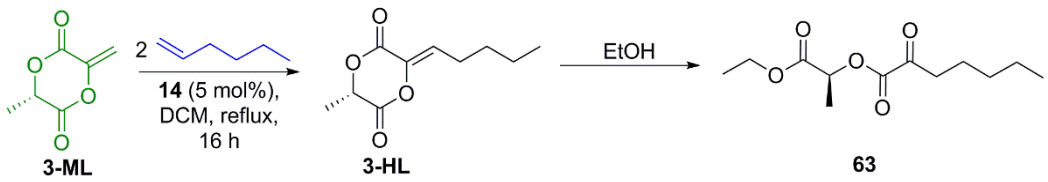

Scheme 2.9 *Formation of 3-HL via olefin CM and subsequent alcoholysis with ethanol.*

ROP of 3-HL would mirror the same degradation pathway as 3-ML, forming non-polymerisable substrates and consumption of the active initiator. To prevent degradation by nucleophilic ring-opening it was hypothesised that hydrogenation of the double bond post metathesis would generate a stable monomer capable of polymerisation. Cossy *et al.* reported a one-pot tandem CM/hydrogenation reaction using **14** and PtO_2 to generate substituted lactones.[26] Based on their work, a one-pot, one-step tandem CM/hydrogenation of 3-ML with dec-1-ene was compared to a one-pot, two-step CM/hydrogenation (**Scheme 2.10**). Analysis by ^{1}H NMR spectroscopy indicated formation of lactide (37 % conversion) during the one-pot, one-step CM/hydrogenation route. CM must be preferential to hydrogenation yielding a higher conversion to the hydrogenated cross product (63 %). The formation of lactide can be accounted for by a few factors, firstly, as the rates of hydrogenation and CM are in competition, 3-ML may undergo hydrogenation at a faster rate than CM. Secondly, a portion of dec-1-ene could also have been hydrogenated, removing its ability to act as a cross partner in CM. Alternatively a one-pot, two-step CM/hydrogenation removed any competition between these reactions and eliminated any formation of lactide. The latter route was chosen moving forward.

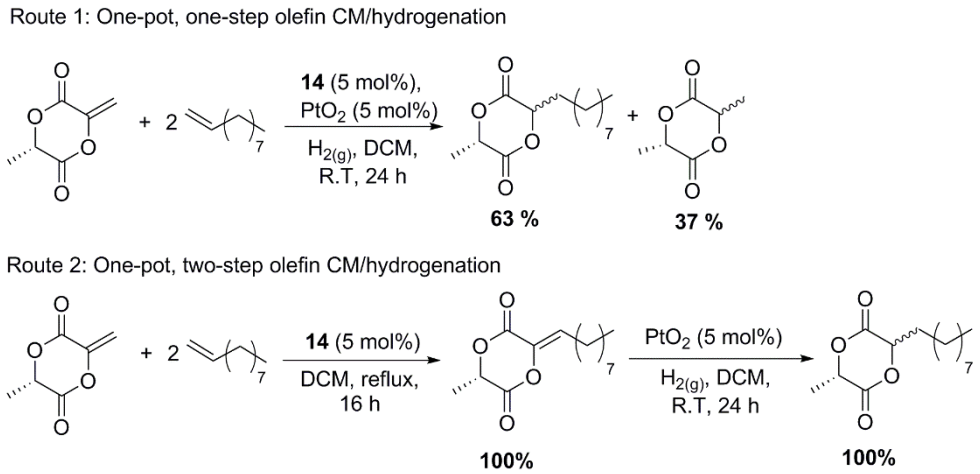

Scheme 2.10 *Comparison of a one-pot, one step cross-metathesis/hydrogenation vs a one-pot two step cross-metathesis/hydrogenation.*

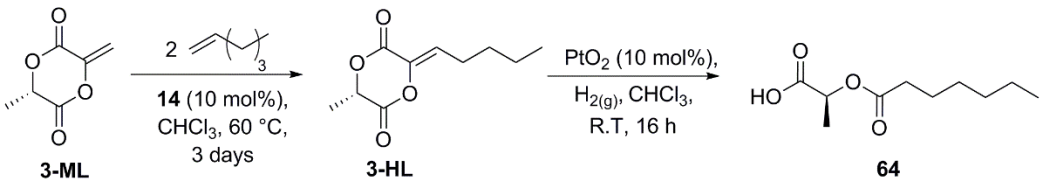

Scheme 2.11 *Olefin cross-metathesis and hydrogenation of 3-ML to yield ring-opened hydrogenated product* ***64****.*

A one-pot, two-step CM/hydrogenation of 3-ML with hex-1-ene was carried out (**Scheme 2.11**). Analysis of the crude product mixture showed disappearance of the characteristic olefin proton of the hex-1-ene functionality of 3-HL, which suggested successful hydrogenation of the olefin moiety. Purification was carried out using column chromatography on silica gel. Unexpectedly, 2D NMR spectroscopy (COSY, HSQC and HMBC) of the isolated product confirmed formation of **64** (**Scheme 2.11**). Comparison of this spectrum to the crude spectra obtained for the above reactions (**Scheme 2.10**) using dec-1-ene contained matching resonances, confirming the same transformation had occurred irrespective of the cross-partner or reaction conditions used. It was theorised that during hydrogenation with PtO_2, β-C-O bond cleavage was promoted followed by sequential hydrogenation to yield **64**. This is an unusual pathway but offers a unique route to synthesise these ring opened derivatives.

To identify whether this pathway was favoured with other hydrogenation catalysts, the reaction was repeated with Pd/C. Analysis identified successful hydrogenation to yield 3-hydogenated hexenyl lactide, (3-HHL) without C-O bond cleavage (**Scheme 2.12**). **Figure 2.5** compares the ^{1}H NMR spectra obtained for the hydrogenation of 3-HL with both PtO_2 and Pd/C. It is evident the characteristic proton (proton **i**, **Figure 2.5**) of the desired hydrogenated product is absent in the reaction using PtO_2. Moreover the characteristic diasterotopic protons (**j**, **Figure 2.5**) support formation of 3-HHL.

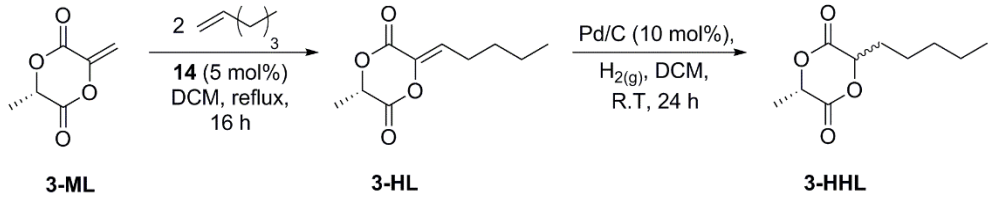

Scheme 2.12 *Hydrogenation of 3-HL with Pd/C to generate 3-HHL.*

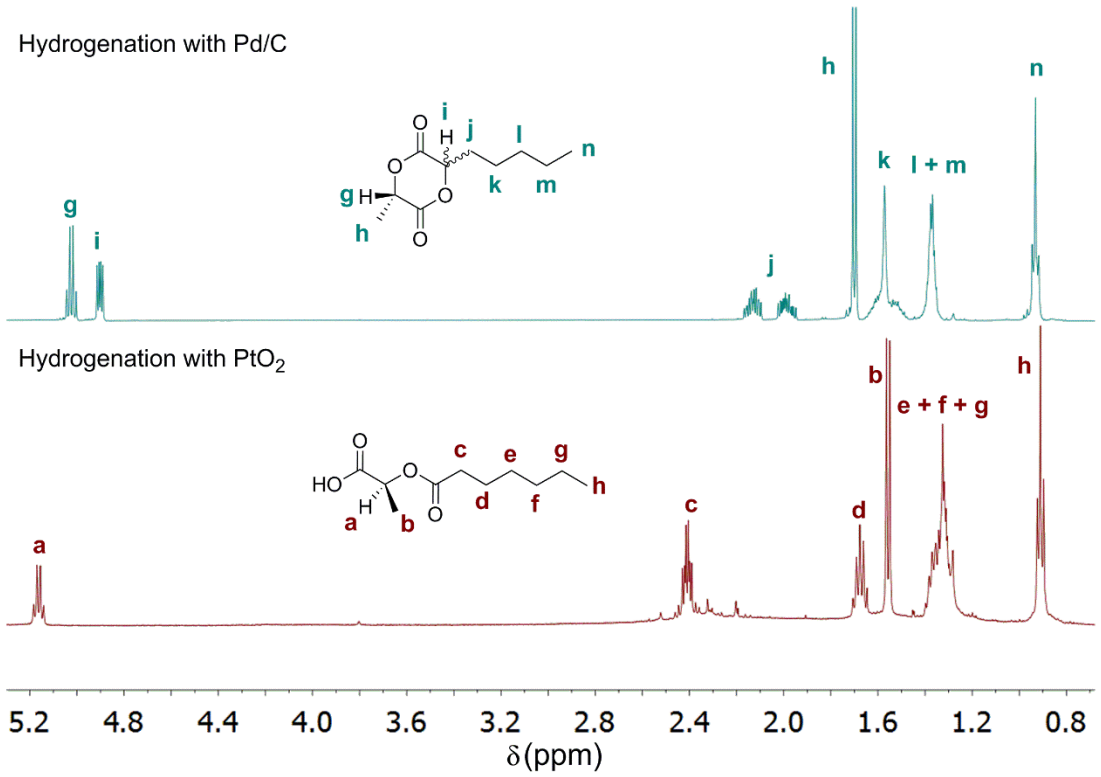

Figure 2.5 *^{1}H NMR spectroscopy comparison of the hydrogenation of 3-HL using PtO_2 and Pd/C*

The results of screening the hydrogenation conditions are shown in **Table 2.6**. Performing the reaction at R.T with a 10 mol% catalyst loading led to a conversion of 77 % (Entry 1). Increasing the reaction temperature to 35 °C increased the conversion to 96

Table 2.6 *Optimisation of the hydrogenation conditions of 3-HL using Pd/C.*

3-HL **3-HHL**

Entry	Pd/C (mol %)	Temperature (°C)	Conversion to 3-HHL (%)[a]
1	10	R.T	77
2	10	35	96
3	7	35	94

[a]Determined by ^{1}H NMR spectroscopy monitored by consumption of the olefin proton of 3-HL and appearance of the new proton alpha to the carbonyl in 3-HHL.

% (Entry 2). Finally, decreasing the catalyst loading to 7 mol% at 35 °C gave almost an identical conversion to using 10 mol% (Entry 3). Thus the conditions used for further hydrogenation were 7 mol% Pd/C, at 35 °C, for 24 hours. Assuming no epimerization of the un-modified methine carbon during both metathesis and hydrogenation, two diastereomeric products can form, (S,S) 3-HHL and (S,R) 3-HHL (**Figure 2.6**). The product mixture was purified *via* column chromatography and ^{1}H NMR spectroscopy revealed the presence of one major product (>98 %). 2D nOe NMR spectroscopy was performed to identify the relative position of proton **c** with respect to either methine **a** or methyl **b**. Cross peaks are evident for the coupling in space of protons **c** and **a**, suggesting that (S,S) 3-HHL is the major diastereomer resulting from the hydrogenation of 3-HL.

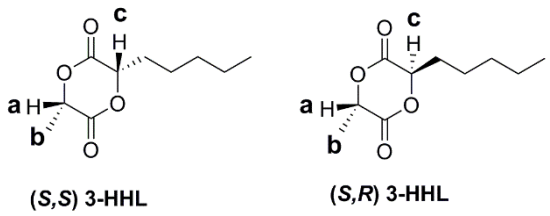

Figure 2.6 *Two diastereomeric products from the hydrogenation of 3-HL.*

2.4.4 Ring-opening polymerisation of 3-hydrogenated hexyl lactide

ROP of 3-HHL was attempted using three different catalysts; TBD **51**, $Sn(Oct)_2$ **52** and aluminium salen **53**. The results are illustrated in **Table 2.7** and confirm all catalysts are active in the ROP of 3-HHL to produce an oily polymer. As expected, this confirms hydrogenation of 3-HL eliminates degradation *via* alcoholysis, generating a stable monomer suitable for polymerisation. Assuming complete conversion the targeted theoretical molecular weight was 10,000 g mol^{-1}. ROP using TBD (Entry 1) is rapid, complete in less than 15 minutes. Polymerisation using $Sn(Oct)_2$ was stopped after 18 hours showing no change in conversion compared to 3 hours previous, reaching 92 % (Entry 2). Similarly, polymerisation using the slowest of the three catalysts aluminium salen was stopped after 24 hours also showing no increase in conversion compared to 3 hours previous with a conversion of 89 % (Entry 3). Dispersity of the polymers generated from TBD (Entry 1) and aluminium salen (Entry 2) are broad, indicating potential

Table 2.7 *Ring-opening polymerisation of 3-HHL under various reactions conditions.*

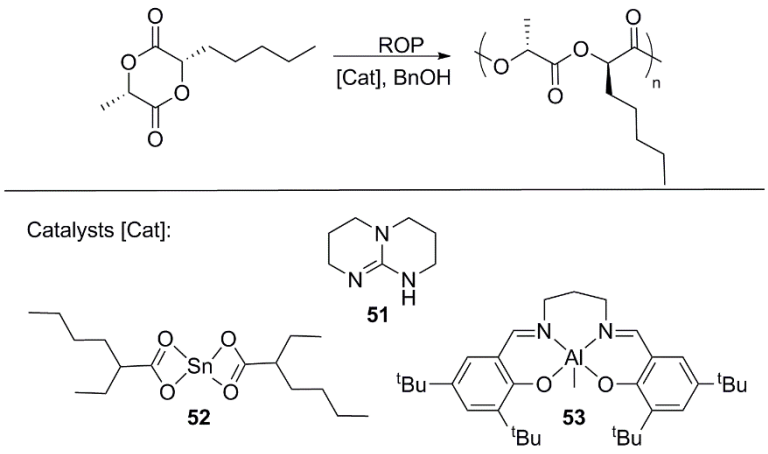

Entry	Cat.	Solvent	Temp. (°C)	Time (h)	Conversion (%)[b]	Đ[c]	M_n (Da)[c]	T_g (°C)
1[a]	**51**	DCM-d_2	R.T	0.25	>99	1.56	6,300	-14
2[a]	**52**	Toluene-d_8	120	18	92	1.29	9,700	1
3[a]	**53**	Toluene-d_8	85	24	89	1.42	4,400	-13

[a]Catalyst: initiator: monomer, 50:1:1. [b]Determined by ^{1}H NMR spectroscopy by comparison of monomer to polymer resonances. [c]Determined by triple detection GPC.

transesterification. ROP with $Sn(Oct)_2$ generated a polymer with molecular weight in good agreement with the theoretical molecular weight and a dispersity narrower than that of the former two catalysts, indicating $Sn(Oct)_2$ is the best choice of catalyst for controlled ROP of 3-HHL.

Thermal analysis of the three polymers was performed using (DSC) **Figure 2.7**. As mentioned earlier, Möller *et al.* previously reported the synthesis of monomer **33** bearing a pentyl group in place of one methyl group in lactide. They report a T_g of -17 °C (for M_n = ~4,600), which is dramatically lower than that of L-lactide (T_g ~60 °C).[6] 3-HHL has a hexyl group incorporated thus a T_g similar to -17 °C was expected. Results indicate the homopolymers formed from reaction with catalysts **51** and **53** (Entries 1 and 3 **Table 2.7**) have a similar T_g that is in close agreement to that observed for monomer **33** of similar M_n. Whereas catalyst **52** produced a homopolymer with a higher T_g of 1 °C, which can be accounted for by its greater M_n (Entry 2). The low T_g is consistent with the introduction of a long flexible chain to induce free motion compared to a small methyl group as seen in lactide which comparatively enables more efficient packing of the polymer chains.

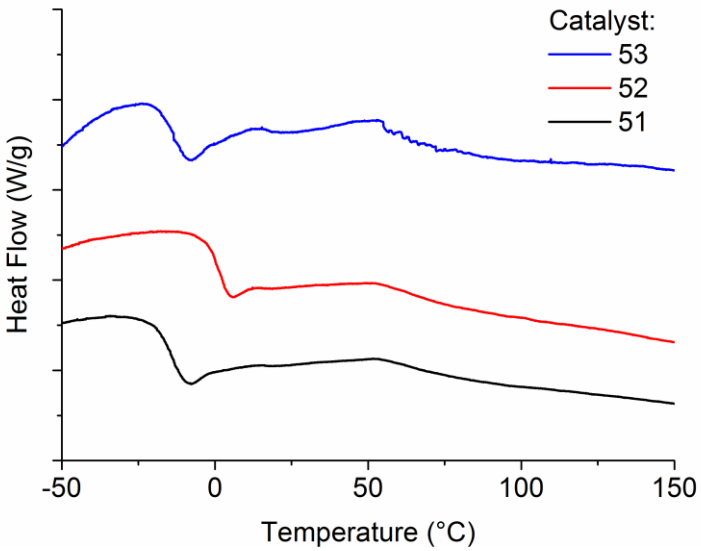

Figure 2.7 *DSC of homopolymers synthesised from catalysts* ***51****,* ***52*** *and* ***53.***

2.5 Conclusions and future work

To conclude, a novel olefin containing derivative of lactide, MML was successfully synthesised. It's metathesis, degradation and polymerisation is summarised in **Scheme 2.13**. Route **a)** demonstrates the optimal conditions explored for the methylenation of lactide using 2 equivalents of the Tebbe reagent, at an addition rate of 0.1ml/min at 0 °C to generate MML to a low isolated yield. To improve the conversion of MML, further optimisation of the methylenation step could be attempted, including fine tuning of the equivalents of the Tebbe reagent and attempting the reaction at a higher concentration. It was discovered that MML undergoes thermal rearrangement to generate **49** (route **b)**) and in its solid state will degrade into volatile by products at room temperature. To fully understand the degradation products of MML, NMR spectroscopy could be used in the presence of an internal standard to monitor the loss of product when exposed to air and heat (>100 °C). ROP of MML was unsuccessful with catalyst **53** (route **c)**). Further screening using alternative catalysts is yet to be tried. Olefin cross-metathesis with itself showed no dimerisation, but CM with Type I olefin hex-1-ene worked efficiently to generate HML (route **d)**), categorising MML as a Type III olefin.

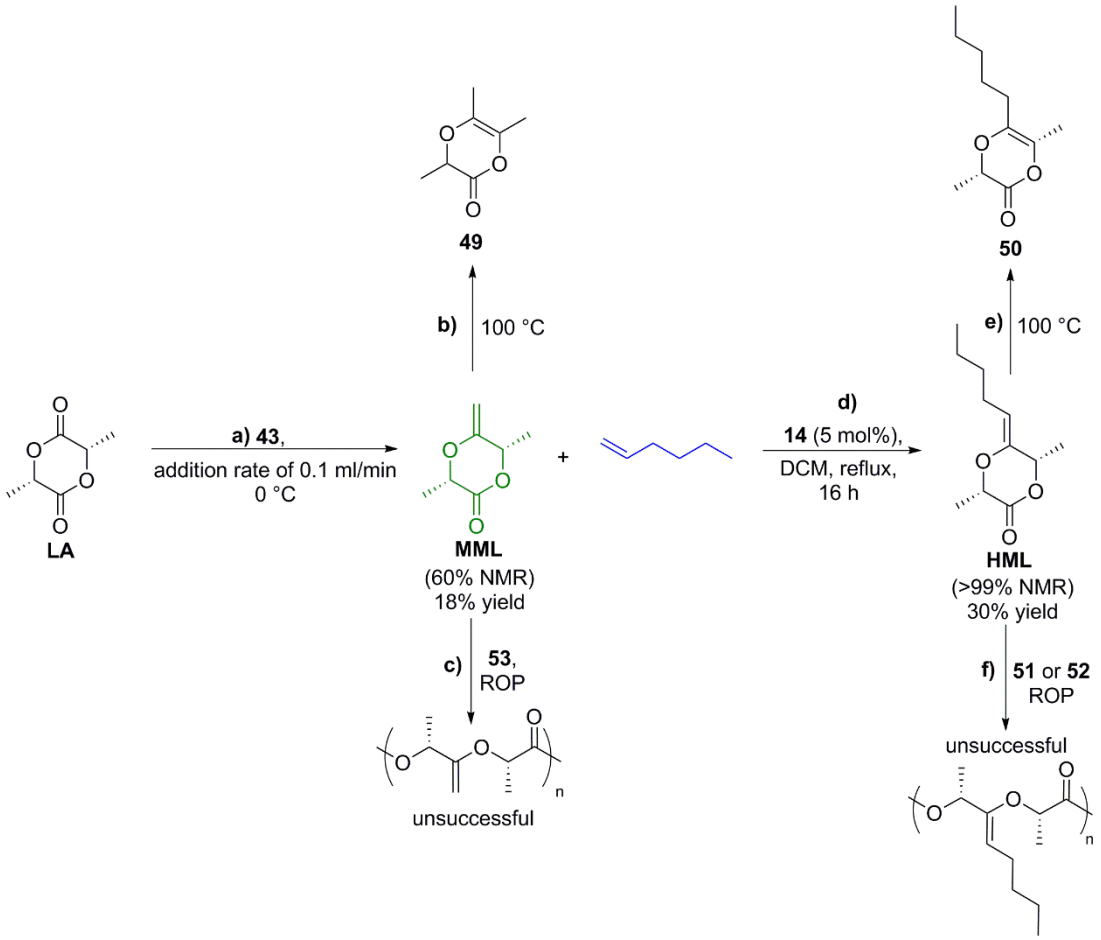

Scheme 2.13 *Summary of the reactions of MML: a) methylenation, b) thermal rearrangement, c) ring-opening polymerisation, d) olefin cross-metathesis, e) thermal rearrangement, f) ring-opening polymerisation.*

To widen the substrate scope of olefin cross-partners other Type I olefins should be tried such as allyltrimethylsilane, 5-hexenyl acetate and longer aliphatic alkenes like dodec-1-ene. HML was also found to undergo thermal re-arrangement but at a slower rate than MML to produce **50** (route **e)**). ROP of HML was attempted using catalysts **51** and **52** but no polymerisation was observed (route **f)**). Catalyst choice and reaction conditions are an area of further research and pre-polymerisation hydrogenation should be investigated.

A second olefin containing derivative of lactide 3-ML, already reported in the literature, was explored as a monomer for polymerisation and CM. Its reactions are summarised in **Scheme 2.14**. Attempted ring-opening polymerisation of 3-ML with an array of catalysts was unsuccessful (route **a)**), however, it was noted this monomer was highly susceptible to alcoholysis and in the presence of methanol, product **57** formed (route **b)**). Its ability

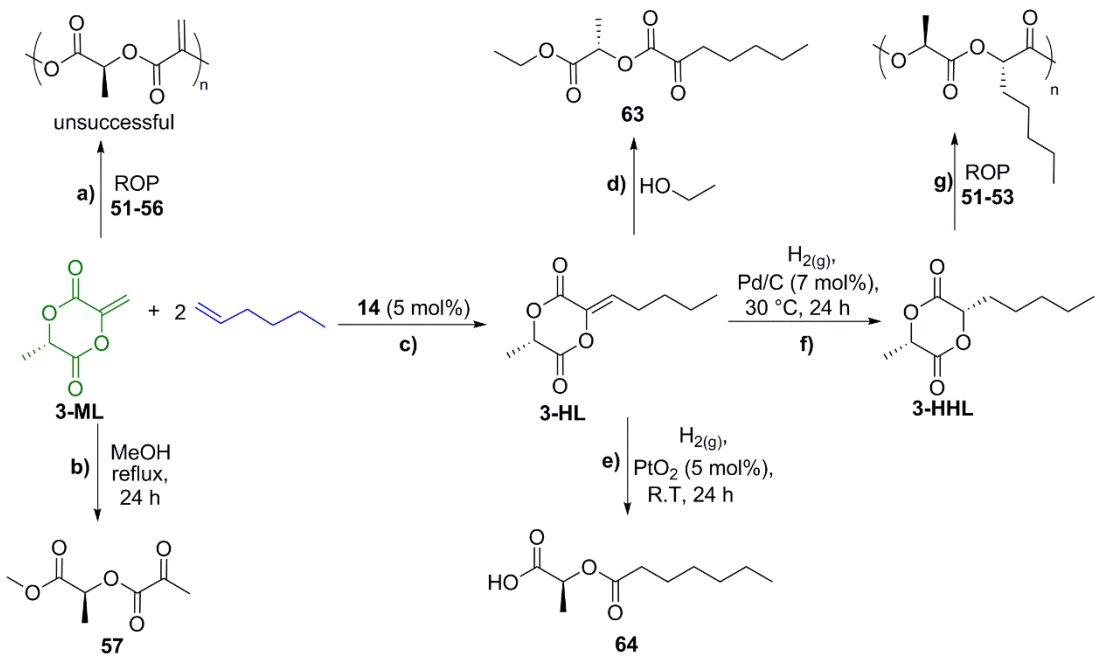

Scheme 2.14 *Summary of the reactions of 3-ML: a) ring-opening polymerisation, b) alcoholysis, c) olefin CM, d) alcoholysis, e) hydrogenation using PtO_2, f) hydrogenation using Pd/C, g) ring-opening polymerisation.*

to react with a range of alcohols led to the synthesis of a family of compounds from reaction of 3-ML with various alcohols and this observation accounted for its inability to polymerise. Olefin CM with itself resulted in no homodimerisation and a wide substrate scope of cross-partners ranging from Type I to Type II olefins were explored. Only long chain aliphatic olefins, hex-1-ene to dodec-1-ene, were incorporated, categorising 3-ML as a Type III olefin. For comparative purposes hex-1-ene was chosen as the cross-partner to generate 3-HL (route **c)**). It was discovered during purification, 3-HL was susceptible to alcoholysis with ethanol to generate **63** (route **d)**). To overcome alcoholysis hydrogenation was investigated using PtO_2 but this catalyst promoted beta-elimination to form **64** (route **e)**). Alternatively Pd/C was capable of generating the desired hydrogenated product (3-HHL) (route **f)**). ROP of 3-HHL was attempted using catalysts **51**-**53** (route **g)**). All catalysts were active in producing a novel functionalised derivative of PLA. Thermal analysis indicated the polymers had associated T_g's of 1 °C and below, consistent with the introduction of a long flexible chain, which would be expected to reduce T_g.

Testing should be carried out in order to identify what effect hex-1-ene incorporation has on the polymers mechanical properties such as its Young's Modulus and elongation to break. This polymer may have the potential to act as a plasticiser during PLA synthesis to

help overcome PLA's inherent brittleness. 3-HHL could be copolymerised with lactide to form random and block structures and its effect on PLA's thermal and mechanical properties should be tested. The product from olefin CM of 3-ML with 5-hexenyl acetate should be isolated in order to examine and compare its properties to hex-1-ene incorporation.

2.6 References

(1) Becker, J. M.; Pounder, R. J.; Dove, A. P. *Macromol. Rapid Commun.* **2010**, *31* (22), 1923–1937.

(2) Yin, M.; Baker, G. L. *Macromolecules* **1999**, *32* (23), 7711–7718.

(3) Simmons, T. L.; Baker, G. L. *Biomacromolecules* **2001**, *2* (3), 658–663.

(4) Tianqi, L.; Simmons, T. L.; Bohnsack, D. A.; Mackay, M. E.; Smith, M. R.; Baker, G. L. *Macromolecules* **2007**, *40* (17), 6040–6047.

(5) Jing, F.; Smith, M. R.; Baker, G. L. *Society* **2007**, *40*, 9304–9312.

(6) Trimaille, T.; Möller, M.; Gurny, R. *J. Polym. Sci. Part A Polym. Chem.* **2004**, *42* (17), 4379–4391.

(7) Saulnier, B.; Coudane, J.; Garreau, H.; Vert, M. *Polymer* **2006**, *47* (6), 1921–1929.

(8) Leemhuis, M.; Akeroyd, N.; Kruijtzer, J. A. W.; van Nostrum, C. F.; Hennink, W. E. *Eur. Polym. J.* **2008**, *44* (2), 308–317.

(9) Marcincinova-Benabdillah, K.; Boustta, M.; Coudane, J.; Vert, M. *Biomacromolecules* **2001**, *2* (4), 1279–1284.

(10) Borchmann, D. E.; Brummelhuis, N.; Weck, M. *Macromolecules* **2013**, *46*, 4426–4431.

(11) Kalelkar, P. P.; Alas, G. R.; Collard, D. M. *Macromolecules* **2016**, *49* (7), 2609–2617.

(12) Scheibelhoffer, A. S.; Blose, W. A.; Harwood, H. *J. Polym. Prepr. (Am. Chem. Soc., Div. Polym. Chem.)* **1969**, *10*, 1375–1380.

(13) Jing, F.; Hillmyer, M. A.; Chen, L.; Qin, D. Y.; Cramer, C. J.; Yao, L.; Young, V. G. *J. Am. Chem. Soc* **2008**, *130*, 13826–13827.

(14) Fiore, G. L.; Jing, F.; Young, Jr., V. G.; Cramer, C. J.; Hillmyer, M. A. *Polym. Chem.* **2010**, *1* (6), 870–877.

(15) Fuoco, T.; Finne-Wistrand, A.; Pappalardo, D. *Biomacromolecules* **2016**, *17* (4), 1383–1394.

(16) Tebbe, F. N.; Parshall, G. W.; Reddy, G. S. *J. Am. Chem. Soc* **1978**, *100* (11), 3611–3613.

(17) Schiøtt, B.; Jørgensen, K. A. *J. Chem. Soc., Dalton Trans.* **1993**, No. 2, 337–344.

(18) Hartley, R.; McKiernan, G. *J. Chem. Soc. Perkin Trans. 1* **2002**, 2763–2793.

(19) Hughes, D. L.; Payack, J. F.; Cai, D.; Verhoeven, T. R.; Reider, P. J. *Organometallics* **1996**, *15* (2), 663–667.

(20) Lee, J. B.; Ott, K. C.; Grubbs, R. H. *J. Am. Chem. Soc* **1982**, *104*, 7491–7496.

(21) Chatterjee, A. K.; Choi, T. L.; Sanders, D. P.; Grubbs, R. H. *J. Am. Chem. Soc.* **2003**, *125* (37), 11360–11370.

(22) Hormnirun, P.; Marshall, E. L.; Gibson, V. C.; Pugh, R. I.; White, A. J. P. *Proc. Natl. Acad. Sci. U. S. A.* **2006**, *103* (42), 15343–15348.

(23) Hormnirun, P.; Marshall, E. L.; Gibson, V. C.; White, A. J. P.; Williams, D. J. *J. Am. Chem. Soc.* **2004**, *126* (9), 2688–2689.

(24) Miyake, G. M.; Zhang, Y.; Chen, E. Y. X. *J. Polym. Sci. Part A Polym. Chem.* **2015**, *53* (12), 1523–1532.

(25) Samojłowicz, C.; Bieniek, M.; Grela, K. *Chem. Rev.* **2009**, *109* (8), 3708–3742.

(26) Cossy, J.; Bargiggia, F.; Bouzbouz, S. *Org. Lett.* **2003**, *5* (4), 459–462.

Chapter 3. Olefin Cross-Metathesis of β-Heptenolactone and its Copolymers with Lactide

3.1 Polyhydroxyalkanoates

Polyhydroxyalkanoates (PHA's) are a family of biodegradable, biologically-synthesised polyesters that accumulate in strains of bacteria as an intracellular carbon and energy reserve (**Figure 3.1**).[1] Due to the stereo specificity of the biosynthetic enzymes used for PHA synthesis, all monomers are found in their R-configuration. Poly((R)3-hydroxybutyrate), P((R)3HB), is the most explored of the family of PHA's; it is a hydrophobic, highly crystalline, thermoplastic polymer that has commercial significance as a biodegradable plastic under the brand name Biopol (**Figure 3.1**).[2] Yet, bulk industrial biosynthesis of P((R)3HB) is not economically viable and cannot currently compete with petroleum derived polymers.[2] Chemical synthesis offers an alternative route to P(3HB) with a range of microstructures. One route of emerging importance is the ROP of β-butyrolactone (β-BL) (**Figure 3.1**). The inherent ring strain associated with four-membered rings makes its synthesis challenging,[3] however, ring-expansion carbonylation of epoxides has been shown to generate an array of functionalised β-lactones.[3]

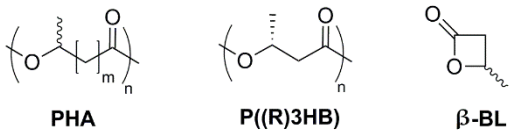

Figure 3.1 *Left: poly(hydroxyalkanoate) (PHA), middle: poly((R)3-hydroxybutyrate) P((R)3HB), right: β-butyrolactone (β-BL).*

3.1.1 Carbonylation of epoxides to β-lactones

Catalyst development has aided the success of epoxide carbonylations. Alper *et al.* first reported the use of $[((C_6H_5)_3P=)_2N]Co(CO)_4$ in the presence of a Lewis acid $BF_3.Et_2O$ to catalyse the carbonylation of epoxides to excellent yields with trace amounts of regio-isomers.[4] Carbonylation reactions can give rise to competing side-products such as regio-isomers, ketones and polyesters, as observed in the earlier work of Drent and co-workers.[5] Coates, the leader in catalyst design for the carbonylation of epoxides to lactones, based his system off the following ion pair $[Lewis\ Acid]^+[Co(CO)_4]^-$ and proposed the following mechanism shown in **Scheme 3.1**.[3] The first step involves epoxide coordination and activation by a Lewis acid, with attack of $Co(CO)_4^-$ to the less hindered carbon. Next, the epoxide ring-opens and CO inserts into the C-Co bond, which is followed by ring-closing to re-generate the active catalyst and yield the corresponding β-lactone. Inversion of configuration is generally observed at the site of attack, which is indicative of an S_N2-type process.

Coates developed a series of Lewis acid catalysts, including aluminium- and titanium-based catalysts **65** and **66**, respectively (**Figure 3.2**). Both catalysts demonstrate regio-selective carbonylation of both epoxides and aziridines.[6] **65** was also used in the double

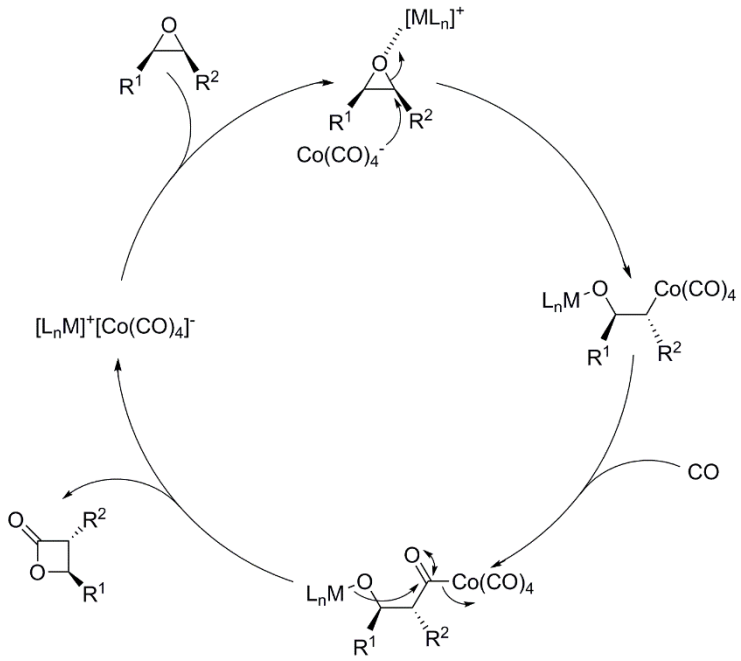

Scheme 3.1 *Catalytic cycle for the carbonylation of epoxides.*

carbonylation of epoxides to form succinic anhydrides.[7] These catalysts were joined by a more active chromium catalyst **67**, which allows carbonylation of both mono- and bicyclic epoxides.[3] Modification of the porphyrin framework led to the formation of **68**, which displays an even higher activity than **67**, leading to expansion in the substrate scope to include epoxides with ester and amide side chains.[8] The authors hypothesised the associated increase in activity with **68** was attributed in part to its higher solubility. The aforementioned processes require high temperatures (~60 °C) and pressures (200-900 psi). To produce a more practical and less expensive process, Coates demonstrated the successful carbonylation of 1,2-epoxybutane using catalyst **69** at room temperature and 1 atm of CO. Moreover, no trace of ketone was observed (an unwanted side product that is dominant at low temperatures).[9] Thus catalyst development for carbonylation reactions has successfully expanded the scope of available PHA's.

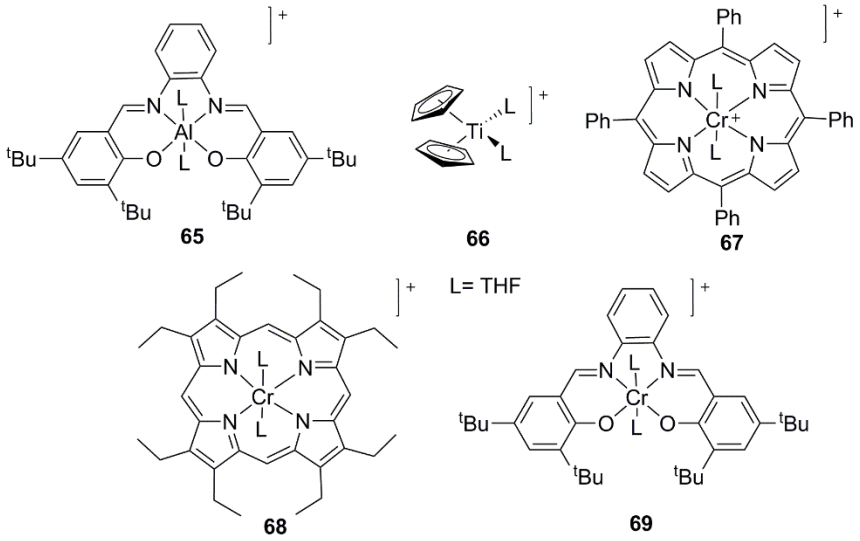

Figure 3.2 *Lewis acid carbonylation catalysts.* ***65*** *aluminium(salph),* ***66*** *titanium cyclopentadienyl,* ***67*** *and* ***68*** *chromium porphyrin,* ***69*** *chromium(salph).*[3,6-9]

3.1.2 Ring-opening polymerisation and modification of β-lactones

Bacteria mediated polymerisation gives rise to only isotactic (R)-P(3HB), thus an added advantage of chemical synthesis of P(3HB) is the ability to control the polymer microstructure. Racemic β-BL has been polymerised to generate atactic P(3HB)[10] and also

syndiotactically enriched P(3HB) from a chain-end control mechanism.[11,12] More recently, Thomas and Coates *et al.* reported sequential syndiospecific polymerisation of enantiomerically pure but different β-lactones to generate polymers of an alternating monomer sequence.[13]

Co-polymerisation of β-BL with biodegradable monomers, ε-caprolactone and lactide has been reported to generate random and block copolymers with unique properties.[14–16] More recently, Shaver *et al.* expanded the scope of β-lactones in the synthesis of ABA block copolymers with L-lactide to investigate the effect of alkyl chain length on microphase separation. The authors compared β-BL to β-valerolactone (β-VL) and β-heptanolactone (β-HAL) (**Scheme 3.2**). They discovered for ABA block polymers (with a middle lactone block), β-BL and β-VL gave a single T_g at all compositions where as β-HAL produced two T_g's when the blocks contained similar degrees of polymerisation. This is indicative of phase separation, which was confirmed by small- and wide-angle X-ray scattering.[17]

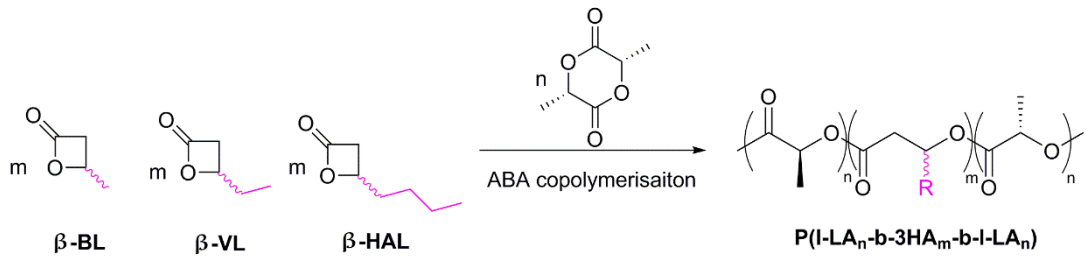

Scheme 3.2 *ABA block copolymers of L-LA with β-lactones.*[17]

Carbonylation of epoxides allows the preparation of functionalised β-lactones including olefin containing β-lactones. The olefin moiety is attractive as it offers the possibility of modification *via* both pre- and post-polymerisation techniques to alter the properties of the corresponding polymer. One such example is β-heptenolactone (β-HL), which is synthesised *via* the carbonylation of 1,2-epoxy-5-hexene (**Scheme 3.3**).[9]

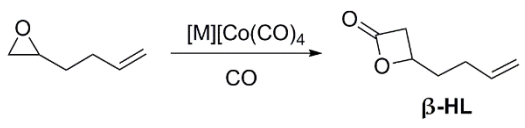

Scheme 3.3 *Synthesis of β-Heptenolactone (β-HL) via the carbonylation of 1,2-epoxy-5-hexene.*[9]

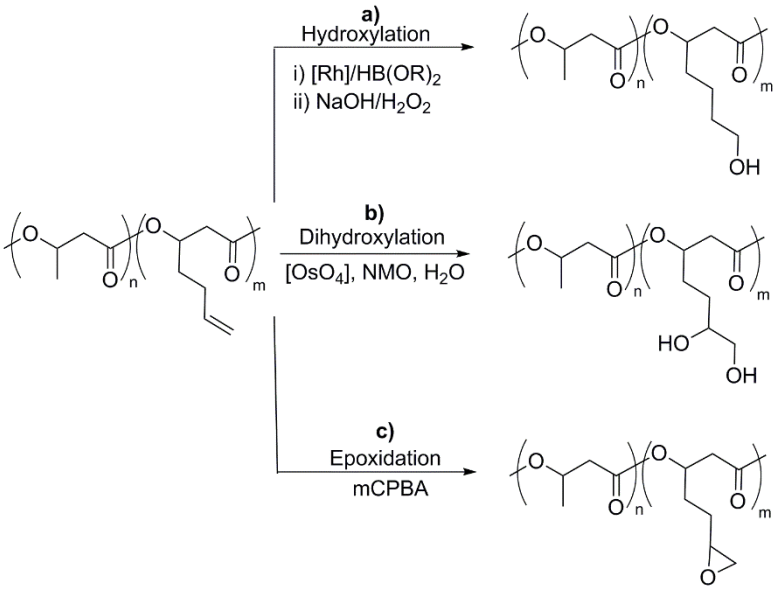

Scheme 3.4 *Modification of copolymers of β-BL and β-HL: a) hydroxylation, b) dihydroxylation and c) epoxidation.*[18]

ROP of rac-β-HL was first reported by Carpentier *et al.* in 2009 using an yttrium-amido complex.[18] The authors generated syndiotactic homo- and random copolymers of β-HL with β-BL. The latent olefin functionality allowed for the modification of the copolymers containing up to 11 mol% β-HL *via* hydroxylation, dihydroxylation and epoxidation (routes **a)**, **b)** and **c) Scheme 3.4**). Thermal analysis indicated homopolymer poly(β-heptenolactone) (P(β-HL)) is an amorphous material with a T_g of -44 °C. Copolymers with β-BL gave higher T_g's than P(β-HL), however modification of the allyl functionality had only a minor influence on the thermal properties of the copolymers.

Carpentier *et al.* investigated the effect of hydroboration on the olefin moiety of P(β-HL).[19] Pre-polymerisation hydroboration was successful but resulted in a non-polymerisable monomer. Conversely, post-polymerisation hydroboration worked and dramatically increased the T_g of the polymer from <-44 °C to -4 °C (**Scheme 3.5**).

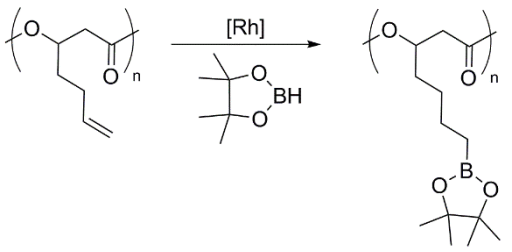

Scheme 3.5 *Hydroboration of P(β-HL).*[19]

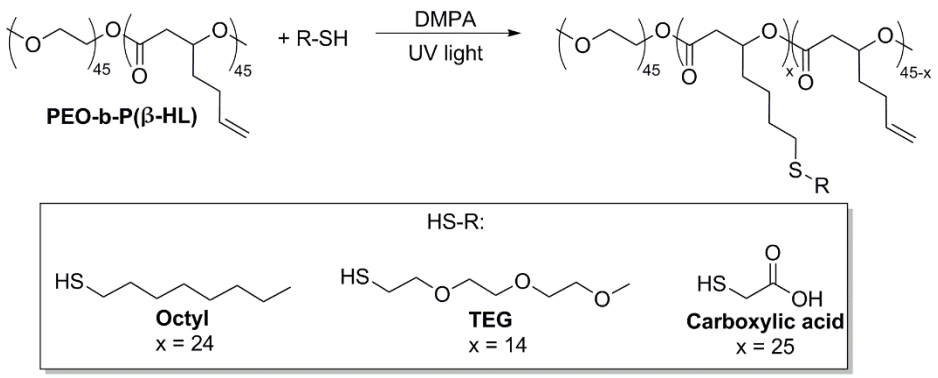

Scheme 3.6 *Thiolene addition of PEO-b-P(β-HL) with octyl, TEG and carboxylic acid thiols.*[20]

More recently, in 2017, Gillies and Shaver *et al.* synthesised block copolymers of ethylene oxide (EO) and β-HL (PEO-b-P(β-HL)) using an aluminium salen catalyst.[20] The authors used thiolene chemistry to functionalise the copolymer and monitor the effect this had on both its thermal properties and self-assembly. They incorporated and compared octyl, triethylene glycol (TEG) and carboxylic acid functional groups (**Scheme 3.6**). Although none of the reactions resulted in complete modification of the olefin moieties, analysis by DSC showed incorporation of the carboxylic acid inhibited crystallisation of the PEO block, producing a copolymer with no T_m. In regards to morphology, octyl incorporation gave "worm like" assemblies while TEG and carboxylic acid incorporation produced small nanoparticles. The authors also demonstrated successful thiolene addition of an anti-cancer therapeutic and a fluorophore.

As discussed, various olefin transformations have been used to alter the properties of P(β-HL) and its copolymers but olefin CM is an alternative modification strategy yet to be explored. Furthermore, copolymerisation of β-HL with lactide presents the possibility of modifying the properties of PLA.

3.2 Olefin cross-metathesis of β-hepteneolactone and its homopolymer

3.2.1 Pre-polymerisation olefin cross-metathesis

Two strategies can be used to modify the olefin moiety of β-HL; pre-polymerisation olefin CM or post-polymerisation olefin CM. Initial research focussed on pre-polymerisation

olefin CM which offers the advantage of preparing a fully functionalised polymer, which is not always accessible *via* post-polymerisation modification. β-HL was prepared in good yields and short reaction times *via* the carbonylation of 1,2-epoxy-5-hexene with chromium catalyst **5** using a modified literature procedure.[9]

Olefin-Type determination was carried out in order to identify the reactivity and substrate scope accessible to β-HL. Hoveyda-Grubbs second generation catalyst **14**, was chosen for all CM reactions due to its high functional group tolerance. Self-metathesis of β-HL was carried out (**Scheme 3.7**) and analysis by ^{1}H NMR spectroscopy showed disappearance of original olefin protons **e** and **f** and appearance of new olefin protons **g** belonging to the dimer (**Figure 3.3**). According to Grubbs' model,[21] this categorises β-HL as either a Type II olefin that is able to homodimerise but the dimers formed are only sparingly consumed in a second CM reaction. Otherwise it can be categorised as a Type I olefin which undergoes rapid homodimerisation and the dimers formed are readily consumed in a second CM reaction. To probe its reactivity further the dimer of β-HL was subject to a second CM reaction with a less reactive Type II olefin, 3-butene-2-one (**Scheme 3.7**). This olefin should preferentially react with the dimer (if the dimer is a Type I olefin) as opposed to react with itself. Successful CM with > 95 % incorporation of 3-butene-2-one was evidenced by disappearance of dimer protons **g** and appearance of new protons **h** and **I,** associated with the newly formed cross-product (**Figure 3.3**). This experiment suggests β-HL can be categorised as a reactive Type I olefin.

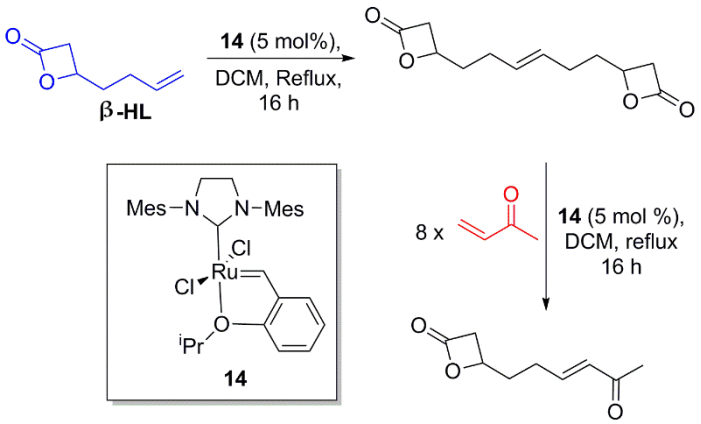

Scheme 3.7 *Olefin Type determination of β-HL. Homodimerisation followed by reaction with a Type II olefin 3-butene-2-one.*

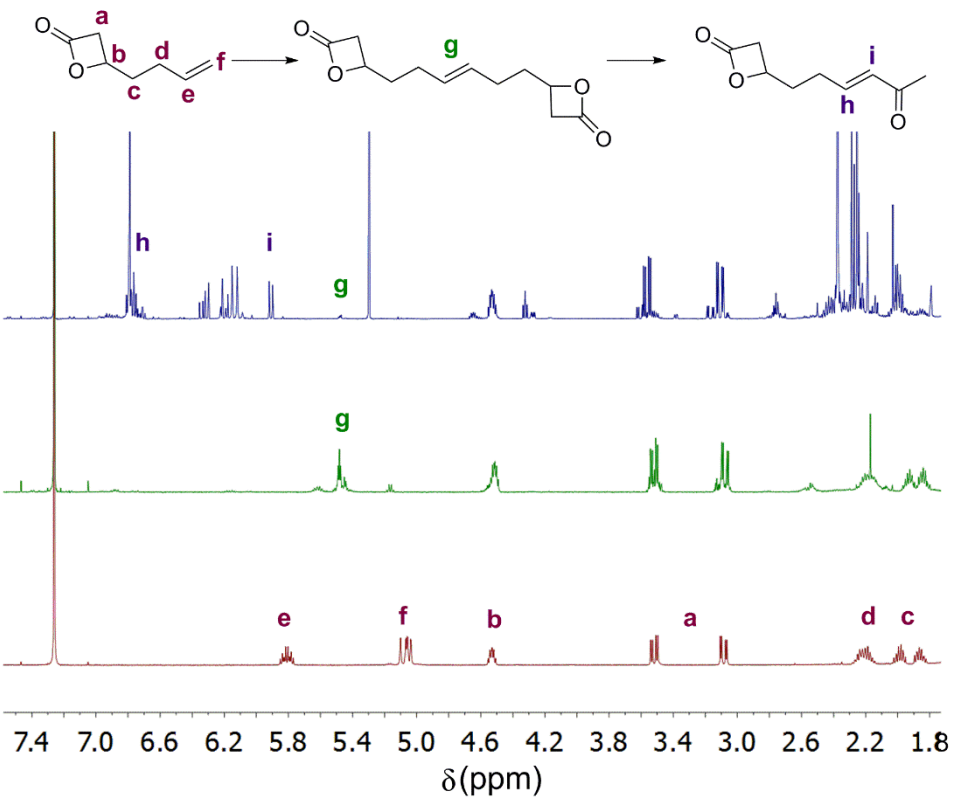

Figure 3.3 *^{1}H NMR spectroscopy comparing the homodimerisation of β-HL and its corresponding olefin cross-metathesis with Type II olefin 3-butene-2-one.*

The high reactivity of β-HL enabled CM with a wide substrate scope of cross-partners ranging from Type I to Type III olefins. A large excess (5-10 equivalents) was used in order to promote high levels of functional group incorporation (**Scheme 3.8**). However, percentage incorporation was difficult to monitor by ^{1}H NMR spectroscopy due to the range of metathesis products present in the mixture. This included unreacted β-HL, the homodimer of β-HL, unreacted cross-partner, the homodimer of the cross-partner and the desired cross-product. Moreover purification of the products by column

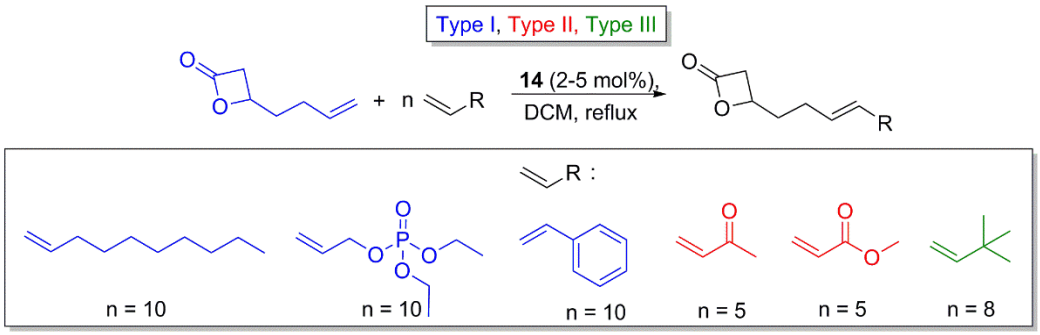

Scheme 3.8 *Olefin cross-metathesis of β-HL with Type I-Type III olefins.*

chromatography was problematic due to the similar retention times of the aforementioned metathesis products across an array of eluents.

Olefin CM of β-HL with the Type II olefins, methyl acrylate and 3-butene-2-one both gave rise to characteristic olefin resonances in the ^{1}H NMR spectra belonging to the cross-products. Thus, determination of conversion of these olefins was viable and in both cases CM led to full functional group incorporation. Consequently, the CM of β-HL with methyl acrylate was chosen for attempted purification by column chromatography. Purification was successful but required two successive columns to isolate a clean sample of the cross-product **70**, **Scheme 3.9**, which possessed high stereoselectivity (trans:cis, 97:3) (**Figure 3.4**).

ROP of **70** was mediated by aluminium salen catalyst **53**. Polymerisation was slow reaching 93 % conversion in 27 hours to give polymer **71** (**Scheme 3.9**). The observed slow rate is consistent with the ROP of other long chain β-propiolactones, as previously reported by Shaver using the same catalytic system.[17] Analysis by GPC revealed a M_n of 4,200, which was much lower than the theoretical molecular weight of 18,400, with an associated broad Đ of 1.65. This lack of control suggests transesterification dominated over controlled propogation giving rise to a broad dispersity. This is potentially due to competing non-productive coordination of the acrylate functionality to the Lewis acidic aluminium centre, suppressing the control and thus leading to enhanced transesterification. The low molecular weight, which cannot be accounted for by transesterification, suggests the presence of a chain transfer agent such as water. Although

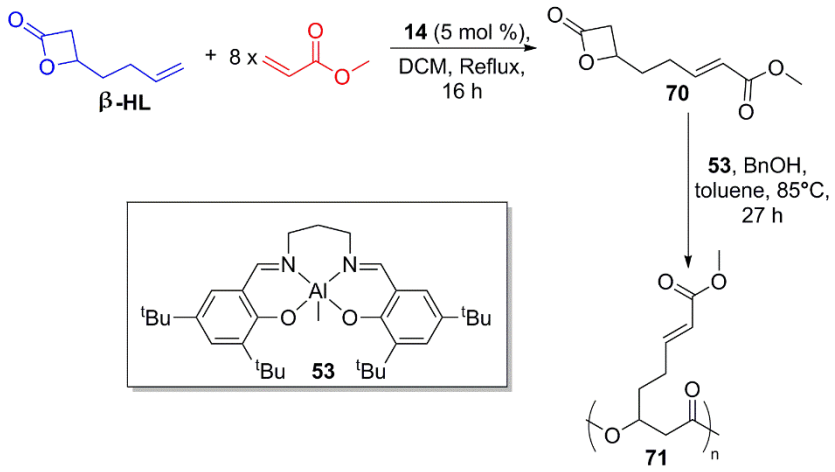

Scheme 3.9 *Olefin cross-metathesis of β-HL with methyl acrylate followed by ROP (monomer:Catalyst:BnOH, 100:1:1).*

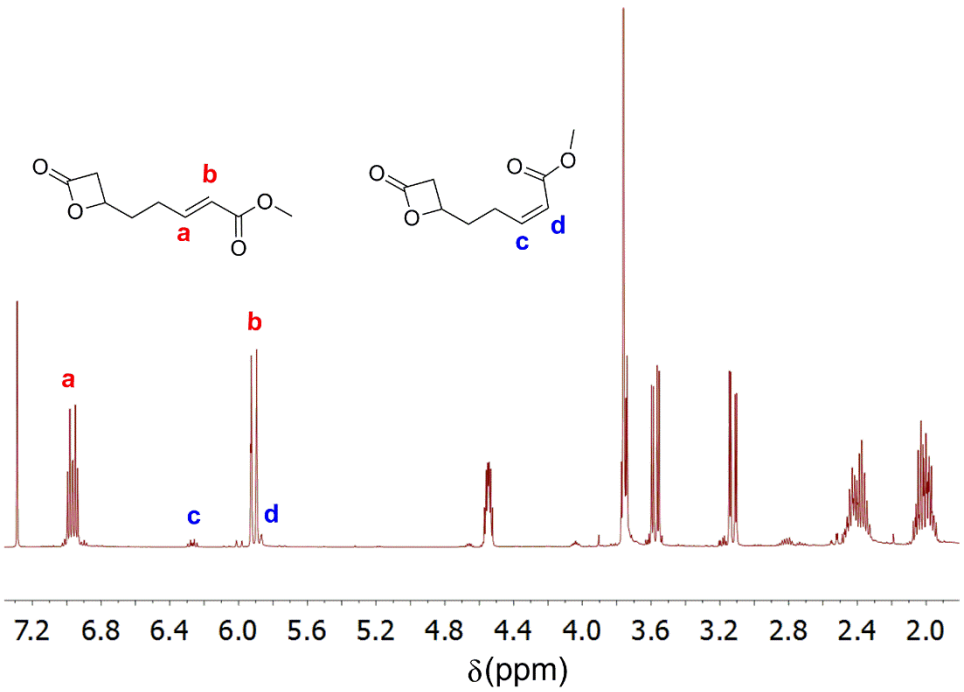

Figure 3.4 *^{1}H NMR spectrum of the trans- and cis-products obtained in the olefin cross-metathesis of β-HL with methyl acrylate.*

NMR spectroscopy showed the monomer to be pure, trace impurities may have been present below the detectable limit.

The synthesis of **70** represents one of only a handful of monomers functionalised by olefin CM that is used in subsequent polymerisation. While pre-polymerisation olefin CM is a promising route to functionalise β-HL, challenges with both monomer purification and polymerisation control led to no further optimisation. Attention was focussed on post-polymerisation olefin CM.

3.2.2 Post-polymerisation olefin cross-metathesis

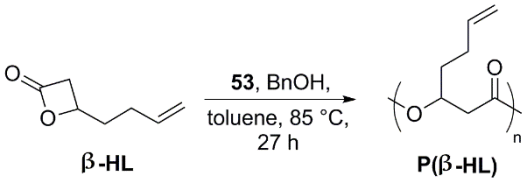

Scheme 3.10 *ROP of β-HL to generate P(β-HL) (monomer:catalyst:BnOH, 100:1:1).*

Homopolymerisation of β-HL was mediated by aluminium salen, **53**, at 85 °C for 27 hours in the presence of BnOH initiator to generate P(β-HL) (**Scheme 3.10**). Kinetic data

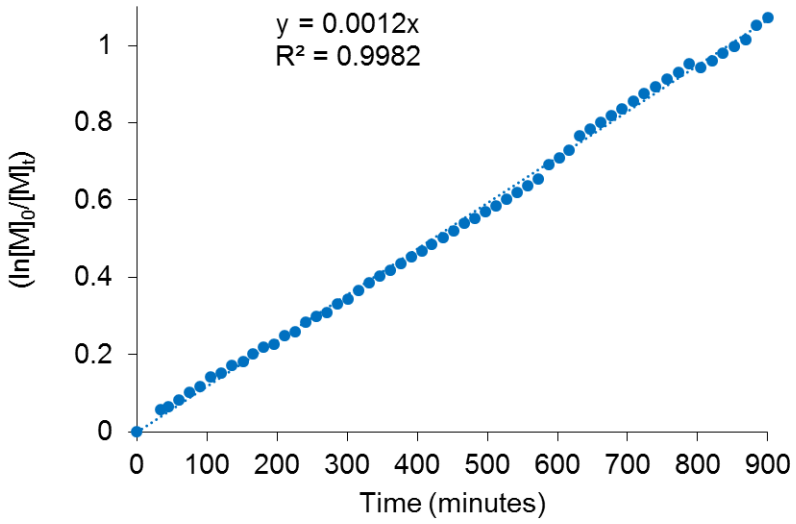

Figure 3.5 *Plot of ln($[M]_0/[M]_t$) versus time for the homopolymerisation of β-HL in C_6D_6.*

reveals the reaction follows first-order kinetics for monomer conversion, indicative of a controlled polymerisation and is complete within ~14 hours (**Figure 3.5**). In contrast to monomer **70**, the polymerisation was well controlled. GPC analysis indicated a molecular weight in good agreement to the theoretical molecular weight ($M_{n,theo}$ = 12,700 $M_{n,GPC}$ = 12,100) and a narrow Đ of 1.09. Although kinetic data highlights the reaction is complete within 14 hours it is evident by the obtained molecular weight and Đ of P(β-HL) that limited transesterification occurs when the polymer is left to react for extended periods of time.

β-HL was categorised as a reactive Type I olefin thus its corresponding polymer should be of similar reactivity. Olefin CM of P(β-HL) was investigated with a large excess (x 8) of two cross-partners of different Types; methyl acrylate (Type II olefin) and 1,2-epoxy-5-hexene (Type I olefin) to synthesise polymers **72** and **73** respectively (**Table 3.1**) P(β-HL) is an amorphous oil with no observed T_m, consequently precipitation of the polymer post-metathesis was not possible. While column chromatography was problematic for functionalised monomer **70**, it proved effective for the purification of polymers **72** and **73**. Non-polymer metathesis products were flushed out the column leaving the polymers attached to the silica. Using methanol washings, the polymers were extracted and isolated *via* filtration. Analysis by ^{1}H NMR spectroscopy identified that both methyl acrylate and 1,2-epoxy-5-hexene gave complete incorporation of the new functionality into the polymer (**Figure 3.6**). Consumption of the parent olefin protons **a** and **b** was observed

Table 3.1 *Analysis of the polymers obtained from olefin cross-metathesis of P(β-HL) with two cross-partners.*

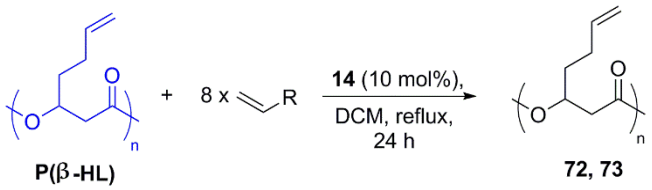

Entry	Polymer	R	Conv. (%)[a]	M_n (Da)[b]	Đ[b]	$T_{5\%}$ (°C)[c]	T_{max} (°C)[c]	T_g (°C)[d]
1	**P(β-HL)**	none	>99	12,100	1.09	265	289	-38
2	**72**	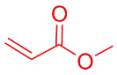	>99	13,400	1.84	216	254	-13
3	**73**	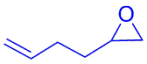	>99	11,300	1.42	230	262	10

[a]Determined by ^{1}H NMR spectroscopy monitored by consumption of P(β-HL) olefin protons and appearance of cross-product protons. [b]Determined by GPC analysis, conventional calibration uncorrected vs polystyrene standards. [c]Determined by thermal gravimetric analysis. [d]Determined by differential scanning calorimetry

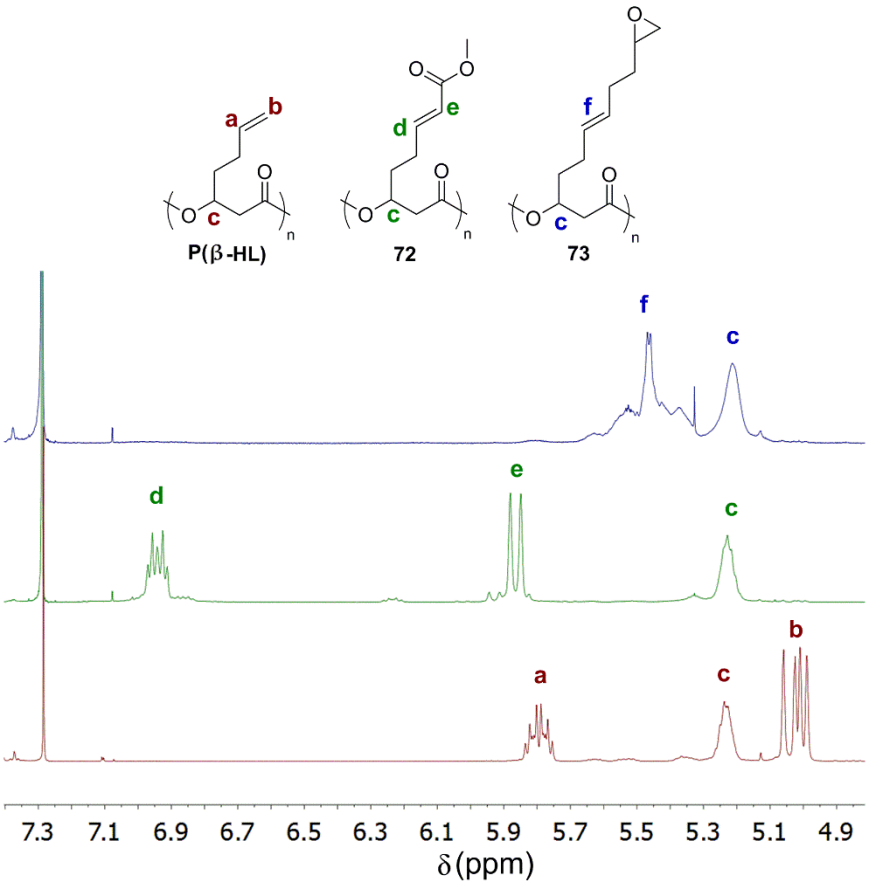

Figure 3.6 *Overlay of ^{1}H NMR spectra of P(βHL) and its functionalised polymers* ***72*** *and* ***73*** *synthesised via the olefin cross-metathesis with methyl acrylate and 1,2-epoxy-5-hexene.*

and new olefin protons **d-f** appeared corresponding to the functionalised polymers. It was noted that a small portion of cis-product was observed in the spectrum of polymer **72**.

GPC analysis indicated a notable increase in Đ for polymers **72** and **73**, particularly for methyl acrylate incorporation, **72** (**Table 3.1**, compare Entries 2 and 3). This suggests a small amount of cross-linking (polymer self-metathesis) may be occurring, that was undetectable by ^{1}H NMR spectroscopy. The long chain of the epoxide could hinder approach of another polymer chain, limiting polymer cross-linking, consistent with the largest increase in Đ being observed for methyl acrylate incorporation. Self-metathesis of P(β-HL) was investigated by reaction with itself in the presence of **14**, but the reaction formed an insoluble cross-linked network that was unable to be analysed by conventional means.

The M_n obtained by GPC analysis showed an insignificant increase post-metathesis functionalisation (Entries 2 and 3 **Table 3.1**). This reflects a negligible change in hydrodynamic volume, a result seen previously in the literature for other functionalised polyester containing olefins.[22]

To understand the significance of functional group incorporation on the properties of the functionalised polymers, thermal analysis was performed using both thermal gravimetric analysis (TGA) and differential scanning calorimetry (DSC), as illustrated in **Table 3.1**. TGA shows both methyl acrylate and 1,2-epoxy-5-hexene induced a significant decrease in the onset thermal degradation temperature ($T_{5\%}$). A decrease of 49 °C and 35 °C in $T_{5\%}$ was observed for polymers **72** and **73** respectively (**Table 3.1** and **Figure 3.7**). Derivative thermogravimetry (DTG) depicts the temperature at which degradation rate is fastest, T_{max}. This also decreased significantly by 35 °C and 27 °C for polymers **72** and **73** respectively (**Table 3.1** and **Figure 3.8**). These results indicate functional group incorporation aids thermal degradation of P(β-HL) by reducing $T_{5\%}$ and T_{max}. It was hypothesised that upon heating, side group elimination may occur first to help promote chain scission and thus decrease the temperature required to degrade the polymer backbone. The shape of the curve of polymer **73** in **Figure 3.7** shows two distinct mass loss processes, the first of which corresponds to ~40 % mass loss. The weight of the epoxide functional group relative to the polymer backbone accounts for ~40 % of the

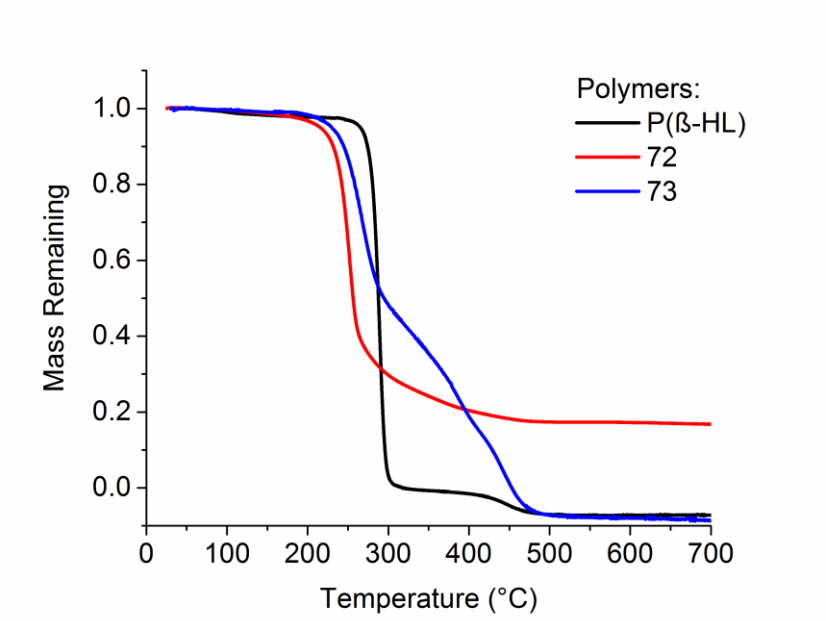

Figure 3.7 *TGA comparison of P(β-HL) to functionalised polymers* ***72*** *and* ***73****.*

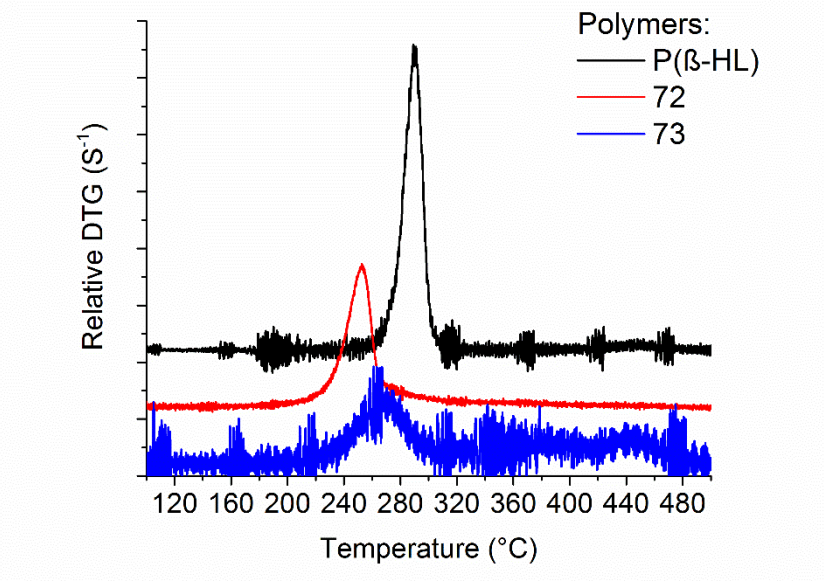

Figure 3.8 *DTG overlay of P(β-HL) with functionalised polymers* ***72*** *and* ***73****.*

polymer mass. Thus this observation supports the theory of side chain group elimination prior to decomposition of the polymer backbone.

DSC identified a substantial increase in the T_g of P(β-HL) (T_g = -38 °C) by 25 °C and 48 °C for polymers **72** and **73** respectively (**Table 3.1** and **Figure 3.9**). The long, flexible, pendent olefin arm of P(β-HL) contributes to its low T_g. Incorporation of methyl acrylate

introduces steric bulk, decreasing bond rotation and likely accounts for the observed increase in T_g. Introduction of a cyclic moiety as seen with 1,2-epoxy-5-hexene could enhance chain stiffness, which can account for its large increase in T_g. Thermal analysis of the functionalised polymers demonstrate olefin CM can serve as an effective tool for altering the properties of P(β-HL). With this knowledge in hand the copolymerisation of β-HL with lactide was explored to enable a viable route to modify the properties of PLA.

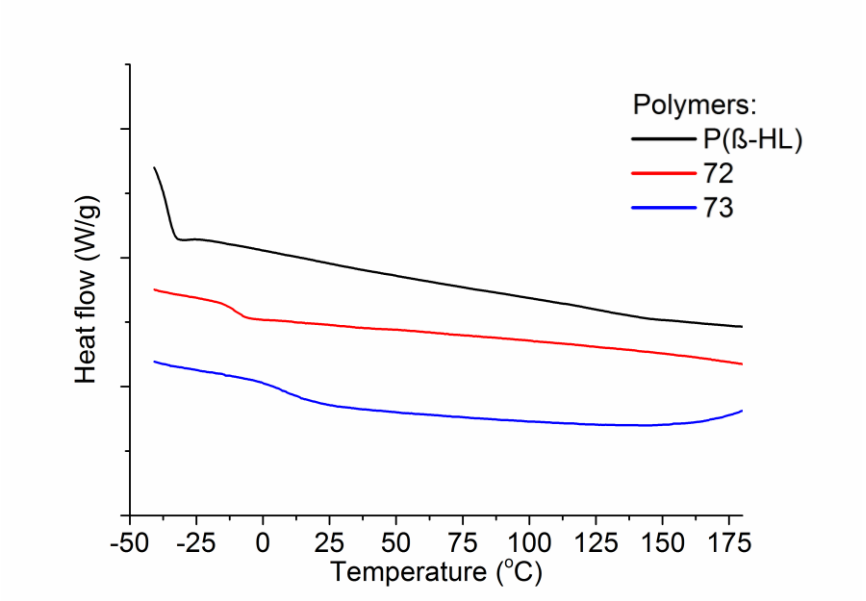

Figure 3.9 *DSC comparison of P(β-HL) to functionalised polymers* ***72*** *and* ***73****.*

3.3 Copolymerisation of lactide with β-heptenolactone

3.3.1 Synthesis of poly(LA_{86}-co-β-HL_4)

The aim was to target a copolymer of L-lactide and β-HL containing minimal β-HL incorporation, at a level that still produced a change in polymer properties upon functionalisation *via* olefin CM. The initial target was to synthesise a copolymer with a ratio of LA:β-HL of 90:10 (P(lactide$_{90}$-co-β-heptenolactone$_{10}$), P(LA_{90}-co-β-HL_{10})) (**Table 3.2**). The rate of polymerisation of LA is ten times greater than that of β-HL (**Figure 3.10**), thus a gradient copolymer is expected to form upon simultaneous monomer addition. Initial reactions were left for 21 hours using catalyst **53** and BnOH initiator (**Table 3.2**). Analysis of the crude ^{1}H NMR spectrum revealed complete

Table 3.2 *Effect of reaction time on the physical properties of the co-polymerisation of lactide with β-HL.*

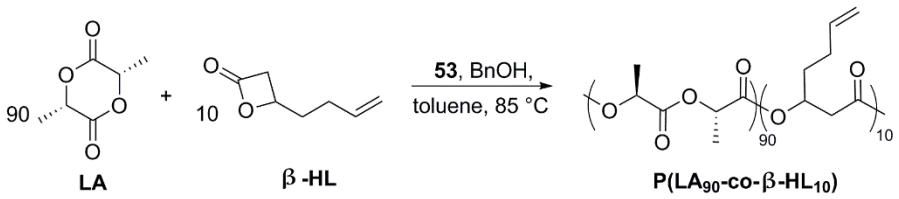

LA β -HL $P(LA_{90}\text{-co-}\beta\text{-}HL_{10})$

Entry	Time (h)	Conv. (%)[a]	Mn (Da)[b]	Đ[b]
1	24	>99	14,800	1.40
2	6	76	15,000	1.13

[a] Conversion of β-HL to P(β-HL) determined by ^{1}H NMR spectroscopy monitored by comparison of monomer to polymer resonances. [b]Determined by triple detection GPC analysis.

conversion of lactide and β-HL but the Đ obtained by GPC was broad (1.40) suggesting significant transesterification (Entry 1, **Table 3.2**). The reaction was repeated for a shorter reaction time of 6 hours, however, the conversion to P(β-HL) dropped to 76 % and the Đ remained above 1.1 (Entry 2, **Table 3.2**). As discussed previously ROP of β-HL mediated by **54** demonstrates good control and the Đ remains narrow even when the reaction is left up to 10 hours past full monomer consumption. The broad Đ (**Table 3.2**) was unexpected, particularly in the case of Entry 2 with incomplete conversion of β-HL.

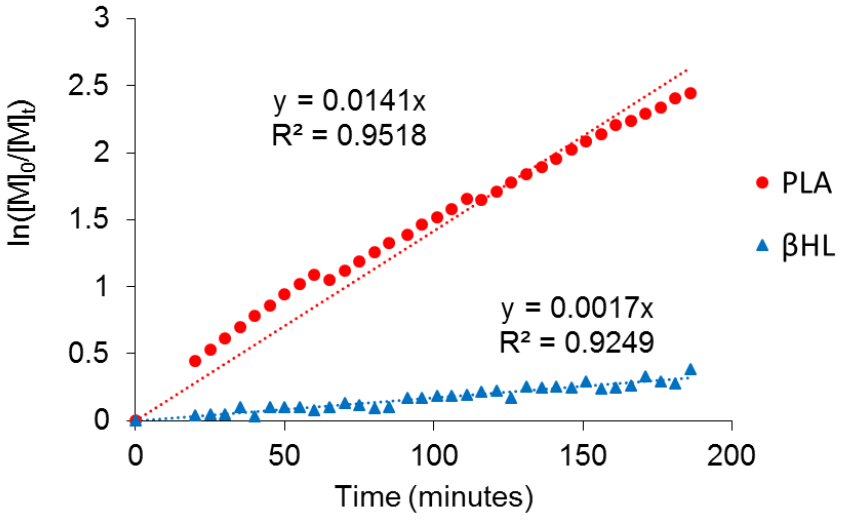

Figure 3.10 *Plot of ln($[M]_0/[M]_t$) versus time for the copolymerisation of lactide with β-HL in C_6D_6.*

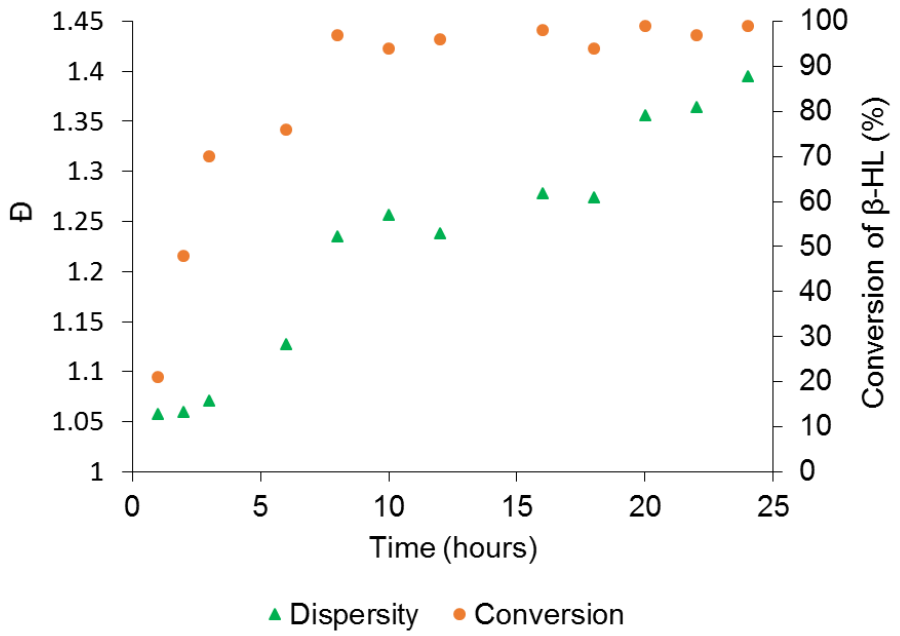

Figure 3.11 *Comparing Đ of P(LA-co-β-HL) with conversion of β-HL vs time.*

To further probe the unexpectedly broad Đ's, a series of identical copolymerisation reactions were carried out and quenched at various reaction times (between 1 hour and 24 hours), **Figure 3.11**. Conversion to P(β-HL) in the copolymer (determined by analysis of the crude sample by ^{1}H NMR spectroscopy) versus time was plotted against its corresponding Đ (determined by triple detection GPC). It can be seen that the Đ of the copolymer remains low for the first 3 hours with a P(β-HL) conversion of ~70 %, but Đ gradually increases as reaction time and conversion increases.

From the kinetic data in **Figure 3.10**, it is evident LA polymerisation to PLA is complete within 3 hours, which corresponds to the same time frame as the low Đ's in **Figure 3.11**. This data suggests that once LA is consumed, the rate of transesterification competes with the rate of β-HL insertion. To maintain a narrow Đ copolymer, the reaction was quenched after 2.5 hours to produce P(LA$_{86}$-co-β-HL$_4$), the first example of a copolymer of LA with

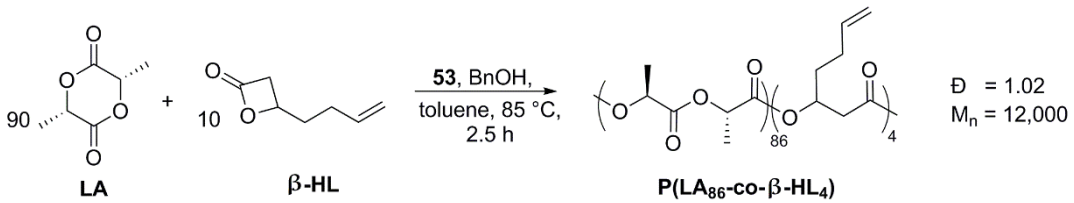

Scheme 3.11 *Copolymerisation of LA with β-HL to synthesise P(LA$_{86}$-co-β-HL$_4$).*

β-HL, **Scheme 3.11**. A LA:β-HL ratio of 86:4 was determined by calculating the % conversion of each polymer unit in the crude ^{1}H NMR spectrum and relating this to the ratio initially incorporated. GPC analysis by triple detection indicated a controlled polymerisation generating a narrow Đ polymer (1.02).

3.3.2 Olefin cross-metathesis of poly(LA$_{86}$-co-β-HL$_4$)

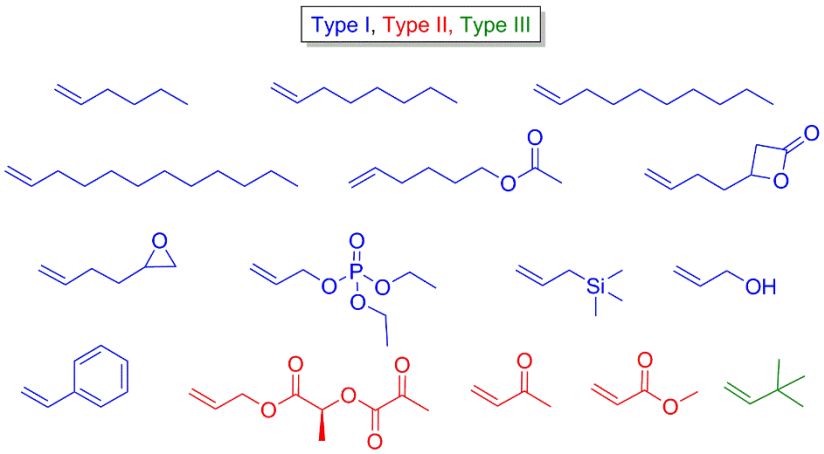

Figure 3.12 *Olefin cross-partners used in olefin Cross-metathesis reactions of copolymers of LA with β-HL.*

Due to the semi-crystalline nature of the PLA segment within P(LA$_{86}$-co-β-HL$_4$), precipitation of this polymer and its functionalised derivatives post-metathesis was possible in cold methanol. This was advantageous compared to P(β-HL), which required column chromatography to isolate the functionalised polymers from the non-polymer metathesis products. The ease of isolation combined with the high reactivity of the β-HL segment within the copolymer enabled a large substrate scope of cross-partners to be explored (**Figure 3.12**). This included Type I to Type III olefins, encompassing alkyl, acrylate, lactone, epoxide, phosphonate, silyl, alcohol and styrene functionalities.

The allyl ester dione **59**, **Scheme 3.12**, is a novel olefin that was synthesised from the

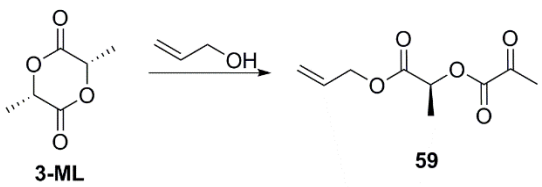

Scheme 3.12 *Alcoholysis of 3-ML to generate novel olefin **59** used as a cross-partner in olefin cross-metathesis.*

Table 3.3 *Thermal and physical properties of P(LA$_{86}$-co-β-HL$_4$) post olefin cross-metathesis functionalisation with Type I- Type III olefins.*

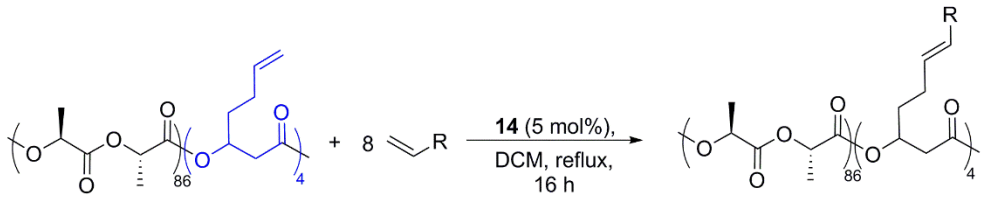

Entry	R	M_n (Da)[a]	Đ[a]	$T_{5\%}$ (°C)[b]	T_{max} (°C)[b]	T_g (°C)[c]	T_c (°C)[c]	T_m (°C)[c]
1	none	12,000	1.02	308	352	55	90	157
2		14,800	1.02	304	360	54	92	156
3		22,000[d]	1.47[d]	302	362	54	90	157
4		11,400	1.02	308	368	55	88	157
5		12,700	1.06	287	351	51	86	157
6	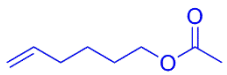	12,300	1.03	n.d	n.d	50	82	157
7	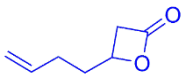	14,000	1.03	262	369	54	91	156
8	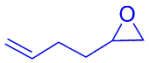	20,500[d]	1.33[d]	226	364	55	93	157

9	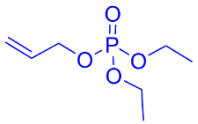	12,300	1.01	317	370	54	89	157
10	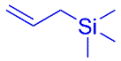	13,900	1.02	215	371	57	93	158
11	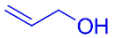	16,400	1.42	n.d	n.d	57	91	156
12	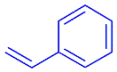	13,000	1.04	308	370	59	93	157
13	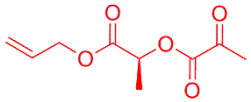	16,200	1.20	304	367	57	94	156
14		17,300	1.01	310	371	n.d	n.d	n.d
15	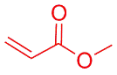	16,800	1.07	305	370	53	n.o	157
16		12,300	1.04	295	365	n.d	n.d	n.d

[a]Determined by triple detection GPC analysis. [b]Determined by thermal gravimetric analysis. [c]Determined by differential scanning calorimetry. [d]Determined by conventional calibration uncorrected vs polystyrene standards. n.o. = not observed. n.d. = not determined.

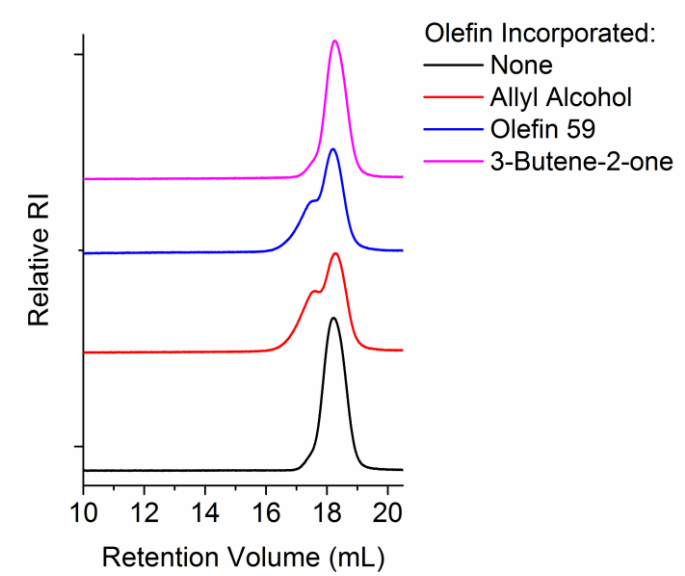

Figure 3.13 *GPC comparison of refractive index of copolymers functionalised with various olefins.*

alcoholysis of 3-ML, as discussed in Chapter 2. This olefin is able to homodimerise but not to completion, likely categorising it as a Type II olefin.

CM of P(LA_{86}-co-β-HL_4) was carried out using a large excess of cross-partner (~8 equivalents) with 5 mol % of **14**. The physical and thermal properties of the resulting functionalised polymers are displayed in **Table 3.3**. GPC analysis illustrates that the majority of functionalised polymers display narrow Đ's (<1.1), suggesting no chain degradation and minimal polymer cross-linking. Copolymers functionalised with allyl alcohol (Entry 11) and olefin **59** (Entry 13) have associated broad Đ's (1.42 and 1.20 respectively) and high M_n's. Upon analysis of the GPC traces (**Figure 3.13**), unimodal traces were not observed as seen in the case of 3-butene-2-one incorporation (representative of the traces obtained for incorporation of the other cross-partners). Instead, a high molecular weight shoulder was present for both allyl alcohol and olefin **59** incorporation, indicating potential cross-linking which can account for the observed broad Đ's and high M_n's. As seen with the homopolymer P(β-HL), there is no observable increase in molecular weight post olefin CM. The low percentage incorporation of β-HL in the copolymer made it difficult to accurately quantify incorporation of the functional groups by ^{1}H NMR integration. However, the resulting thermal properties as observed by TGA and DSC (Entries 2-16, Table 3.3) indicate a clear change compared to the parent copolymer (Entry 1). TGA shows a dramatic decrease in $T_{5\%}$ for both epoxide (Entry 8)

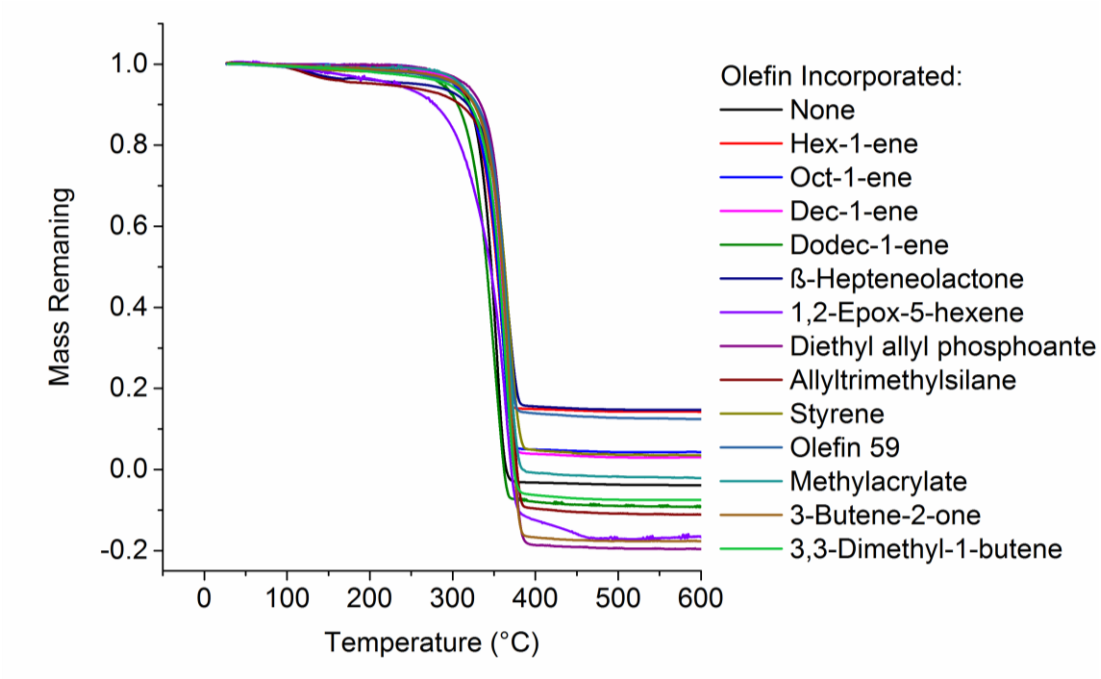

Figure 3.14 *TGA of functionalised P(LA$_{86}$-co-β-HL$_4$).*

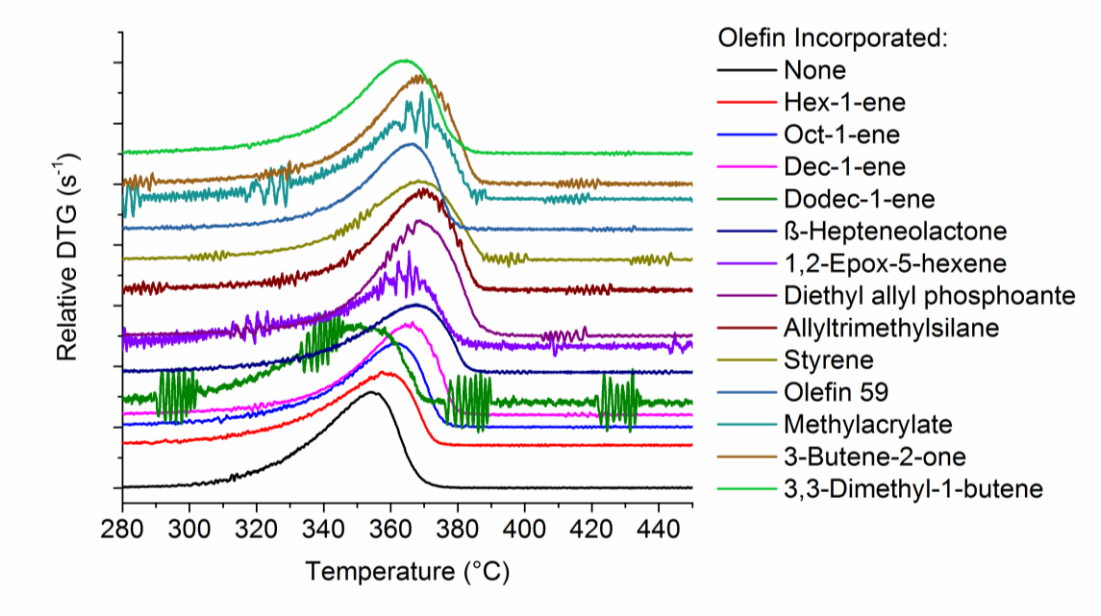

Figure 3.15 *DTG of functionalised P(LA$_{86}$-co-β-HL$_4$).*

and allyltrimethylsilane (Entry 10) incorporation, decreasing by 82 °C and 93 °C respectively (**Figure 3.14**). It can be observed that some of the functionalised polymers display a remaining mass that may be accounted for by minor cross-linking. Moreover, some of the polymers display a mass loss below zero which was attributed to recycled pans for analysis.

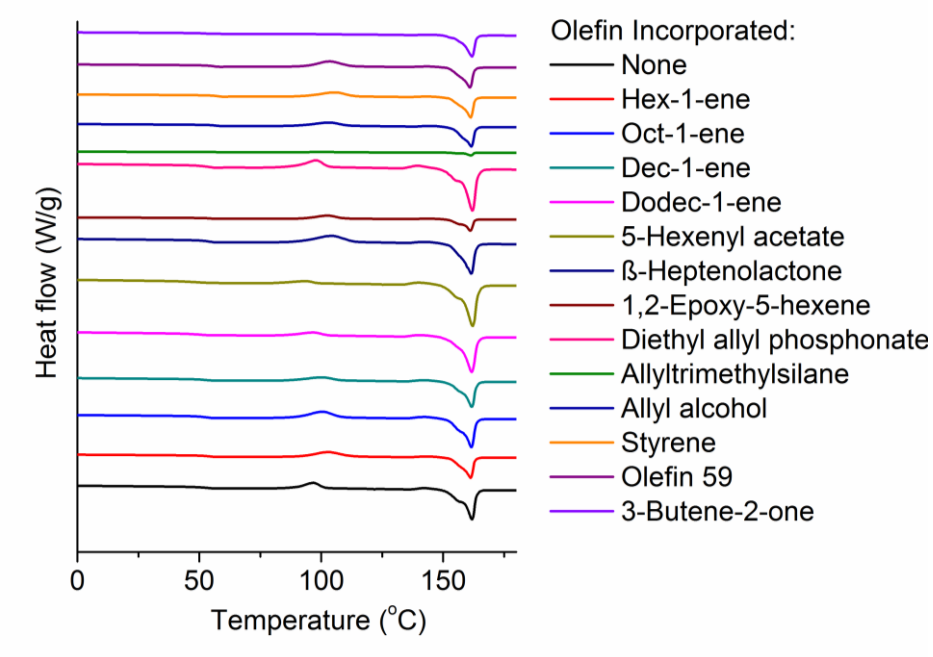

Figure 3.16 *DSC of functionalised P(LA$_{86}$-co-β-HL$_4$).*

DTG displays an increase in T_{max} by 8-19 °C for almost all samples, highlighting that a higher temperature and thus more energy is required for maximum weight loss of the functionalised copolymers, compared to non-functionalised P(LA$_{86}$-co-β-HL$_4$) (**Table 3.3** and **Figure 3.15**).

DSC shows that a minimal change in T_g was observed for all functionalities (**Figure 3.16**). Incorporation of styrene led to the largest increase in T_g, by 4 °C (Entry 12, **Table 3.3**). This is consistent with the introduction of a rigid aromatic ring, which will induce stiffness and minimise rotation within the copolymer. The lowest T_g copolymers are associated with the long alkyl chains, dodec-1-ene and 5-hexenyl acetate (Entries 5 and 6 respectively), which promote flexibility and rotation. The biggest change in T_c was observed with 5-hexenyl acetate incorporation that resulted in a decrease in T_c by 8 °C (Entry 5). Similarly, an increase in alkyl chain length from hex-1-ene through to dodec-1-ene, gave rise to a decrease in T_c (compare Entries 2-5), while minimal change is observed in T_m across the olefin cross-partners.

3.3.3 Olefin cross-metathesis of poly(LA_{85}-co-β-HL_{19})

Functional group incorporation altered the thermal properties of P(LA_{86}-co-β-HL_4) with only a small number of β-HL units present. To monitor whether increasing the incorporation of β-HL could lead to a greater impact on the thermal properties, a copolymer was sought with an increased quantity of β-HL. Consequently, a copolymer with a LA:β-HL ratio of 85:15 was targeted. With the knowledge that stopping the

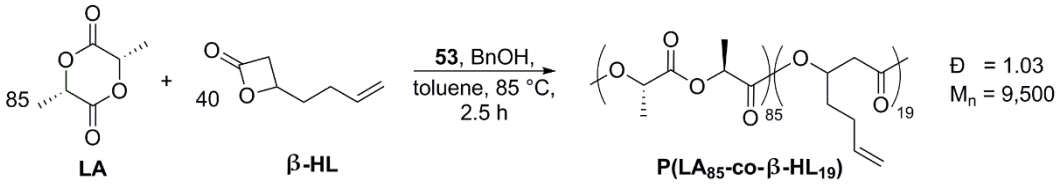

Scheme 3.13 *Copolymerisation of LA with β-HL to generate P(LA_{85}-co-β-HL_{19}).*

copolymerisation after 2.5 hours results in ~ 40 % β-HL conversion to P(β-HL), an excess of β-HL was added into the polymerisation mixture to yield the targeted ratio. For example, a targeted LA:β-HL ratio of 85:15 involved the addition of 85:40 equivalents of LA:β-HL. Analysis by crude ^{1}H NMR revealed ~48 % conversion to P(β-HL), thus 48 % of the 40 equivalents added initially yields 19 repeat units of P(β-HL). Full conversion of LA to PLA was observed, thus a novel copolymer P(LA_{85}-co-β-HL_{19}) was generated (**Scheme 3.13**).

Olefin CM of P(LA_{85}-co-β-HL_{19}) was carried out using the same olefin cross-partners shown in **Figure 3.12** using 5 mol% **14** with an excess of cross-partner. The physical and thermal properties are displayed in **Table 3.4**. The higher incorporation of β-HL in P(LA_{85}-co-β-HL_{19}) compared to P(LA_{86}-co-β-HL_4) enabled functional group incorporation to be estimated from peak integrations by ^{1}H NMR spectroscopy. Type I olefins gave incomplete incorporation of the functional groups into the polymer (**Table 3.4**, Entries 2 -12). In order to try and react the remaining parent olefins, these polymers (excluding allyl alcohol) were precipitated and subject to a second metathesis. Reactions used the same olefin cross-partner but a higher catalyst loading of 10 mol%. Under these conditions copolymers containing hex-1-ene and 1,2-epoxy-5-hexene (Entries 2 and 8 respectively) resulted in full functional group incorporation. The remaining copolymers contained a persistent parent olefin moiety ranging from 10-40 %, dependent on the

Table 3.4 Thermal and physical properties of P(LA_{85}-co-β-HL_{19}) post olefin cross-metathesis functionalisation with Type I- Type III olefins.

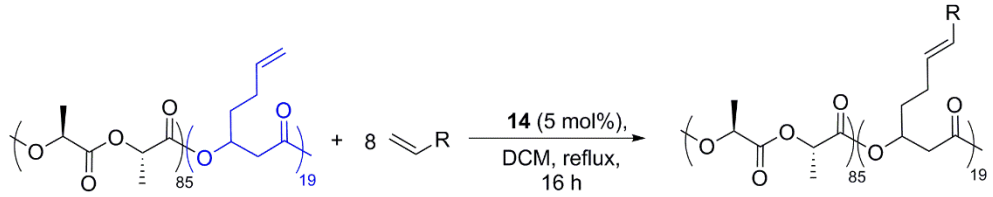

Entry	R	Conv. (%)[a]	M_n (Da)[b]	Đ[b]	$T_{5\%}$(°C)[c]	T_{max} (°C)[c]	T_g (°C)[d]	T_c (°C)[d]	T_m (°C)[d]
1	none		9,500	1.04	293	345	45	94	134
2		>95	n.d	n.d	272	361	43	94	136
3		76	9,900	1.03	274	358	40	93	134
4		87	10,400	1.04	n.d	n.d	n.o	95	137
5		87	11,300	1.18	277	359	37	92	134
6	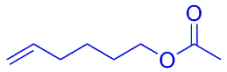	55	10,700	1.04	278	360	40	93	134
7	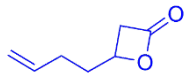	74	16,100	1.98	267	344	47	99	139
8	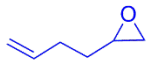	>99	11,600	1.08	236	343	44	97	138

9	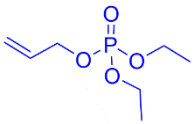	76	9,600	1.06	286	364	45	97	136
10	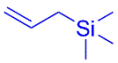	n.d	9,300	1.04	280	361	46	97	136
11		n.d	29,400	4.25	295	351	54	111	143
12	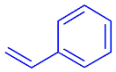	71	12,600	1.24	266	360	53	104	139
13	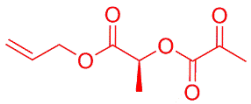	>99	23,800	2.39	233	362	49	n.o	n.o
14		>99	9,800	1.03	299	355	48	101	139
15	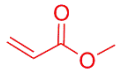	>99	12,100	1.02	297	350	46	98	136
16		>99	8,000	1.05	294	359	50	101	137

[a]Determined by ^{1}H NMR spectroscopy monitored by consumption of olefin protons of P(LA_{85}-co-β-HL_{19}) and appearance of cross-product protons. [b]Determined by triple detection GPC analysis. [c]Determined by thermal gravimetric analysis. [d]Determined by differential scanning calorimetry. n.o. = not observed. n.d. = not determined.

functional group. It was hypothesised the lack of full incorporation was a result of the competing olefin metathesis reactions accessible in the presence of two Type I olefins. These include homodimerisation of the olefin cross-partner, selective cross-metathesis of the olefin cross-partner with the copolymer and secondary metathesis of the functionalised copolymer. Moreover, steric hindrance of the attached olefin on the copolymer may inhibit approach and reaction of both catalyst and cross-partner. This theory is consistent with the incorporation of 5-hexenyl acetate, which, after two CM reactions resulted in the lowest incorporation (~55%). The long flexible aliphatic chain coupled with the sterics of the acetate group likely inhibits approach and reaction of further olefin cross-partners. Estimation of percentage incorporation of allyltrimethylsilane and allyl alcohol were unsuccessful due to overlapping peaks in the ^{1}H NMR spectrum.

Optimisation of reaction conditions using dec-1-ene as the cross-partner was attempted (**Table 3.5**). Increasing the catalyst loading from 5 to 15 mol% had no effect on the conversion (compare Entries 1 and 2). Increasing the temperature to 60 °C (Entry 3) and decreasing the equivalents of dec-1-ene and performing two consecutive metathesis reactions (Entries 4 and 5 respectively) gave a slight improvement to conversion.

Table 3.5 *Optimisation of reaction conditions of the olefin cross-metathesis of P(LA$_{85}$-co-β-HL$_{19}$) with dec-1-ene.*

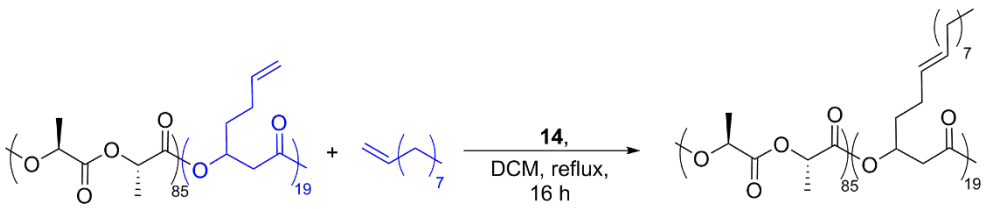

Entry	Temperature (°C)	**14** (mol%)	Equivalents of dec-1-ene	% lactone remaining[a]
1	40	5	12	11
2	40	15	12	11
3	60	5	12	6
4	60	5	6	8
5	60	5 + 5[b]	12	5

[a]Determined by ^{1}H NMR spectroscopy monitored by consumption of olefin protons in P(LA$_{85}$-co-β-HL$_{19}$) and appearance of cross-product protons. [b]One reaction using 5 mol% catalyst followed by a second reaction post precipitation using 5 mol% catalyst.

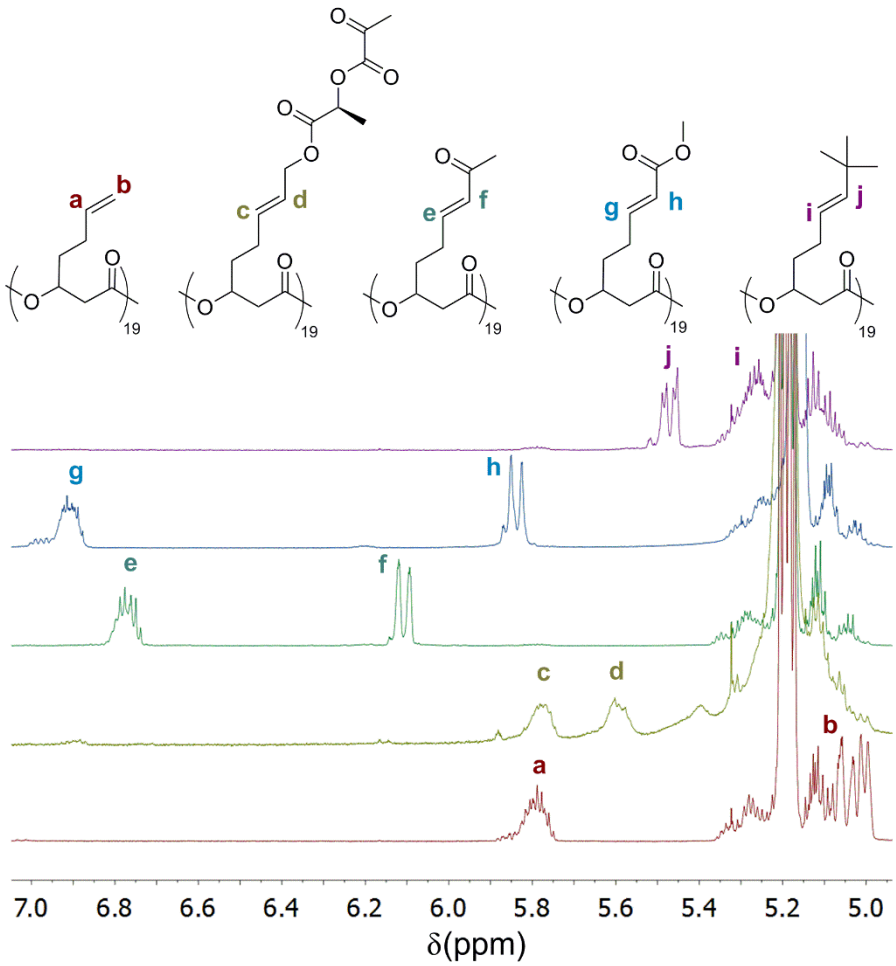

Figure 3.17 *Overlay of ^{1}H NMR spectra of functionalised copolymers of P(LA$_{85}$-co-β-HL$_{19}$).*

Although not a comprehensive screening this suggests the reaction conditions have minimal effect on the functional group incorporation and instead olefin reactivity dictates conversion. This is further evidenced by the metathesis of the less reactive Type II and III olefins, which gave full incorporation, irrespective of their steric bulk (Entries 13-16). The slow rate of homodimerisation of the Type II olefins and the inability of the Type III olefin to homodimerise promotes selective CM with the copolymer. **Figure 3.17** displays an overlay of the ^{1}H NMR spectra obtained for the functionalised copolymers, with the Type II and Type III olefins. It is evident that parent olefin protons **a** and **b** have disappeared in all functionalised copolymers and are replaced with new olefin protons **c**-**j**, where proton **i** belonging to the Type III olefin, 3,3-dimethylbut-1-ene, is hidden under the quartet of PLA.

GPC analysis displays narrow Đ values (<1.1) for the majority of the functionalised copolymers, suggesting no chain degradation and minimal polymer cross-linking. As seen

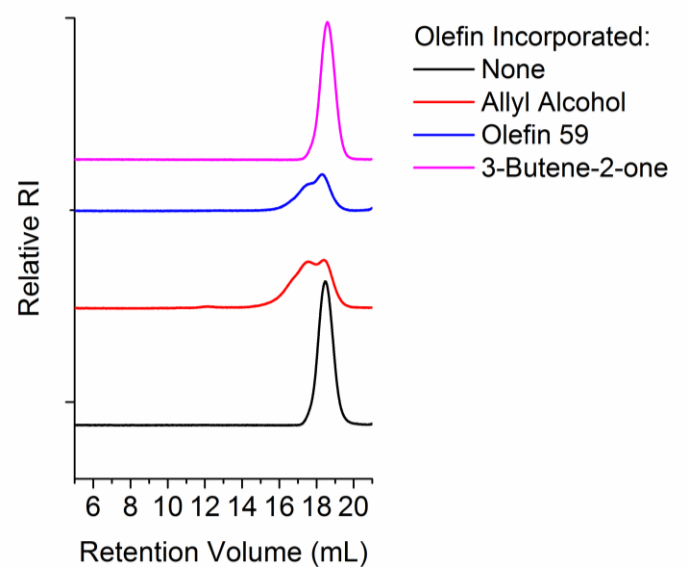

Figure 3.18 *GPC comparison of refractive index of copolymers functionalised with various olefins.*

with P(LA_{86}-co-β-HL_4) the copolymers functionalised with allyl alcohol and olefin **59** exhibited the highest Đ values (4.25 and 2.39 respectively), with M_n's higher than expected. Upon analysis of the GPC traces a clear high molecular weight shoulder is present for both of these copolymers,compared to 3-butene-2-one (representative of the other olefin cross-partners), which displays a unimodal trace (**Figure 3.18**).

A more notable difference in thermal properties was observed with these functionalised copolymers compared to functionalised P(LA_{86}-co-β-HL_4). TGA analysis shows a shows a significant decrease in $T_{5\%}$ for both epoxide and olefin **59** incorporation, by 63 °C and 66 °C respectively (Entries 8 and 13, **Table 3.4** and **Figure 3.19**). DTG analysis shows an increase in T_{max} between 6 °C and 19 °C for the majority of the functionalised copolymers highlighting a higher temperature, thus more energy, is required for maximum weight loss of the functionalised copolymers compared to P(LA_{85}-co-β-HL_{19}) (**Table 3.4** and **Figure 3.20**).

DSC (**Figure 3.21**) shows the largest decrease in T_g (by up to 8 °C) is associated with long aliphatic alkyl chains as observed previously in the functionalisation of P(LA_{86}-co-β- HL_4). An increase in chain length gave a decrease in T_g, consistent with the introduction of long flexible chains to induce free motion (**Table 3.4**, Entries 2-5). Incorporation of allyl alcohol and styrene increases T_g's by 9° C and 8 °C respectively. The rigidity of the styrene ring and its ability to form π-π interactions along with the hydrogen bonding introduced

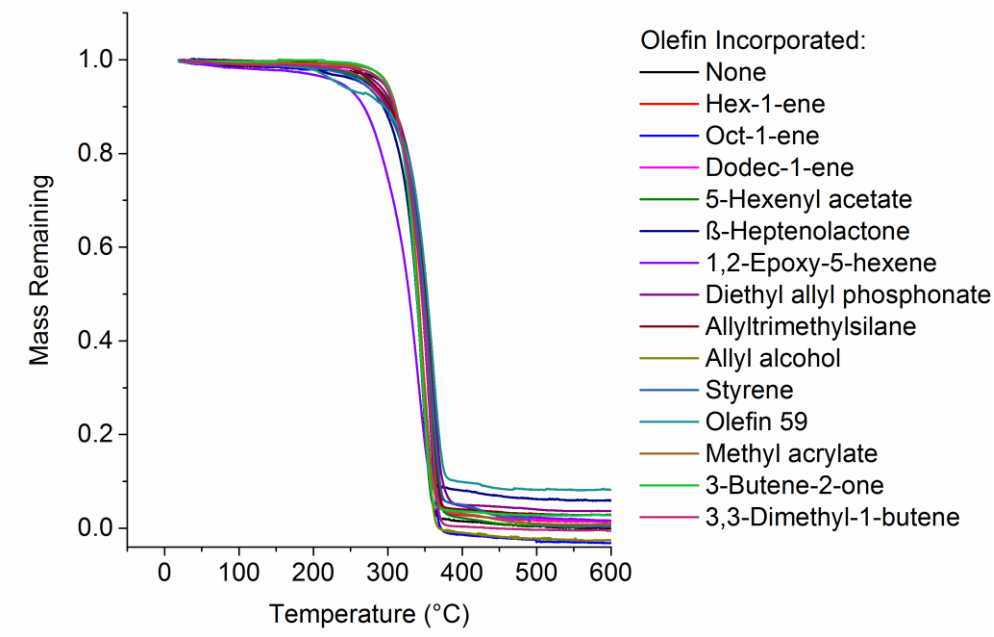

Figure 3.19 *TGA of functionalised P(LA$_{85}$-co-β-HL$_{19}$).*

with allyl alcohol may account for the observed increase in T_g's. Similarly, a significant increase in T_c and T_m were observed for both allyl alcohol and styrene incorporation. Allyl alcohol gave an increase in T_c of 17 °C and an associated increase in T_m of 9 °C. This suggests the copolymer forms strong crystalline domains, likely a result of the increased hydrogen bonding. Equally, incorporation of styrene resulted in an increase in T_c of 10 °C and to a lesser extent an increase in T_m of 5 °C. Strong intermolecular bonding induced by π-π stacking of the styrene rings may account for the increase in both temperatures.

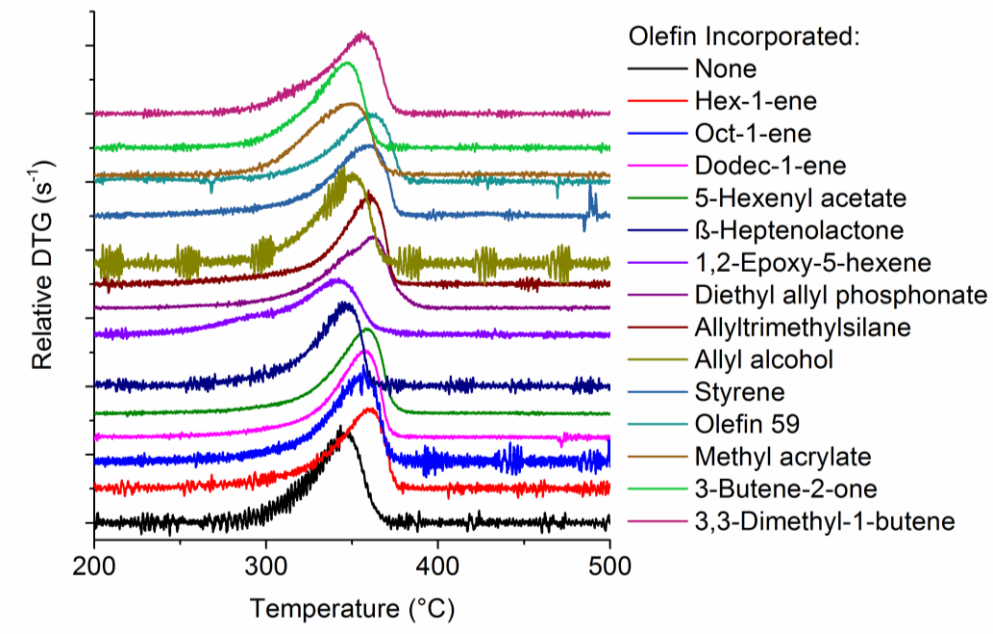

Figure 3.20 *DTG of functionalised P(LA$_{85}$-co-β-HL$_{19}$).*

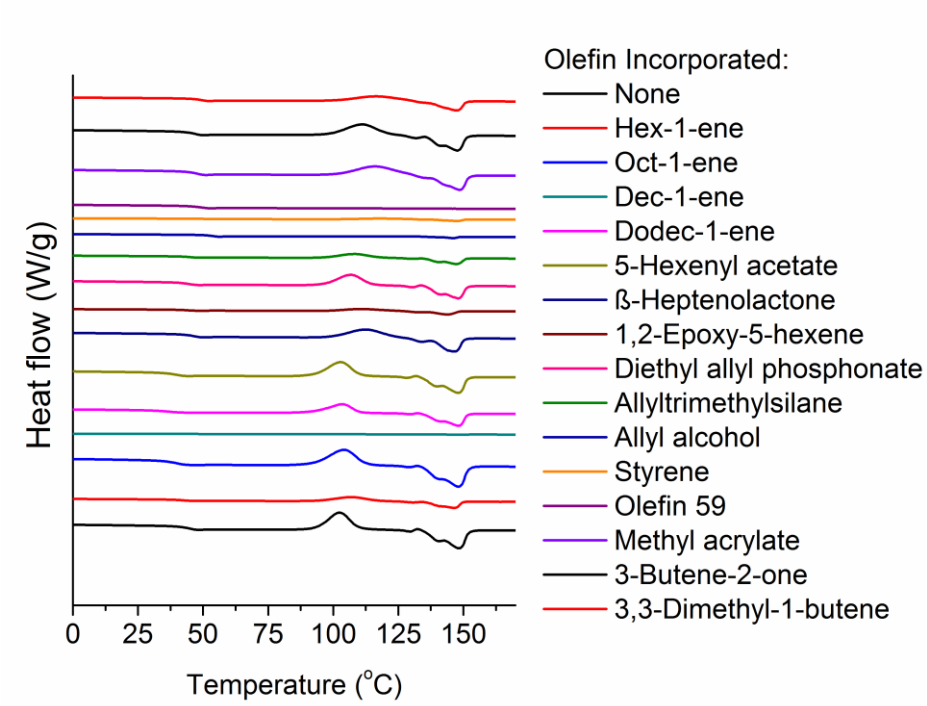

Figure 3.21 *DSC of functionalised P(LA_{85}-co-β-HL_{19}).*

3.3.4 Double metathesis of poly(LA-co-β-HL)

The above experiments show that the thermal properties of PLA can be modified by copolymerisation and subsequent chemical modification using olefin CM. The most efficient olefin cross-partners, which enabled full functional group incorporation, were the less reactive Type II and Type III olefins, due to non-competitive homodimerisation. In contrast, the more active Type I olefins led to incomplete incorporation regardless of conditions. Although an apparently negative outcome, it facilitated the development of a new methodology to introduce two unique olefin functionalities into the copolymer, based on manipulation of olefin Types.

Incomplete functional group incorporation presented an opportunity to introduce a second olefin cross-partner, in order to consume the remaining parent olefins of the pendent arm. To develop this methodology, we exploited the differences in reactivity of the olefin cross-partners (**Scheme 3.14** and **Table 3.6**). In Scenario 1, **Scheme 3.14**, the copolymer was reacted first with the Type II olefin methyl acrylate followed by precipitation in methanol. Following, the functionalised copolymer **74**, was reacted with the Type I olefin 1,2-epoxy-5-hexene which, post-precipitation, generated copolymer **75**.

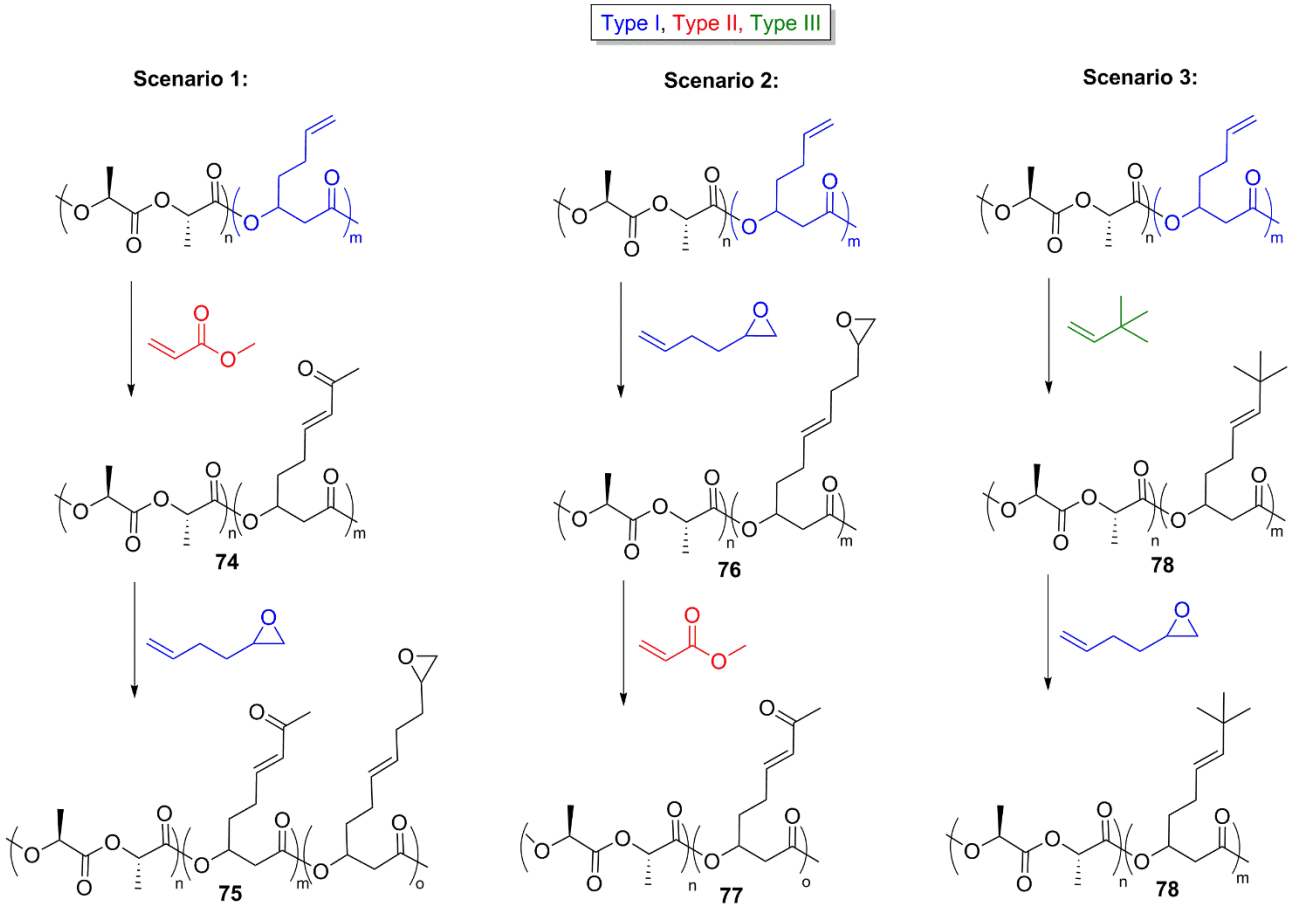

Scheme 3.14 *Double olefin CM. Scenario 1: CM with a Type II olefin followed by a Type I olefin. Scenario 2: CM with a Type I olefin followed by a Type II olefin. Scenario 3: CM with a Type III olefin followed by a Type I olefin.*

This copolymer displayed incorporation of both functionalities in an almost 1:1 ratio as determined by integration of product protons of both functionalities by ^{1}H NMR spectroscopy (Entry 1,**Table 3.6**). Reversing the order of addition of the olefins as in Scenario 2, **Scheme 3.14**, led to copolymer **77** with only incorporation of the Type II olefin, methyl acrylate, (Entry 2, **Table 3.6**). This scenario suggests the rate of secondary metathesis of copolymer **76** functionalised with the epoxide, is faster than the rate of homodimerisation of the Type II olefin methyl acrylate. Consequently, replacement of all the functionalised epoxide with methyl acrylate was favoured. On the other hand, in Scenario 1, the rate of secondary metathesis of copolymer **74**, functionalised with methyl acrylate must be slower than the rate of homodimerisation of the epoxide, generating copolymer **75** functionalised with both olefins. Interestingly, reacting the polymer with a Type III olefin first followed by a Type I olefin gave copolymer **78**, Scenario 3, **Scheme 3.14**, functionalised with the Type III olefin only (Entry 3, **Table 3.6**). This suggests copolymer **78** is likely categorised as an inactive Type IV olefin that is inert towards secondary metathesis

To investigate whether double metathesis would work similarly in the presence of other Type I olefins, the epoxide was changed to diethyl allyl phosphonate. Double metathesis involved mimicking the conditions used in Entry 1, **Table 3.6**, and the copolymer was reacted first with Type II olefin methyl acrylate followed by an excess of Type I olefin diethyl allyl phosphonate (Entry 4). Analysis by ^{1}H NMR spectroscopy showed a ratio of methyl acrylate:diethyl allyl phosphonate of 0.36:1, whereas Entry 1 gave a ratio of methyl acrylate:epoxide of 1:0.78. These ratios suggest the rate of homodimerisation of allyl phosphonate is slower than the rate of homodimerisation of the epoxide, consequently leading to a greater replacement of methyl acrylate (functionalised on the copolymer) when reacted in the presence of diethyl allyl phosphonate. This highlights the nuances that exist within olefin categories; while both diethyl allyl phosphonate and the epoxide can be categorised as reactive Type I olefins, a gradient of reactivity also exists within the category based on the preference of the olefins to homodimerise. The steric bulk associated with diethyl allyl phosphonate likely explains its associated decrease in rate of homodimerisation compared to the epoxide. The ratio of diethyl allyl phosphonate was lowered which resulted in less functional group incorporation, as expected (Entry 5).

Table 3.6 *Double Cross-metathesis of the copolymer with two different olefins.*

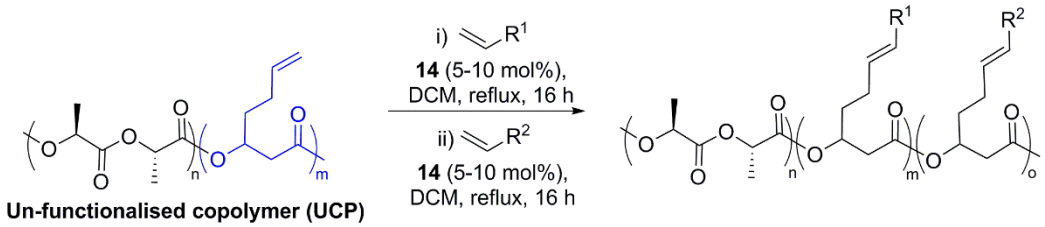

Un-functionalised copolymer (UCP)

Entry	R	Equiv. of R^1	UCP (%)[a]	R	Equiv. of R^2	(UCP:R^1:R^2)[a]
1	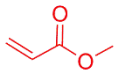	1	13	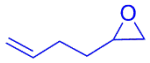	8	0:1:0.78
2	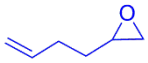	12	13	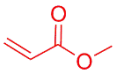	5	0:0:1
3		8	0	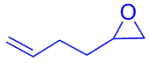	0.3	0:1:0
4	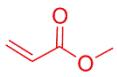	1	18	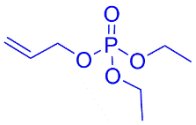	5	0:0.36:1
5	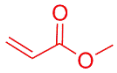	8	0	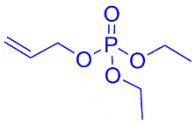	0.3	0:1:0.25
6		8	6	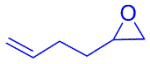	0.3	0.26:0.9:1

[a]Determined by ^{1}H NMR spectroscopy monitored by consumption of olefin protons of copolymer and appearance of cross-product protons.

To highlight the gradient of reactivity within the less active Type II olefins, methyl acrylate was replaced by 3-butene-2-one, which was reacted in the double metathesis with the epoxide (Entry 6,**Table 3.6**). Interestingly, parent olefins of the copolymer remained and almost a 1:1 ratio of ketone:epoxide was observed even when a small excess of epoxide was used (compare to Entry 1, which used a large excess of epoxide). This suggests 3-butene-2-one is more reactive than methyl acrylate, and the copolymer functionalised with this ketone has a higher susceptibility towards secondary metathesis than the copolymer functionalised with methyl acrylate. The low equivalents of epoxide (Entry 6) may account for the remaining parent olefin observed. Moreover, remaining parent olefins (~6 %) after the first metathesis highlights the higher susceptibility of the ketone to homodimerise compared to methyl acrylate. **Figure 3.22** displays an overlay of the ^{1}H NMR spectra

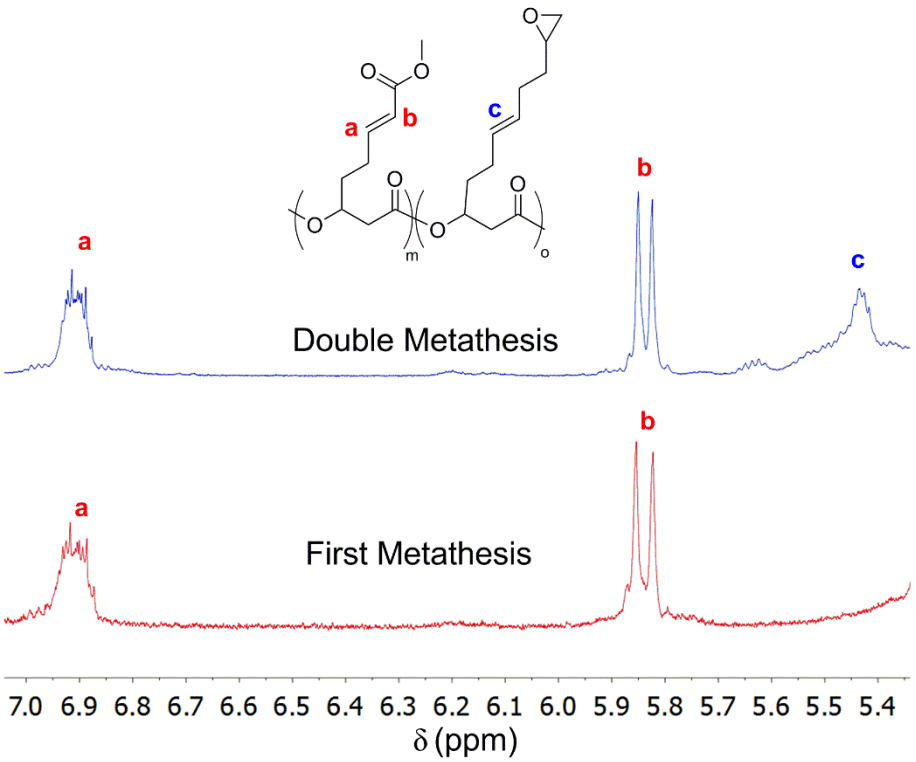

Figure 3.22 *Overlay of the ^{1}H NMR spectra for double metathesis with methyl acrylate and 1,2-epoxy-5-hexene.*

obtained from Entry 1, **Table 3.6** for the double metathesis with methyl acrylate and the epoxide. It is apparent both functionalities are incorporated due to inclusion of protons **a** and **b** of methyl acrylate after the first metathesis and appearance of olefin protons **c** belonging to the epoxide after the second metathesis. These results highlight the importance of understanding olefin Type categorisation and the gradient of reactivity within each category. Through manipulation and careful selection of olefins, it is possible to effectively introduce two unique functionalities into the copolymer. Normally, the introduction of two unique functionalities into a system requires different chemical reactions and steps. Double metathesis offers the ability to do this with just one transformation in two steps. It also allows further control and tuning of the thermal properties of the copolymers.

The copolymers successfully synthesised *via* double metathesis are displayed in **Figure 3.23** along with their parent copolymers that differ slightly in lactide composition. Copolymer **79** generated functionalised copolymer **80**, while copolymer **81** generated functionalised copolymers **82** and **83**. Thermal and physical properties of the copolymers post-double metathesis are illustrated in **Table 3.7** and **Figure 3.24** to **Figure 3.26**. In

general, all functionalised copolymers (Entries 2, 4 and 5, **Table 3.7**) display a broad Đ post double CM compared to just single metathesis (as illustrated previously in

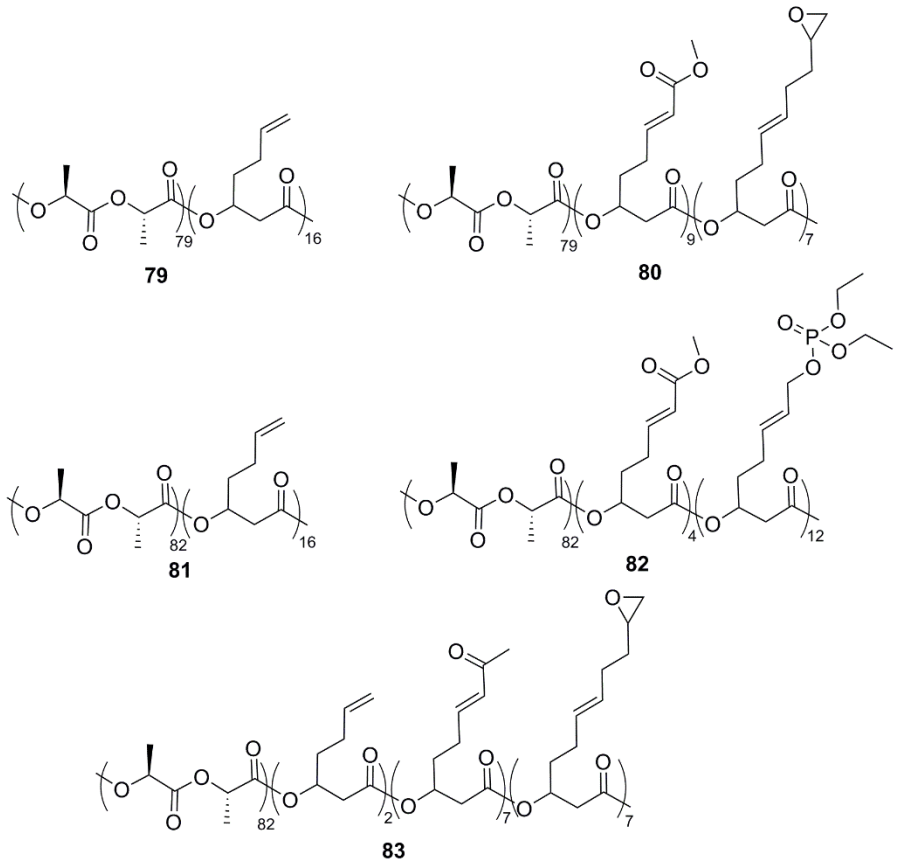

Figure 3.23 *Copolymers and functionalised copolymers from double metathesis. Copolymer **79** generated functionalised copolymer **80**. Copolymer **81** generated functionalised copolymers **82** and **83**.*

Table 3.7 *Thermal and physical properties of the functionalised copolymers synthesised from double metathesis*

Entry	Copolymer	M_n (Da)[a]	Đ[a]	$T_{5\%}$ (°C) [b]	T_{max} (°C)[b]	T_g (°C)[c]	T_c (°C)[c]	T_m (°C)[c]
1	**79**	10,400	1.03	289	342	43	97	135
2	**80**[d]	20,700	1.25	290	355	46	101	137
3	**81**	9,800	1.02	301	350	44	93	133
4	**82**[e]	22,000	2.34	288	368	49	102	140
5	**83**[e]	21,200	1.76	291	364	51	103	140

[a]Determined by triple detection GPC analysis.[b]Determined by thermal gravimetric analysis. [c]Determined by differential scanning calorimetry. [d]Synthesised from copolymer **79**. [e]Synthesised from copolymer **81**.

Table 3.4). This is expected assuming a non-equal distribution of both olefins is observed per polymer chain giving rise to chains with varying composition and mass. The TGA and DTG data is depicted in **Figure 3.24** and **Figure 3.25** and highlight that the largest change in $T_{5\%}$ and T_{max} was observed for copolymer **82**. It gave a decrease in $T_{5\%}$ by 13 °C and an increase in T_{max} by 18 °C (Entry 4, **Table 3.7**). DSC, **Figure 3.26**, shows that all functionalised copolymers have an associated increase in T_g, T_c and T_m, as shown in **Table 3.7**. This route provides a platform to tune the properties by altering both the Type and ratio of olefins incorporated.

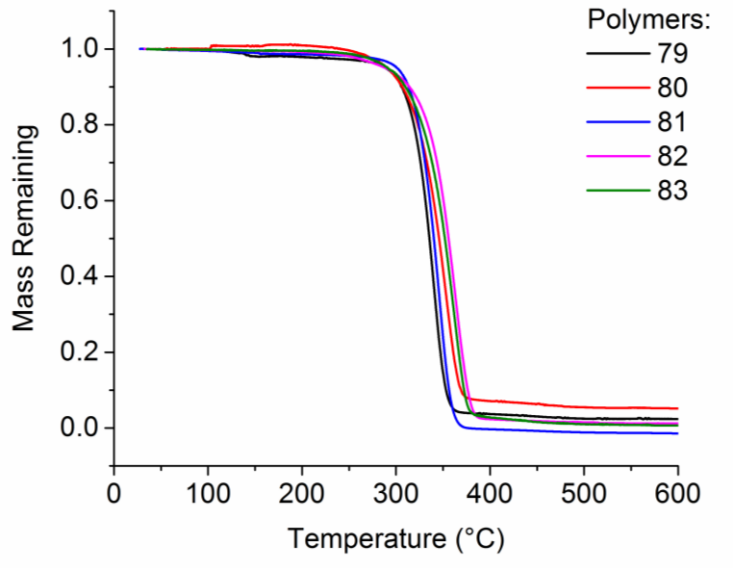

Figure 3.24 *TGA of functionalised copolymers obtained from double metathesis.*

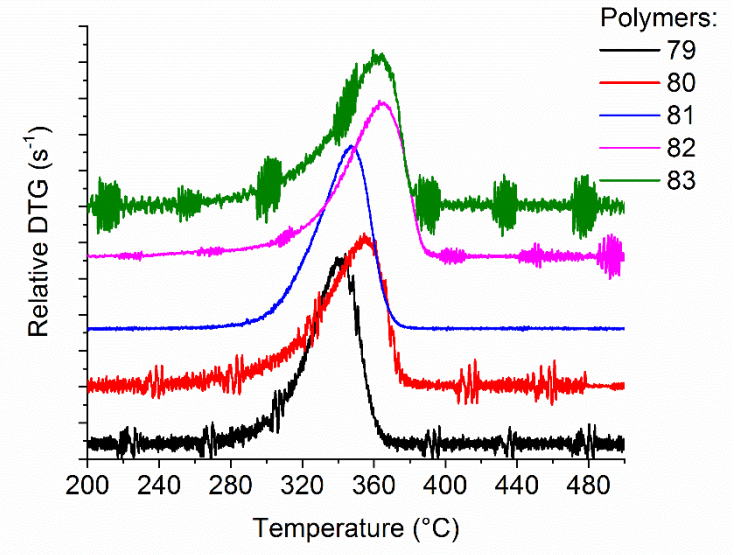

Figure 3.25 *DTG of functionalised copolymers obtained from double metathesis.*

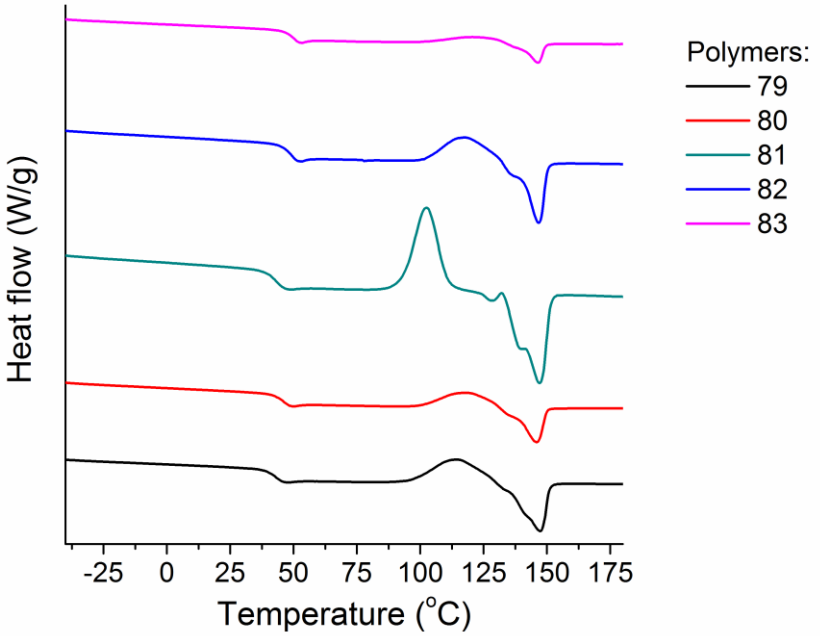

Figure 3.26 *DSC of functionalised copolymers obtained from double metathesis.*

3.4 Conclusions and future work

To conclude, β-HL was a successful monomer in both pre- and post-polymerisation olefin CM (**Scheme 3.15**). Through experimental deduction, β-HL was categorised as a reactive Type I olefin, which enabled a large substrate scope of cross-partners to be incorporated. However, due to the range of possible metathesis products formed, both conversion and purification was difficult. CM between β-HL and Type II olefin methyl acrylate, generated a novel monomer (route **a)**) that was isolated and successfully polymerised (route **b)**). This work demonstrates one of only a handful of reports that functionalise a monomer *via* olefin CM and demonstrate its subsequent polymerisation. The polymerisation was uncontrolled, likely due to interference of the functional group, highlighting that pre-polymerisation olefin CM of β-HL is not a viable route to obtain functionalised polymers.

Polymerisation of β-HL was well controlled as evidenced by the narrow Đ (route **c)**). Olefin CM of the homopolymer was carried out using two different olefins; Type II olefin methyl acrylate and Type I olefin 1,2-epoxy-5-hexene (route **d)**). CM was successful with full functional group incorporation of both olefins as evidenced by ^{1}H NMR spectroscopy. Incorporation of the olefins had a dramatic effect on the thermal properties

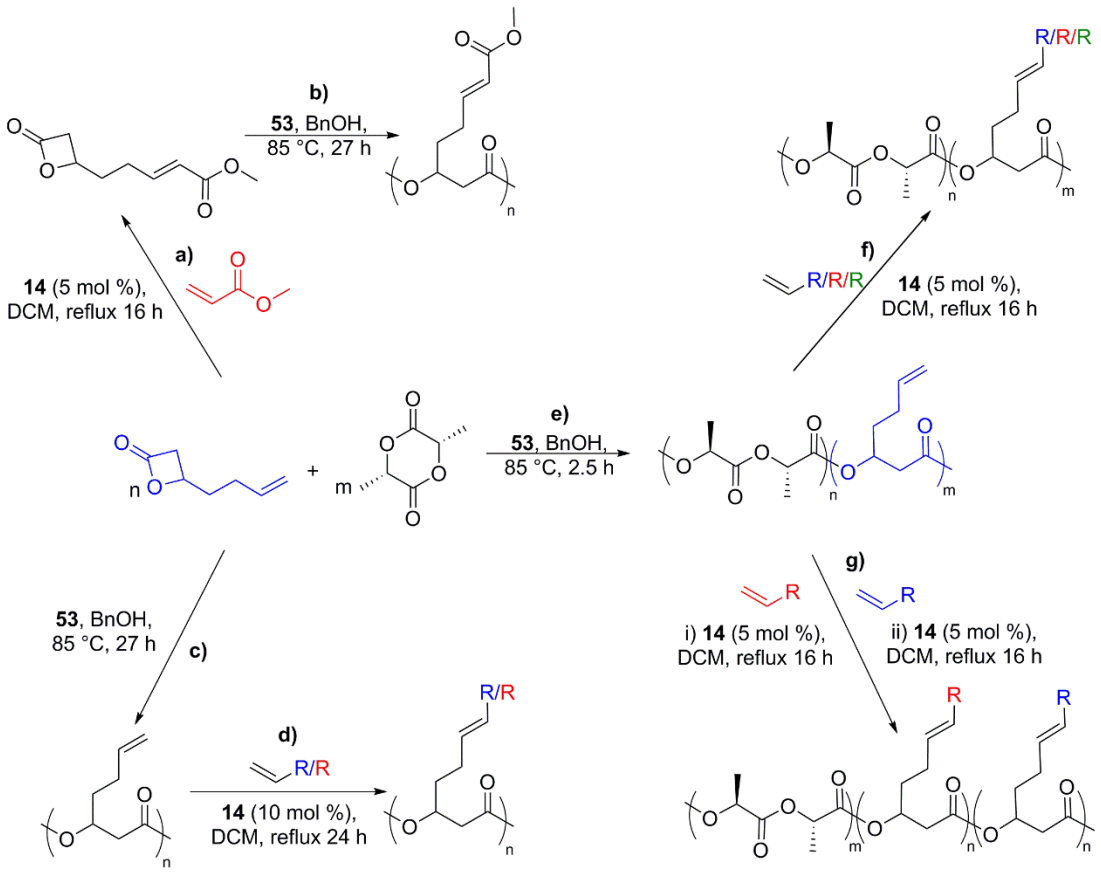

Scheme 3.15 *Summary of the CM reactions involving β-HL: a) pre-polymerisation CM with methyl acrylate, b) polymerisation of novel monomer, c) homopolymersiation of β-HL, d) post-polymerisation CM with a Type I and Type II olefin, e) copolymerisation of β-HL and L-lactide, f) post-polymerisation CM with 15 different olefins ranging from Type I to Type III, g) double metathesis of copolymer.*

of the functionalised homopolymers, as determined by DSC and TGA. In particular, a substantial increase in the T_g was observed. To expand the applications of this polymer, block copolymers (AB) should be explored with lactide. Generation of a β-HL block first followed by PLA should be attempted and olefin CM of this block copolymer post-polymerisation should be explored. Alteration of the length of the functionalised β-HL – segment should be monitored with respect to its properties. Similarly, block copolymers (ABA) of β-HL and lactide (containing a β-HL middle block) should be investigated to generate a phase separated material with the potential of functional group modification *via* olefin CM.

Copolymerisation of β-HL and lactide synthesised gradient copolymers of varying monomer ratios; LA:β-HL, 86:4 and 85:19 (route **e)**). These polymers represent the first copolymers of lactide and β-HL. The high reactivity of β-HL enabled a wide substrate scope of cross partners to be investigated and the copolymers were successfully reacted

with 15 different olefins ranging from Type I to Type III olefins (route **f)**). Functional group incorporation as determined by ^{1}H NMR spectroscopy, was difficult to determine for the copolymers containing a LA:β-HL ratio of 86:4. Thermal analysis by DSC and TGA was used to confirm a change in the copolymer properties. Generally, a larger change in thermal properties was observed with the copolymer containing a LA:β-HL ratio of 85:19. The largest change was associated with styrene and allyl alcohol incorporation. Determination of conversion of these functionalised copolymers was possible by ^{1}H NMR spectroscopy, with the less reactive Type II and Type III olefins leading to complete incorporation, likely due to their slow rate or inability to homodimerise. Copolymers functionalised with the Type I olefins were subject to a second round of metathesis but still incomplete incorporation was observed, likely due to the selectivity problems that arise between reaction of two Type I olefins. Mechanical testing on these functionalised copolymers should be investigated to determine what effect functional group incorporation had on their Young's modulus and elasticity. Moreover a truly random copolymer could be targeted by controlling the rate of addition of lactide via a syringe pump.

The lack of complete incorporation of the Type I olefins led to the development of a novel methodology to introduce two unique functionalities into the copolymer (route **g)**). Manipulation of olefin Type reactivity identified that reaction with a less reactive Type II olefin first, followed by reaction with a Type I olefin generates a copolymer containing both olefins. This route offers the ability to introduce two unique functionalities through the same organic transformation with the potential to tune polymer properties. Optimisation of this route should include attempting a one-pot two-step process to remove the precipitation step in-between the second CM reaction. Moreover synthesis of an ABA block copolymer with a lactide middle block and two end blocks of β-HL should be targetted. This offers the potential to generate an ABA block copolymer with two different functionalised β-HL segments through manipulation of cross-partner reactivities.

It is of interest to also investigate incorporation of a third functionality on the unreacted olefins *via* a different olefin transformation. Various routes could be explored including hydroboration, epoxidation and thiolene addition.

3.5 References

(1) Lin, K.-W.; Lan, C.-H.; Sun, Y.-M. *Polym. Degrad. Stab.* **2016**, *134*, 30–40.

(2) Anjum, A.; Zuber, M.; Zia, K. M.; Noreen, A.; Anjum, M. N.; Tabasum, S. *Int. J. Biol. Macromol.* **2016**, *89*, 161–174.

(3) Schmidt, J. A. R.; Mahadevan, V.; Getzler, Y. D. Y. L.; Coates, G. W. *Org. Lett.* **2004**, *6* (3), 373–376.

(4) Lee, J. T.; Thomas, P. J.; Alper, H. *J. Org. Chem.* **2001**, *66* (16), 5424–5426.

(5) Drent, E.; Kragtwijk, E. *Eur. Pat. Appl. EP 577, 206; Chem. Abstr.* **1994**, *120*, 191517c.

(6) Mahadevan, V.; Getzler, Y. D. Y. L.; Coates, G. W. *Angew. Chemie - Int. Ed.* **2002**, *41* (15), 2781–2784.

(7) Getzler, Y. D. Y. L.; Kundnani, V.; Lobkovsky, E. B.; Coates, G. W. *J. Am. Chem. Soc.* **2004**, *126* (22), 6842–6843.

(8) Schmidt, J. A. R.; Lobkovsky, E. B.; Coates, G. W. *J. Am. Chem. Soc.* **2005**, *127* (32), 11426–11435.

(9) Kramer, J. W.; Lobkovsky, E. B.; Coates, G. W. *Org. Lett.* **2006**, *8* (17), 3709–3712.

(10) Rieth, L. R.; Moore, D. R.; Lobkovsky, E. B.; Coates, G. W. *J. Am. Chem. Soc.* **2002**, *124* (51), 15239–15248.

(11) Hori, Y.; Hagiwara, T. *Int. J. Biol. Macromol.* **1999**, *25* (1–3), 237–245.

(12) Amgoune, A.; Thomas, C. M.; Ilinca, S.; Roisnel, T.; Carpentier, J. F. *Angew. Chemie - Int. Ed.* **2006**, *45* (17), 2782–2784.

(13) Kramer, J. W.; Treitler, D. S.; Dunn, E. W.; Castro, P. M.; Roisnel, T.; Thomas, C. M.; Coates, G. W. *J. Am. Chem. Soc.* **2009**, *131* (44), 16042–16044.

(14) Li, S. M.; Pignol, M.; Gasc, F.; Vert, M. *Macromolecules* **2004**, *37* (26), 9798–9803.

(15) Hiki, S.; Miyamoto, M.; Kimura, Y. *Polymer 2***000**, *41* (20), 7369–7379.

(16) Jaimes, C.; Collet, A.; Giani-Beaune, O.; Schué, F.; Amass, W.; Amass, A. *Polym. Int.* **1998**, *45*, 5–13.

(17) MacDonald, J. P.; Parker, M. P.; Greenland, B. W.; Hermida-Merino, D.; Hamley, I. W.; Shaver, M. P. *Polym. Chem.* **2015**, *6* (9), 1445–1453.

(18) Ajellal, N.; Thomas, C. M.; Carpentier, J.-F. *J. Polym. Sci. Part A Polym. Chem.* **2009**, *47*, 3177–3189.

(19) Guillaume, C.; Ajellal, N.; Carpentier, J.-F.; Guillaume, S. M. *J. Polym. Sci. Part A Polym. Chem.* **2011**, *49* (4), 907–917.

(20) Raycraft, B. M.; MacDonald, J. P.; McIntosh, J. T.; Shaver, M. P.; Gillies, E. R. *Polym. Chem.* **2017**, *8* (3), 557–567.

(21) Chatterjee, A. K.; Choi, T. L.; Sanders, D. P.; Grubbs, R. H. *J. Am. Chem. Soc.* **2003**, *125* (37), 11360–11370.

(22) Fournier, L.; Robert, C.; Pourchet, S.; Gonzalez, A.; Williams, L.; Prunet, J.; Thomas, C. M. *Polym. Chem.* **2016**, *7* (22), 3700–3704.

Chapter 4. Uranium and Cerium Complexes for the Ring-Opening Polymerisation of Lactide

4.1 Lanthanides and actinides as catalysts for the ring-opening polymerisation of lactide

f-Block cations are emerging as potential ROP catalysts that are often overlooked due to misconceptions of excessive oxophilicity and scarcity. In particular, lanthanide rare-earth metal complexes are of growing interest in the ROP of cyclic esters, including lactide. The stability and catalytic properties of rare-earth metals are dictated by the choice of metal centre and coordination environment. To control this, various ancillary ligands have been incorporated in rare-earth metals to impart stability and selectivity. Yao *et al.* reported the synthesis of bimetallic lanthanide (Nd, Sm and Y) amido complexes stabilised by rigid phenylene-bridged bis(β-diketiminate) ligands, **84**, **Figure 4.1**.[1] The authors demonstrated that all complexes were extremely active in the ROP of L-lactide with reaction times as low as 5 minutes. The order of reactivity increased with increasing ionic radii (Nd>Sm>Y), a trend observed in many lanthanide ROP systems.[2] However, although highly active, the polymerisations were not well controlled as observed by broad Đ's. The complexes gave a moderate level of heterotacticty (P_r = 0.65-0.73) in the ROP of rac-lactide.

Single-site lanthanide catalysts can often offer more control during ROP. Shen *et al.* synthesised lanthanide (Y, Nd, Sm, Yb) monoborohydride complexes stabilised by bis(amidinate) ligands, **85**, **Figure 4.1**.[3] A high level of heterotacticty was observed during the ROP of rac-lactide using Y (P_r = 0.85), while an increase in ionic radii led to a decrease

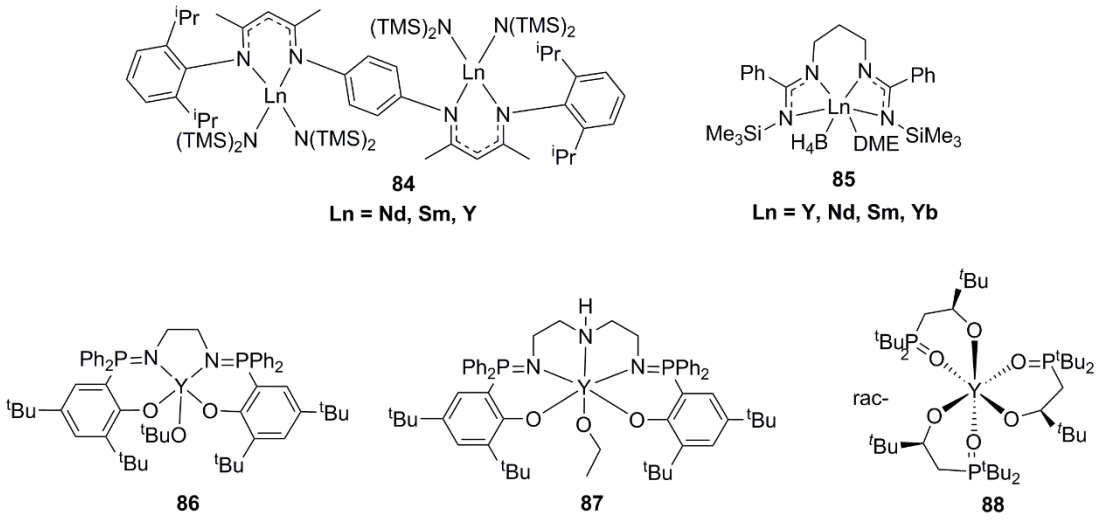

Figure 4.1 *f-Block complexes as ROP catalysts for lactide.*[1,3-6]

in heterotacticity, Nd (P_r = 0.69). This suggested that a crowded coordination environment promoted higher stereocontrol.

Williams *et al.* synthesised the first yttrium phosphosalen alkoxide complexes, which demonstrated superior activity to its salen counter-parts in the ROP of lactide **86**, **Figure 4.1**.[4] This was hypothesised to arise from an increase in electron density and thus a decrease in the Lewis acidity of the yttrium centre, enabling a more labile metal-alkoxide bond to enhance lactide insertion. More recently, the authors demonstrated successful iso-selective ROP of rac-lactide using yttrium-phosphosalen alkoxide complexes **87** **Figure 4.1**, where tacticity could be switched to heterotactic through ligand modification.[5] This was dictated by a chain end control mechanism. Alternatively, Arnold *et al.* demonstrated iso-selective ROP of rac-lactide using a mixture of two homochiral lanthanide complexes through an enantiomorphic site control mechanism **88**, **Figure 4.1**.[6]

The literature discussed above represents just a few examples of the research on f-block cations for the ROP of lactide. Less common initiators for the ROP of lactide are cerium and uranium. Cerium complexes for ROP of lactide are virtually unknown and only a few examples exist in the literature[7–9] Most interestingly, Diaconescu *et al.* demonstrated the first example of a metal-based redox switch, which is not part of a supporting ligand, for the ROP of lactide. Cerium(III), complex **89**, (**Figure 4.2**) was synthesised and found to react faster than its oxidised counterpart, Ce(IV), which was inactive at room temperature. The difference in activity was attributed to electronic factors associated with the lower

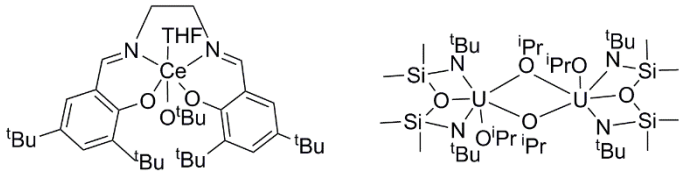

89 **90**

Figure 4.2 *Uranium and cerium complexes reported for the ROP of lactide.*[8,11]

electrophilicity of Ce(III), which would increase the nucleophilicity of the alkoxide ligand. *In situ* switching between the two catalysts was performed at ambient temperature. Oxidation of **89** Ce(III), to Ce(IV) was able to halt the polymerisation, while reduction back to Ce(III) was able to trigger the restart of polymerisation without any loss in activity of the catalyst.[8]

Uranium is highly oxophilic with the expectation that in the presence of oxygen-containing substrates catalytic activity would decrease. Consequently, literature on uranium initiators for the ROP of lactide is rare. However, reports by Eisen et *al.* and Carpentier and Leznoff *et al.* demonstrate successful ROP of lactide in the presence of uranium complexes without deactivation.[10,11] In the latter example, the authors synthesised new diamido uranium alkoxide complexes including **90**, **Figure 4.2**, which demonstrated excellent control in the ROP of lactide with narrow Đ's at short reaction times. ROP of rac-lactide using **90** in a coordinating solvent gave a heterotactic enriched polymer (P_r = 0.73) but at the expense of a reduced reaction rate and a low conversion (~50 %).[11]

The scarcity of both uranium and cerium initiators for the ROP of lactide merits research into further complexes. Arnold *et al.* recently synthesised a set of new heterobimetallic uranium- group 10 metal complexes **91**, (**Figure 4.3**) comparing Ni(0), Pd(0) and Pt(0).[12] The authors discovered when X = I, shorter U-I bonds were present in the bimetallic complexes compared to in the parent monometallic derivative. They also observed an increase in U-M bond strength from U-Pt to U-Ni. This was supported by a higher bond-order, determined by computational studies, and shorter U-M distances, determined by crystallography.

Using the U-Ni derivative the effect of the ligand X *trans* to Ni, was investigated and iodide was substituted with both fluoride and trimethylsiloxide. The authors discovered

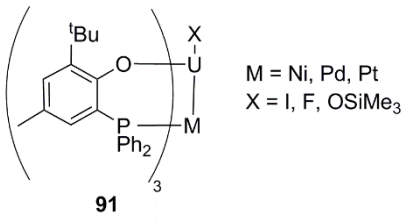

Figure 4.3 *Bimetallic uranium-metal complexes.*[12]

ligand substitution led to a strengthening of the U-Ni bond in the order Ni-U-I< Ni-U-F< Ni-U-$OSiMe_3$. This was attributed to the *inverse trans influence* which is the mutual strengthening of two trans-coordinated ligands, specific to f-block complexes. It predicts a stronger U-Ni bond *trans* to the ligand, which in the case of Ni-U-F was supported further by a shorter U-Ni bond length compared to in the Ni-U-I analogue. This work overall showcased the shortest U-transition metal bond reported to date.

Arnold *et al.* hypothesised these heterobimetallic uranium-metal complexes alongside their monomeric precursors could serve as effective initiators in the ROP of lactide. The authors synthesised the following complexes shown in **Figure 4.4**; bimetallic Ni(0)-U(IV)-$OSiMe_3$ (**U-Ni)**, monometallic U(IV)-$OSiMe_3$ (**U-1**), a monometallic uranium(IV) complex with the absence of any siloxide ligand (**UL_4**) and a cerium(IV) analogue of the monometallic species Ce-$OSiMe_3$ (**Ce-1**). In a collaborative project we compared the ability of these complexes as initiators in the ROP of both L- and rac-lactide.

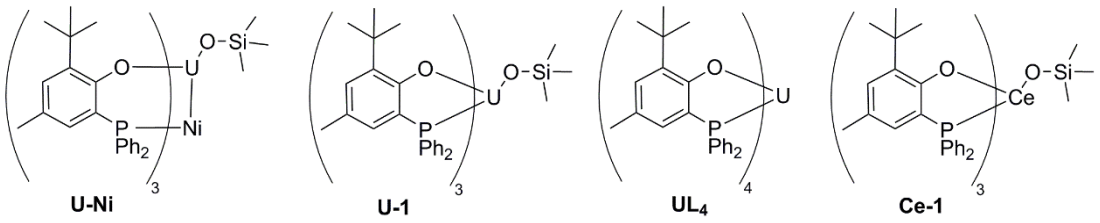

Figure 4.4 *Uranium and cerium catalysts synthesised by Arnold et al. used in the ROP of L-and rac-lactide for this chapter.*

4.2 Ring-opening polymerisation of L-lactide

In order to investigate the ability of the complexes as initiators in the ROP of lactide, initial studies focused on the ROP of L-lactide. Screening reactions were carried out under living conditions in the absence of any external BnOH, with a monomer:catalyst ratio of 200:1 (**Table 4.1**). Comparing uranium and cerium analogues **U-1** and **Ce-1** respectively,

Table 4.1 *Ring-opening polymerisation of L-lactide.*

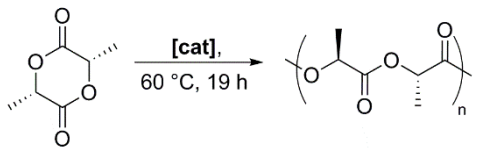

Entry	[cat]	Solvent	Conversion (%)[a]	$M_{n,th}$ (Da)[b]	$M_{n,GPC}$ (Da)[c]	Đ[c]
1[d]	**U-1**	Toluene	98	28,300	26,500	1.04
2[d]	**U-1**	Benzene-d_6	98	28,300	22,400	1.11
3[d]	**U-1**	Dichloroethane	94	27,200	20,700	1.11
4[e]	**U-1**	Toluene	>99	14,200[f]	15,700	1.07
5[g]	**U-1**	Toluene	>99	4,900[h]	4,900	1.10
6[d]	**UL$_4$**	Toluene	>99	28,500[i]	56,600	1.27
7[g]	**UL$_4$**	Toluene	>99	5,900[j]	5,100	1.26
8[d]	**U-Ni**	Toluene	2	N/A	N/A	N/A
9[g]	**U-Ni**	Toluene	25	N/A	N/A	N/A
10[d]	**Ce-1**	Toluene	94	27,200	25,900	1.24
11[d]	**Ce-1**	Benzene-d_6	98	28,300	39,800	1.47
12[d]	**Ce-1**	Dichloroethane	80	23,200	35,900	1.64
13[e]	**Ce-1**	Toluene	98	14,200[f]	9,100	1.18
14[g]	**Ce-1**	Toluene	>99	4,900[h]	7,300	1.18

[a]Determined by ^{1}H NMR spectroscopy monitored by comparison of monomer to polymer resonances. [b]$M_{n,th}$ = (% conv. x ($MW_{(monomer)}$ x2)) + $MW_{(HOSi(Me)3)}$. [c]Determined by triple detection GPC using *dn/dc* value of 0.05. [d]Monomer: catalyst (200:1). [e]Monomer: catalyst: BnOH (200:1:1). [f]$M_{n,th}$ = (% conv. x ($MW_{(monomer)}$ x2))/2 + $MW_{((HOSi(Me)3 + BnOH)/2)}$. [g]Monomer: catalyst: BnOH (200:1:5). [h]$M_{n,th}$ = (% conv. x ($MW_{(monomer)}$ x2))/6 + $MW_{((HOSi(Me)3 + BnOH)/2)}$. [i]$M_{n,th}$ = % conv. X ($MW_{(monomer)}$ x2). [i]$M_{n,th}$ (% conv. x ($MW_{(monomer)}$ x2))/5 + $MW_{(BnOH)}$.

both catalysts were active, displaying molecular weights in good agreement to the theoretical molecular weights (compare Entries 1 and 10, **Table 4.1**). However, less control is observed with **Ce-1**, as shown by broader Đ's. Solvent screening was carried out in toluene, benzene and dichloroethane. Control was maintained with **U-1** in all three solvents (Entries 1-3), while **Ce-1** gave a lower conversion and a higher molecular weight than predicted in dichloroethane (Entry 12). This result suggests potential catalyst degradation which may arise as a result of the harder nature of Ce(IV) compared to U(IV) making it more likely to abstract chloride from the halogenated solvent.

To determine the role of the siloxide ligand during polymerisation homoleptic **UL_4** was used (Entry 6). It was found insertion into the aryloxide of the ligand was slow, forming polymers with molecular weights double the theoretical values expected. This shows the significance and preference of the siloxide ligand to act as the reactive initiator.

It was hypothesised the heterobimetallic complex, **U-Ni**, may impart a change in tacticity control during the ROP of rac-lactide, compared to its monometallic analogue **U-1**, due to a change in the coordination environment surrounding the uranium centre. First, its activity was monitored using L-lactide (Entry 8) but unfortunately negligible polymerisation occurred. In **U-1**, the phosphorous ligands are labile and only weakly coordinated to the uranium centre. Introduction of nickel into the system will favour P-Ni bonding compared to P-U, producing a less labile and more conformationally rigid complex. This change in lability may be responsible for the lack of polymerisation, by hampering monomer access. Another hypothesis is the *Inverse Trans Influence* (ITI), which predicts incorporation of nickel *trans* to the siloxide would strengthen the U-$OSiMe_3$ bond. This would reduce the nucleophilicity of the siloxide ligand and could prevent lactide insertion. To help promote polymerisation the reaction was repeated with **U-Ni** under immortal conditions using 5 times excess of BnOH (Entry 9). It was theorised the decrease in sterics of benzyl alkoxide compared to the siloxide could perhaps favour monomer coordination, if steric congestion was hampering polymerisation. However, only a minor improvement in conversion was observed.

Immortal polymerisation offers the advantage of a reduction in catalyst loading. Thus polymerisations were repeated under immortal conditions using a monomer:catalyst:BnOH ratio of 200:1:5. Expectedly, **UL_4** showed an improvement in control under immortal conditions where GPC analysis revealed molecular weights in close agreement to the theoretical values (Entry 7). This highlights benzyl alkoxide promotes efficient initiation compared to the sluggish nature of **UL_4** in the absence of BnOH. Both **U-1** and **Ce-1** maintained excellent control under immortal conditions (Entries 5 and 14).

4.3 Polymerisation kinetics

In-situ monitoring of the polymerisation was conducted using ^{1}H NMR spectroscopy in order to investigate and compare the reactivities of **U-1** and **Ce-1**, illustrated in **Figure 4.5** and **Figure 4.6** respectively. Interestingly, a significant difference was observed in the reaction rates of the two catalysts. k_{obs} for **U-1** was 0.0189 s^{-1} and the polymerisation of L-lactide was complete in ~160 minutes compared to **Ce-1** where the polymerisation took 600 minutes with a k_{obs} of 0.0052 s^{-1}. It was hypothesised that the higher affinity of the phosphorous donor atom for the uranium centre will result in a fixed coordination geometry ensuring lactide coordination to the productive siloxide face. Conversely, the weaker nature of the phosphorous-cerium bond will generate a more labile ligand which can create a more open and flexible coordination geometry. This could favour non-productive lactide coordination, *i.e trans* to the growing chain, which would account for the observed decrease in rate. Moreover, the greater Lewis acidity of **Ce-1** may decrease the lability of the Ce-siloxide bond reducing the efficiency of lactide insertion.

It was expected a similar trend in rate would be observed under immortal conditions (monomer:catalyst:BnOH, 200:1:5) but unexpectedly, the reactivity of the catalysts switched and the observed rate constants for **U-1** and **Ce-1** were 0.0782 s^{-1} and 0.1646 s^{-1} respectively. (**Figure 4.7** and **Figure 4.8**). It was theorised that the increase in observed

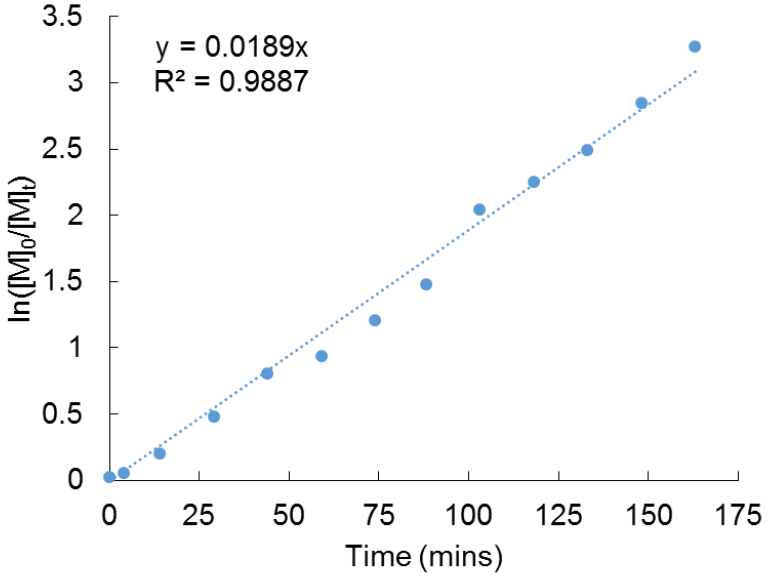

Figure 4.5 *Plot of ln($[M]_0/[M]_t$) versus time for the ROP of L-lactide using catalyst* ***U-1*** *in toluene-d_8.* K_{obs} = 0.0189 s^{-1}.

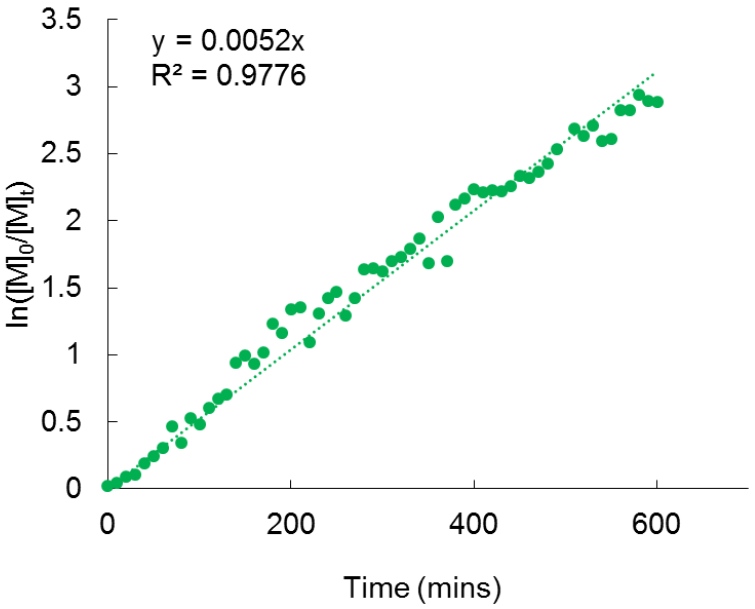

Figure 4.6 *Plot of ln([M]$_0$/[M]$_t$) versus time for the ROP of L-lactide using catalyst* ***Ce-1*** *in toluene-d$_8$.* K_{obs} = 0.0052 s^{-1}.

rate could be rationalised by the excess BnOH participating in chain exchange reactions with both siloxide and the phenoxide ligands. This would alleviate steric congestion, creating a more open coordination environment easing lactide access to the Lewis acidic metal centres. The greater Lewis acidity of Ce(IV) compared to U(IV) may account for the switch in reactivity.

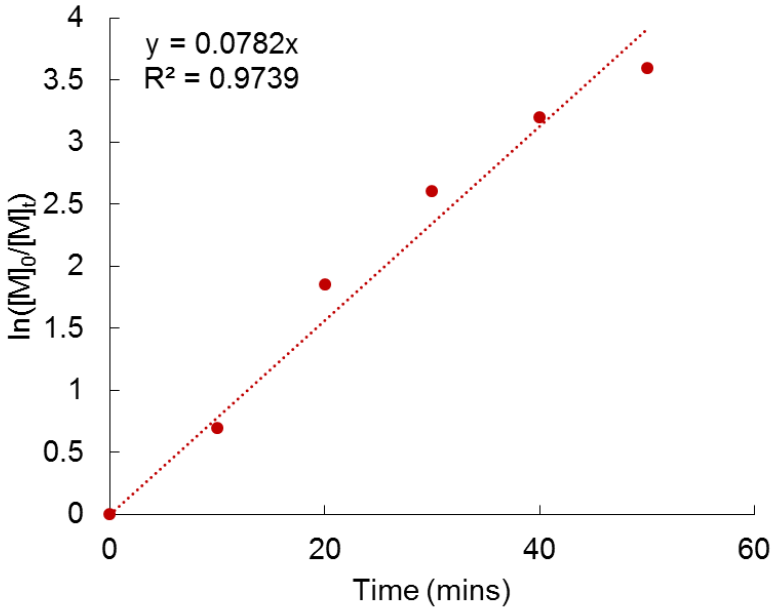

Figure 4.7 *Plot of ln([M]$_0$/[M]$_t$) versus time for the ROP of L-lactide under immortal conditions using catalyst* ***U-1*** *in toluene-d$_8$.* K_{obs} = 0.1646 s^{-1}.

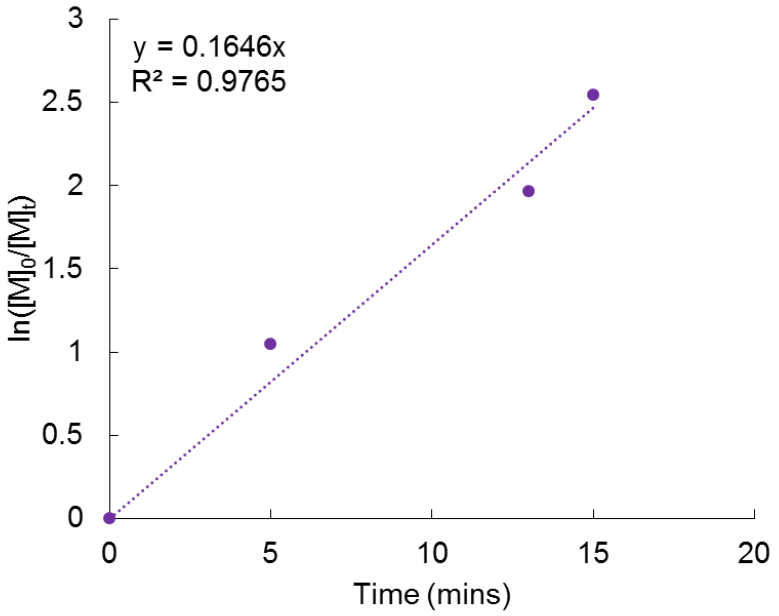

Figure 4.8 *Plot of ln([M]$_0$/[M]$_t$) versus time for the ROP of L-lactide under immortal conditions using catalyst* ***Ce-1*** *in toluene-d_8.* K_{obs} = 0.1646 s^{-1}.

^{31}P NMR spectroscopy supports the idea of BnOH-promoted ligand displacement. The peak corresponding to free phosphorous ligand HOAr^{p} appears to grow on addition of BnOH (compare spectra **a** and **b** in **Figure 4.9**). Furthermore ^{1}H NMR indicates replacement of siloxide with benzyl alkoxide as evidenced by disappearance of the siloxide group in spectrum **b** compared to **a** (**Figure 4.10**).

To confirm BnOH end-group incorporation, 2D NMR spectroscopy (COSY, HSQC, and HMBC) was carried out on a polymer prepared from **Ce-1** under immortal conditions. Characteristic resonances corresponding to benzyl protons **g** were apparent along with a quartet belonging to proton **c** from an end-group capped with an OH (**Figure 4.11**). To further confirm this analysis MALDI-TOF mass spectrometry of the same sample was carried out (**Figure 4.12**). The mass spectrum identifies a major population of BnOH terminated chains, $[M + Na]^+$ for $C_7H_7O(C_6H_8O_4)_{30}H$. Increments of 72 Da between consecutive peaks were evident, suggesting significant transesterification occurred.

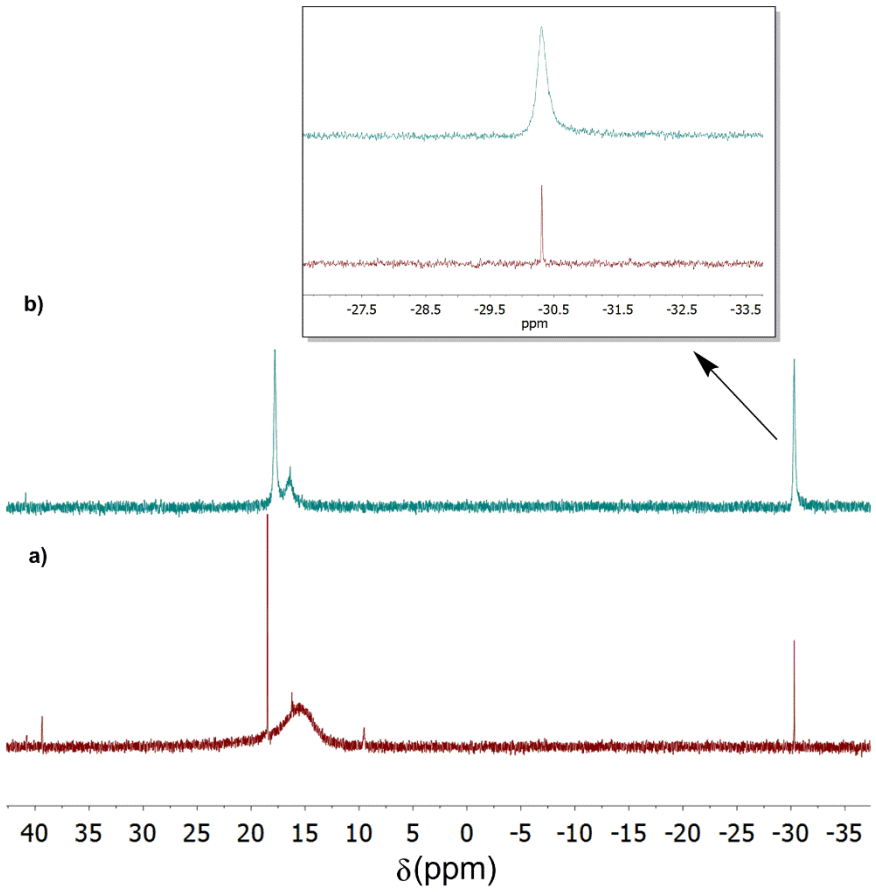

Figure 4.9 *$^{31}P\{^{1}H\}$ NMR spectra of **Ce-1**. a) absense of BnOH, b) presence of BnOH (5 equivalents) in toluene-d_8 at 333K.*

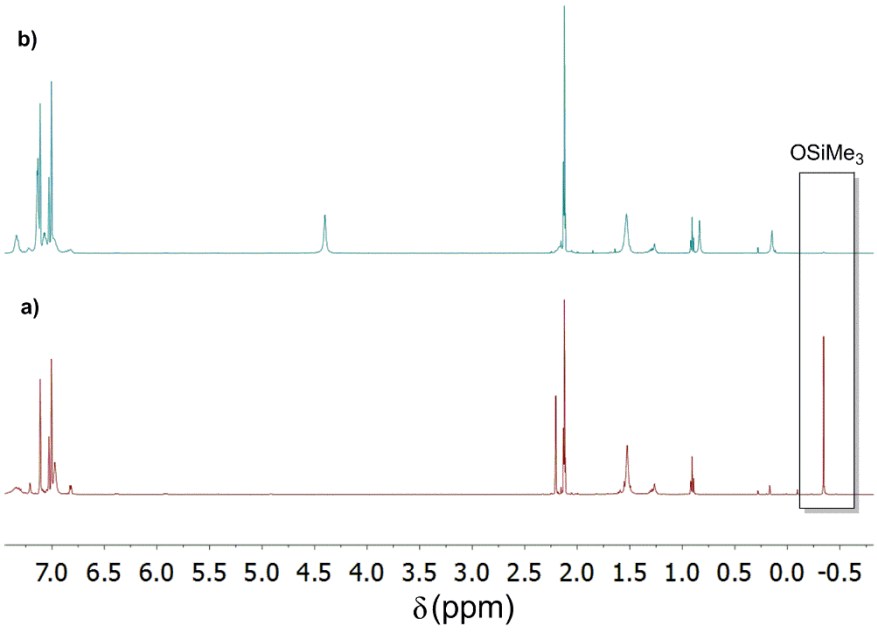

Figure 4.10 *^{1}H NMR spectra of **Ce-1**. a) absence of BnOH, b) presence of BnOH (5 equivalents) in toluene-d_8 at 333K.*

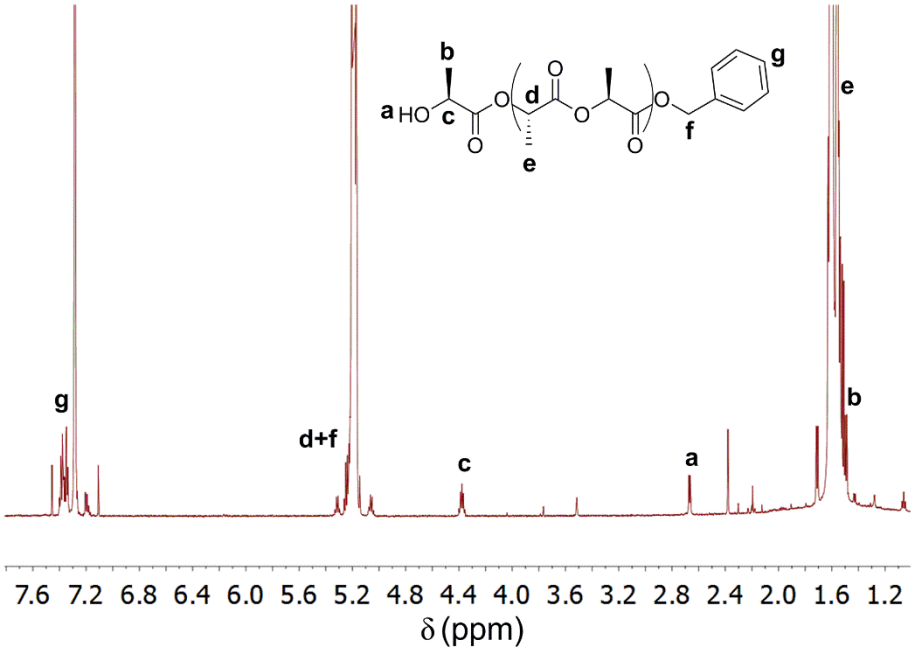

Figure 4.11 *^{1}H NMR spectrum of poly-* L*-lactide made from catalyst* ***Ce-1*** *for end-group analysis in $CDCl_3$ at 300 K.*

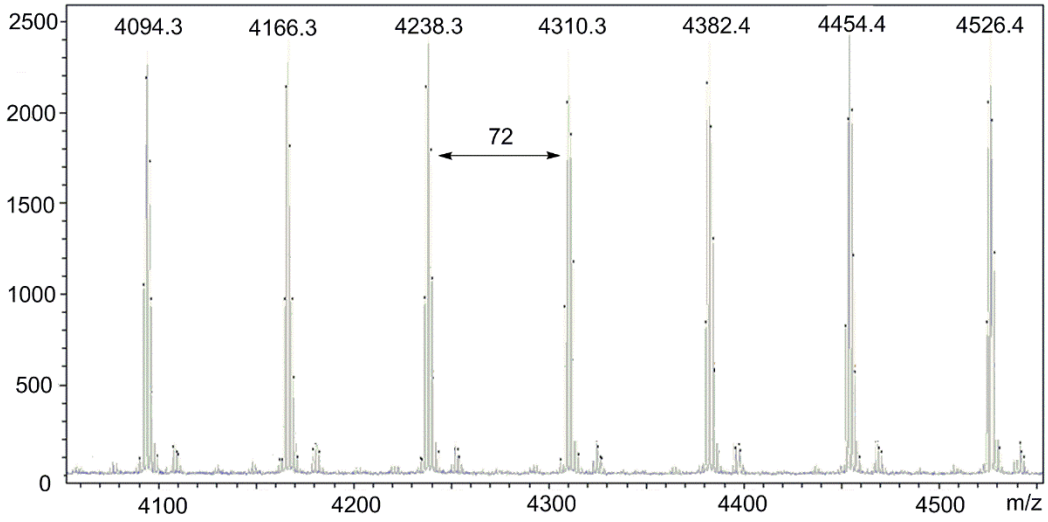

Figure 4.12 *MALDI mass spectrometry for end-group analysis of PLA from* ***Ce-1*** *under immortal conditions.*

4.4 Ring-opening polymerisation of rac-lactide

To explore what control these catalysts exhibited on the stereoselectivity of polymerisations, ROP of rac-lactide was examined using **U-1** and **Ce-1**. The screening reactions were carried out with a monomer:catalyst ratio of 200:1 using various solvents and temperatures. It was discovered that **U-1** favoured the formation of heterotactically-enriched PLA, (**Scheme 4.1** and Entry 1, **Table 4.2**). This structure is favoured when the

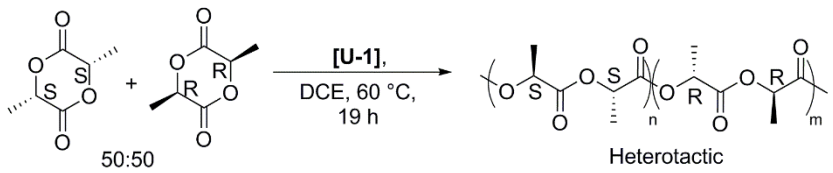

Scheme 4.1 *Polymerisation of rac-lactide using U-1 to form heterotactic PLA.*

catalyst alters coordination of one enantiomer followed by the opposite, to generate a polymer with the following stereosequence- -RR-SS-RR-SS-. **Ce-1** enforced no stereocontrol during the polymerisation (Entry 8, **Table 4.2**). It was hypothesised that the more rigid coordination environment in **U-1** generated from the strong phosphorous-uranium bonding promotes chain end control stereoselectivity. On the other hand, **Ce-1** displays a more flexible coordination sphere due to the greater lability of the phosphorous ligands, leading to no preference of monomer coordination (L- or D-lactide) producing atactic PLA.

Altering the reaction conditions had no impact on the stereocontrol induced by **Ce-1** (Entries 8-13), giving rise to atactic PLA under all conditions. However, solvent choice influenced the tacticity observed with **U-1**. The highest stereoselectivity was observed when dichloroethane was used as the solvent, generating heterotactic PLA, with $P_r = 0.79$ (Entry 2). Dichloroethane likely offers the best results due to the higher solubility of rac-lactide in this solvent compared to toluene or benzene. To the best of our knowledge, this is the highest tacticity value for any uranium catalyst for lactide ROP. Expectedly, the use of dichloroethane with **Ce-1** resulted in a decrease in conversion for reasons discussed previously (Entries 9 and 10). Moreover, temperature impacted the heterotacticity obtained. Increasing the temperature from 60 °C to 90 °C using **U-1** led to a decrease in tacticity (compare Entries 4 and 5), a trend commonly observed in the literature,[13] while decreasing the temperature appeared to have a negligible influence (compare Entries 5 and 6).

As discussed above immortal polymerisation of L-lactide, with a 5 times excess of BnOH using either **U-1** or **Ce-1**, gave rise to faster reaction rates compared to in the absence of BnOH. It was hypothesised a more open coordination environment was created under immortal conditions enabling easier lactide coordination. Based on this hypothesis, a less sterically crowded and fixed coordination environment would expect a loss of

Table 4.2 *Ring-opening polymerisation of rac-lactide.*

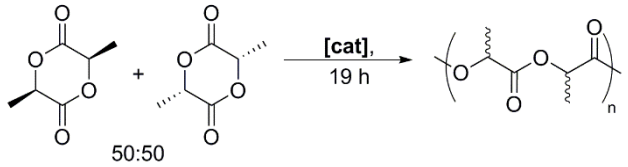

Entry	[cat]	Solvent	Temperature (°C)	P_r[a]	Conversion (%)[b]	$M_{n,th}$ (Da)[c]	$M_{n,GPC}$ (Da)[d]	Đ[d]
[e]	**U-1**	Toluene	60	0.68	98	28,300	23,100	1.35
2[e]	**U-1**	Dichloroethane	60	0.79	96	27,800	24,600	1.31
3[e]	**U-1**	Dichloroethane	45	0.75	95	27,500	28,000	1.19
4[e]	**U-1**	Benzene-d_6	90	0.62	>99	28,600	23,700	1.47
5[e]	**U-1**	Benzene- d_6	60	0.71	>99	28,600	25,700	1.28
6[e]	**U-1**	Benzene- d_6	50	0.73	74	21,400	29,000	1.16
7[f]	**U-1**	Benzene- d_6	60	0.58	>99	4,900[g]	6,600	1.32
8[e]	**Ce-1**	Toluene	60	0.37	95	27,500	22,400	1.64
9[e]	**Ce-1**	Dichloroethane	60	0.45	70	20,300	32,800	1.83
10[e]	**Ce-1**	Dichloroethane	45	0.51	71	20,600	31,500	1.66
11[e]	**Ce-1**	Benzene- d_6	90	0.32	>99	28,600	23,200	2.61
12[e]	**Ce-1**	Benzene- d_6	60	0.4	92	28,600	28,500	1.57
13[e]	**Ce-1**	Benzene- d_6	50	0.58	83	24,000	23,400	1.93
14[e]	**Ce-1**	Toluene	60	0.42	>99	4,900[g]	7,900	1.23

[a]Determined by homodecoupled ^{1}H NMR spectroscopy. [b]Determined by ^{1}H NMR spectroscopy monitored by comparison of monomer to polymer resonances. [c]$M_{n,th}$ = (% conv. X ($MW_{(monomer)}$ x2)) + $MW_{(HOSi(Me)3)}$. [d]Determined by triple detection GPC using *dn/dc* of 0.05. [e]Monomer: catalyst (200:1). [f]Monomer: catalyst: BnOH (200:1:5). [g]$M_{n,th}$ = (% conv. X ($MW_{(monomer)}$ x2))/6 + $MW_{((HOSi(Me)3 + BnOH)/2)}$.

heterotacticity. To test this theory polymerisation of rac-lactide using **U-1** and **Ce-1** were repeated under immortal conditions (monomer:catalyst:BnOH, 200:1:5). Expectedly, no stereocontrol was observed with **Ce-1** (Entry 14), yet, a decrease in heterotacticity from P_r = 0.71 to P_r = 0.58 was observed for **U-1** (compare Entries 5 and 7). This result is consistent with the proposed theory, thus a less conformationally rigid complex, decreases the chain end influence, which leads to a decrease in the heterotactic bias.

4.5 Conclusions and future work

To summarise, a group of uranium (IV) and cerium (IV) catalysts have been synthesised for the ROP of lactide, successfully expanding the scope of the currently limited uranium and cerium ROP catalysts previously reported. Reactions using these catalysts are shown in **Scheme 4.2**. Heterobimetallic complex **U-Ni** was effectively inactive in the ROP of L-lactide under living and immortal conditions (route **a)**). This is hypothesised to be a combination of both an increase in steric crowding preventing monomer coordination and strengthening of the U-OSiMe$_3$ bond as a result of the *inverse trans influence*. A stoichiometric experiment between LA and **U-Ni** would be of interest to observe whether LA coordination occurs and whether a single monomer can be ring-opened *via* monitoring a change in the ^{1}H resonances in the NMR spectrum.

Uranium complex **U-1** displayed excellent control giving a narrow Đ polymer (route **b)**), while removal of the siloxide group as in **UL$_4$** generated a polymer with molecular weight double that expected (route **c)**). This highlights the importance of the siloxide as the initiator during polymerisation.

Cerium complex **Ce-1** is analogous to **U-1** and displayed good control but with an associated broader dispersity compared to **U-1** (route **d)**). Kinetic studies illustrated that **U-1** polymerises lactide at a faster rate than **Ce-1**. Introducing an excess of BnOH, (immortal polymerisation) using **U-1** and **Ce-1** (routes **e)** and **f)** respectively) gave much faster reaction rates compared to in the absence of BnOH. It was discovered BnOH is capable of displacing both the siloxide and some phosphorous ligands to create a more open geometry and thus an associated increase in rate. Under these conditions **Ce-1**, polymerised lactide at a faster rate than **U-1**.

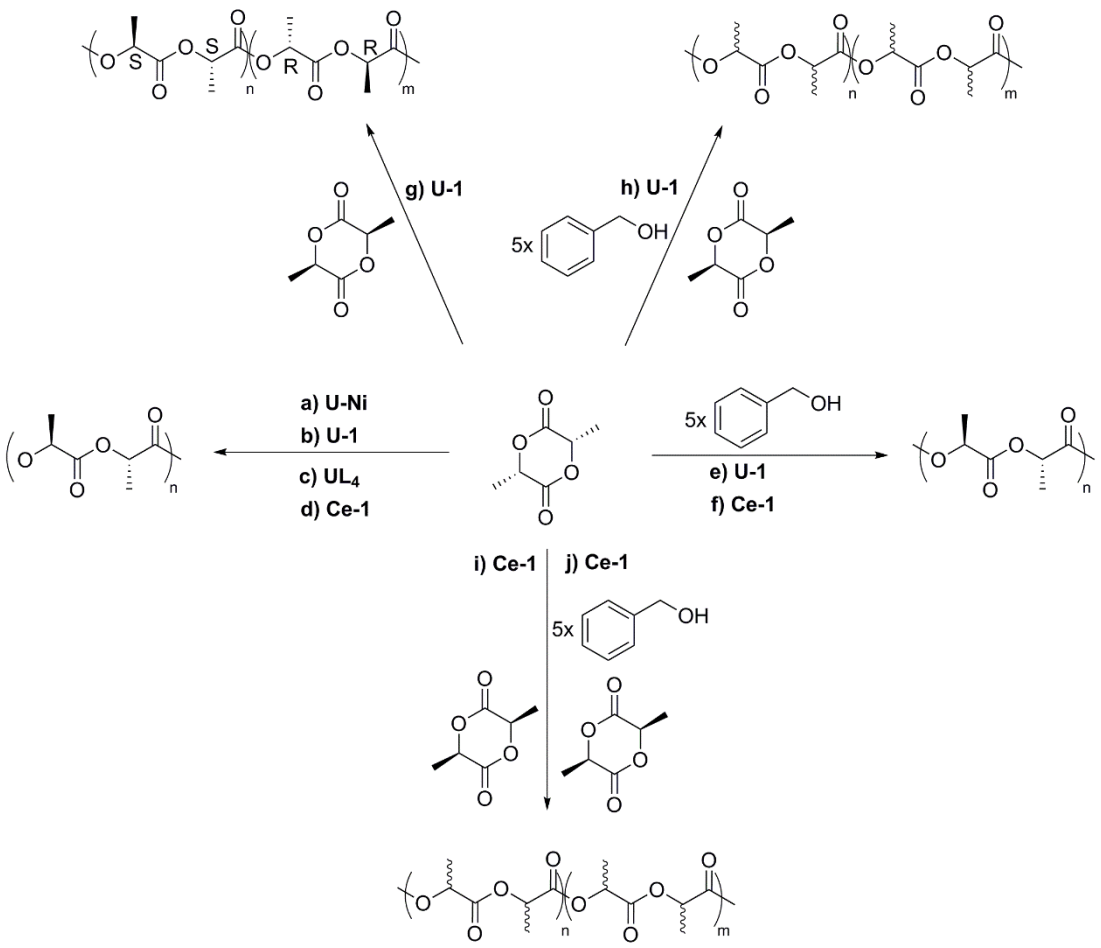

Scheme 4.2 *Summary of the different polymerisation routes of L- and rac-lactide using uranium and cerium initiators.*

It would be of interest to attempt to grow single crystals suitable for X-ray diffraction of **U-1** and **Ce-1** from 5 x excess of BnOH to try and identify the structures formed under immortal conditions. This should provide evidence of ligand displacement of the phosphorous ligands ($HOAr^{P}$) with BnOH.

Polymerisation of rac-lactide using **U-1** produced a heterotactically biased PLA, with to the best of our knowledge, the highest P_r value (0.79) of any uranium catalyst for the ROP of rac-lactide (route **g)**). Tacticity was reduced with an increase in temperature. Conversely, **Ce-1** generates an atactic polymer which is consistent with a less rigid coordination sphere with limited phosphorous coordination (route **i)**). Repeating the polymerisations under immortal conditions removed the stereocontrol imparted by **U-1**, potentially due to opening-up access to the coordination sphere through replacement of phosphorous coordination with BnOH, consequently eliminating chain end control

(route **h)**). ROP of rac-lactide under immortal conditions using **Ce-1** enforced no sterecontrol (route **j)**).

It would be of interest to manipulate the tacticity control by using a temperature profile during the polymerisation of rac-lactide with **U-1**. It may be possible to produce a heterotactic block then increase the temperature to synthesise an atactic block and so forth. Moreover, it is worth expanding the monomer scope and screening these aforementioned catalysts in the ROP of other biodegradable monomers such as ε-caprolactone and β-lactones. This also opens opportunities to generate random and block copolymers of lactide with other biodegradable monomers.

4.6 References

1 Sun, S.; Nie, K.; Tan, Y.; Zhao, B.; Zhang, Y.; Shen, Q.; Yao, Y. *Dalton Trans.* **2013**, *42*, 2870–2878.

2 Nie, K.; Feng, T.; Song, F.; Zhang, Y.; Sun, H.; Yuan, D.; Yao, Y.; Shen, Q. *Sci. China Chem.*, **2014**, *57*, 1106–1116.

3 Li, W.; Xue, M.; Tu, T.; Zhang, Y.; Shen, Q. *Dalton Trans.* **2012**, 41, 7258–7265.

4 Cao, T. P. A.; Buchard, A.; Le Goff, X. F.; Auffrant, A.; Williams, C. K. *Inorg. Chem.*, **2012**, *51*, 2157–2169.

5 Bakewell, C.; Cao, T.-P. A.; Long, N.; Le Goff, X.F.; Auffrant, A.; Williams, C. K. *J. Am. Chem. Soc.*, **2012**, *134*, 20577–20580.

6 Arnold, P. L.; Buffet, J. C.; Blaudeck, R. P.; Sujecki, S.; Blake, A. J.; Wilson, C. *Angew. Chem. Int. Ed.*, **2008**, *47*, 6033–6036.

7 Broderick, E. M.; Diaconescu, P. L. *Inorg. Chem.*, **2009**, *48*, 4701–4706.

8 Broderick, E. M.; Guo, N.; Wu, T.; Vogel, C. S.; Xu, C.; Sutter, J.; Miller, J. T.; Meyer, K.; Cantat, T.; Diaconescu, P. L. *Chem. Commun.*, **2011**, *47*, 9897–9899.

9 Agarwal, S.; Puchner, M.; *Eur. Polym. J.*, **2002**, *38*, 2365–2371.

10 Barnea, E.; Moradove, D.; Berthet, J.C.; Ephritikhine, M.; Eisen, M. S. *Organometallics*, **2006**, *25*, 320–322.

11 Hayes, C. E.; Sarazin, Y.; Katz, M. J.; Carpentier, J. F.; Leznoff, D. B. *Organometallics*, **2013**, *32*, 1183–1192.

12 Hlina, J. A.; Pankhurst, J. R.; Kaltsoyannis, N.; Arnold, P. L. *J. Am. Chem. Soc.*, **2016**, *138*, 3333–3345.

13 Char, J.; Brulé, E.; Gros, P. C.; Rager, M.-N.; Guérineau, V.; Thomas, C. M. *J. Organomet. Chem.*, **2015**, *796*, 47–53.

Chapter 5. Conclusions

The aim of this research was to modify the thermal properties of PLA *via* olefin CM. An in-depth conclusion and future work section can be found at the end of each chapter, this chapter summarises the thesis as a whole. Initial studies focussed on the generation of a novel olefin containing derivative of lactide, mono-methylenated lactide (MML). MML was categorised as a low reactivity Type III olefin with a narrow substrate scope. Associated stability issues rendered MML inactive in ROP. A second olefin containing derivative of lactide, 3-methylenated lactide (3-ML) was synthesised. Olefin categorisation determined 3-ML was a Type III olefin that demonstrated successful CM with long chain aliphatic Type I olefins, hex-1-ene to dodec-1-ene. Pre-polymerisation hydrogenation of hex-1-ene functionalised 3-ML, produced a stable monomer capable of ROP. The T_g of the resulting polymer was lower than room temperature, showcasing that pre-polymerisation olefin CM can successfully alter the thermal properties of PLA.

β-Heptenolactone (β-HL), which contained olefin functionality, was explored in both pre- and post-polymerisation olefin CM. Although pre-polymerisation olefin CM was challenging, post-polymerisation olefin CM on Poly(β-heptenolactone) P(β-HL), was successful, generating functionalised homopolymers of substantially increased T_g's compared to P(β-HL). Two copolymers of lactide were synthesised; P(LA_{86}-co-β-HL_4) and P(LA_{85}-co-β-HL_{19}). Olefin CM with 15 different cross partners ranging from Type I to Type III was explored. Full functional group incorporation was achieved with the less active Type II and Type III olefins. Thermal analysis indicated P(LA_{85}-co-β-HL_{19}) displayed a more substantial change in the thermal properties compared to P(LA_{86}-co-β-HL_4). Incorporation of both allyl alcohol and styrene gave the biggest changes in the thermal properties with an associated increase in both T_g and T_m. Following from the observed incomplete incorporation of the Type I olefins during olefin CM, a novel methodology to introduce two unique functionalities into the polymer backbone was developed through manipulation of olefin Type reactivities. This work demonstrates the properties of PLA can be altered and tuned through copolymerisation and functionalisation using olefin CM.

Finally, in a collaborative project, uranium(IV) and cerium(IV) complexes were investigated as initiators in the ROP of lactide. ROP of L-lactide gave better control using the uranium complex compared to the cerium complex with an associated faster rate. Polymerisations under immortal conditions were investigated and the reactivity was reversed, where the cerium catalyst was more active than the uranium catalyst. These observations were linked to the changes in coordination geometry around the metal centres. Polymerisation of rac-lactide using the cerium complex produced atactic PLA, while the uranium complex produced heterotactically biased PLA. The heterotacticity observed with the uranium complex could be tuned with temperature and switched off under immortal conditions. Thus, new catalyst design has expanded the scope of achiral complexes available for the stereocontrolled ROP of rac-lactide.

The work of this thesis has demonstrated successful modification of the properties of PLA through novel monomer synthesis, copolymerisation with an olefin containing monomer and tacticity control. Of significance is the successful utilisation of olefin CM as an effective tool for altering the properties of PLA. Continued development and research into biodegradable polymers, derived from renewable resources, is key for a sustainable future. Research needs to focus on further development of new functionalised polyesters with an outlook on new synthetic strategies and new catalysts. Although challenges exist with both matching the polymer properties to current petroleum derived polymers and maintaining a competitive financial advantage, the future looks promising for PLA and other renewably sourced biodegradable polymers.

Chapter 6. Experimental

6.1 General methods and characterisation

All experiments involving air- and moisture-sensitive compounds were performed under a nitrogen atmosphere using either an MBraun LABmaster sp or Vigor glovebox system equipped with a −35 °C freezer and [H_2O] and [O_2] analysers or using standard Schlenk techniques. Dichloromethane (DCM), tetrahydrofuran (THF) and toluene were obtained from an Innovative Technologies solvent purification system incorporating columns of alumina and copper catalysts and were de-gassed by three freeze-pump-thaw cycles prior to use. Carbon monoxide (99.9%, BOC) and hydrogen (high purity BOC) gas were used as received. High-pressure carbonylation was preformed in a 100 mL pressure reactor with a carbon monoxide detector. Gel permeation chromatography (GPC) was performed using a Malvern Instruments Viscotek 270 GPC Max triple detection system with 2 × mixed bed styrene/DVB columns (300 × 7.5 mm) in THF at a flow rate of 1 mL min^{-1} and an injection volume of 100 μL or 200 μL. Samples for analysis were pre-dissolved in chloroform at a concentration of ~8–12 mg/mL. The *dn/dc* value for poly(lactic acid) was 0.05.[1] The *dn/dc* value for β-heptenolcatone was calculated to be 0.063 using OmniSEC 5.0 software. Calculation of the *dn/dc* value was obtained from five samples of known concentrations of the same molecular weight. OmniSEC 5.0 software was used to obtain a calculated *dn/dc* value for each concentration and an average value was used as the input *dn/dc* value of the polymer. Triple detection GPC was used for all analysis except where concentration of samples was low and conventional calibration was used instead (indicated on Table footnotes). Unlike with homopolymers, triple detection GPC is not suitable for obtaining absolute M_n for copolymers as *dn/dc* cannot be determined. However, this did not affect analysis of the copolymers in this thesis as M_n was unaffected by functionalisation. ^{1}H NMR spectra were recorded at 298 K using BrukerAvance spectrometers (400, 500 or 600 MHz). ^{13}C NMR spectra were recorded using BrukerAvance spectrometers (126 MHz). 2D NMR analyses (COSY, HSQC, HMBC and NOSEY) were recorded using BrukerAvance spectrometers (500 or 600 MHz). ^{31}P{^{1}H} NMR spectra were obtained using a BrukerAvance spectrometer (202

MHz). ^{29}Si NMR spectra were obtained using a BrukerAvance spectrometer (99 MHz). ^{1}H homodecoupled NMR was recorded using BrukerAvance spectrometer (600 MHz), using a standard pulse programme: zghd.2 irradiating at 1.59 ppm (949.18 Hz). Chloroform-d_1, benzene-d_6, dichloromethane-d_2 or toluene-d_8 were used as solvents for all NMR analyses. Differential scanning calorimetry (DSC) from Chapter 3 was carried out by Long Chen and Dr Barnaby Greenland from the University of Reading using TA Instruments DSC Q2000. DSC from Chapter 2 was performed using TA Instruments DSC 2500, both through a heat/cool/heat cycle between −90 °C to 200 °C at a rate of 10 °C min^{-1}. Values of T_g, T_m and T_c were obtained from the second heating scan. Thermogravimetric analysis (TGA) measurements were performed on a SDTQ600. Samples were heated from room temperature to 800 °C at a rate of 10 °C min^{-1} using recycled pans. Cooling baths at 0 °C, -41 °C and -72 °C were prepared using ice, dry ice/acetonitrile and dry ice/ethanol respectively. MALDI mass spectrometry was run on an AB Voyager MALDI at the EPSRC UK National Mass Spectrometry Facility at Swansea University. The sample was analysed in positive-linear and reflectron modes, with dithranol matrix and NaOAc additive. Mass spectra (EI/ESI) were recorded using Bruker MicroToF II spectrometer.

6.2 Materials

Hoveyda-Grubbs second generation catalyst, paraformaldehyde, trimethylaluminium (2 M in toluene), methylmagnesium chloride (3 M in THF), *N,N'*-diphenylethylenediamine and 1,5,7-triazabicyclodec-5-ene (TBD), were purchased from Sigma-Aldrich and used as received. Hex-1-ene, benzoyl peroxide, tin(IV) chloride and 2,4-diaminonaphthaline, were purchased from Fisher Scientific UK Ltd. and used as received. Tin(II) 2-ethylhexanoate, triethylamine, benzyl alcohol, diethyl allyl phosphonate, octafluorotoluene and chloroform-d_1 were purchased from Sigma Aldrich, dried over calcium hydride for 24 h under reflux, then either distilled under nitrogen or vacuum, or transferred *via* filter cannula under an atmosphere of nitrogen prior to being degassed by three freeze-pump-thaw cycles. Toluene-d_8 and benzene-d_6 were purchased from Sigma-Alrdich and dried over potassium for 72 h under reflux, distilled under nitrogen and degassed by three freeze-pump-thaw cycles. 3-Butene-2-one, dichloromethane-d_2 and dichloroethane were purchased from Sigma Aldrich, de-gassed by three freeze-pump-thaw cycles and dried for

24 h using molecular sieves (3Å) in the glove box. Dicobalt octacarbonyl was purchased from Acros Organics and used as received. 1,2-Epoxy-5-hexene, allyl alcohol, allyltrimethylsilane, 3,3-dimethyl-1-butene and oct-1-ene were purchased from Acros Organics, dried over calcium hydride for 24 h under reflux and transferred *via* filter cannula under an atmosphere of nitrogen prior to being degassed by three freeze-pump-thaw cycles. Dec-1-ene and 5-hexenyl acetate were purchased from Alfa Aesar, dried over calcium hydride for 24 h under reflux and transferred *via* filter cannula under an atmosphere of nitrogen prior to being degassed by three freeze-pump-thaw cycles. Methyl acrylate was purchased from Alfa Aesar, dried over calcium hydride for 24 h under reflux and vacuum transferred prior to being degassed by three freeze-pump-thaw cycles. 1-Dodec-1-ene was purchased from Merck Millipore dried over calcium hydride for 24 h under reflux, before being vacuum transferred and degassed by three freeze-pump-thaw cycles. Styrene was purchased from Merck Millipore, dried over calcium hydride for 24 h under reflux and a vacuum transfer was used prior to being degassed by three freeze-pump-thaw cycles. N-bromosuccinimide, 2,4-di-*tert*-butylphenol, 2,4-dichlorophenol, 1,8-diazabicycloundec-7-en (DBU), chromium(II) chloride and *o*-phenylenediamine, were purchased from VWR International Ltd. and used as received. L- and *rac*-lactide were supplied from Corbion and purified *via* vacuum sublimation three times prior to use. 3,5-Di-*tert*-butylsalicylaldehyde, $^{ClEtN\text{-}Bn}$[salan]H_2, $^{t\text{BuPr}}$[salen]H_2, $^{t\text{BuNapth}}$[salen]H_2, $^{ClEtN\text{-}Bn}$[salan]AlMe, $^{t\text{BuPr}}$[salen]AlMe, $^{t\text{BuNapth}}$[salen]AlMe, [salph]CrCl and $Cp_2TiClCH_2AlMe_2$ (the Tebbe reagent) were synthesised *via* literature procedures.[2–6] $Me_3SiOU(\mu\text{-}OAr^P\text{-}1\kappa^1O,2\kappa^2P)_3Ni$, $Me_3SiOU(OC_6H_2\text{-}6\text{-}Bu^t\text{-}4\text{-}Me\text{-}2\text{-}PPh_2\text{-}\kappa^2O,P)_3$ and $Me_3SiOCe(OC_6H_2\text{-}6\text{-}Bu^t\text{-}4\text{-}Me\text{-}2\text{-}PPh_2\text{-}\kappa^2O,P)_3$, were synthesised and provided by Jordann Wells, Johann Hilna and Professor Polly Arnold from the University of Edinburgh.

6.3 Synthesis for chapter two

6.3.1 Representative methylenation of L-lactide using the Tebbe reagent

In a glove box L-lactide (0.85 g, 5.897 mmol) was dissolved in THF (17 mL) and added to an oven-dried ampoule. In a second ampoule the Tebbe reagent (3.360 g, 11.794 mmol)

was dissolved in toluene (68 mL). Outside the box, both solutions were cooled to 0 °C and the Tebbe solution was transferred dropwise to the lactide solution *via* cannula transfer under an atmosphere of nitrogen. Once the addition was complete the ampoule was sealed under nitrogen and the reaction was stirred for 1 h. The reaction was then diluted with diethyl ether (100 mL), filtered through ceilte, washed with diethyl ether and concentrated *in vacuo* to yield an orange oil. The product was purified *via* column chromatography on silica gel (petroleum ether:ethyl acetate, 85:15). Evaporation of the combined fractions was carried out at 0 °C using a stream of nitrogen to afford mono-, di- methylenated lactide and residual lactide (isolation method developed by Dr Vincent Gauchot).

Mono-methylenated lactide (MML): (70 % by NMR), 0.150 g, 18 %.

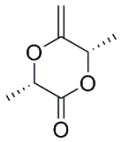

^{1}H NMR ($CDCl_3$, ppm): δ 5.06 (qd, J = 6.4 Hz, 1 Hz, 1H), 4.70 (q, 6.5 Hz, 1H), 4.52 (dd, J = 2.3 Hz, 1 Hz, 1H), 4.25 (m, 1H), 1.59 (d, J = 6.4 Hz, 3H,), 1.57 (d, J = 6.5 Hz, 3H). ^{13}C NMR {^{1}H} ($CDCl_3$, ppm): δ 170.4, 155.4, 87.4, 71.9, 69.9 17.0, 16.0. HRMS (ESI^+): m/z calculated 143.0703 $[M + H]^+$ m/z found 143.0713 $[M + H]^+$

Di- methylenated lactide (DML): (14 % by NMR), negligible yield.

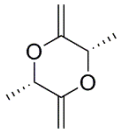

^{1}H NMR ($CDCl_3$, ppm): δ 4.80 (qd, J = 6.3 H_z, 1 Hz, 2H), 4.34 (dd, 2.0 Hz, 1.0 Hz, 2H), 4.05 (m, 2H), 1.45 (d, J = 6.3 Hz, 6H). ^{13}C NMR {^{1}H} ($CDCl_3$, ppm): δ 159.4, 84.71, 68.1, 17.2. HRMS (ESI^+): m/z calculated 141.0910 $[M + H]^+$ m/z found 141.0913 $[M + H]^+$

6.3.2 Representative ring-opening polymerisation of MML

In a glove box to a Young's NMR tube MML (0.030 g, 0.211 mmol), $^{t\text{BuPr}}$[salen]AlMe (0.0023 g, 4.22 x10^{-3} mmol) and BnOH (0.4 μL, 4.22 x10^{-3} mmol) were dissolved in C_6D_6 (0.5 mL). Outside the box the solution was heated at 85 °C for 15 h. The reaction was quenched with a drop of methanol and the solution was concentrated using a stream of of nitrogen at 0 °C. ^{1}H NMR analysis confirmed the polymerisation was unsuccessful.

6.3.3 Representative olefin cross-metathesis of MML

In a glove box MML (0.060 g, 0.422 mmol), hex-1-ene (0.106 g, 0.282 mmol) and Hoveyda-Grubbs Second Generation catalyst (0.013 g, 0.021 mmol) were dissolved in DCM (3 mL) and added to an oven dried ampoule. Outside the box the solution was de-gassed by one freeze-pump-thaw cycle and heated at reflux for 16 h. The solvent was evaporated using a stream of nitrogen at 0 °C. The product was then purified *via* column chromatography on silica gel (petroleum spirits : ethyl acetate, 70:30). Evaporation of the combined fractions was carried out at 0 °C using a stream of nitrogen to afford the product as a colourless oil. (85 % by NMR), 0.025 g, 30 %.

Formation of HML

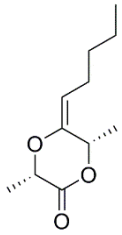

^{1}H NMR ($CDCl_3$, ppm): δ 5.05 (m, 1H), 4.68 (q, 6.6 Hz, 1H), 4.65 (m, 1H), 2.08-2.14 (m, 2H), 1.57 (d, 6.6 Hz, 3H), 1.54 (d, 6.3 Hz, 3H), 1.38-1.33 (m, 4H), 0.92 (m, 3H). ^{13}C NMR {^{1}H} ($CDCl_3$, ppm): δ 170.8, 147.2, 105.0, 72.7, 70.1, 31.5, 22.3, 23.7, 17.1, 16.4, 13.9. HRMS (ESI^+): m/z calculated 199.1329 $[M + H]^+$ m/z found 199.1322 $[M + H]^+$

6.3.4 NMR degradation of MML and HML

In two separate Young's NMR tubes, MML and HML were dissolved in $CDCl_3$ and placed in a pre-heated oil bath at 60 °C. Degradation with time was monitored (6 days) by ^{1}H NMR spectroscopy. The temperature was increased gradually, reaching a maximum of 105 °C.

MML degradation to 49

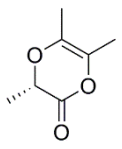

^{1}H NMR ($CDCl_3$, ppm): δ 4.32 (q, J = 6.7 Hz, 1H), 1.92 (q, J = 1.1 Hz, 3H), 1.83 (q, J = 1.1 Hz, 3H), 1.56 (d, J = 6.7 Hz, 3H). ^{13}C NMR {^{1}H} ($CDCl_3$, ppm): δ 166.5, 132.2, 129.1, 70.4, 15.6, 14.3, 14.1. HRMS (ESI^+): m/z calculated 165.0522 $[M + Na]^+$ m/z found 165.0536 $[M + Na]^+$

HML degradation to 50

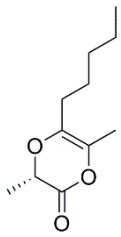

^{1}H NMR ($CDCl_3$, ppm): δ 4.29 (q, J = 6.8 Hz, 1H), 2.14-2.11 (m, 2H), 1.92 (s, 3H), 1.55 (d, 6.8 Hz, 3H), 1.53- 1.50 (m, 2H), 1.34-1.31 (m, 4H), 0.92 (m, 3H). ^{13}C NMR {^{1}H} ($CDCl_3$, ppm): δ 166.6, 135.8, 129.3, 70.5, 31.3, 28.5, 26.6, 22.4, 15.6, 14.0, 14.0. HRMS (ESI^+): m/z calculated 221.1148 $[M + Na]^+$ m/z found 221.1154 $[M + Na]^+$.

6.3.5 Representative ring-opening polymerisation of HML

In a glove box HML (0.025 g, 0.126 mmol), TBD (0.6 mg, 4.206 x10^{-3} mmol) and BnOH (0.4 μL, 4.206 x10^{-3} mmol) were dissolved in dichloromethane-d_2 (0.6 mL) and added to an oven dried ampoule. Outside the box the reaction was left at room temperature for 24 h. The same molar ratio of reagents was used as above for catalyst $Sn(Oct)_2$ which was left to react for 24 h at 120 °C. Polymerisations were unsuccessful as determined by ^{1}H NMR spectroscopy.

6.3.6 Synthesis of 3-ML

Synthesis of 3-bromo-3,6-dimethyl-1,4-dioxane-2,5-dione (3-BL)

L-Lactide (20 g, 138.76 mmol) and *n*-bromosuccinimide (27.2 g, 152.8 mmol) were dissolved in benzene (100 mL) and heated at reflux. Benzoyl peroxide (0.668 g, 2.76 mmol) in benzene (10 mL) was added *via* syringe over ~30 mins. The reaction was left to reflux for a further 12 h before the solution was cooled and filtered. The solvent was removed *in vacuo* to yield pale yellow crystals. The crystals were dissolved in DCM and extracted using washings of saturated sodium bisulfite (3x 10 mL) and saturated sodium chloride (1x 10 mL). The organic layer was dried ($MgSO_4$) and concentrated *in vacuo* to yield a yellow solid. The solid was recrystallized from hot hexane and ethyl acetate and cooled in the freezer for 16 h. Following the solution was filtered to collect white crystals. (>99 % $_{NMR}$), 19.5 g, 63%. ^{1}H and ^{13}C NMR spectroscopy characterisation was consistent with literature reports.[7]

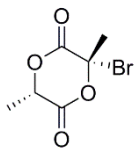

^{1}H NMR ($CDCl_3$, ppm): δ 5.50 (q, J = 6.8 Hz, 1H), 2.34 (s, 3H), 1.73, (d, 6.8 Hz, 3H). ^{13}C NMR {^{1}H} ($CDCl_3$, ppm): δ 164.7, 161.2, 81.4, 73.7, 29.7, 16.5.

Synthesis of 3-methylene-6-methyl-1,4-dioxane-2,5-dione (3-ML)

3-BL (19.5 g, 87.4 mmol) was dried under vacuum for 2 h prior to use. To this DCM (~100 mL) was added *via* cannula under an atmosphere of nitrogen and the flask was cooled to 0 °C. Triethylamine (13 mL, 96.1 mmol) was added dropwise *via* syringe and the reaction was stirred for 1 h at 0 °C, then warmed to room temperature and stirred for a further 1 h. The mixture was extracted with HCl (0.2 M, 3x 10 mL), and NaCl (1x 10 mL), dried ($MgSO_4$) and concentrated *in vacuo* to yield a pale yellow solid. The product was then purified *via* column chromatography on silica gel (DCM) to afford a white solid. (>99 % by NMR) 6.12 g, 49%. ^{1}H and ^{13}C NMR spectroscopy characterisation was consistent with literature reports.[7]

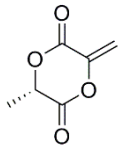

^{1}H NMR ($CDCl_3$, ppm): δ 5.97 (d, J = 2.5 Hz, 1H), 5.57 (d, J = 2.5 Hz, 1H), 5.06 (q, J = 7.0 Hz, 1H), 2.34 (s, 3H), 1.74, (d, 7.0 Hz, 3H). ^{13}C NMR {^{1}H} ($CDCl_3$, ppm): δ 162.9, 157.3, 143.0, 110.5, 72.5, 17.4.

6.3.7 Representative ring-opening polymerisation of 3-ML

In a glove box 3-ML (0.1 g, 0.704 mmol), [salan]AlMe, $^{t\text{BuPr}}$ (0.0077 g, 0.014 mmol) and BnOH (1.5 μL, 0.014 mmol) were dissolved in toluene (1 mL) and added to an oven dried ampoule. Outside the box the ampoule was heated to 85 °C for 24 h and a crude sample was taken for NMR analysis to determine conversion. The same molar ratio of reagents was used as above for the following catalysts at various temperatures; $Sn(oct)_2$, $^{ClEtN\text{-}Bn}$[salen]AlMe, $^{t\text{BuNapth}}$[salen]AlMe, TBD and DBU. Polymerisations were unsuccessful as determined by ^{1}H NMR spectroscopy.

6.3.8 Representative alcoholysis of 3-ML

In a glove box 3ML (0.02 g, 0.141 mmol) was weighed and added to an oven dried ampoule. Outside the box methanol (1 mL) was syringed into the ampoule under an atmosphere of nitrogen. The reaction was then de-gassed by one freeze-pump-thaw cycle and heated for 24 h at 70 °C under static vacuum. The excess methanol was then removed under vacuum to yield a colourless oil. All alcoholysis reactions were performed as above in an excess of alcohol and results were quantitative with no purification required.

Formation of 57

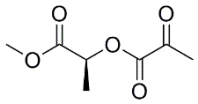

^{1}H NMR ($CDCl_3$, ppm): δ 5.23 (q, J = 7.1 Hz, 1H), 3.80 (s, 3H), 2.53 (s, 3H), 1.63 (d, 7.1 Hz, 3H). ^{13}C NMR {^{1}H} ($CDCl_3$, ppm): δ 190.9, 169.7, 159.8, 70.3, 52.7, 26.8, 16.8. HRMS (ESI^+): m/z calculated 197.0420 $[M + Na]^+$, m/z found 197.0418 $[M + Na]^+$.

Formation of 58

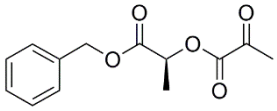

^{1}H NMR ($CDCl_3$, ppm): δ 7.41-7.35 (m, 5H), 5.32-5.19 (m, 3H), 2.49 (s, 3H), 1.63 (d, 7.1 Hz, 3H). ^{13}C NMR {^{1}H} ($CDCl_3$, ppm): δ 191.0, 169.3, 160.0, 135.0-127, 70.4, 67.4, 26.7, 16.7. HRMS (ESI^+): m/z calculated 273.0734 $[M + Na]^+$, m/z found 273.0728 $[M + Na]^+$.

Formation of 60

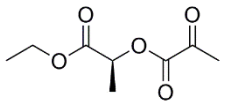

^{1}H NMR ($CDCl_3$, ppm): δ 5.20 (q, J = 7.1 Hz, 1H), 4.26 (q, J = 7.2 Hz, 2H), 2.52 (s, 3H), 1.63 (d, 7.1 Hz, 3H), 1.31 (t, J = 7.2 Hz, 3H). ^{13}C NMR {^{1}H} ($CDCl_3$, ppm): δ 191.1, 169.4, 160.0, 70.4, 61.8, 26.8, 16.8, 14.1. HRMS (ESI^+): m/z calculated 211.0577 $[M + Na]^+$, m/z found 211.0571 $[M + Na]^+$.

Formation of 61

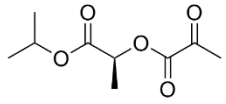

^{1}H NMR ($CDCl_3$, ppm): δ 5.16 (q, J = 7.1 Hz, 1H), 5.12-5.07 (m, 1H), 2.52 (s, 3H), 1.62 (d, 7.1 Hz, 3H), 1.32-1.23 (m, 6H). ^{13}C NMR {^{1}H}

($CDCl_3$, ppm): δ 191.1, 169.0, 160.0, 70.6, 69.7, 26.8, 21.6, 16.7. HRMS (ESI^+): m/z calculated 225.0734 $[M + Na]^+$, m/z found 225.0722 $[M + Na]^+$.

Formation of 62

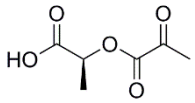

^1H NMR ($CDCl_3$, ppm): δ 5.26 (q, J = 7.2 Hz, 1H), 2.53 (s, 3H), 1.67 (d, 7.2 Hz, 3H). ^{13}C NMR $\{^1H\}$ ($CDCl_3$, ppm): δ 190.9, 173.4, 159.8, 69.8, 26.7, 16.7. HRMS $(ESI)^+$: m/z calculated 161.0445 $[M + H]^+$, m/z found 161.0518 $[M + H]^+$.

6.3.9 Synthesis of olefin 59

In a glove box, 3-ML (0.250 g, 1.76 mmol) was dissolved in DCM (1 mL) and added to an oven dried ampoule. Outside the box allyl alcohol (0.135 mL, 1.94 mmol) was added under an atmosphere of nitrogen using a syringe. The solution was then degassed by three freeze-pump-thaw cycles and heated to 85 °C for 24 h. The crude product was distilled under vacuum to afford the product as a colourless oil.

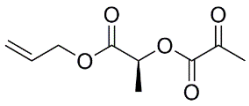

^1H NMR ($CDCl_3$, ppm): δ 5.91 (ddt, J = 17.2, 10.4, 5.7 Hz, 1H), 5.36-5.26 (m, 2H), 5.22 (q, J = 7.1 Hz, 1H), 4.70-4.67 (m, 2H), 2.50 (s, 3H), 1.62 (d, J = 7.1 Hz, 3H). ^{13}C NMR {1H} ($CDCl_3$, ppm): δ 190.9, 169.1, 159.9, 131.2, 119.0, 70.2, 66.2, 26.7, 16.8. MS (EI): m/z 113.0 (M-87, 100%), 157.1 (M-43, 47.46%), 129.1 (M-71, 20.47%).

6.3.10 Representative olefin cross-metathesis of 3-ML

In a glove box 3-ML (0.02 g, 0.140 mmol), hex-1-ene (0.024 g, 0.282 mmol) and Hoveyda-Grubbs Second Generation catalyst (0.0044 g, 7 $x10^{-3}$ mmol) were dissolved in DCM (1 mL) and added to an oven dried ampoule. Outside the box the ampoule was de-gassed by one freeze-pump-thaw cycle and heated at reflux for 16 h. The reaction was cooled to room temperature and analysed *via* ^1H NMR spectroscopy.

Formation of 3-HL (> 99% by NMR):

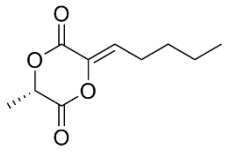

^{1}H NMR ($CDCl_3$, ppm): δ 6.45 (t, J = 7.9 Hz, 1H), 4.99 (q, J = 7.0 Hz, 1H), 2.39-2.35 (m, 2H), 1.72 (d, J = 7.0 Hz, 3H), 1.52-1.47 (m, 2H), 1.42-1.31 (m, 2H), 0.95 (t, 7.3 Hz, 3H). ^{13}C NMR {^{1}H} ($CDCl_3$, ppm): δ 163.5, 158.6, 136.8, 129.8, 72.0, 30.1, 25.0, 22.3, 17.2, 13.7.

Attempted purification of 3-HL, which generated 63

3-HL was purified *via* column chromatography on silica gel (flushed with petroleum spirits, followed by DCM (stabilised with 0.2% ethanol)). Degradation *via* alcoholysis of 3-HL with ethanol (present in the DCM) occurred to afford **63** as a pale yellow oil (>99 % by NMR).

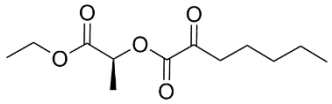

^{1}H NMR ($CDCl_3$, ppm): δ 5.17 (q, J = 7.1 Hz, 1H), 4.23 (q, J = 7.2 Hz, 2H), 2.87-2.81 (m, 2H), 1.69-1.63 (m, 2H), 1.59 (d, J = 7.1 Hz, 3H), 1.36-1.31 (m, 4H), 1.28 (t, J = 7.2 Hz, 3H), 0.9-0.88 (m, 3H). ^{13}C NMR {^{1}H} ($CDCl_3$, ppm): 193.9, 169.6, 160.5, 70.2, 61.8, 30.4, 31.1, 22.6, 22.3, 14.1, 13.8. HRMS (ESI^+): m/z calculated 267.1203 $[M + Na]^+$, m/z found 267.1191 $[M + Na]^+$.

6.3.11 Representative tandem olefin cross-metathesis and hydrogenation of 3-ML

Method A. In a glove box 3-ML (0.5 g, 3.518 mmol), dec-1-ene (0.998 g, 7.036 mmol), and Hoveyda Grubbs Second Generation catalyst (0.11g, 0.176 mmol) were dissolved in DCM (15 mL) and added an oven-dried ampoule. Outside the box the ampoule was de-gassed by one freeze-pump-thaw cycle and heated at reflux for 16 h. A crude NMR was taken, then Pt_2O (0.048 g, 0.176 mmol) was added to the ampoule which was de-gassed by three freeze-pump-thaw cycles. Hydrogen gas (1 bar, 14 psi) was then introduced into the vessel and stirred at room temperature for 24 h. The product was purified *via* column chromatography on silica gel (flushed with petroleum spirits followed by ethyl acetate) to yield the ring-opened product **64** from β-elimination during the hydrogenation (>99 % by NMR).

Formation of 64

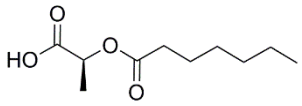

^{1}H NMR ($CDCl_3$, ppm): δ 5.16 (q, J = 7.1 Hz, 1H), 2.43-2.38 (m, 2H), 1.68 (p, J = 7.5 Hz), 1.56 (d, J = 7.1 Hz, 3H), 1.42-1.30 (m, 6H), 0.91 (t, J = 6.9 Hz). ^{13}C NMR {^{1}H} ($CDCl_3$, ppm): δ 173.8, 173.3, 67.8, 33.9, 31.4, 28.8, 24.7, 22.5, 16.1, 14.0, HRMS (ESI^{+}): m/z found 225.1089 $[M + Na]^{+}$, m/z calculated 225.1097 $[M + Na]^{+}$.

Method B. In a glove box 3-ML (0.5 g, 3.518 mmol), hex-1-ene (0.6 g, 7.036 mmol), and Hoveyda Grubbs Second Generation catalyst (0.110 g, 0.176 mmol) were dissolved in DCM (15 mL) and added to an oven-dried ampoule. Outside the box the ampoule was de-gassed by one freeze-pump thaw cycle and heated at reflux for 16 h. A crude NMR was taken (93 % by NMR), then Pd/C (0.027 g, 0.254 mmol) was added to the ampoule which was de-gassed by three freeze-pump thaw cycles. Next, hydrogen gas (1 bar, 14 psi) was introduced into the vessel and stirred at 35 °C for 24 h. The product was filtered to remove Pd/C and purified *via* column chromatography on silica gel (petroleum spirits: ethyl acetate, 70:30) to afford 3-HHL, a white solid, (>99 % by NMR), 296 mg, 42%.

Formation of 3-HHL

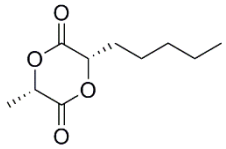

^{1}H NMR ($CDCl_3$, ppm): δ 5.02 (q, J = 6.7 Hz, 1H), 4.9 (dd, J = 7.7 Hz, 4.3 Hz, 1H), 2.13 (dddd, J = 14.8 Hz, 10.4 Hz, 5.9 Hz, 4.3 Hz, 1H), 1.98 (dddd, J = 14.8 Hz, 10.4 Hz, 7.7 Hz, 4.9 Hz, 1H), 1.7 (d, J = 6.7 Hz, 3H), 1.6-1.52 (m, 2H), 1.37-1.38 (m, 4H), 0.93-0.88 (m, 3H). ^{13}C NMR {^{1}H} ($CDCl_3$, ppm): δ 167.8, 167.4, 75.9, 72.3, 31.2, 30.0, 24.0, 22.3, 13.9, 15.9. NOSEY analysis shows coupling in space between protons δ 5.02 and δ 4.90 indicating a cis-relationship as shown above. HRMS (ESI^{+}): m/z calculated 223.0940 $[M + Na],^{+}$ m/z found 223.0933 $[M + Na].^{+}$

6.3.12 Representative ring-opening polymerisation of 3-HHL

In a glove box to a Young's NMR tube 3-HHL (0.08 g, 0.398 mmol), TBD (0.0011 g, 7.96 x10^{-3} mmol) and BnOH (0.8 μL, 7.96 x10^{-3} mmol) were dissolved in dichlromethane-

d_2 (0.8 mL). Outside the box the reaction was monitored by NMR and quenched after 0.25 h with benzoic acid (0.003 g). The polymer was precipitated to yield an oil. The same molar ratio of reagents was used as above for the following catalysts; $Sn(oct)_2$ at 120 °C for 18 hr and $^{t\text{BuPr}}$[salen]AlMe at 85 °C for 24 h.

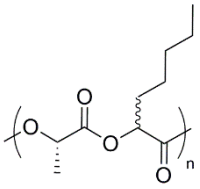

^{1}H NMR ($CDCl_3$, ppm): δ 5.20 (br, 1H, C*H*CH_3), 5.09 (br, 1H, C*H*$CH_aH_b(CH_2)_3CH_3$), 1.97 (br, 1H, CH(C*H*$_a$$H_b(CH_2)_3CH_3$), 1.90 (br, 1H, CH($CH_aH_b$)$_3CH_3$), 1.56 (br, 3H, CHC*H*$_3$), 1.46 (br, 2H, $CH_aH_bCH_2(CH_2)_2CH_3$), 1.31-1.32 (br, 4H, $CH_aH_bCH_2(CH_2)_2CH_3$), 0.9 (br, 3H, $CH_aH_bCH_2(CH_2)_2CH_3$). ^{13}C NMR {^{1}H} ($CDCl_3$, ppm): δ 169.3, 169.1, 72.7, 69.0, 31.2, 30.8, 24.6, 22.3, 16.8, 13.9. **TBD**: M_n = 6,318, Đ = 1.56. **Sn(oct)$_2$**: M_n = 9,650, Đ = 1.29. **[salan]AlMe$^{t\text{BuPr}}$**: M_n = 4,425, Đ = 1.42.

6.4 Synthesis for chapter three

6.4.1 Synthesis of β-HL

In a glove box [salph]CrCl (0.159 g, 0.255 mmol) and $Co_2(CO)_8$, (0.131 g, 0.382 mmol) were dissolved in THF (12 mL) and added to an oven dried ampoule. Outside the box 1,2-epoxy-5-hexene (2.5 g, 25.47 mmol), was weighed in a vial, added to an ampoule and de-gassed by three freeze-pump-thaw cycles. The Cr/Co solution was transferred to the ampoule containing the epoxide *via* cannula transfer under an atmosphere for nitrogen. Using a second cannula transfer under nitrogen, the contents were moved to a 100 mL pressure reactor, which had been pre-heated and evacuated prior to use. The pressure reactor was purged three times with carbon monoxide (~50 psi), then pressurised to 200 psi. The reaction was then heated to 50 °C for ~4 h or until the carbon monoxide level ceased to decrease. The product was purified *via* vacuum distillation to yield a colourless oil. ^{1}H and ^{13}C NMR spectroscopy characterisation was consistent with literature reports.[8]

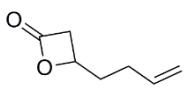

^{1}H NMR ($CDCl_3$, ppm): δ 5.83 (ddt, J = 16.9, 10.0, 6.6 Hz, 1H), 5.10-5.03 (m, 2H), 4.55-4.50 (m, 1H), 3.54 (dd, J = 16.3, 5.7 Hz, 1H), 3.11 (dd, 16.3, 4.3 Hz, 1H), 2.28-2.13 (m, 2H), 2.03-1.94 (m, 1H), 1.89-1.82 (m, 1H) ^{13}C NMR {^{1}H} ($CDCl_3$, ppm): δ 168.1, 136.4, 116.8, 70.6, 42.9, 33.9, 29.1.

6.4.2 Representative olefin cross-metathesis of β-HL.

In a glove box β-HL (0.3 g, 2.4 mmol), methyl acrylate (1.64 g, 19 mmol) and Hoveyda Grubbs Second generation catalyst (0.0745 g, 0.12 mmol) were dissolved in DCM (2 mL) and added to an oven dried ampoule. Outside the box the ampoule was de-gassed by one freeze-pump-thaw cycle and heated at reflux for 16 h.

Formation of 70: eluent system on silica gel: (EtOAc:hexane, 10:90) followed by a second column (EtOAc:DCM 10:90) to afford the product as a yellow oil, (>99 % by NMR) 0.14 g, 32%.

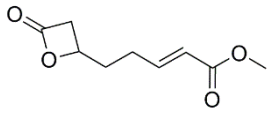

^{1}H NMR ($CDCl_3$, ppm): δ 6.94 (dt, J = 15.6, 6.9 Hz, trans 1H), 6.24 (dt, J = 11.4, 7.7 Hz, cis, 1H), 5.88 (dt, J = 15.6, 1.6 Hz, trans, 1H), 5.85 (dt 1H, cis, 1H) 4.52 (dtd, J = 8.0, 5.5, 4.3 Hz, 1H), 3.73 (s, 3H), 3.55 (dd, J = 16.3, 5.8, 1H), 3.10 (dd, J = 16.3, 4.3 Hz,1H), 2.47 – 2.26 (m, 2H), 2.08 – 1.88 (m, 2H). ^{13}C NMR {^{1}H} ($CDCl_3$, ppm): δ 167.4, 166.6, trans (146.4, 122.3) cis (147.5, 120.8), 70.1, 51.5, 43.0, 33.6, 27.6. MS (EI): m/z 113.1 (M-71, 100.00%), 81.1 (M-103, 76.97%), 153.1 (M-31, 19.08%).

6.4.3 Ring-opening polymerisation of 70 to form 71

In a glove box **70** (0.09 g, 0.489 mmol), ^{t}BuPr[salen]AlMe (0.0027 g, 4.89 x10^{-3} mmol) and benzyl alcohol (0.5 μL, 4.89 x10^{-3} mmol) were dissolved in toluene (0.5 mL) and added to an oven dried ampoule. Outside the box the mixture was heated to 85 °C for 27 h and quenched with the addition of a few drops of methanol. The product was concentrated under reduced pressure to yield a dark brown oil **71**:

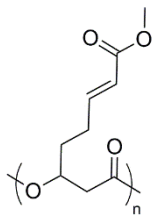

^{1}H NMR ($CDCl_3$, ppm): δ 6.91 (br, 1H, CH_2CH=CH), 5.84 (br, 1H, CH_2CH=C*H*), 5.20 (br, 1H, C=OCH_2CH), 3.71 (brs, 3H, CH_3), 2.57 (br, 2H, C=OCH_2CH), 2.24 (br, 2H, CH_2CH=CH), 1.78 (br, 2H, CH_2CH_2CH=CH). ^{13}C NMR {^{1}H} ($CDCl_3$, ppm): δ 169.2, 166.7, 147.5, 121.7, 70.0, 51.4, 38.9, 32.2, 27.9. M_n = 2,400, Đ = 1.65.

6.4.4 Ring-opening polymerisation of β-HL to form P(β-HL)

In a glove box β-HL (3 g, 23.8 mmol), $^{t\text{Bu}Pr}$[salen]AlMe (0.130 g, 0.238 mmol) and benzyl alcohol (0.0257 g, 0.238 mmol) were dissolved in toluene (15mL) and added to an oven dried ampoule. Outside the box the mixture was heated at 85 °C for 27 h and quenched with the addition of a few drops of methanol. The product was concentrated under reduced pressure to yield a light brown oil, **P(β-HL).**

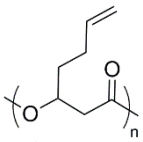

^{1}H NMR ($CDCl_3$, ppm): δ 5.80 (ddt, J = 16.9, 10.3, 6.6 Hz, 1H, C*H*=CH_2), 5.02 (br, 2H, CH=CH_2), 5.23 (br, 1H, C=OCH$_2$C*H*), 2.57 (br, 2H, C=OCH_2CH), 2.09 (br, 2H, CH_2CH=CH_2), 1.72 (br, 2H CH_2CH$_2$CH=CH_2). ^{13}C NMR {1H} ($CDCl_3$, ppm): δ 169.4, 137.0, 115.5, 70.2, 39.0, 33.0, 29.3. M_n = 12,100, Đ = 1.09.

Homopolymer Kinetics

In-situ observation of homopolymerisation: Ring-opening polymerisations were monitored using ^{1}H NMR spectroscopy. In a glove box to a Young's NMR tube, β-HL (0.126 g, 1 mmol), $^{t\text{Bu}Pr}$[salen]AlMe (0.0055 g, 0.01 mmol) and BnOH (0.001 g, 0.01 mmol) were dissolved in toluene-d_8 (0.7 mL). The tube was sealed and placed in the spectrometer probe which was pre-heated to 358 K (85 °C). Spectra were taken in 15-minute intervals.

6.4.5 Representative post polymerisation metathesis of P(β-HL)

In a glove box P(β-HL) (0.250 g), alkene cross partner methyl acrylate (1.7 g, 19.8 mmol) and Hoveyda Grubbs second generation catalyst (0.124 g, 0.1982 mmol) were dissolved in DCM (4 mL) and added to an oven dried ampoule. The solution was degassed by one freeze-pump-thaw cycle and heated under reflux for 16 h with occasional de-gassing. The crude polymer was purified using column chromatography on silica gel (DCM) to elute non-polymer alkene products. The polymer was then extracted from the silica using methanol washings and was filtered to yield the product as a dark brown oil.

Formation of 72

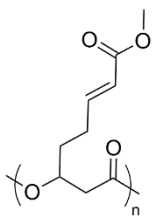

^{1}H NMR ($CDCl_3$, ppm): δ 6.91 (dt, J = 14.7, 6.7 Hz, 1H, trans CH_2CH=CH), 6.86 (br, 1H, cis CH_2CH=CH) 5.92 (br, 1H, cis CH_2CH=CH) 5.84 (br, 1H, trans CH_2CH=CH), 5.20 (br, 1H C=OCH_2CH), 3.71 (brs, 3H, CH_3), 2.57 (br, 2H, C=OCH_2CH), 2.24 (br, 2H, CH_2CH=CH), 1.78 (br, 2H, CH_2CH_2CH=CH). ^{13}C from HSQC and HMBC ($CDCl_3$, ppm): 169.3, 166.7, trans (147.7, 121.7) cis (142.6, 124.6), 70.2, 51.5, 38.8, 32.2, 27.9. M_n = 13, 400, Đ = 1.84.

Formation of 73

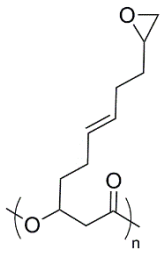

^{1}H NMR ($CDCl_3$, ppm): δ 5.63 (br, 1H, cis C=O$CH_2CH$$CH_2CH_2CH$=$CH$), 5.46 (br, 2H, trans C=O$CH_2CH$$CH_2CH_2CH$=$CH$), 5.36 (br, 1H, cis C=O$CH_2CH$$CH_2CH_2CH$=CH), 5.21 (br, 1H, C=O$CH_2CH$), 2.93 (br, 1H, CH_2CH-O-CH_aH_b), 2.77 (br, 1H, CH_2CH-O-CH_aH_b), 2.56 (br, 2H, C=OCH_2CH), 2.50 (br, 1H, $CH_2CHOCH_aH_b$), 2.18 (br, 2H, CH_2CH_2CH-O-CH_aH_b), 2.03 (br, 2H, C=O$CH_2CHCH_2CH_2$), 1.68 (br, 2H C=O$CH_2CHCH_2CH_2$), 1.61 (2H, CH_2CH_2CH-O-CH_aH_b). ^{13}C from HSQC and HMBC ($CDCl_3$, ppm): δ 169.4, trans (130.0), cis (129.6, 125.0), 70.3, 51.7, 47.3, 38.9, 33.7, 32.4, 29.1, 28.2. M_n = 11,300, Đ = 1.42.

6.4.6 Representative copolymer synthesis

Copolymer dispersity analysis with conversion

In a glove box β-HL (0.019 g, 0.143 mmol), L-lactide (0.2 g, 1.38 mmol), $^{t\text{BuPr}}$[salen]AlMe (0.008 g, 0.015 mmol) and benzyl alcohol (0.002 g, 0.015 mmol) were dissolved in toluene (1 mL) and added to an oven dried ampoule. Outside the box the mixture was heated at 85 °C for 24 h and subsequently precipitated in cold methanol. The same procedure was repeated at different reaction times ranging from 2 hr to 24 h. Conversion was determined by ^{1}H NMR spectroscopy of the crude mixtures and Đ was determined by GPC analysis. A plot of Đ and conversion versus time was made to observe trends.

Formation of P(LA_{86}-co-β-HL_4)

In a glove box β-HL (0.39 g, 3.1 mmol), L-lactide (4 g, 28 mmol), $^{t\text{BuPr}}$[salen]AlMe (0.169 g, 0.31 mmol) and benzyl alcohol (0.034 g, 0.31 mmol) were dissolved in toluene (20 mL) and added to an oven dried ampoule. Outside the box the mixture was heated at 85 °C for 2.5 h and precipitated in cold methanol:

Formation of P(LA_{85}-co-β-HL_{19})

In a glove box β-HL (1.44 g, 11 mmol), L-lactide (3.5 g, 24 mmol), $^{t\text{BuPr}}$[salen]AlMe (0.156 g, 0.28 mmol) and benzyl alcohol (0.031 g, 0.28 mmol) were dissolved in toluene (20 mL) and added to an oven dried ampoule. Outside the box the mixture was heated at 85 °C for 2.5 h and precipitated in cold methanol:

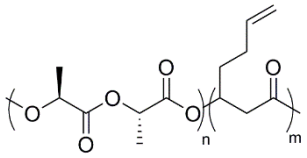

^{1}H NMR ($CDCl_3$, ppm): δ 5.78 (br, 1H, C*H*=CH_2) 5.26 (br, 1H, C=OCH_2C*H*), 5.16 (q, J = 7.1 Hz, 1H, C*H*CH_3), 5.02 (br, 2H, CH=C*H*$_2$), 2.68 (br, 2H, C=OC*H*$_2$CH), 2.10 (br, 2H, C*H*$_2$CH=CH_2), 1.75 (br, 2H C*H*$_2$$CH_2$CH=$CH_2$), 1.58 (d, J = 7.1 Hz, 3H, CHC*H*$_3$). ^{13}C NMR {^{1}H} ($CDCl_3$, ppm): δ 169.7, 169.5, 137.2, 115.4, 70.8, 69.0, 38.8, 33.0, 29.3, 16.6. **P(LA_{86}-co-β-HL_4):** M_n = 12,000, Đ = 1.02. **P(LA_{85}-co-β-HL_{19}):** M_n = 9,500, Đ = 1.04.

Co-polymer kinetics

In-situ observation of copolymerisation: Ring-opening polymerisations were monitored using ^{1}H NMR spectroscopy. In a glove box to a Young's NMR tube, β-HL (0.0114 g, 0.090 mmol), lactide (0.116 g, 0.81 mmol), $^{t\text{BuPr}}$[salen]AlMe (0.0049 g, 0.009 mmol) and BnOH (9.7 x10^{-4} g, 0.009 mmol) were dissolved in toluene-d_8 (0.7 mL). The tube was sealed and placed in the spectrometer probe which was pre-heated to 358 K (85 °C). Spectra were taken in 5-minute intervals.

6.4.7 Representative olefin cross metathesis of copolymers

In a glove box P(LA_{85}-co-β-HL_{19}) (0.1 g), hex-1-ene (0.09 g, 1.08 mmol) and Hoveyda Grubbs second generation catalyst (0.0042 g, 6.74 x10^{-3} mmol) were dissolved in DCM (2

mL) and added to an oven dried ampoule. Outside the box the mixture was degassed by one freeze-pump-thaw cycle and heated under reflux for 16 h with occasional de-gassing. The reaction was quenched with a few drops of ethyl vinyl ether and precipitated in cold methanol (~20 mL) and washed with cold diethyl ether (~20 mL) and cold hexane (~20 mL).

Hex-1-ene incorporation

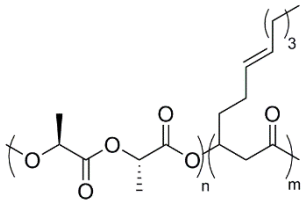

^{1}H NMR ($CDCl_3$, ppm): δ 5.53 (br, 1H, CH=C*H*$(CH_2)_3CH_3$), 5.43 (br, 1H, CH=C*H*$(CH_2)_3CH_3$), 5.35 (br, 1H, C*H*=CH$(CH_2)_3CH_3$), 5.31 (br, 1H, C*H*=CH$(CH_2)_3CH_3$), 5.26 (br, 1H C=OCH2CH), 5.19 (q, J = 7.1 Hz, 1H, C*H*CH_3), 2.68 (br, 2H, C=OC*H*$_2$CH), 2.03 (br, 2H C=OCH_2CHCH_2C*H*$_2$), 1.99 (br, 1H, CH=CHC*H*$_2(CH_2)_2CH_3$), 1.70 (br, 2H, C=OCH_2CHC*H*$_2$), 1.60 (d, J = 7.1 Hz, 3H, CHC*H*$_3$), 1.34-1.25 (m, 4H, CH=CHCH_2*(CH*$_2)_2$$CH_3$), 0.90 (br, 3H, CH=CH$(CH_2)_3$C*H*$_3$). ^{13}C from HSQC and HMBC ($CDCl_3$, ppm): δ 169.7, 169.5, cis & trans (131.9, 135.5, 128.1, 123.3), 71.3, 69.0, 38.5, 33.7, 32.2, (31.7-22.2), 28.1, 16.7, 14.0. **P(LA$_{86}$-co-β-HL$_4$):** M_n = 14,800, Đ = 1.02. **P(LA$_{85}$-co-β-HL$_{19}$):** M_n = n.d, Đ = n.d.

Oct-1-ene incorporation

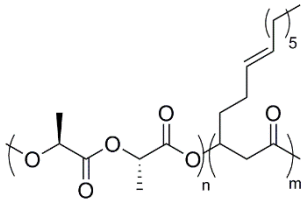

^{1}H NMR ($CDCl_3$, ppm): δ 5.53 (br, 1H, CH=C*H*$(CH_2)_5CH_3$), 5.43 (br, 1H, CH=C*H*$(CH_2)_5CH_3$), 5.35 (br, 1H, C*H*=CH$(CH_2)_5CH_3$), 5.31 (br, 1H, C*H*=CH$(CH_2)_5CH_3$), 5.26 (br, 1H C=OCH_2C*H*), 5.19 (q, J = 7.1 Hz, 1H, C*H*CH_3), 2.68 (br, 2H, C=OC*H*$_2$CH), 2.03 (br, 2H C=OCH_2CHCH_2C*H*$_2$), 1.99 (br, 1H, CH=CHC*H*$_2(CH_2)_4CH_3$), 1.70 (br, 2H, C=OCH_2CHC*H*$_2$), 1.60 (d, J = 7.1 Hz, 3H, CHC*H*$_3$), 1.35-1.22 (m, 4H, CH=CH*(CH*$_2)_5$$CH_3$), 0.90 (br, 3H, CH=CH$(CH_2)_5$C*H*$_3$). ^{13}C from HSQC and HMBC ($CDCl_3$, ppm): δ 169.7, 169.5, cis & trans (131.9, 135.5, 128.1, 123.3), 71.3, 69.0, 38.5, 33.7, 32.2, (31.8-22.6), 28.1, 16.7, 14.0. **P(LA$_{86}$-co-β-HL$_4$):** M_n = 22,000, Đ = 1.47. **P(LA$_{85}$-co-β-HL$_{19}$):** M_n = 9,900, Đ = 1.03.

Dec-1-ene incorporation

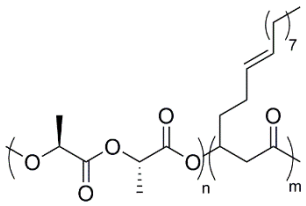

^{1}H NMR ($CDCl_3$, ppm): δ 5.53 (br, 1H, CH=C*H*$(CH_2)_7CH_3$), 5.43 (br, 1H, CH=C*H*$(CH_2)_7CH_3$), 5.35 (br, 1H, C*H*=CH$(CH_2)_7CH_3$), 5.31 (br, 1H, C*H*=CH$(CH_2)_7CH_3$), 5.26 (br, 1H C=OCH_2C*H*), 5.19 (q, J = 7.1 Hz, 1H, C*H*CCH_3), 2.68 (br, 2H, C=OC*H*$_2$CH), 2.03 (br, 2H C=OCH_2CHCH_2C*H*$_2$), 1.99 (br, 1H, CH=CHC*H*$_2$$(CH_2)_6CH_3$), 1.70 (br, 2H, C=O$CH_2$CHC*H*$_2$), 1.60 (d, J = 7.1 Hz, 3H, CHCC*H*$_3$), 1.38-1.24 (m, 4H, CH=CH*(CH*$_2$*)*7CH3), 0.90 (br, 3H, CH=CH$(CH_2)_7$C*H*$_3$). ^{13}C from HSQC and HMBC ($CDCl_3$, ppm): δ 169.7, 169.5, cis & trans (131.9, 135.5, 128.1, 123.3), 71.3, 69.0, 38.5, 33.7, 32.2, (~31.7-22.2), 28.1, 16.7, 14.0. **P(LA$_{86}$-co-β-HL$_4$):** M_n = 11,400, Đ = 1.02. **P(LA$_{85}$-co-β-HL$_{19}$):** M_n = 10,400, Đ = 1.04.

Dodec-1-ene incorporation

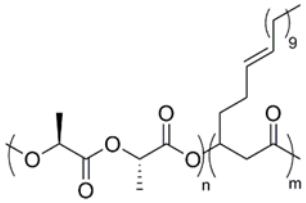

^{1}H NMR ($CDCl_3$, ppm): δ 5.53 (br, 1H, CH=C*H*$(CH_2)_9CH_3$), 5.43 (br, 1H, CH=C*H*$(CH_2)_9CH_3$), 5.35 (br, 1H, C*H*=CH$(CH_2)_9CH_3$), 5.31 (br, 1H, C*H*=CH$(CH_2)_9CH_3$), 5.26 (br, 1H C=OCH_2C*H*), 5.19 (q, J = 7.1 Hz, 1H, C*H*CCH_3), 2.68 (br, 2H, C=OC*H*$_2$CH), 2.03 (br, 2H C=OCH_2CHCH_2C*H*$_2$), 1.99 (br, 1H, CH=CHC*H*$_2$$(CH_2)_8CH_3$), 1.70 (br, 2H, C=O$CH_2$CHC*H*$_2$), 1.60 (d, J = 7.1 Hz, 3H, CHCC*H*$_3$), 1.38-1.23 (m, 4H, CH=CH*(CH*$_2$*)*$_9$$CH_3$), 0.90 (br, 3H, CH=CH$(CH_2)_9$C*H*$_3$). ^{13}C from HSQC and HMBC ($CDCl_3$, ppm): δ 169.7, 169.5, cis & trans (131.9, 135.5, 128.1, 123.3), 71.3, 69.0, 38.5, 33.7, 32.2, (32.1-22.6), 28.1, 16.7, 14.0. **P(LA$_{86}$-co-β-HL$_4$):** M_n = 12,700, Đ = 1.06. **P(LA$_{85}$-co-β-HL$_{19}$):** M_n = 11,300, Đ = 1.18.

5-Hexenyl acetate incorporation

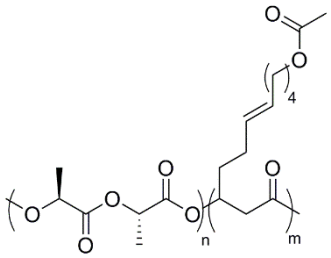

^{1}H NMR ($CDCl_3$, ppm): δ 5.52 (br, 1H, C*H*=CH$(CH_2)_4$OC=OCH_3), 5.42 (br, 1H, C*H*=CH$(CH_2)_4$OC=OCH_3), 5.38 (br, 1H, CH=C*H*$(CH_2)_4$OC=OCH_3), 5.33 (br, 1H, CH=C*H*$(CH_2)_4$OC=OCH_3), 5.26 (br, 1H C=OCH_2C*H*), 5.19 (q, J = 7.1 Hz, 1H, C*H*CH_3), 4.07 (br, 2H, CH=C*H*$(CH_2)_3$C*H*$_2$OC=OCH_3), 2.68 (br, 2H, C=OC*H*$_2$CH), 2.06 (brs, 3H, OC=OCH3), 2.03 (br, 2H, CH=CHC*H*$_2$$(CH_2)_3$),

2.02 (br, 2H, C=OCH$_2$CHCH$_2$C*H$_2$*), 1.71 (br, 2H, C=OCH$_2$CHC*H$_2$*CH$_2$), 1.65 (br, 2H, CH=CH(CH$_2$)$_2$C*H$_2$*CH$_2$OC=OCH$_3$), 1.60 (d, J = 7.1 Hz, 3H, CHC*H$_3$*), 1.41 (br, 2H, CH=CHCH$_2$C*H$_2$*(CH$_2$)$_2$OC=OCH$_3$). ^{13}C from HSQC and HMBC (CDCl$_3$, ppm): δ 171.8, 169.7, 169.5, cis & trans (134.6, 131.0, 128.9, 124.0), 71.3, 69.0, 64.3, 38.5, 33.6, 32.1, 28.1, 28.0, 25.4, 21.0, 16.7. **P(LA$_{86}$-co-β-HL$_4$):** M$_n$ = 12,300, Đ = 1.03 **P(LA$_{85}$-co-β-HL$_{19}$):** M$_n$ = 10,700, Đ = 1.04.

β-HL incorporation:

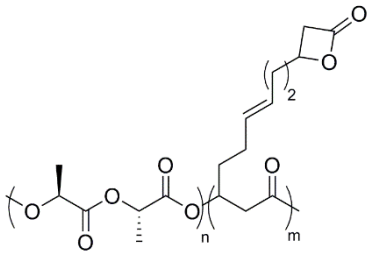

^{1}H NMR (CDCl$_3$, ppm)**:** δ 5.44 (br, 1H, C=OCH$_2$CH(CH$_2$)$_2$C*H*=C*H*), 5.26 (br, 1H C=OCH$_2$C*H*), 5.19 (q, J = 7.1 Hz, 1H, C*H*CH$_3$), 4.53 (br, 1H CH=CHCH$_2$(CH$_a$H$_b$)C*H*OC=OCH$_c$H$_d$), 3.53 (br, 1H, CH=CHCH$_2$CH$_a$H$_b$CHOC=OC*H$_c$*H$_d$), 3.08 (br, 1H, CH=CHCH$_2$CH$_a$H$_b$CHO C=OCH$_c$*H$_d$*), 2.68 (br, 2H, C=OC*H$_2$*CH), 2.15 (br, 2H, CH=CHC*H$_2$*(CH$_a$H$_b$), 2.04 (br, 2H, C=OCH$_2$CHCH$_2$C*H$_2$*), 1.94 (br, 1H, CH=CHCH$_2$(C*H$_a$*H$_b$), 1.82 (br, 1H, CH=CHCH$_2$(CH$_a$*H$_b$*), 1.71 (br, 2H, C=OCH$_2$CHC*H$_2$*CH$_2$), 1.60 (d, J = 7.1 Hz, 3H, CHC*H$_3$*). ^{13}C from HSQC and HMBC (CDCl$_3$, ppm): δ 169.7, 169.5, 168.2, 130.2 129.3, 71.3, 70.6, 69.0, 42.9, 38.5, 34.37, 33.4, 28.0, 28.0 16.7. **P(LA$_{86}$-co-β-HL$_4$):** M$_n$ = 14,000, Đ = 1.03. **P(LA$_{85}$-co-β-HL$_{19}$):** M$_n$ = 16,100, Đ = 1.98.

1,2-Epoxy-5-hexene incorporation

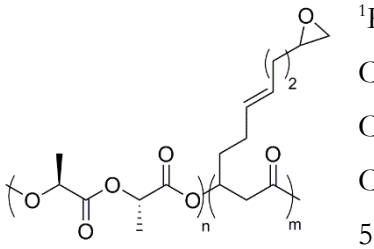

^{1}H NMR (CDCl$_3$, ppm)**:** δ 5.54 (br, 1H, C=OCH$_2$CH(CH$_2$)$_2$CH=C*H*), 5.46 (br, 2H, C=OCH$_2$CH(CH$_2$)$_2$C*H*=C*H*), 5.37 (br, 1H, C=OCH$_2$CH(CH$_2$)$_2$C*H*=CH), 5.26 (br, 1H C=OCH2CH), 5.19 (q, J = 7.1 Hz, 1H, C*H*CH$_3$), 2.91 (br, 1H, CH$_2$C*H*-O-CH$_a$H$_b$), 2.74 (br, 1H, CH$_2$CH-O-C*H$_a$*H$_b$), 2.69 (br, 2H, C=OC*H$_2$*CH), 2.47 (br, 1H, CH2CH-O-CH$_a$*H$_b$*), 2.17 (br, 2H, C*H$_2$*CH$_2$CH-O-CH$_a$H$_b$), 2.02 (br, 2H, C=OCH$_2$CHCH$_2$C*H$_2$*), 1.68 (br, 2H C=OCH$_2$CHC*H$_2$*CH$_2$), 1.61 (2H, CH$_2$C*H$_2$*CH-O-CH$_a$H$_b$), 1.60 (d, J = 7.1 Hz, 3H, CHC*H$_3$*). ^{13}C from HSQC and HMBC (CDCl$_3$, ppm): δ

169.7, 169.5, cis & trans (130.0, 129.84, 124.0), 71.3, 69.0. 51.8, 47.2, 38.5, 33.7, 32.4, 29.0, 28.2, 16.7. **P(LA$_{86}$-co-β-HL$_4$):** M_n = 20,500, Đ = 1.33. **P(LA$_{85}$-co-β-HL$_{19}$):** M_n = 11,600, Đ = 1.08.

Diethyl allyl phosphonate incorporation

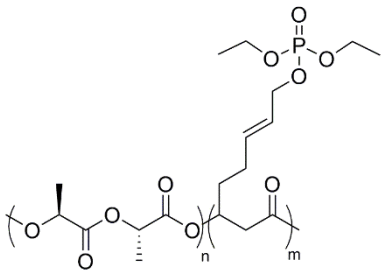

^{1}H NMR ($CDCl_3$, ppm): δ 5.58 (br, 1H, C*H*=CHCH$_2$P=O), 5.45 (br, 1H, CH=C*H*CH$_2$P=O), 5.26 (br, 1H C=OCH$_2$C*H*), 5.19 (q, J = 7.1 Hz, 1H, C*H*CH$_3$), 4.11 (br, 4H O=P(OC*H$_2$*CH$_3$)$_2$), 2.68 (br, 2H, C=OC*H$_2$*CH), 2.54 (br, 2H, CH=CHC*H$_2$*P=O), 2.08 (br, 2H, C=OCH$_2$CHC*H$_2$*CH$_2$), 1.71 (br, 2H, C=OCH$_2$CHC*H$_2$*CH$_2$), 1.60 (d, J = 7.1 Hz, 3H, CHC*H$_3$*), 1.33 (br, 6H, O=P(OCH$_2$C*H$_3$*)$_2$). ^{13}C from HSQC and HMBC ($CDCl_3$, ppm): δ 169.7, 169.5, 134.2, 120.0, 71.3, 69.0, 61.8, 38.5, 30.9, 33.2, 28.2, 16.7, 16.4. ^{31}P {^{1}H} ($CDCl_3$, ppm): δ 27.58. **P(LA$_{86}$-co-β-HL$_4$):** M_n = 12,300, Đ = 1.01. **P(LA$_{85}$-co-β-HL$_{19}$):** M_n = 9,600, Đ = 1.06.

Allyltrimethylsilane incorporation

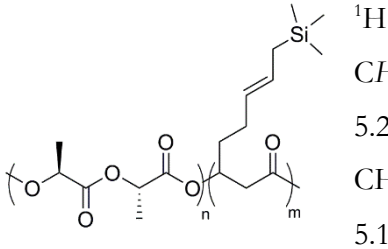

^{1}H NMR ($CDCl_3$, ppm)**:** δ 5.52 (br, 1H, C*H*=CHCH$_2$Si(CH$_3$)$_3$), 5.41 (br, 1H, C*H*=CHCH$_2$Si(CH$_3$)$_3$), 5.26 (br, 1H C=OCH$_2$C*H*), 5.20 (br, 1H, CH=C*H*CH$_2$Si(CH$_3$)$_3$), 5.19 (q, J = 7.1 Hz, 1H, C*H*CH$_3$), 5.16 (br, 1H, CH=C*H*CH$_2$Si(CH$_3$)$_3$), 2.68 (br, 2H, C=OC*H$_2$*CH), 2.02 (br, 2H, C=OCH$_2$CHCH$_2$C*H$_2$*), 1.68 (br, 2H, C=OCH$_2$CHC*H$_2$*CH$_2$), 1.60 (d, J = 7.1 Hz, 3H, CHC*H$_3$*), 1.46 (br, 2H, CH=CHC*H$_2$*Si(CH$_3$)$_3$), 0.06-0.01 (br, 9H, CH=CHCH$_2$Si(C*H$_3$*)$_3$). ^{13}C from HSQC and HMBC ($CDCl_3$, ppm): δ 169.7, 169.5, cis & trans (131.47, 127.6, 126.9, 121.7), 71.3, 69.0, 38.5, 34.1, 28.5, 22.7, 16.7. 3, (-1.23 to -1.91). **P(LA$_{86}$-co-β-HL$_4$):** M_n = 13,900, Đ = 1.02. **P(LA$_{85}$-co-β-HL$_{19}$):** M_n = 9,300, Đ = 1.04.

Allyl alcohol incorporation:

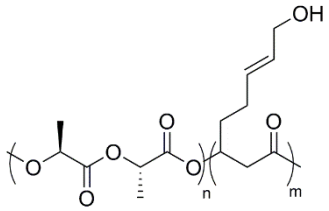

^{1}H NMR ($CDCl_3$, ppm)**:** δ 5.53 (br, 1H, C*H*=CHCH$_2$OH), 5.33 (br, 1H, CH=C*H*CH$_2$OH), 5.26 (br, 1H C=OCH$_2$C*H*),), 5.19 (q, J = 7.1 Hz, 1H, C*H*CH$_3$), 2.68 (br, 2H, C=OC*H*$_2$CH), 2.02 (br, 2H, C=OCH$_2$CHCH$_2$C*H*$_2$), 1.71 (br, 2H, C=OCH$_2$CHC*H*$_2$CH$_2$), 1.60 (d, J = 7.1 Hz, 3H, CHC*H*$_3$). Note: not all protons were observed. ^{13}C from HSQC and HMBC ($CDCl_3$, ppm): δ 169.7, 169.5, 71.3, 69.0, 38.5, 33.7, 27.0, 16.7. Note: no alkene carbons obtained from HSQC, data too weak. **P(LA$_{86}$-co-β-HL$_4$):** M_n = 16,400, Đ = 1.42. **P(LA$_{85}$-co-β-HL$_{19}$):** M_n = 29,400, Đ = 4.25.

Styrene incorporation

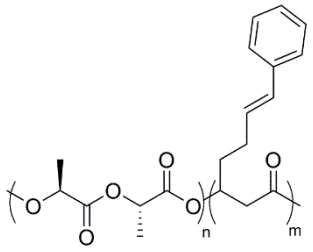

^{1}H NMR ($CDCl_3$, ppm): δ 7.38-7.21 (br, 5H, C$_6$*H*$_5$), 6.39 (br, 1H, CH=C*H*C$_6$H$_5$), 6.16 (br, 1H, C*H*=CHC$_6$H$_5$), 5.28 (br, 1H C=OCH$_2$C*H*), 5.19 (q, J = 7.1 Hz, 1H, C*H*CH$_3$), 2.68 (br, 2H, C=OC*H*$_2$CH), 2.23 (br, 2H, (br, 2H, C=OCH$_2$CHCH$_2$C*H*$_2$), 1.83 (br, 2H, C=OCH$_2$CHC*H*$_2$CH$_2$), 1.60 (d, J = 7.1 Hz, 3H, CHC*H*$_3$). ^{13}C from HSQC and HMBC ($CDCl_3$, ppm):: δ 169.7, 169.5, 130.8, 128.9, benzene carbons (126-131), 71.5, 69.0, 38.5, 33.4, 28.6, 16.7. **P(LA$_{86}$-co-β-HL$_4$):** M_n = 13,000, Đ = 1.04. **P(LA$_{85}$-co-β-HL$_{19}$):** M_n = 12,600, Đ = 1.24.

Olefin 59 incorporation

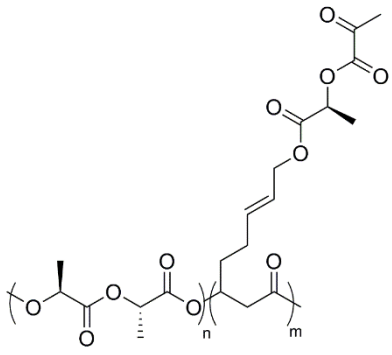

^{1}H NMR ($CDCl_3$, ppm): δ 5.59 (br, 1H, CH=C*H*CH$_2$OC=O), 5.77 (br, 1H, C*H*=CHCH$_2$OC=O), 5.28 (br, 1H C=OCH$_2$C*H*), 5.22 (CH=CHCH$_2$OC=OC*H*CH$_3$), 5.19 (q, J = 7.1 Hz 1H, C*H*CH$_3$), 4.61 (br, 2H, CH=CHC*H*$_2$OC=O), 2.68 (br, 2H, C=OC*H*$_2$CH), 2.52 (brs, 3H, C=OC=OC*H*$_3$), 2.12 (br, 2H, C=OCH$_2$CHCH$_2$C*H*$_2$), 1.76 (br, 2H, C=OCH$_2$CHC*H*$_2$CH$_2$), 1.60 (d, J = 7.1 Hz, 3H, CHC*H*$_3$), 1.60 (br, 3H, CH=CHCH$_2$OC=OCHC*H*$_3$). ^{13}C from HSQC and HMBC ($CDCl_3$, ppm): δ 191.0, 179.4, 169.7, 169.5, 169.0, 135.2, 124.1, 71.5, 70.0, 69.0, 66.0, 38.5, 32.8, 26.8, 27.4, 16.7. **P(LA$_{86}$-co-β-HL$_4$):** M_n = 16,200, Đ = 1.20. . **P(LA$_{85}$-co-β-HL$_{19}$):** M_n = 23,800, Đ = 2.39.

3-Butene-2-one incorporation

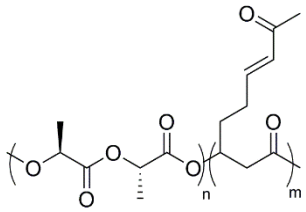

^{1}H NMR ($CDCl_3$, ppm)**:** δ 6.75 (br, 1H, C*H*=CHC=OCH_3), 6.08 (br, 1H, CH=C*H*C=OCH_3), 5.26 (br, 1H C=OCH_2C*H*), 5.19 (q, J = 7.1 Hz 1H, C*H*CH_3), 2.68 (br, 2H, C=OC*H*$_2$CH), 2.27 (br, 2H, C=OCH_2CHCH_2C*H*$_2$), 2.24 (brs, 3H, C*H*=CHC=OC*H*$_3$), 1.82 (br, 2H, C=OCH2CHCH2CH2), 1.60 (d, J = 7.1 Hz, 3H, CHC*H*$_3$). ^{13}C from HSQC and HMBC ($CDCl_3$, ppm): δ 198.3, 169.7, 169.5, 145.9, 131.8, 70.0, 69.0, 38.6, 32.2, 28.0, 27.0, 16.7. **P(LA$_{86}$-co-β-HL$_4$):** M_n = 17,300, 1.01. Đ = 1.092. **P(LA$_{85}$-co-β-HL$_{19}$):** M_n = 9,800, Đ = 1.03.

Methyl acrylate incorporation

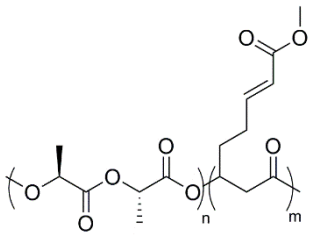

^{1}H NMR ($CDCl_3$, ppm)**:** δ 6.91 (br, 1H, C*H*=CHC=OOCH_3), 5.84 (br, 1H, CH=C*H*C=OOCH_3), 5.26 (br, 1H C=OCH_2C*H*), 5.19 (q, J = 7.1 Hz, 1H, C*H*CH_3), 3.72 (brs, 3H CH=CHC=OOCH3), 2.68 (br, 2H, C=OC*H*$_2$CH), 2.24 (br, 2H, C=OCH_2CHCH_2C*H*$_2$), 1.81 (br, 2H, C=OCH_2CHC*H*$_2$CH_2), 1.60 (d, J = 7.1 Hz, 3H, CHC*H*$_3$). ^{13}C from HSQC and HMBC ($CDCl_3$, ppm): δ 169.7, 169.5, 166.8, 147.4, 121.8, 70.2, 69.0, 51.5, 38.5, 32.2, 27.8, 16.7. **P(LA$_{86}$-co-β-HL$_4$):** M_n = 16,800, Đ = 1.07. **P(LA$_{85}$-co-β-HL$_{19}$):** M_n = 12,100, Đ = 1.02.

3,3-Dimethyl-1-butene incorporation

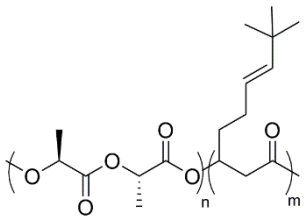

^{1}H NMR ($CDCl_3$, ppm)**:** δ 5.47 (br, 1H, CH=C*H*C(CH_3)$_3$), 5.27 (br, 1H, C*H*=CHC(CH_3)$_3$), 5.26 (br, 1H C=OCH_2C*H*), 5.19 (q, J = 7.1 Hz, 1H, C*H*CH_3), 2.68 (br, 2H, C=OC*H*$_2$CH), 2.02 (br, 2H, C=OCH_2CHCH_2C*H*$_2$), 1.71 (br, 2H, C=OCH_2CHC*H*$_2$CH_2), 1.60 (d, J = 7.1 Hz, 3H, CHC*H*$_3$), 0.99 (br, C*H*=C(*C*H_3)$_3$). ^{13}C from HSQC and HMBC ($CDCl_3$, ppm): δ 169.7, 169.5, 142.9, 122.8, 71.3, 69.0, 38.5, 33.8, 32.7, 29.7, 28.2, 16.7. **P(LA$_{86}$-co-β-HL$_4$):** M_n = 12,300, Đ = 1.04. **P(LA$_{85}$-co-β-HL$_{19}$):** M_n = 8,000, Đ = 1.05.

6.4.8 Representative double olefin cross-metathesis

Copolymer **75**: In a glove box copolymer (85:19) (0.2 g), methyl acrylate (0.023 g, 0.27 mmol) and Hoveyda Grubbs second generation catalyst (0.0084 g, 0.013 mmol) were dissolved in DCM (1 mL) and added to an oven dried ampoule. The mixture was degassed by one freeze-pump-thaw cycle and heated for 16 h under reflux with occasional de-gassing. The reaction was quenched with a few drops of ethyl vinyl ether, precipitated in cold methanol (~20 mL) and washed with cold diethyl ether (~20 mL) and hexane (~20 mL). The polymer was dried under vacuum and taken into the box. Following this the functionalised polymer (0.12 g), 1,2-epoxy-5-hexene (0.13 g, 1.3 mmol) and Hoveyda Grubbs second generation catalyst (0.01 g, 0.016 mmol) were dissolved in DCM (0.5 mL) in an oven dried ampoule. The mixture was degassed by one freeze-pump-thaw cycle and heated for 16 h under reflux with occasional de-gassing. The reaction was quenched with a few drops of ethyl vinyl ether, precipitated in cold methanol (~20 mL) and washed with cold diethyl ether (~20 mL) and cold hexane (~20 mL).

6.5 Synthesis for chapter four

6.5.1 Representative ring-opening polymerisation of lactide

ROP using U-1 or Ce-1

L-Lactide (0.086 g, 0.6 mmol) and **U-1** (0.0041 g, 0.003 mmol) were dissolved in toluene (0.6 mL) and added to an oven dried ampoule to give a 1.0 M solution of lactide. The reaction mixture was heated at 60 °C for 19 h. The product was quenched and precipitated in cold methanol with a small amount of of dilute hydrochloric acid. The polymer was collected *via* filtration to yield a white solid.

ROP using UL_4

L-Lactide (0.086 g, 0.6 mmol) and **UL_4** (0.0049 g, 0.003 mmol) were dissolved in toluene (0.6 mL) and added to an oven dried ampoule to give a 1.0 M solution of lactide. The

reaction mixture was heated at 60 °C for 19 h. The product was quenched in cold methanol with a small amount of dilute hydrochloric acid. No polymer precipitated. The same reaction was repeated under immortal conditions (monomer:catalyst:BnOH (200:1:5)) to produce a polymer.

ROP using U-Ni

L-Lactide (0.086 g, 0.6 mmol) and **U-Ni** (0.0043 g, 0.003 mmol) were dissolved in toluene (0.6 mL) and added to an oven dried ampoule to give a 1.0 M solution of lactide. The reaction mixture was heated at 60 °C for 19 h. The product was quenched in cold methanol with a small amount of dilute hydrochloric acid. No polymer precipitated. The same reaction was repeated under immortal conditions but still no polymer formation.

6.5.2 Representative Immortal ring-opening polymerisation of lactide

ROP using U-1 or Ce-1: (0.086 g, 0.6 mmol), **U-1** (0.0041 g, 0.003 mmol) and BnOH (0.0016 g, 0.015 mmol) were dissolved in toluene (0.6 mL) and added to an oven dried ampoule to give a 1.0 M solution of lactide. The reaction mixture was heated at 60 °C for 19 h. The product was quenched and precipitated in cold methanol with a small amount of of dilute hydrochloric acid. The polymer was collected *via* filtration to yield a viscous oil.

End-group analysis

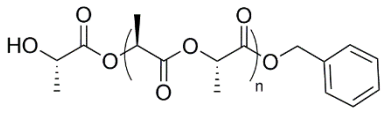

^{1}H NMR ($CDCl_3$, ppm): δ 7.34-7.38 (m, 5H, *Ph*CH_2O-(polymer end group)), δ 5.18 (m, 2H, PhCH_2O-(polymer end group)), δ 5.16 (q, J = 7.1 Hz, 1H, C*H*CH_3), 4.37 (m, 1H, HOC*H*CH_3C=OO-(polymer end group)), 2.67 (br, 1H, *H*OCHCH_3C=OO-(polymer end group)), 1.58 (d, J = 7.1 Hz, 3H, CHC*H*$_3$), 1.51 (d, 3H, HOCHC*H*$_3$C=OO-(polymer end group)). ^{13}C NMR {^{1}H} ($CDCl_3$, ppm): 175.1, 169.6, 135.1, 128.6-128.3, 69.0, 67.2, 66.69, 20.54, 16.65.

6.5.3 Representative kinetics

Example of *in-situ* observation of LA polymerisation: Ring-opening polymerisations were monitored using ^{1}H NMR spectroscopy. In a glove box to a Young's NMR tube, lactide, catalyst and BnOH (if required) were dissolved in toluene-d_8 to make a 1 M solution. The tube was sealed and placed in the spectrometer probe, which was pre-heated to 333 K (60 °C). Spectra were taken at 10-minute intervals.

6.6 References

1 Cross, E. D.; Allan, L. E. N.; Decken. A.; Shaver, M. P.; *J. Polym. Sci. Part A Polym. Chem.*, **2013**, *51*, 1137–1146.

2 Hormnirun, P.; Marshall, E. L.; Gibson, V. C.; White, A. J. P.; Williams, D. J.; *J. Am. Chem. Soc.*, **2004**, *126*, 2688–2689.

3 Hormnirun, P.; Marshall, E. L.; Gibson, V. C.; Pugh, R. I.; White, A. J. P.; *Proc. Natl. Acad. Sci. U. S. A.*, **2006**, *103*, 15343–8.

4 Doyle, D. J.; Gibson, V. C.; White, A. J. P.; *Dalton. Trans.*, **2007**, 358–363.

5 Kramer, J. W.; Lobkovsky, E. B.; Coates, G. W. *Org. Lett.*, **2006**, *8*, 3709–3712.

6 Lee, J. B.; Ott, K. C.; Grubbs, R. H. *J. Am. Chem. Soc*, **1982**, *104*, 7491–7496.

7 Jing, F.; Hillmyer, M. A.; Chen, L.; Qin, D. Y.; Cramer, C. J.; Yao, L.; Young, V. G. *J. Am. Chem. Soc*, **2008**, *130*, 13826–13827.

8 Guillaume, C.; Ajellal, N.; Carpentier, J.-F.; Guillaume, S. M. *J. Polym. Sci. Part A Polym. Chem.*, **2011**, *49*, 907–917.